Supporting information for *Effectiveness of UNAIDS targets and HIV vaccination across 127 countries*

Jan Medlock[a,1], Abhishek Pandey[b], Alyssa S. Parpia[b], Amber Tang[b], Laura A. Skrip[b], and Alison P. Galvani[b]

[a]Department of Biomedical Sciences, Oregon State University, 106 Dryden Hall, Corvallis, OR 97331-4801
[b]Center for Infectious Disease Modeling and Analysis, Yale School of Public Health, 135 College Street, New Haven, CT 06510-2483
[1]To whom correspondence should be addressed. Email: jan.medlock@oregonstate.edu.

March 9, 2017

We developed a mathematical model of HIV transmission and progression that stratifies HIV infection into acute, chronic undiagnosed, chronic diagnosed, chronic treated, chronic virally suppressed, and AIDS, along with uninfected unvaccinated and vaccinated people (Section S1 & Fig. S1), tailored to each of 127 countries. Simulations of our model project the number of people in each HIV stratum from 2015 to 2035, from which statistics such as prevalence and incidence were calculated. To evaluate the impact of the 90–90–90 and 95–95–95 UNAIDS goals, model transition rates were adjusted dynamically to meet intervention goals for diagnosis, treatment, viral suppression, and vaccination coverage (Section S2). Data and estimates from many sources, including The World Bank and UNAIDS, were used to parametrize the model (Section S3). Country-specific transmission rates were fitted to estimates of the historical trajectories of incidence and prevalence, spanning from as early as 1990 for some countries (Section S4). For every scenario of intervention combinations, we conducted 1000 model simulations, sampling values of model parameters from empirical distributions for each simulation, and reported the results with median and percentiles (Section S5). The effectiveness of the UNAIDS goals and vaccination was estimated for each of the 127 countries and aggregated by region and globally (Section S6).

The model simulation and analysis tools, written in Python, are publicly available (1).

S1 Model structure

Within each country, our model divides people aged 15 years and older into non-overlapping HIV states. We focused on this age group because it accounts for the vast majority of global PLHIV (2), 93% in 2014; because population-level HIV estimates and demographic data are typically only estimated for ages 15–49; and to capture the continuing burden of infections in people ages 50 and older. Our model has 8 HIV states (Fig. S1): susceptible to HIV infection (S is the number of people susceptible), vaccinated against HIV (R), acute HIV infection (A), undiagnosed HIV infection (U),

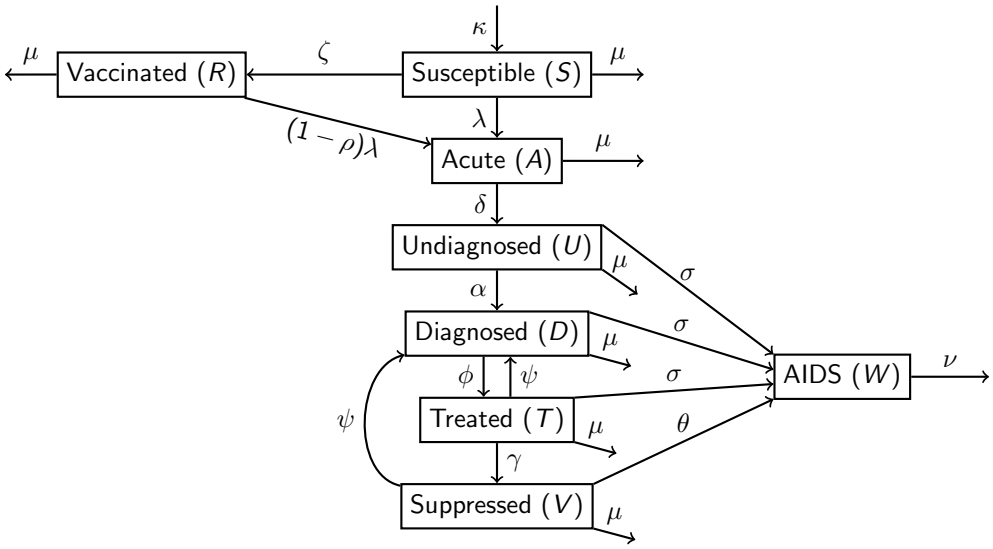

Fig. S1. Model diagram.

diagnosed but untreated HIV infection (D), treated without viral suppression (T), viral suppression (V), and having AIDS (W).

Transitions between model states are governed by a system of differential equations parametrized using values found in other studies, along with transmission rates derived from UNAIDS estimates of incidence and prevalence (Table S1). The model is deterministic, but uncertainty in the parameters was treated by running the model 1000 times with samples from the parameter distributions (Section S5) and summarizing the model outcomes using the median and percentiles. Each country was modeled separately (Figs. S14–S140) and the country simulations were aggregated to calculate global and regional outcomes (Figs. S4–S13).

People susceptible to HIV (S) are at risk of becoming infected according to the force of infection (λ), which depends on the HIV transmission rate, estimated from the country-specific incidence and prevalence data (Section S4), adjusted for the current number of acutely infected, untreated or ineffectively treated, and virally suppressed PLHIV. Upon infection, people transition into acute infection (A), characterized by high viral loads for an average of 2.90 [95% confidence interval 1.23, 6.00] months (5). (We converted these durations to rates like $1/2.90$ month$^{-1} \approx 4.14$ y^{-1} and set the parameter using random samples from Triangular$(2, 4.14, 9.6)$ y^{-1} to capture the uncertainty in its value. See Section S5 for the definition of Triangular(a, b, c) and other distributions.) Acute infection progresses into the chronic undiagnosed class (U), from which diagnosis occurs at the rate α, which is determined by the country's current diagnosis level and its diagnosis target under the different scenarios (Section S2). Upon diagnosis, people transition into the diagnosed class (D). From the diagnosed class, people transition to the treated compartment (T) upon starting ART at the rate ϕ, dependent on the country's current treatment level and its treatment target (Section S2). Treated people transition to the viral suppression (V) at the rate γ, sampled from Uniform$(0.5, 1.5)$ y^{-1}: thus, viral suppression occurs after between 8 months and 2 years on treatment (7). Disengagement from treatment moves people from treated (T) and viral suppression (V) back to the diagnosed class (D) at the rate ψ, dependent on the current level of viral suppression and the country's target

Table S1. Model parameters.

	Definition	Value	References
μ	Background death rate	Country specific, Dataset 2	(3)
κ	Recruitment rate	Country specific, Dataset 2	(3, 4)
δ	Rate of progression from acute infection	Triangular$(2, 4.14, 9.6)$ y^{-1}	(5)
σ	Rate of developing AIDS without viral suppression	0.1064 y^{-1}	(6)
θ	Rate of developing AIDS with viral suppression	Eq. **2**	—
γ	Rate of viral suppression	Uniform$(0.5, 1.5)$ y^{-1}	(7)
ν	Death rate from AIDS	0.5 y^{-1}	(6)
ρ	Vaccine efficacy	50% [30%, 70%]	—
ω	Reduction in life expectancy with viral suppression	Uniform$(5, 8)$ y	(8, 9)
τ_A	Transmissibility per coital act during acute phase	Triangular$(0.0039, 0.0082, 0.0150)$	(10, 11)
τ_U	Transmissibility per coital act after acute phase	Triangular$(0.00077, 0.0014, 0.00251)$	(12)
ϵ	Relative transmissibility per coital act with viral suppression	Beta-PERT$(0.08, 0.002, 0.57)$	(13–17)
n	Coital acts per year	Uniform$(96, 108)$	(10, 18)
α	Diagnosis rate	Eq. **12**	—
ϕ	Treatment rate	Eq. **15**	—
ψ	Rate of relapse to untreated	Eq. **17**	—
ζ	Vaccination rate	Eq. **19**	—

Triangular, Uniform, and Beta-PERT are sampling distributions (Section S5).
For vaccine efficacy, 50% was the baseline, and 30% and 70% were also assessed in sensitivity analysis.

(Section S2).

PLHIV without viral suppression (compartments U, D, and T) develop AIDS (compartment W) after an average duration of 10.4 years (6), i.e. with transition rate $\sigma = 0.1064$ y^{-1}. Viral suppression greatly reduces the rate of progression to AIDS (θ) and improves longevity, such that life expectancy is only 5–8 y shorter than average country-specific life expectancy (8, 9). This reduction in life expectancy was quantified by randomly sampling the parameter ω from Uniform$(5, 8)$ y. Thus, in the absence of relapse to untreated, the duration of viral suppression is

$$\frac{1}{\theta + \mu} = \frac{1}{\mu} - \omega - \frac{1}{\nu}. \qquad [1]$$

The left-hand side of the equation is the time until leaving viral suppression by either progression to AIDS (at rate θ) or background mortality (at rate μ). The right-hand side of the equation is the life expectancy of uninfected people, minus the reduction in life expectancy attributable to virally suppressed HIV infection, minus the duration of the AIDS stage. Solving for θ gives the rate of progression to AIDS from viral suppression,

$$\theta = \frac{1}{1/\mu - \omega - 1/\nu} - \mu. \qquad [2]$$

In the vaccination scenarios, susceptible people are vaccinated at rate ζ, depending on the country's current vaccination coverage and its coverage target (Section S2), transitioning into the vaccinated compartment (R). The force of infection for vaccinated people is reduced by the efficacy factor ρ. We took the base-case efficacy to be 50%, but varied it to 30% and 70% in sensitivity analysis (Section S5). We did not model specific vaccine dose regime, such that implicit in our efficacy parameter is the assumption that boosters will be used to maintain efficacy over time. Without vaccine, $\zeta = 0$.

The background mortality rate (μ) in each of the 127 countries was collected from published estimates (3). The recruitment rate (κ) into the age 15 y and older group was set by the difference between the country's population growth rate (4) and its background mortality rate (3), as would be true if the population was at its stable age structure. (More on these data sources is in Section S3.)

We also added differential equations to track the cumulative number of new infections (Y) and AIDS deaths (Z) over the simulation period.

The model equations are

$$\begin{aligned}
\frac{\mathrm{d}S}{\mathrm{d}t} &= \kappa N - \lambda S - \zeta S - \mu S,\\
\frac{\mathrm{d}R}{\mathrm{d}t} &= \zeta S - (1-\rho)\lambda R - \mu R,\\
\frac{\mathrm{d}A}{\mathrm{d}t} &= \lambda S + (1-\rho)\lambda R - \delta A - \mu A,\\
\frac{\mathrm{d}U}{\mathrm{d}t} &= \delta A - \alpha U - \mu U - \sigma U,\\
\frac{\mathrm{d}D}{\mathrm{d}t} &= \alpha U + \psi T + \psi V - \phi D - \mu D - \sigma D,\\
\frac{\mathrm{d}T}{\mathrm{d}t} &= \phi D - \psi T - \gamma T - \mu T - \sigma T,\\
\frac{\mathrm{d}V}{\mathrm{d}t} &= \gamma T - \psi V - \mu V - \theta V,\\
\frac{\mathrm{d}W}{\mathrm{d}t} &= \sigma U + \sigma D + \sigma T + \theta V - \nu W,\\
\frac{\mathrm{d}Y}{\mathrm{d}t} &= \lambda\big[S + (1-\rho)R\big],\\
\frac{\mathrm{d}Z}{\mathrm{d}t} &= \nu W,
\end{aligned} \qquad \textbf{[3]}$$

with force of infection

$$\lambda = \frac{\xi\big[\beta_A A + \beta_U(U+D+T) + \beta_V V\big]}{N}, \qquad \textbf{[4]}$$

and sexually active population size $N = S + R + A + U + D + T + V$. We assumed that people with AIDS (W) are too sick to be sexually active.

The relative transmission rates (per unit time), β, from acute (A), unsuppressed (U and T), and suppressed infected (V) people are respectively

$$\begin{aligned}
\beta_A &= 1 - (1-\tau_A)^n,\\
\beta_U &= 1 - (1-\tau_U)^n,\\
\beta_V &= 1 - (1-\epsilon\tau_U)^n,
\end{aligned} \qquad \textbf{[5]}$$

where the τ's are the relative transmissibilities per coital act, n is the annual number of coital acts, and ϵ is the relative transmissibility per coital act with viral suppression. For transmissibility per coital act during the acute phase, we sampled τ_A from Triangular$(0.0039, 0.0082, 0.0150)$ (10, 11). Transmissibility per coital act for unsuppressed people, τ_U, was sampled from Triangular$(0.00077, 0.0014, 0.00251)$ (12). The transmissibility per coital act of people with viral suppression relative to those without suppression has been estimated at 0.08 (95% confidence interval 0.002, 0.57) (13). Due to the extremely long left tail of this confidence interval, we sampled the relative transmissibility per coital act ϵ from Beta-PERT$(0.08, 0.002, 0.57)$ rather than a Triangular distribution. (See Section S5 for a full description of Beta-PERT(a, b, c).) The annual number of coital acts per person n was sampled from Uniform$(96, 108)$ based on survey studies (10, 18). The country-specific transmission rate ξ was derived from country-specific longitudinal trends in HIV prevalence and incidence, primarily from UNAIDS estimates (Section S4).

The model was initiated with country-specific estimates from 2015 of the number of people aged 15–49 years, $M(2015)$; the prevalence, $p_I(2015)$; the proportion diagnosed, $p_D(2015)$; the proportion treated, $p_T(2015)$; and proportion with viral suppression, $p_V(2015)$ were used to initialize the model (Section S3). Although the initial population used ages 15–49 due to the availability of published estimates, model projections allowed for analysis of infected people aging beyond 50 years old. Due to a lack of published estimates of the number of acute infections, and since the acute phase is so much shorter than the other stages, we assumed that initially there were no acute infections. Due to a lack of comprehensive estimates of the number of people with AIDS in each country, we assumed that the proportion of diagnosed, untreated people $(D + W)$ who have AIDS (W) in year 2015 was

$$p_A = \frac{\sigma}{\sigma + \nu}, \qquad [6]$$

which is the equilibrium fraction of diagnosed people $(D+W)$ who have AIDS (W) in the absence of treatment and background mortality. Simulations were initiated with no vaccination. The cumulative number of new infections and AIDS deaths were initially set to 0. Thus, the model initial conditions are

$$\begin{aligned}
S(2015) &= \big(1 - p_I(2015)\big)M(2015),\\
R(2015) &= 0,\\
A(2015) &= 0,\\
U(2015) &= \big(1 - p_D(2015)\big)p_I(2015)M(2015),\\
D(2015) &= \big(1 - p_A\big)p_D(2015)\big(1 - p_T(2015)\big)p_I(2015)M(2015),\\
T(2015) &= p_D(2015)p_T(2015)\big(1 - p_V(2015)\big)p_I(2015)M(2015),\\
V(2015) &= p_D(2015)p_T(2015)p_V(2015)p_I(2015)M(2015),\\
W(2015) &= p_A p_D(2015)\big(1 - p_T(2015)\big)p_I(2015)M(2015),\\
Y(2015) &= 0,\\
Z(2015) &= 0.
\end{aligned} \qquad [7]$$

The parametrized differential equations were solved numerically from 2015 to 2035 using the LSODA routine (1, 19, 20) and four effectiveness outcomes were computed from the solutions.

Cumulative new infections from 2015 to time t was given by $Y(t)$.

Per-capita incidence at each solution time was calculated as

$$i(t_j) = \frac{Y(t_j) - Y(t_{j-1})}{M(t_j)(t_j - t_{j-1})}, \qquad [8]$$

where

$$M(t) = S(t) + R(t) + A(t) + U(t) + D(t) + T(t) + V(t) + W(t) \qquad [9]$$

is the total population size at time t. (The per-capita incidence at the first time point was undefined.)

PLHIV at each solution time was given by

$$A(t) + U(t) + D(t) + T(t) + V(t) + W(t). \qquad [10]$$

Cumulative AIDS-related deaths from 2015 to time t was given by $Z(t)$.

The results from the country simulations were aggregated to the regional and global levels by adding the numbers of people in each compartment over time and then new infections, per-capita incidence, PLHIV, and HIV-related deaths were calculated from the aggregates. (See Dataset 6 for the definitions of UNAIDS regions.)

S2 Target rates

The current proportion of PLHIV who have been diagnosed is

$$p_D(t) = \frac{D(t) + T(t) + V(t) + W(t)}{A(t) + U(t) + D(t) + T(t) + V(t) + W(t)}. \quad \textbf{[11]}$$

The timing and levels of diagnosis under evaluation, whether maintaining status quo or increasing to UNAIDS targets, are given by the target $p_D^*(t)$. (See below.) To achieve this target, we adjusted the diagnosis rate over time according to the function

$$\alpha(t) = \alpha_{\max} H\big(p_D^*(t) - p_D(t)\big), \quad \textbf{[12]}$$

where $H(x)$ is the Heaviside-like function

$$H(x) = \begin{cases} 0 & \text{if } x < 0, \\ x/\chi & \text{if } 0 \le x \le \chi, \\ 1 & \text{if } x > \chi, \end{cases} \quad \textbf{[13]}$$

with $\chi = 0.001$, which rapidly switches from $H = 0$ when $x < 0$ to $H = 1$ when $x > 0$. The linear segment connecting $H = 0$ and $H = 1$ was used to avoid difficulties in computing numerical solutions that occur when using a discontinuous function. The function for the rate of new diagnoses **12** allows new diagnoses ($\alpha(t) > 0$) when the current diagnosis level is below the target ($p_D^*(t) > p_D(t)$), and stops new diagnoses ($\alpha(t) = 0$) when the current diagnosis level is at or above target. We took $\alpha_{\max} = 1\ \text{y}^{-1}$.

The proportion of diagnosed people who are treated is

$$p_T(t) = \frac{T(t) + V(t) + W(t)}{D(t) + T(t) + V(t) + W(t)}. \quad \textbf{[14]}$$

Like the diagnosis rate, the rate of treatment initiation is

$$\phi(t) = \phi_{\max} H\big(p_T^*(t) - p_T(t)\big), \quad \textbf{[15]}$$

with $\phi_{\max} = 10$, allowing new treatment ($\phi(t) > 0$) when the current treatment level is below the target ($p_T^*(t) > p_T(t)$) and stopping new treatment ($\phi(t) = 0$) when the current treatment level is at or above target.

The proportion of people on ART who have achieved viral suppression is

$$p_V(t) = \frac{V(t)}{T(t) + V(t)}. \quad \textbf{[16]}$$

The rate of people relapsing to untreated is

$$\psi(t) = \psi_{\max} H\big(p_V(t) - p_V^*(t)\big), \tag{17}$$

with $\psi_{\max} = 1$, which, unlike diagnosis and treatment rates, prevents relapses ($\psi(t) = 0$) when the current level of viral suppression is below the target ($p_V^*(t) > p_V(t)$) and allows relapses ($\psi(t) > 0$) when the current level of viral suppression is at or above target. We varied the relapse rate to achieve the target level of viral suppression because achieving viral suppression depends on the time on treatment (7).

The proportion of susceptible people vaccinated is

$$p_R(t) = \frac{R(t)}{S(t) + R(t)}. \tag{18}$$

Like diagnosis and treatment, the vaccination rate is

$$\zeta(t) = \zeta_{\max} H\big(p_R^*(t) - p_R(t)\big), \tag{19}$$

with $\zeta_{\max} = 1$, vaccinating people ($\zeta(t) > 0$) when the current vaccine coverage level is below the target ($p_R^*(t) > p_R(t)$).

We modeled 3 different targets for the proportion diagnosed (p_D), the proportion treated (p_T), and the proportion with viral suppression (p_V).

Status quo is maintenance of the proportions p_D, p_T, and p_V at their initial levels going forward. That is,

$$\begin{aligned} p_D^*(t) &= p_D(2015), \\ p_T^*(t) &= p_T(2015), \\ p_V^*(t) &= p_V(2015). \end{aligned} \tag{20}$$

UNAIDS 90–90–90 was implemented as linearly increasing p_D, p_T, and p_V from their 2015 levels, each up to 90% by 2020, and then maintained at 90% from 2020 to 2035. However, if an initial level exceeds 90%, it is maintained at its higher level so that meeting the 90–90–90 goal does not worsen any aspect of the treatment cascade. That is,

$$\begin{aligned} p_D^*(t) &= \begin{cases} F\big(t, 2015, p_D(2015), 2020, 0.9\big) & \text{if } p_D(2015) < 0.9, \\ p_D(2015) & \text{if } p_D(2015) \geq 0.9. \end{cases} \\ p_T^*(t) &= \begin{cases} F\big(t, 2015, p_T(2015), 2020, 0.9\big) & \text{if } p_T(2015) < 0.9, \\ p_T(2015) & \text{if } p_T(2015) \geq 0.9. \end{cases} \\ p_V^*(t) &= \begin{cases} F\big(t, 2015, p_V(2015), 2020, 0.9\big) & \text{if } p_V(2015) < 0.9, \\ p_V(2015) & \text{if } p_V(2015) \geq 0.9, \end{cases} \end{aligned} \tag{21}$$

where

$$F(t, t_0, x_0, t_1, x_1) = \begin{cases} x_0 & \text{if } t < t_0, \\ x_0 + (x_1 - x_0)\frac{t - t_0}{t_1 - t_0} & \text{if } t_0 \leq t < t_1, \\ x_1 & \text{if } t \geq t_1, \end{cases} \tag{22}$$

is constant at x_0 for $t < t_0$, linearly connects x_0 at t_0 to x_1 at t_1 for $t_0 \leq t < t_1$, and is constant at x_1 for $t \geq t_1$.

UNAIDS 95–95–95 is to achieve 90–90–90 by 2020, and then for p_D, p_T, and p_V to all be raised to 95% by 2030. We implemented this target as for 90–90–90 from 2015 to 2020, and then as linear increases from the 2020 levels up to 95% in 2030, again with the exception that if an initial level is above 95% then it remains constant from 2015 to 2035. That is,

$$p_D^*(t) = \begin{cases} G\big(t, 2015, p_D(2015), 2020, 0.9, 2030, 0.95\big) & \text{if } p_D(2015) < 0.9, \\ F\big(t, 2020, p_D(2015), 2030, 0.95\big) & \text{if } 0.9 \le p_D(2015) < 0.95, \\ p_D(2015) & \text{if } p_D(2015) \ge 0.95, \end{cases}$$

$$p_T^*(t) = \begin{cases} G\big(t, 2015, p_T(2015), 2020, 0.9, 2030, 0.95\big) & \text{if } p_T(2015) < 0.9, \\ F\big(t, 2020, p_T(2015), 2030, 0.95\big) & \text{if } 0.9 \le p_T(2015) < 0.95, \\ p_T(2015) & \text{if } p_T(2015) \ge 0.95, \end{cases} \quad \textbf{[23]}$$

$$p_V^*(t) = \begin{cases} G\big(t, 2015, p_V(2015), 2020, 0.9, 2030, 0.95\big) & \text{if } p_V(2015) < 0.9, \\ F\big(t, 2020, p_V(2015), 2030, 0.95\big) & \text{if } 0.9 \le p_V(2015) < 0.95, \\ p_V(2015) & \text{if } p_V(2015) \ge 0.95, \end{cases}$$

where

$$G(t, t_0, x_0, t_1, x_1, t_2, x_2) = \begin{cases} x_0 & \text{if } t < t_0, \\ x_0 + (x_1 - x_0)\frac{t-t_0}{t_1-t_0} & \text{if } t_0 \le t < t_1, \\ x_1 + (x_2 - x_1)\frac{t-t_1}{t_2-t_1} & \text{if } t_1 \le t < t_2, \\ x_2 & \text{if } t \ge t_2, \end{cases} \quad \textbf{[24]}$$

is constant at x_0 for $t < t_0$, linearly connects x_0 at t_0 to x_1 at t_1 for $t_0 \le t < t_1$, linearly connects x_1 at t_1 to x_2 at t_2 for $t_1 \le t < t_2$, and is constant at x_2 for $t \ge t_2$, and F is as in eq. **22**.

For vaccination, we assume in our base case that rollout begins in year $t_V = 2020$ (or $t_V = 2025$ in vaccine scenario analysis, Section S5), with the proportion of susceptible people becoming vaccinated increasing from 0% by $r_V = 25\%$ per year (or $r_V = 10\%$ per year) up to $c_V = 70\%$ (or $c_V = 50\%$ or $c_V = 90\%$), after which the vaccination coverage remains constant. Thus, the target for vaccination coverage at time t is

$$p_R^*(t) = \begin{cases} 0 & \text{if } t < t_V, \\ r_V(t - t_V) & \text{if } t_V \le t < T_V, \\ c_V & \text{if } t \ge T_V, \end{cases} \quad \textbf{[25]}$$

where $T_V = t_V + c_V/r_V$ is the time when rollout reaches the ultimate coverage c_V.

We simulated each of the 3 diagnosis and treatment targets (status quo, 90–90–90, or 95–95–95) with and without vaccination. In sensitivity analysis (Section S5), we varied vaccine efficacy, ultimate coverage, start date of rollout, and speed of rollout.

S3 Data sources

We found sufficient published estimates and data to parametrize our model for 127 countries. Demographic data, including population growth rate (4), death rate (3), and number of people aged 15–49 years (21) were obtained from the World Bank (Dataset 2). Longitudinal HIV prevalence

(Dataset 3) and incidence (Dataset 4) estimates for ages 15–49, spanning from as early as 1990 for some countries to 2015, were primarily obtained from the AIDSinfo database produced by UNAIDS (22). Other sources included UNAIDS Country Progress Reports (23) published from 2012 to 2016 and AIDS Data Hub (24), which compiles data from UNAIDS, UNICEF, WHO, and the Asian Development Bank. These sources were also used to inform the initial conditions for the model regarding the number of people diagnosed with HIV, the number on ART, and the number who have viral suppression or have been retained on treatment for at least 12 months (Dataset 5). Where data or estimates were not available from these sources, alternative resources such as peer-reviewed journal articles and country health ministry reports were consulted. Full information on the sources used for each country is provided in Datasets 2–5. These source tables are also available in our public source-code repository (1).

S4 Model fitting

We tailored our model to each of the 127 countries separately. Using available historical country-specific estimates of prevalence and incidence (Datasets 3 & 4), and published estimates of transmissibility per coital act (10–13), we derived an average country-specific transmission rate, taking into account the differential contributions from the proportions of acute, unsuppressed, and suppressed of the infected population in each country. Using historical data to smooth out short-term variations, our calibration method provided estimates of current country-specific transmission, as detailed below.

We first derived country-specific rates of HIV transmission, $\beta(t)$, for each of the available points in the historical estimates of prevalence and incidence. Approximating the model force of infection **4** by

$$\lambda(t) = \frac{\xi\left[\beta_A A(t) + \beta_U\big(U(t) + D(t) + T(t)\big) + \beta_V V(t)\right]}{N(t)} \approx \beta(t)\frac{I(t)}{N(t)}, \qquad \textbf{[26]}$$

where β is the estimated time-dependent aggregate transmission rate under the approximation that there is no difference in transmission risk among acute, unsuppressed, suppressed, and AIDS classes, and $I = A + U + D + T + V + W$ is the total number of PLHIV, gives the per-capita incidence as

$$i(t) = \lambda(t)\frac{S(t)}{N(t)} \approx \beta(t)\frac{I(t)}{N(t)}\frac{S(t)}{N(t)} = \beta(t)p(t)(1-p(t)), \qquad \textbf{[27]}$$

where $p(t)$ is the prevalence. Thus, we calculated the transmission rate at each historical time point using the incidence and prevalence estimates by

$$\beta(t) \approx \frac{i(t)}{p(t)(1-p(t))}. \qquad \textbf{[28]}$$

To reflect the uncertainty in $\beta(t)$, we assumed that it follows a lognormal distribution (Section S5). For the parameters μ and σ^2 of the lognormal distribution we used the exponentially weighted mean and variance (25) over time (with half-life 1 year) of $\log\beta(t)$ for the year 2015. That is,

$$\begin{aligned} \mu &= \frac{\sum_{i=1}^{n} 2^{t_i}\log\beta(t_i)}{\sum_{i=1}^{n} 2^{t_i}}, \\ \sigma^2 &= \frac{\big(\sum_{i=1}^{n} 2^{t_i}\big)\left[\sum_{i=1}^{n} 2^{t_i}\big(\log\beta(t_i)-\mu\big)^2\right]}{\big(\sum_{i=1}^{n} 2^{t_i}\big)^2 - \sum_{i=1}^{n} 2^{2t_i}}. \end{aligned} \qquad \textbf{[29]}$$

For this exponentially weighted mean and variance over time, a half-life of 1 year means that the estimate of the transmission rate from year i is weighted half as much as the estimate from year $i+1$, a quarter as much as the estimate from year $i+2$, and so on. This approach captured the recent country-specific transmission behavior while simultaneously allowing the use of historical estimates to smooth short-term variations (Fig. S2).

For each of the 1000 simulations per scenario, the country-specific aggregate transmission rate $\bar{\beta}$ was sampled from Lognormal(μ, σ^2) with the parameters given by eqs. **29**. Samples were also drawn for the transmissibilities per coital act of acute and virally unsuppressed infected people, τ_A and τ_U; the transmission reduction due to viral suppression, ϵ; and the average annual number of coital acts per person, n (Section S1). From these samples, the relative transmission rates for the acute phase (β_A), for unsuppressed chronic infections (β_U), and for chronic infections with viral suppression (β_V) were calculated by eqs. **5**. For each sample parameter set, the country-specific transmission rate was then computed by

$$\xi = \frac{\bar{\beta} I(2015)}{\beta_A A(2015) + \beta_U \big(U(2015) + D(2015) + T(2015)\big) + \beta_V V(2015)}, \qquad \textbf{[30]}$$

derived by rearranging eq. **26**, and uses the model initial conditions eq. **7**. This estimate of ξ is derived for the 2015 estimates of the proportion of PLHIV divided among acute infections; undiagnosed, diagnosed, or treated infections; and virally suppressed infections.

A few countries—e.g. Bulgaria, Timor-Leste, and Yemen—are currently estimated by UNAIDS to have low HIV prevalence but relatively high incidence, resulting in large estimated transmission rates and, thus, rapid projected growth of their HIV epidemics. The apparent low prevalence and high incidence may be an artifact of the resolution in UNAIDS estimates (0.1% for prevalence, 0.01% for annual per-capita incidence). Results for these countries should be considered in light of this limitation.

S5 Sensitivity and uncertainty analysis

Latin hypercube sampling (26) was used to draw parameter samples from published parameter distributions (Table S1) and the country-specific estimated distribution of the transmission rate (Section S4) 1000 times for each country. Projections were then generated by running the model simulations with these parameter sets. To compare interventions, as well as status quo projections, we implemented the variance-reduction technique of using the same set of sample parameter values for all interventions, repeating this process for each of the 1000 simulations in every country (27). We report the median, 1st and 3rd quartiles (i.e. 25th and 75th percentiles), and 5th and 95th percentiles for each model outcome. We also calculated partial rank correlation coefficients (PRCC) (26) to measure the independent effect of each non-vaccine parameter on model projections of global HIV incidence from 2015 to 2035 (Fig. S3).

We used several probability distributions to capture the uncertainty in the parameters. (See Section S1 for more on each parameter.)

Uniform was used for parameters where only a broad range was indicated in the literature. Uniform(a, b), with minimum a and maximum b, has density function

$$f_{\text{Uniform}}(x) = \begin{cases} \frac{1}{b-a} & \text{if } a \le x \le b, \\ 0 & \text{otherwise.} \end{cases} \qquad \textbf{[31]}$$

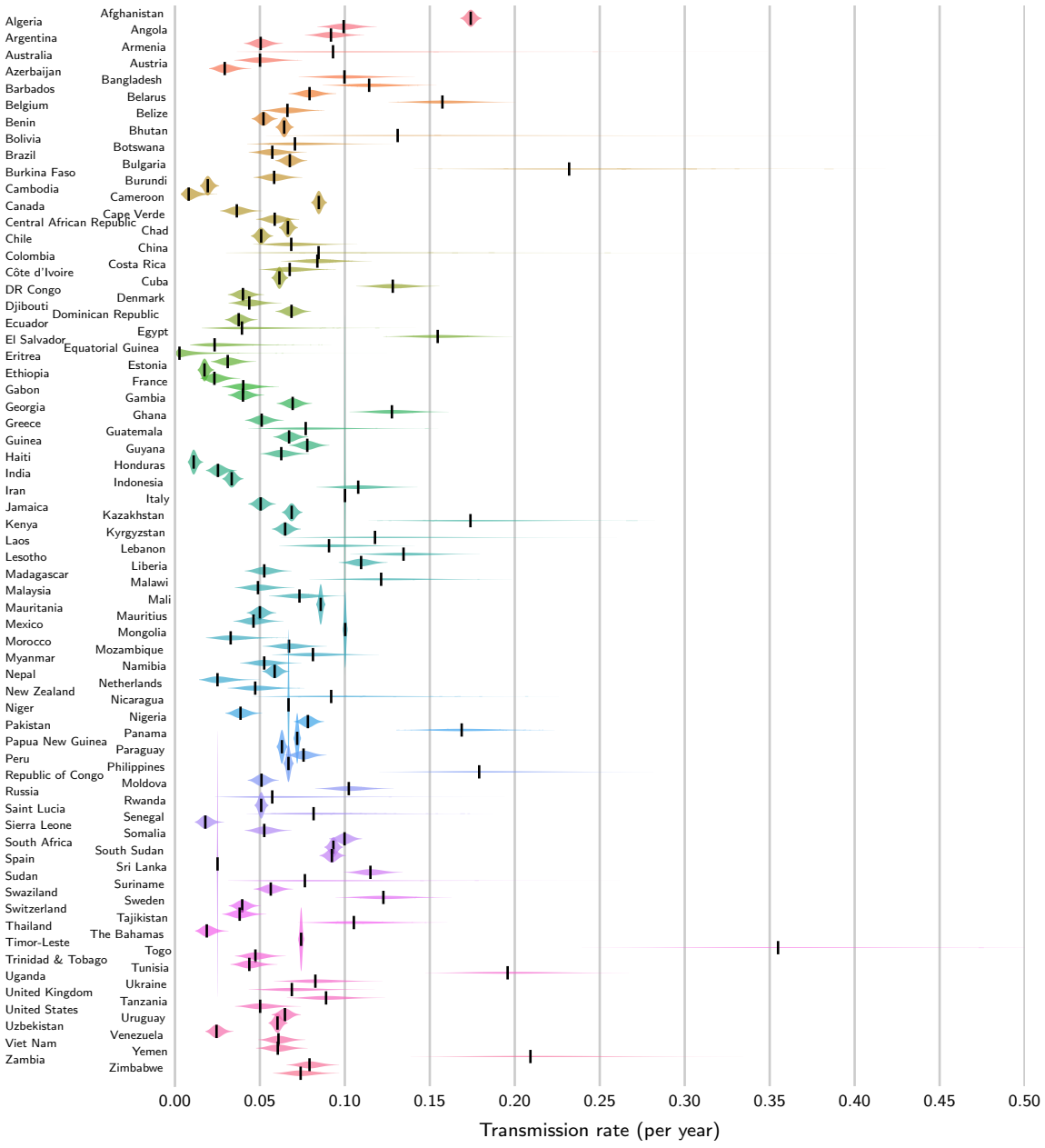

Fig. S2. Country-specific distributions of transmission rate, $\bar{\beta}$, calculated based on UNAIDS historical estimates of country prevalence and incidence. The colored shapes are the sampling distributions and the black bars are the modes of these distributions. See Section S4.

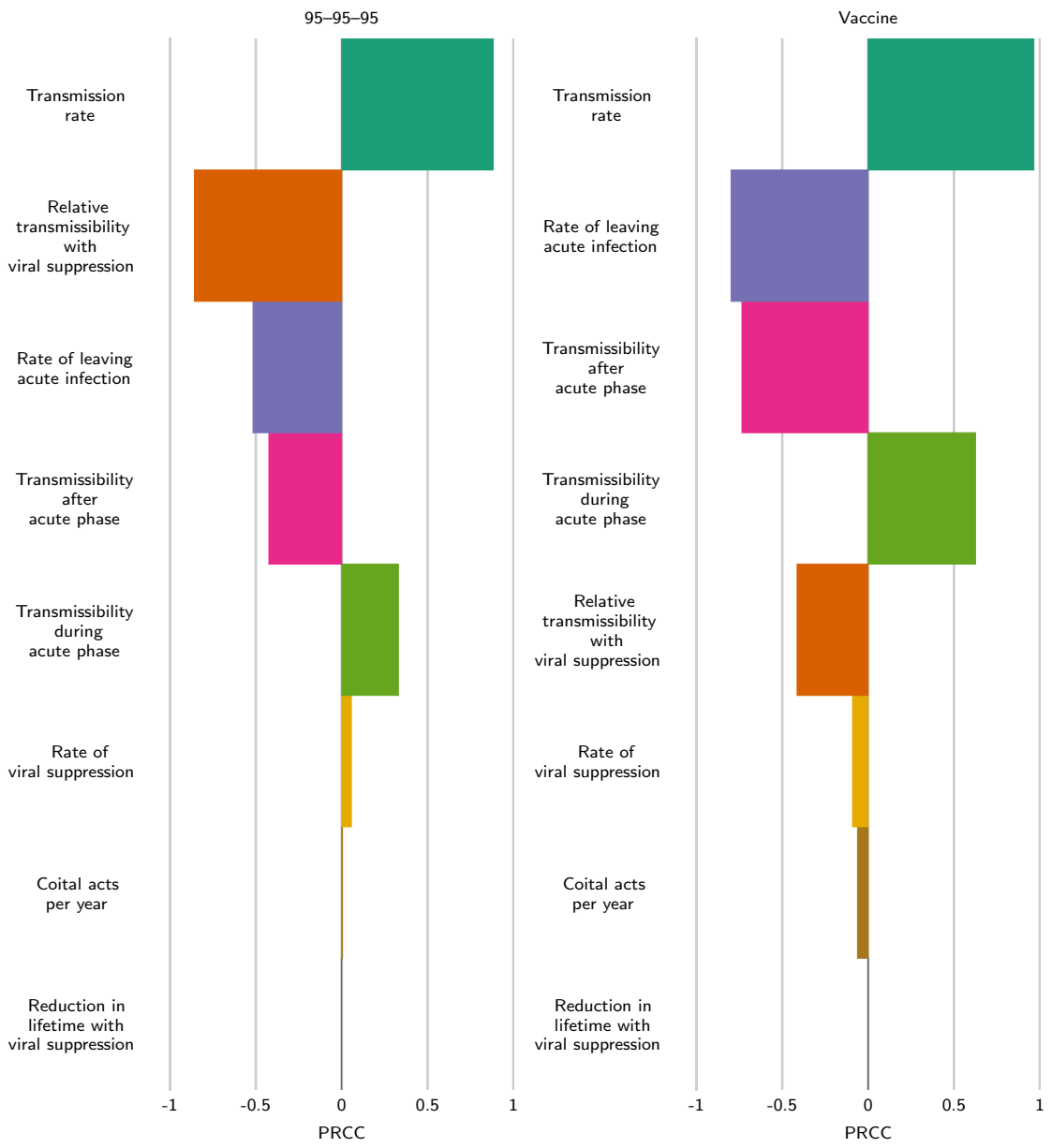

Fig. S3. Sensitivity of global HIV incidence from 2015 to 2035 to model parameters. Left is the sensitivity of infections averted by 95–95–95, relative to status quo. Right is the sensitivity of vaccination with status quo levels of diagnosis and treatment, relative to status quo. Sensitivity is measured by the partial rank correlation coefficient (PRCC).

We defined the mode for the uniform distribution to be the midpoint $\frac{b-a}{2}$.

Triangular was used for parameters where maximum-likelihood estimates and confidence intervals (or similar) were available. Triangular(a, b, c), with minimum a, mode b, and maximum c, has density function

$$f_{\text{Triangular}}(x) = \begin{cases} \frac{2(x-a)}{(c-a)(b-a)} & \text{if } a \leq x \leq b, \\ \frac{2(c-x)}{(c-a)(c-b)} & \text{if } b \leq x \leq c, \\ 0 & \text{otherwise.} \end{cases} \quad \textbf{[32]}$$

Beta-PERT was used for the efficacy of viral suppression at reducing transmission, ϵ, because the confidence interval had an extremely long right tail (13), which would strongly skew the mean and median of a Triangular distribution to the right. Beta-PERT(a, b, c), the Beta-PERT probability distribution (28) with minimum a, mode b, and maximum c, has density function

$$f_{\text{Beta-PERT}}(x) = \begin{cases} \frac{(x-a)^{v-1}(c-x)^{w-1}}{(c-a)^{v+w-2}\,\mathrm{B}(v,w)} & \text{if } a \leq x \leq c, \\ 0 & \text{otherwise,} \end{cases} \quad \textbf{[33]}$$

where

$$\begin{aligned} \mu &= \frac{a + \lambda b + c}{\lambda + 2}, \\ v &= \frac{(\mu - a)(2b - a - c)}{(b - \mu)(c - a)}, \\ w &= \frac{v(a - \mu)}{\mu - c}, \end{aligned} \quad \textbf{[34]}$$

and $\mathrm{B}(v, w)$ is the standard beta function (29, §6.2). We used the standard value of $\lambda = 4$.

Lognormal was used for the country-specific aggregate transmission rates, $\bar{\beta}$. Lognormal(μ, σ^2) has density function

$$f_{\text{Lognormal}}(x) = \frac{1}{x\sigma\sqrt{2\pi}} \exp\left(-\frac{(\log x - \mu)^2}{2\sigma^2}\right). \quad \textbf{[35]}$$

Based on proposed vaccine regimens that include boosters for sustaining immunogenicity (30), we made the simplifying assumption that vaccine efficacy remains constant over time. We chose plausible baseline values for efficacy (50%), ultimate coverage (70%), speed of rollout (25% per year), and date of rollout initiation (2020). We examined sensitivity and uncertainty by simulating 6 additional vaccine scenarios, varying efficacy (30%, 70%), ultimate coverage (50%, 90%), speed of rollout (10% coverage per year), and date of rollout initiation (2025; Fig. 4). The vaccine scenario analysis was done using the modes from the parameter distributions, not samples from these distributions, to reduce the computation time.

References

1. Medlock J, et al. (2016) HIV-95-vaccine. Available at `https://github.com/janmedlock/HIV-95-vaccine/`.

2. UNICEF. UNICEF statistics. Available at http://data.unicef.org/hiv-aids/global-trends.html. Accessed August 18, 2016.

3. The World Bank. Death rate, crude (per 1,000 people) | data. Available at http://data.worldbank.org/indicator/SP.DYN.CDRT.IN. Accessed July 11, 2016.

4. The World Bank. Population growth (annual %) | data. Available at http://data.worldbank.org/indicator/SP.POP.GROW. Accessed July 11, 2016.

5. Hollingsworth TD, Anderson RM, Fraser C (2008) HIV-1 transmission, by stage of infection. *J Infect Dis* 198(5):687–693.

6. Morgan D, et al. (2002) HIV-1 infection in rural Africa: is there a difference in median time to AIDS and survival compared with that in industrialized countries? *AIDS* 16(4):597–603.

7. Currie S, Rogstad KE, Piyadigamage A, Herman S (2009) Time taken to undetectable viral load, following the initiation of HAART. *Int J STD AIDS* 20(4):265–266.

8. Samji H, et al. (2013) Closing the gap: increases in life expectancy among treated HIV-positive individuals in the United States and Canada. *PLoS ONE* 8(12):e81355.

9. UNAIDS (2014) 90–90–90: Ambitious treatment target to help end the AIDS epidemic. Available at http://www.unaids.org/sites/default/files/media_asset/90-90-90_en_0.pdf.

10. Wawer MJ, et al. (2005) Rates of HIV-1 transmission per coital act, by stage of HIV-1 infection, in Rakai, Uganda. *J Infect Dis* 191(9):1403–1409.

11. Skarbinski J, et al. (2015) Human immunodeficiency virus transmission at each step of the care continuum in the United States. *JAMA Intern Med* 175(4):588–596.

12. Hughes JP, et al. (2012) Determinants of per-coital-act HIV-1 infectivity among African HIV-1–serodiscordant couples. *J Infect Dis* 205(3):358–365.

13. Donnell D, et al. (2010) Heterosexual HIV-1 transmission after initiation of antiretroviral therapy: a prospective cohort analysis. *Lancet* 375(9731):2092–2098.

14. Attia S, Egger M, Müller M, Zwahlen M, Low N (2009) Sexual transmission of HIV according to viral load and antiretroviral therapy: systematic review and meta-analysis. *AIDS* 23(11):1397–1404.

15. Wilson DP (2012) HIV treatment as prevention: natural experiments highlight limits of antiretroviral treatment as HIV prevention. *PLoS Med* 9(7):e1001231.

16. Jia Z, et al. (2013) Antiretroviral therapy to prevent HIV transmission in serodiscordant couples in China (2003–11): a national observational cohort study. *Lancet* 382(9899):1195–1203.

17. Rodger AJ, et al. (2016) Sexual activity without condoms and risk of HIV transmission in serodifferent couples when the HIV-positive partner is using suppressive antiretroviral therapy. *JAMA* 316(2):171–181.

18. Abdool Karim Q, et al. (2010) Effectiveness and safety of tenofovir gel, an antiretroviral microbicide, for the prevention of HIV infection in women. *Science* 329(5996):1168–1174.

19. Hindmarsh AC. Brief description of ODEPACK: a systematized collection of ODE solvers. Available at http://www.netlib.org/odepack/opkd-sum. Accessed June 12, 2008.

20. Jones E, Oliphant T, Peterson P, et al. SciPy: Open source scientific tools for Python. Available at https://www.scipy.org/. Accessed August 20, 2016.

21. The World Bank. Health nutrition and population statistics: population estimates and projections | World DataBank. Available at http://databank.worldbank.org/data/reports.aspx?source=health-nutrition-and-population-statistics:-population-estimates-and-projections. Accessed July 11, 2016.

22. UNAIDS. AIDSinfo | UNAIDS. Available at http://aidsinfo.unaids.org/. Accessed June 28, 2016.

23. UNAIDS. Countries | UNAIDS. Available at http://www.unaids.org/en/regionscountries/countries/. Accessed June 28, 2016.

24. HIV/AIDS Asia Pacific Research Statistical Data Information Resources AIDS Data Hub. Country profiles | AIDS, HIV, data, reports, publications. Available at http://www.aidsdatahub.org/Country-Profiles. Accessed June 28, 2016.

25. Holt CC (2004) Forecasting seasonals and trends by exponentially weighted moving averages. *Int J Forecast* 20(1):5–10.

26. Blower SM, Dowlatabadi H (1994) Sensitivity and uncertainty analysis of complex models of disease transmission: an HIV model, as an example. *Int Stat Rev* 62(2):229–243.

27. Shechter SM, Schaefer AJ, Braithwaite RS, Roberts MS (2006) Increasing the efficiency of Monte Carlo cohort simulations with variance reduction techniques. *Med Decis Making* 26(5):550–553.

28. Malcolm DG, Roseboom JH, Clark CE, Fazar W (1959) Application of a technique for research and development program evaluation. *Oper Res* 7(5):646–669.

29. Davis PJ (1972) Gamma function and related functions. *Handbook of Mathematical Functions with Formulas, Graphs, and Mathematical Tables*, eds Abramowitz M, Stegun IA (National Bureau of Standards, Washington, DC), pp 253–266.

30. Gray GE, Laher F, Lazarus E, Ensoli B, Corey L (2016) Approaches to preventative and therapeutic HIV vaccines. *Curr Opin Virol* 17:104–109.

S6 Global, regional, and per-country effectiveness

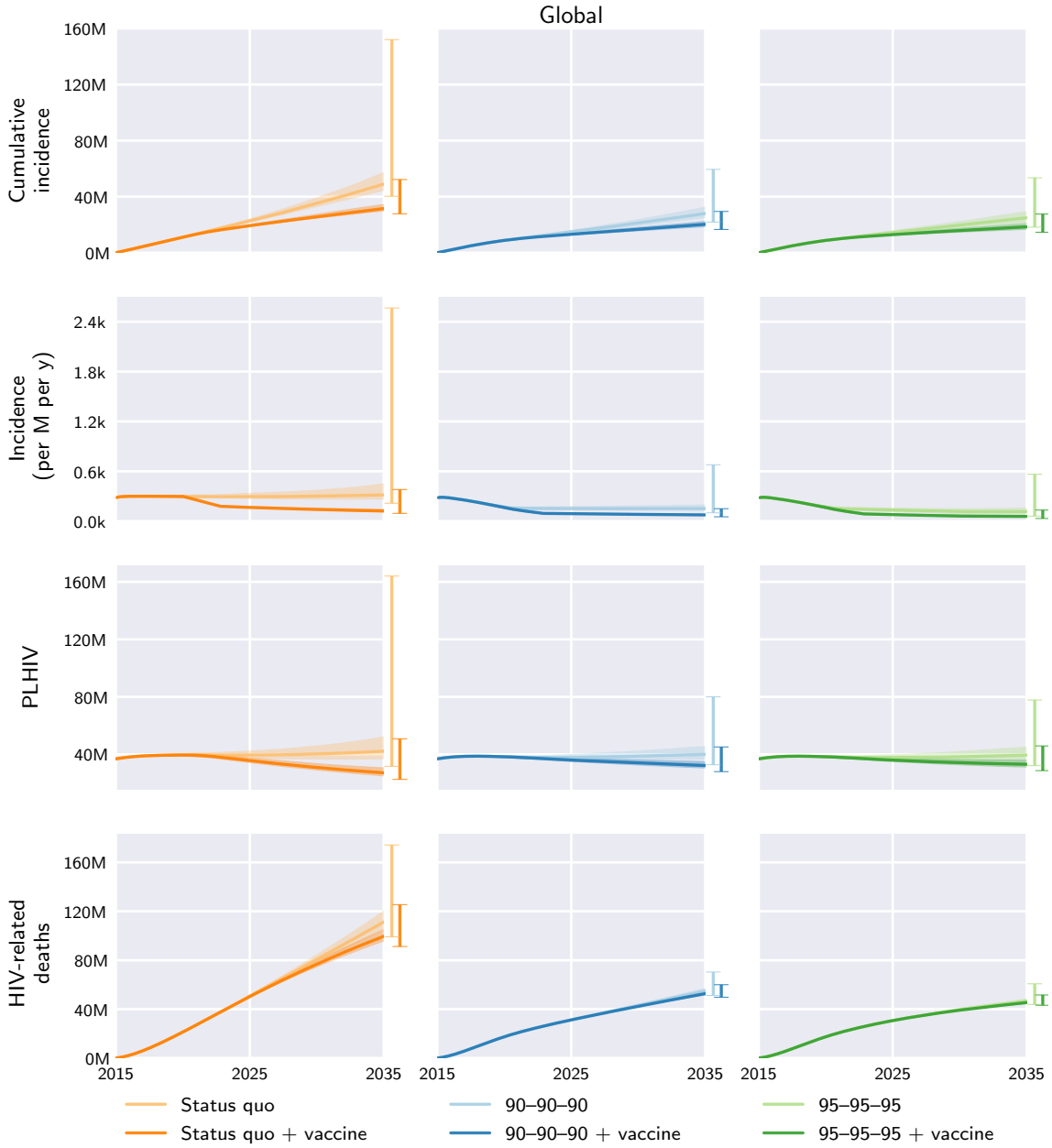

Fig. S4. Global model outcomes under the different diagnosis, treatment, and vaccination scenarios. Central curves show the medians over model runs with 1000 samples from parameter distributions, shaded regions show the 1st and 3rd quartiles (i.e. 25th and 75th percentiles), and vertical bars to the right of each axis show the 5th and 95th percentiles at the end time, 2035. Regional and global outcomes were aggregated from the country-level model outcomes.

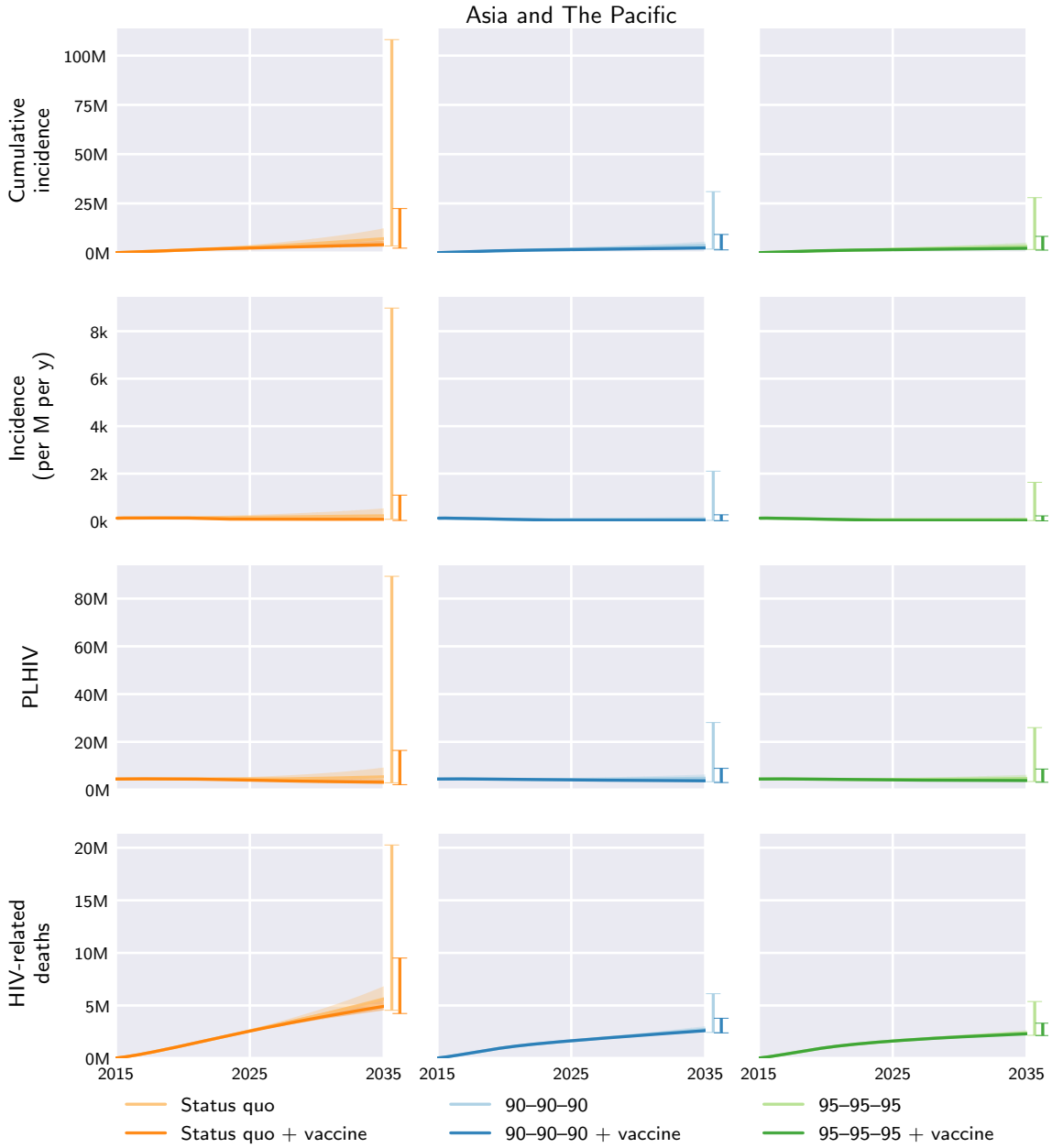

Fig. S5. Asia and The Pacific model outcomes under the different diagnosis, treatment, and vaccination scenarios. Central curves show the medians over model runs with 1000 samples from parameter distributions, shaded regions show the 1st and 3rd quartiles (i.e. 25th and 75th percentiles), and vertical bars to the right of each axis show the 5th and 95th percentiles at the end time, 2035. Regional and global outcomes were aggregated from the country-level model outcomes.

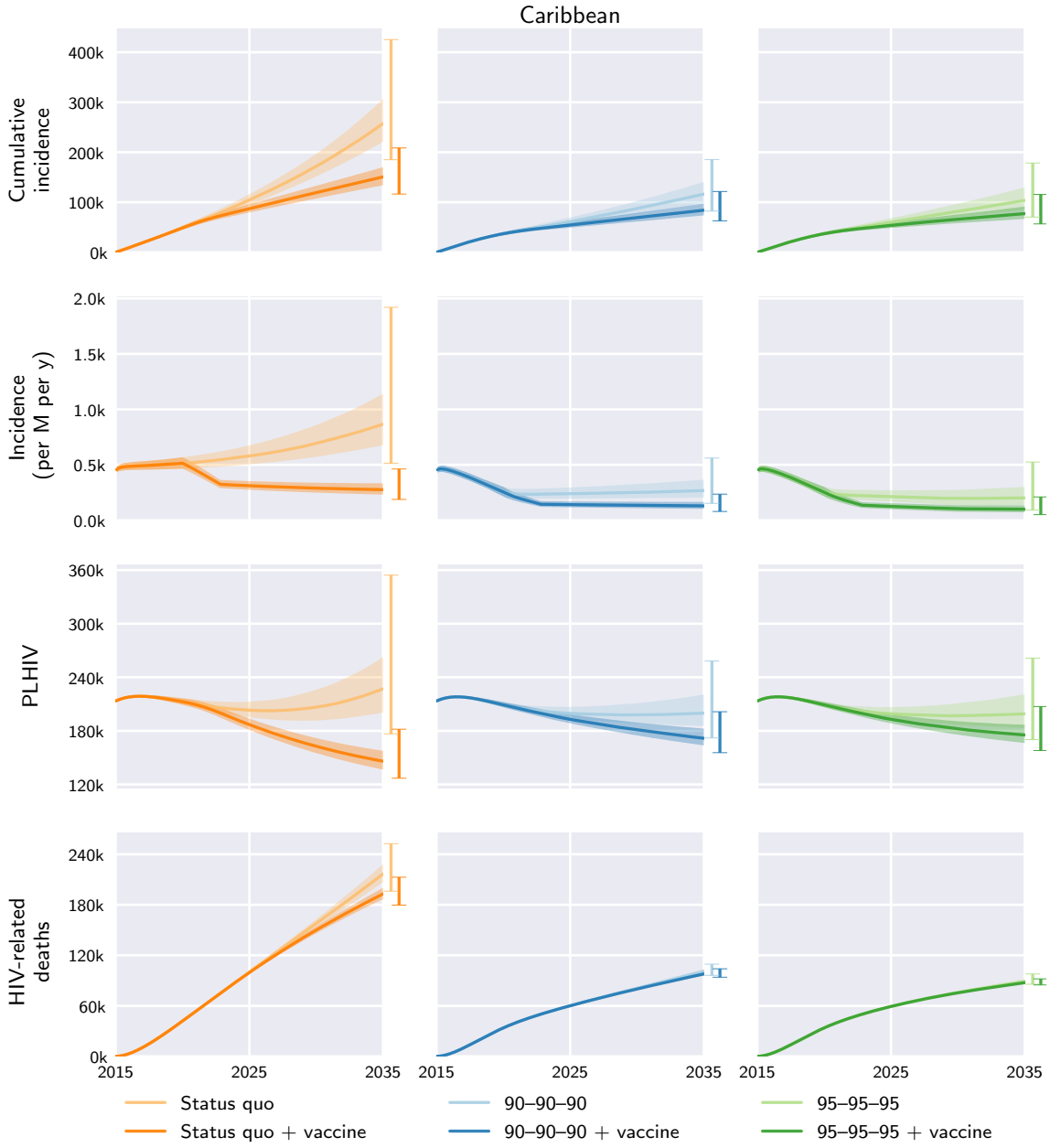

Fig. S6. Caribbean model outcomes under the different diagnosis, treatment, and vaccination scenarios. Central curves show the medians over model runs with 1000 samples from parameter distributions, shaded regions show the 1st and 3rd quartiles (i.e. 25th and 75th percentiles), and vertical bars to the right of each axis show the 5th and 95th percentiles at the end time, 2035. Regional and global outcomes were aggregated from the country-level model outcomes.

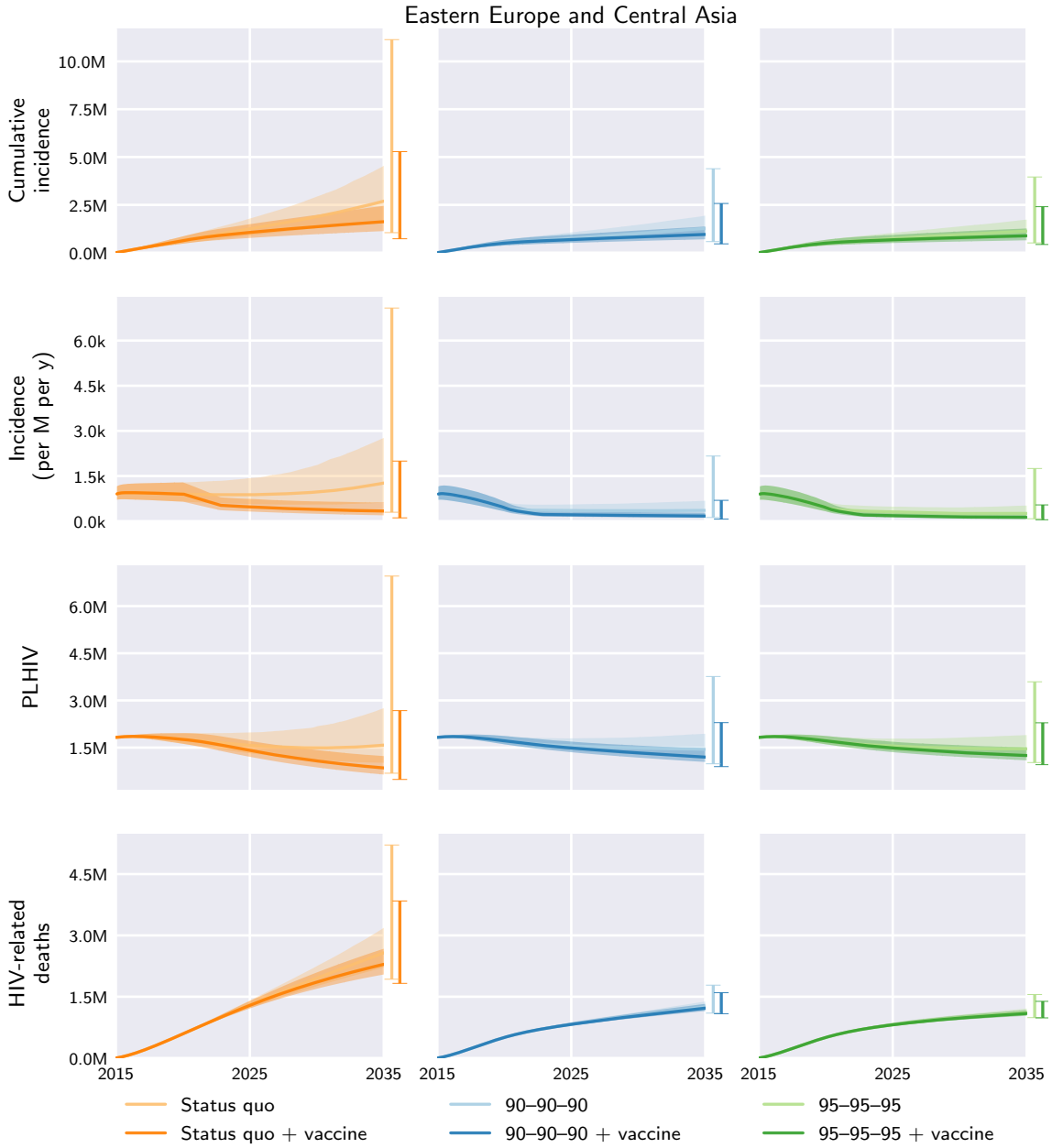

Fig. S7. Eastern Europe and Central Asia model outcomes under the different diagnosis, treatment, and vaccination scenarios. Central curves show the medians over model runs with 1000 samples from parameter distributions, shaded regions show the 1st and 3rd quartiles (i.e. 25th and 75th percentiles), and vertical bars to the right of each axis show the 5th and 95th percentiles at the end time, 2035. Regional and global outcomes were aggregated from the country-level model outcomes.

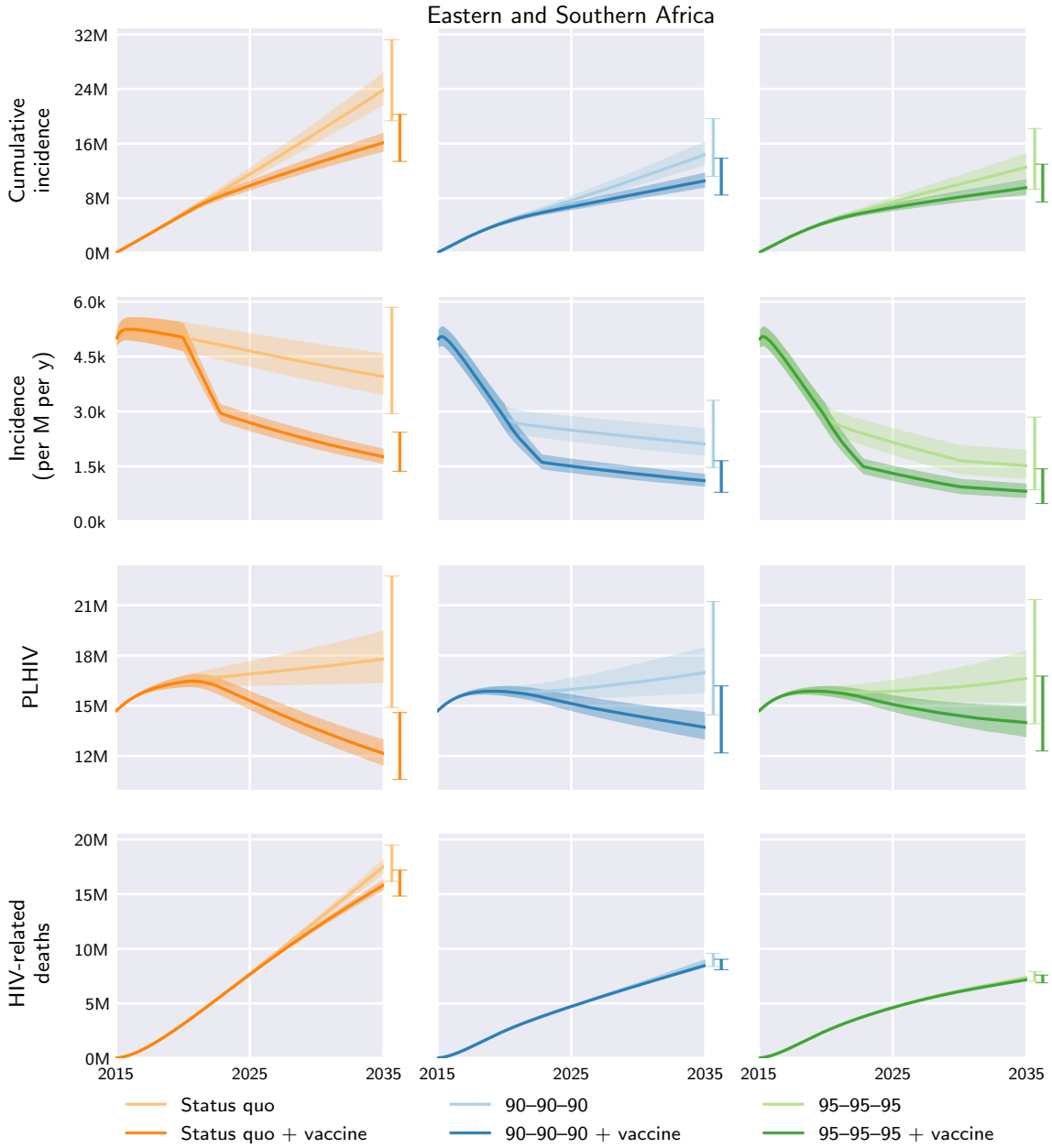

Fig. S8. Eastern and Southern Africa model outcomes under the different diagnosis, treatment, and vaccination scenarios. Central curves show the medians over model runs with 1000 samples from parameter distributions, shaded regions show the 1st and 3rd quartiles (i.e. 25th and 75th percentiles), and vertical bars to the right of each axis show the 5th and 95th percentiles at the end time, 2035. Regional and global outcomes were aggregated from the country-level model outcomes.

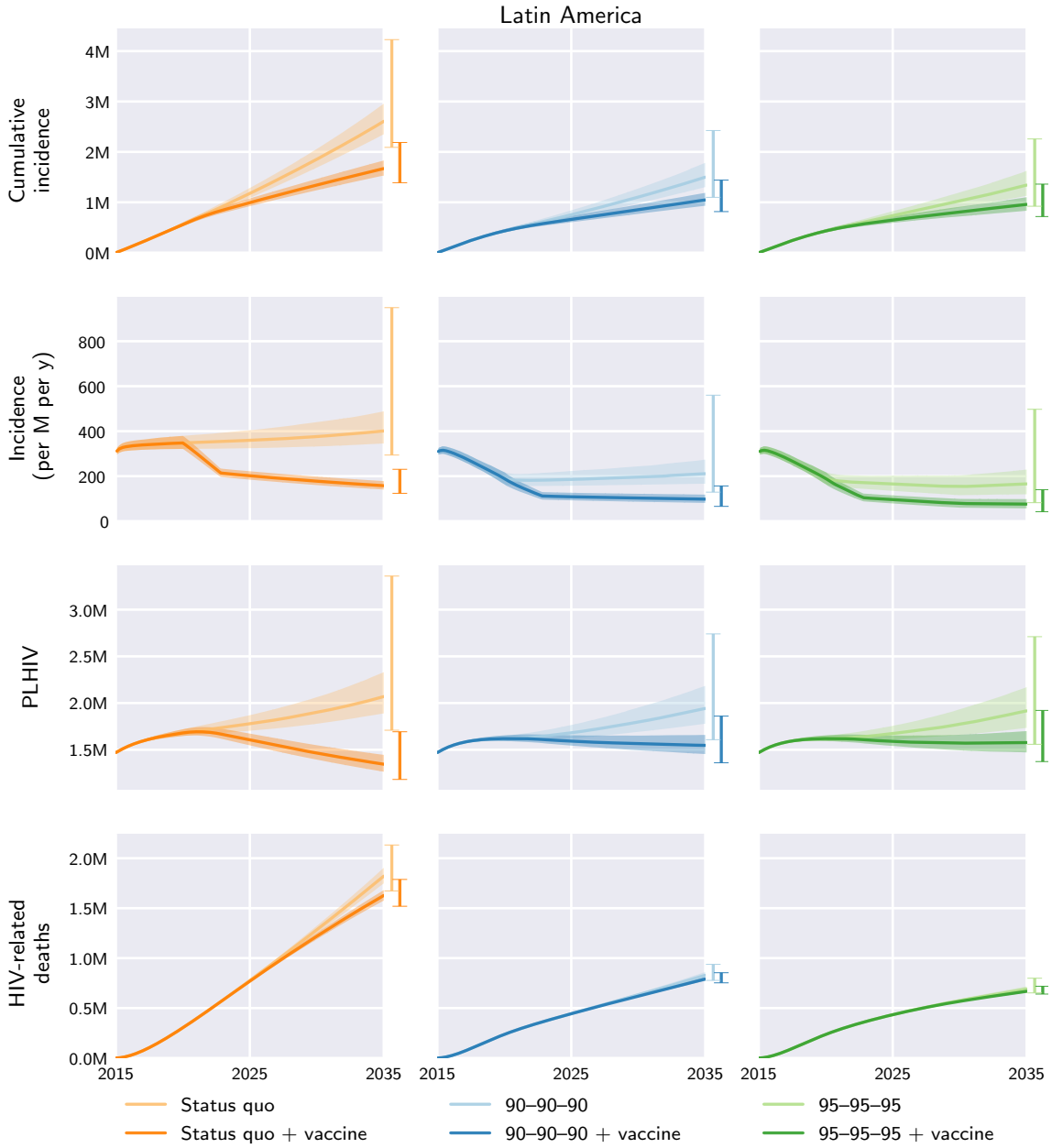

Fig. S9. Latin America model outcomes under the different diagnosis, treatment, and vaccination scenarios. Central curves show the medians over model runs with 1000 samples from parameter distributions, shaded regions show the 1st and 3rd quartiles (i.e. 25th and 75th percentiles), and vertical bars to the right of each axis show the 5th and 95th percentiles at the end time, 2035. Regional and global outcomes were aggregated from the country-level model outcomes.

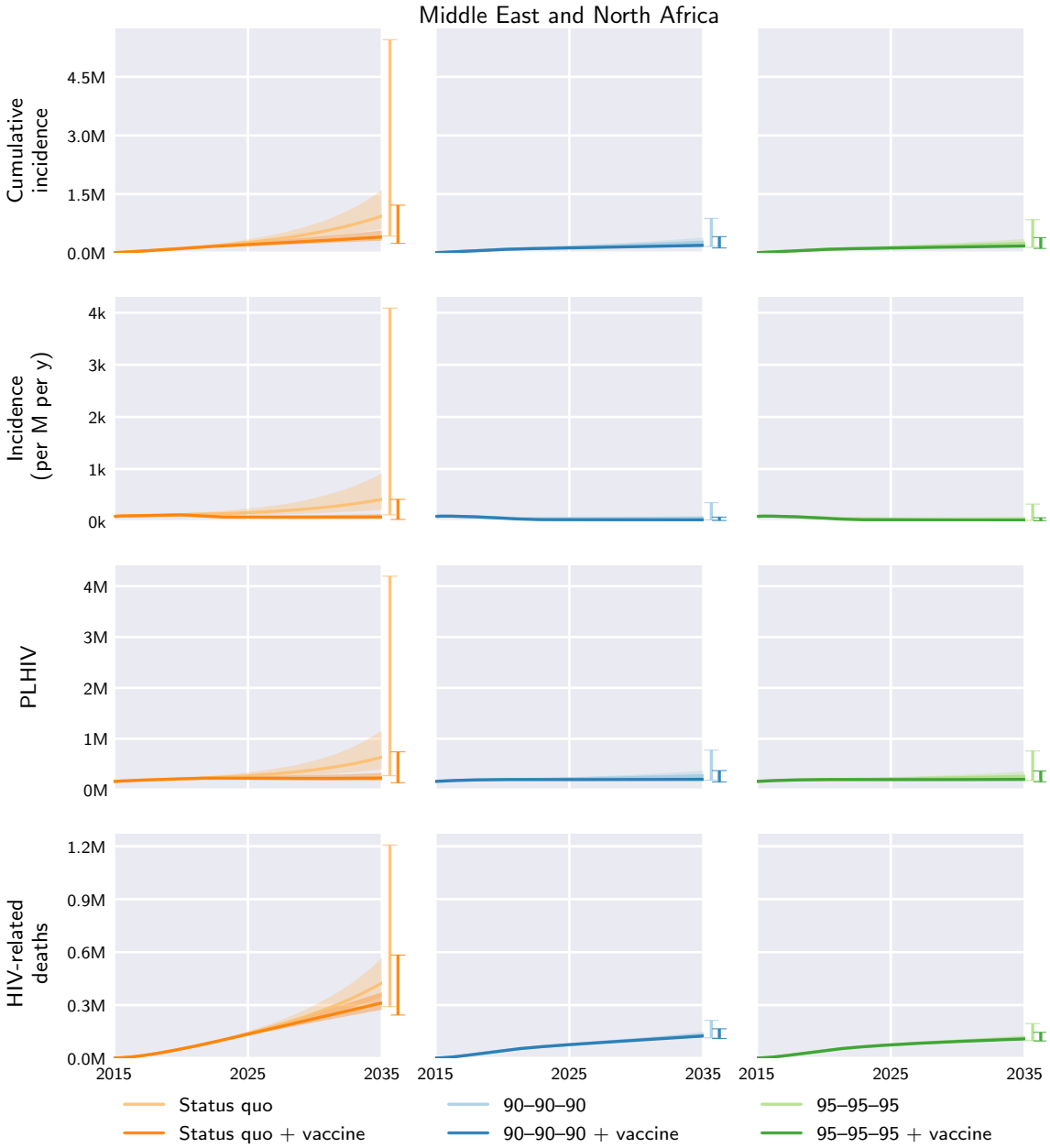

Fig. S10. Middle East and North Africa model outcomes under the different diagnosis, treatment, and vaccination scenarios. Central curves show the medians over model runs with 1000 samples from parameter distributions, shaded regions show the 1st and 3rd quartiles (i.e. 25th and 75th percentiles), and vertical bars to the right of each axis show the 5th and 95th percentiles at the end time, 2035. Regional and global outcomes were aggregated from the country-level model outcomes.

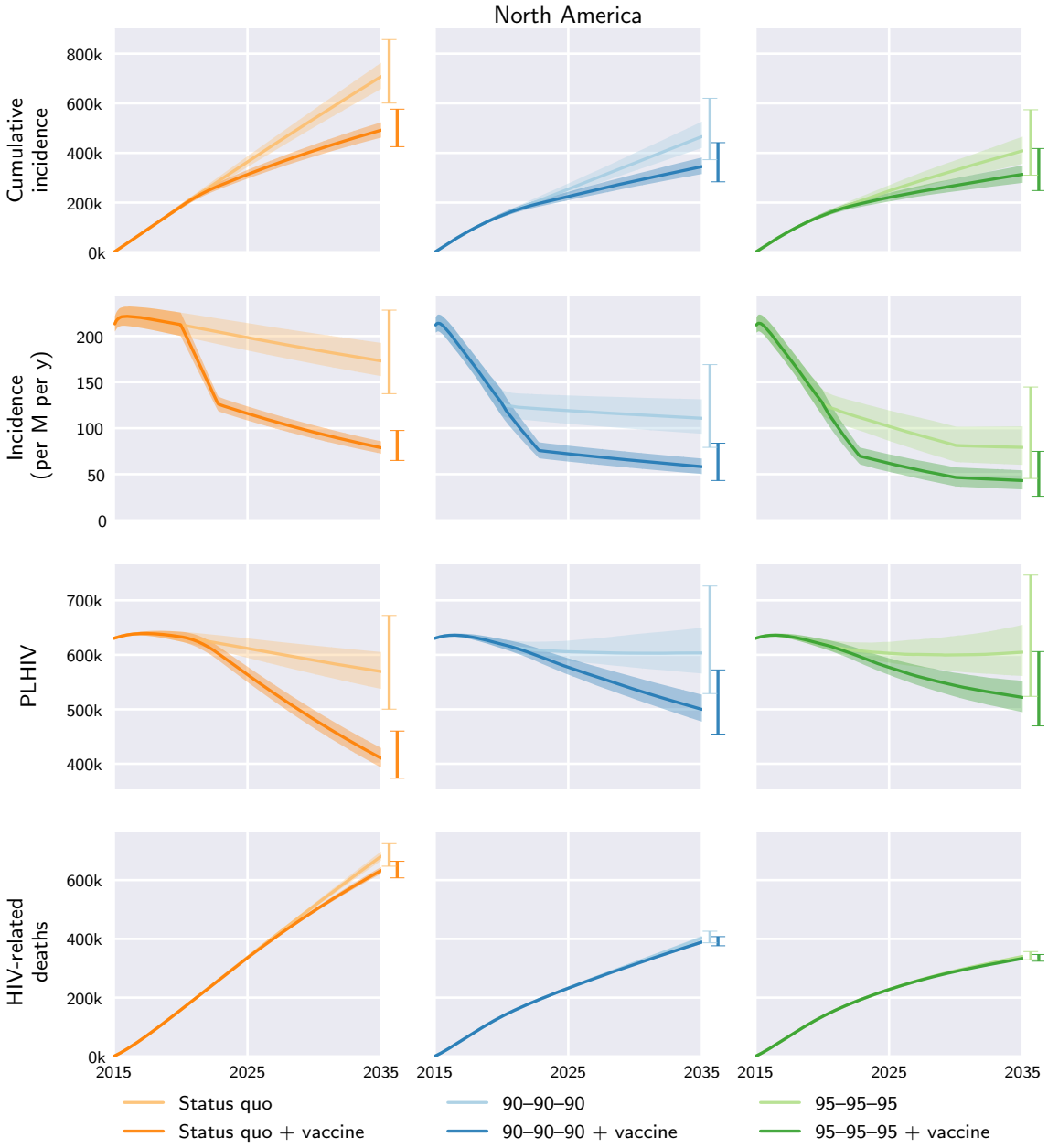

Fig. S11. North America model outcomes under the different diagnosis, treatment, and vaccination scenarios. Central curves show the medians over model runs with 1000 samples from parameter distributions, shaded regions show the 1st and 3rd quartiles (i.e. 25th and 75th percentiles), and vertical bars to the right of each axis show the 5th and 95th percentiles at the end time, 2035. Regional and global outcomes were aggregated from the country-level model outcomes.

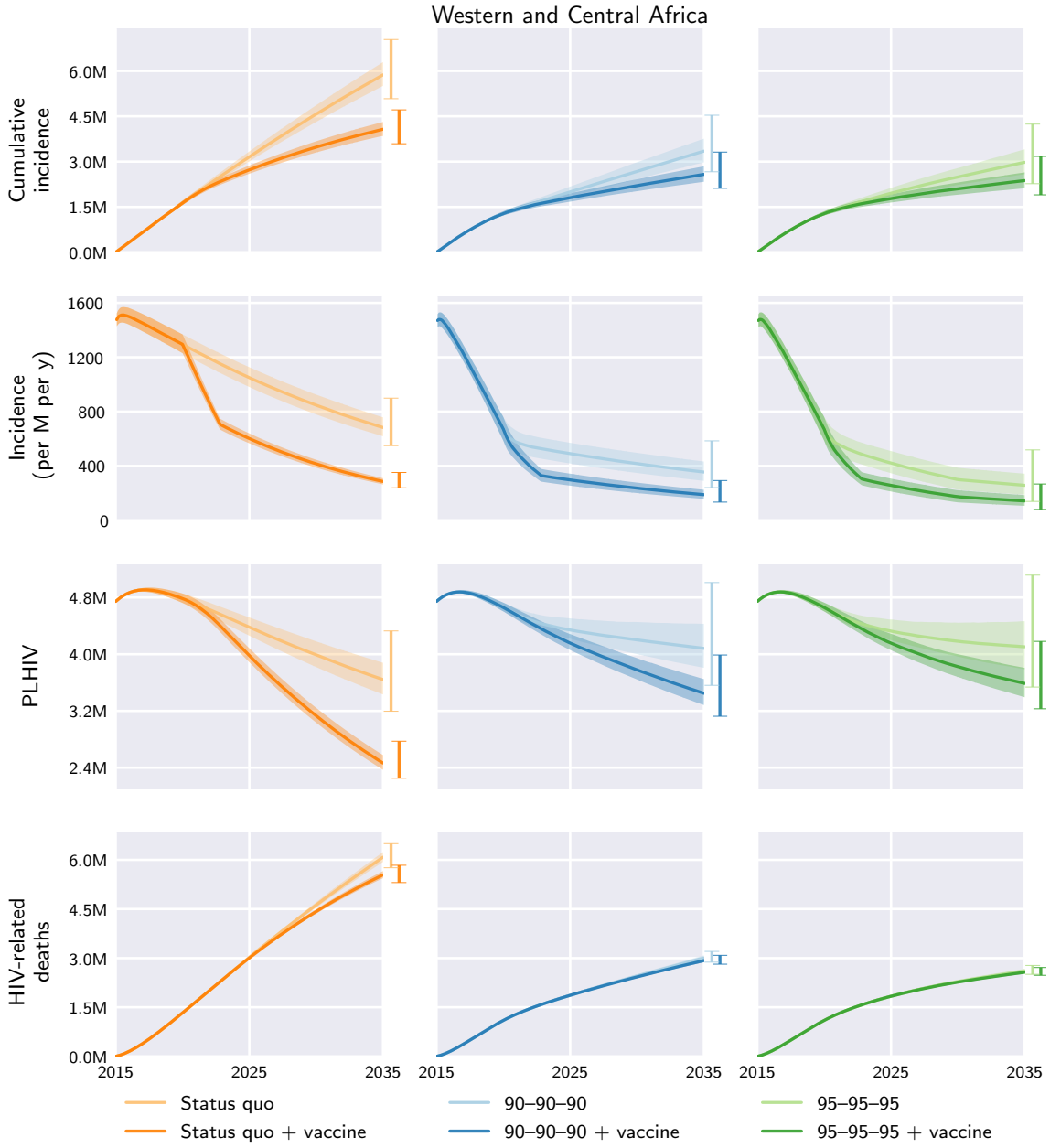

Fig. S12. Western and Central Africa model outcomes under the different diagnosis, treatment, and vaccination scenarios. Central curves show the medians over model runs with 1000 samples from parameter distributions, shaded regions show the 1st and 3rd quartiles (i.e. 25th and 75th percentiles), and vertical bars to the right of each axis show the 5th and 95th percentiles at the end time, 2035. Regional and global outcomes were aggregated from the country-level model outcomes.

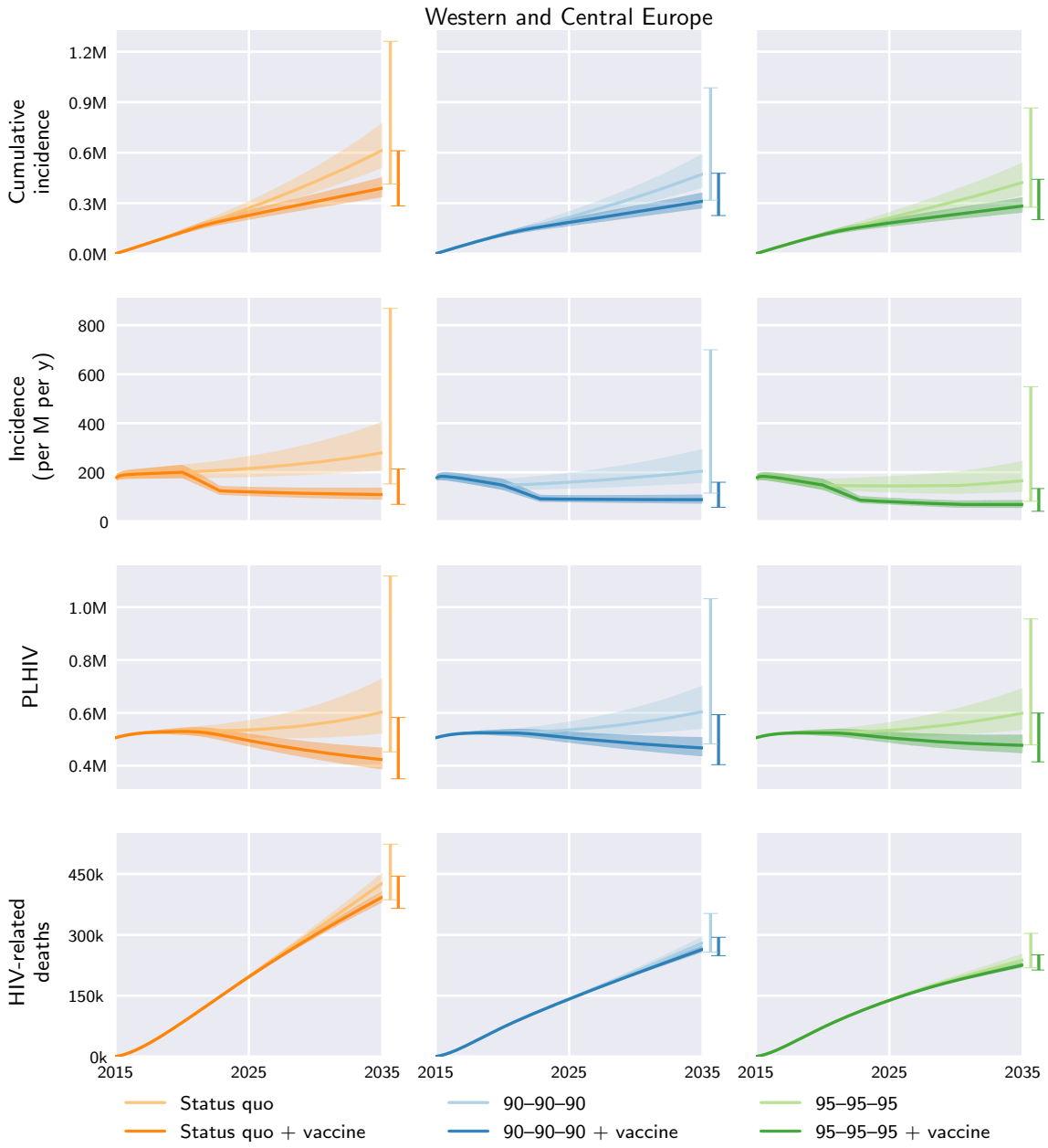

Fig. S13. Western and Central Europe model outcomes under the different diagnosis, treatment, and vaccination scenarios. Central curves show the medians over model runs with 1000 samples from parameter distributions, shaded regions show the 1st and 3rd quartiles (i.e. 25th and 75th percentiles), and vertical bars to the right of each axis show the 5th and 95th percentiles at the end time, 2035. Regional and global outcomes were aggregated from the country-level model outcomes.

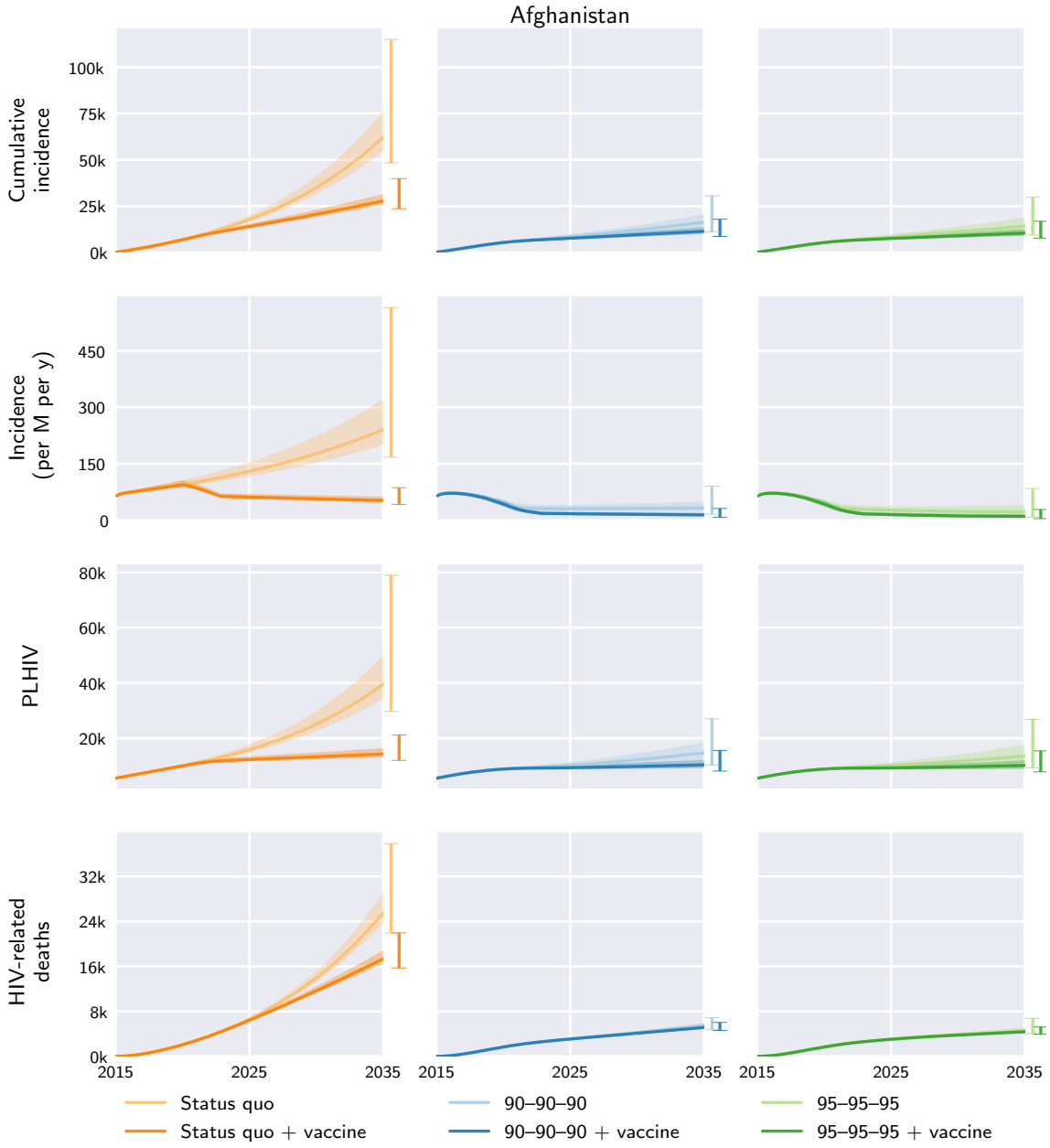

Fig. S14. Afghanistan model outcomes under the different diagnosis, treatment, and vaccination scenarios. Central curves show the medians over model runs with 1000 samples from parameter distributions, shaded regions show the 1st and 3rd quartiles (i.e. 25th and 75th percentiles), and vertical bars to the right of each axis show the 5th and 95th percentiles at the end time, 2035. Regional and global outcomes were aggregated from the country-level model outcomes.

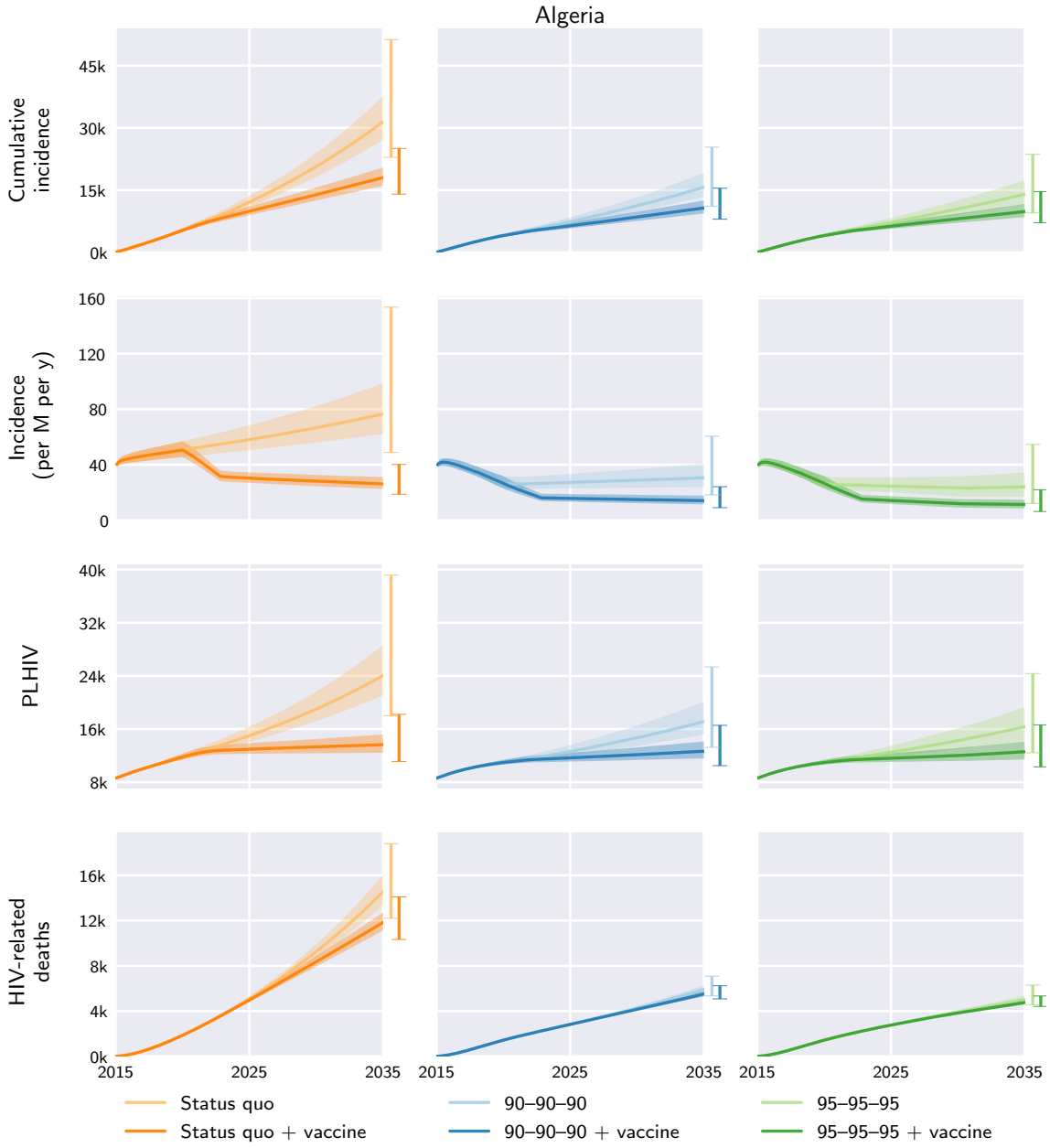

Fig. S15. Algeria model outcomes under the different diagnosis, treatment, and vaccination scenarios. Central curves show the medians over model runs with 1000 samples from parameter distributions, shaded regions show the 1st and 3rd quartiles (i.e. 25th and 75th percentiles), and vertical bars to the right of each axis show the 5th and 95th percentiles at the end time, 2035. Regional and global outcomes were aggregated from the country-level model outcomes.

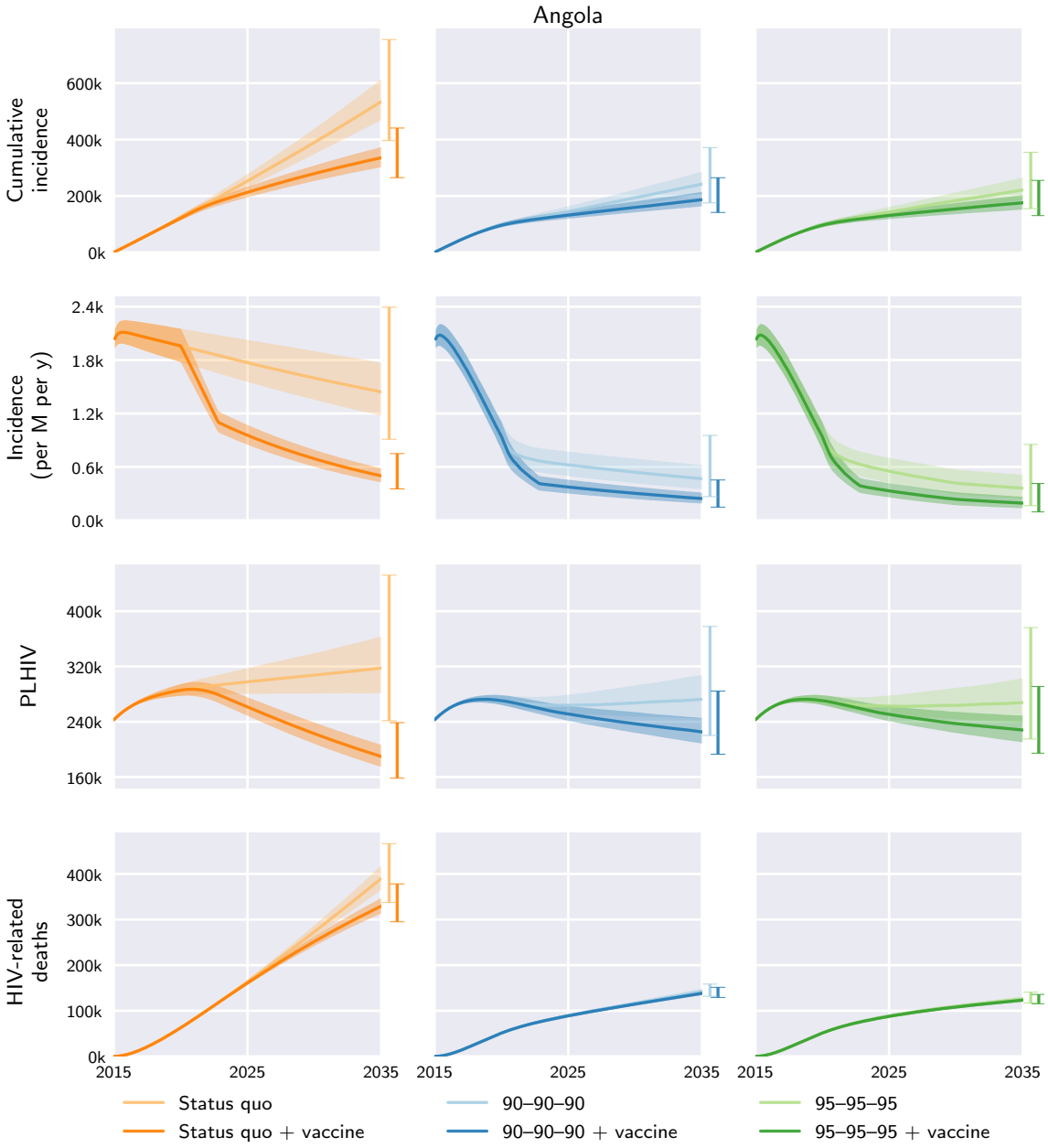

Fig. S16. Angola model outcomes under the different diagnosis, treatment, and vaccination scenarios. Central curves show the medians over model runs with 1000 samples from parameter distributions, shaded regions show the 1st and 3rd quartiles (i.e. 25th and 75th percentiles), and vertical bars to the right of each axis show the 5th and 95th percentiles at the end time, 2035. Regional and global outcomes were aggregated from the country-level model outcomes.

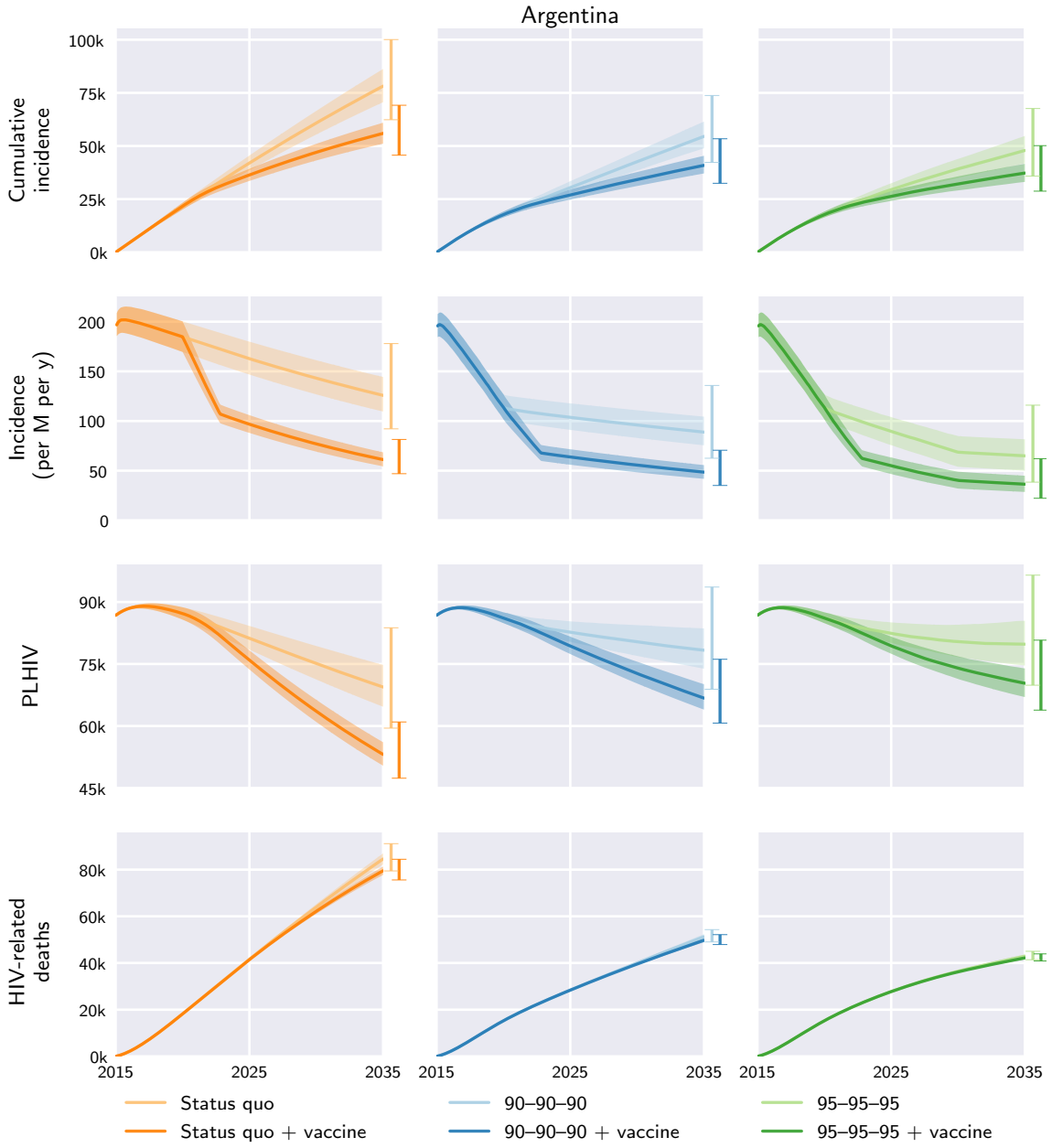

Fig. S17. Argentina model outcomes under the different diagnosis, treatment, and vaccination scenarios. Central curves show the medians over model runs with 1000 samples from parameter distributions, shaded regions show the 1st and 3rd quartiles (i.e. 25th and 75th percentiles), and vertical bars to the right of each axis show the 5th and 95th percentiles at the end time, 2035. Regional and global outcomes were aggregated from the country-level model outcomes.

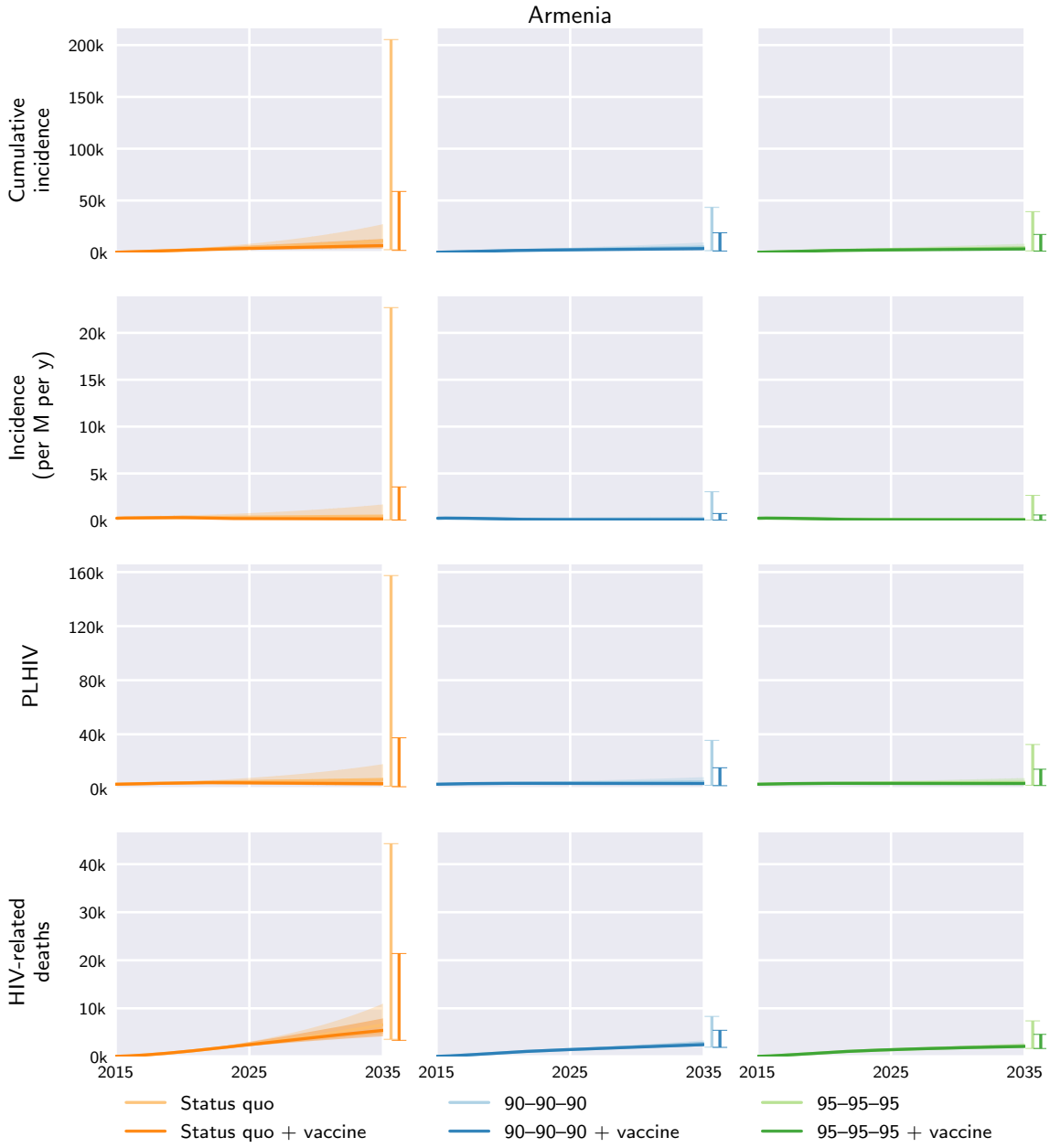

Fig. S18. Armenia model outcomes under the different diagnosis, treatment, and vaccination scenarios. Central curves show the medians over model runs with 1000 samples from parameter distributions, shaded regions show the 1st and 3rd quartiles (i.e. 25th and 75th percentiles), and vertical bars to the right of each axis show the 5th and 95th percentiles at the end time, 2035. Regional and global outcomes were aggregated from the country-level model outcomes.

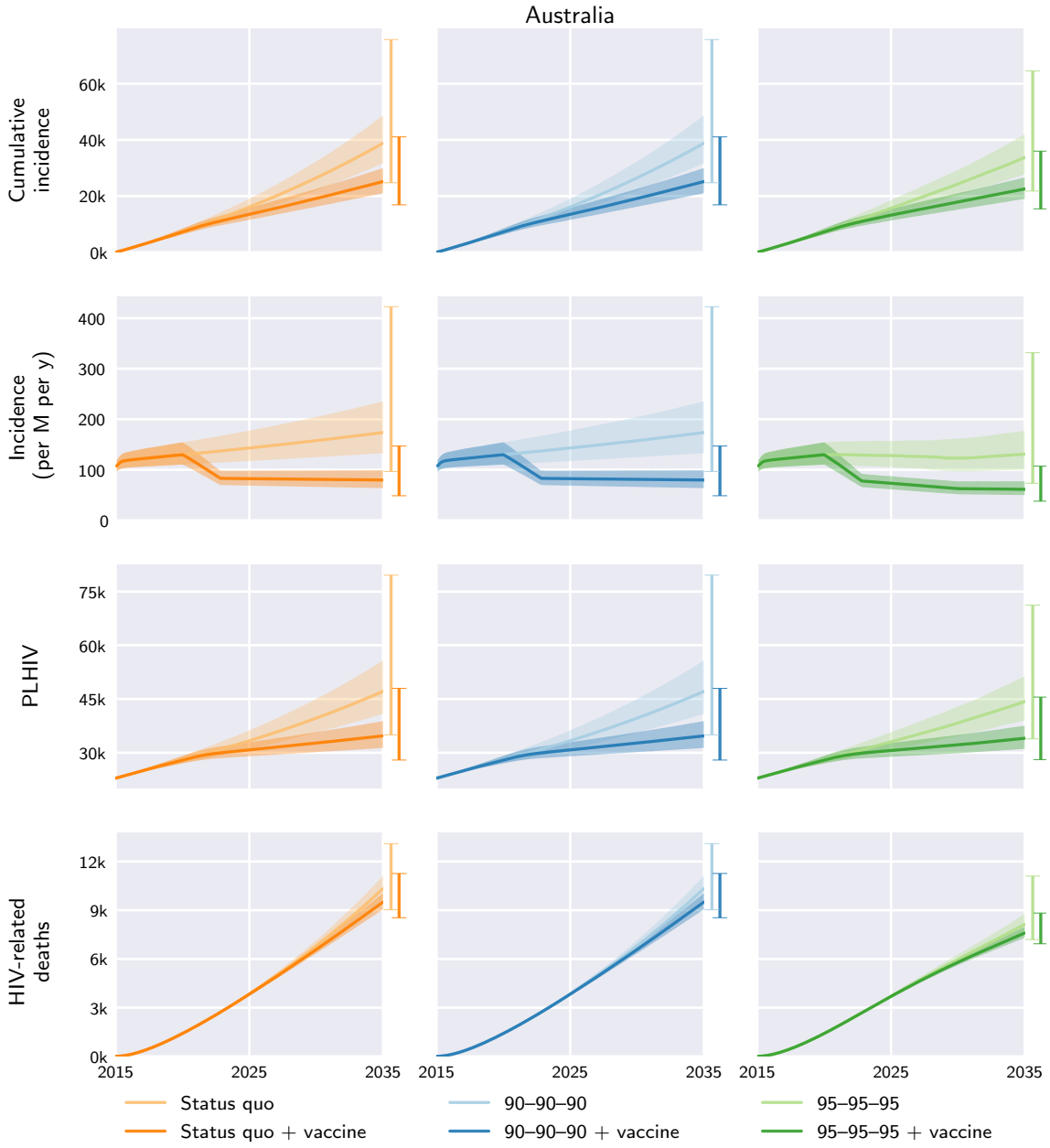

Fig. S19. Australia model outcomes under the different diagnosis, treatment, and vaccination scenarios. Central curves show the medians over model runs with 1000 samples from parameter distributions, shaded regions show the 1st and 3rd quartiles (i.e. 25th and 75th percentiles), and vertical bars to the right of each axis show the 5th and 95th percentiles at the end time, 2035. Regional and global outcomes were aggregated from the country-level model outcomes.

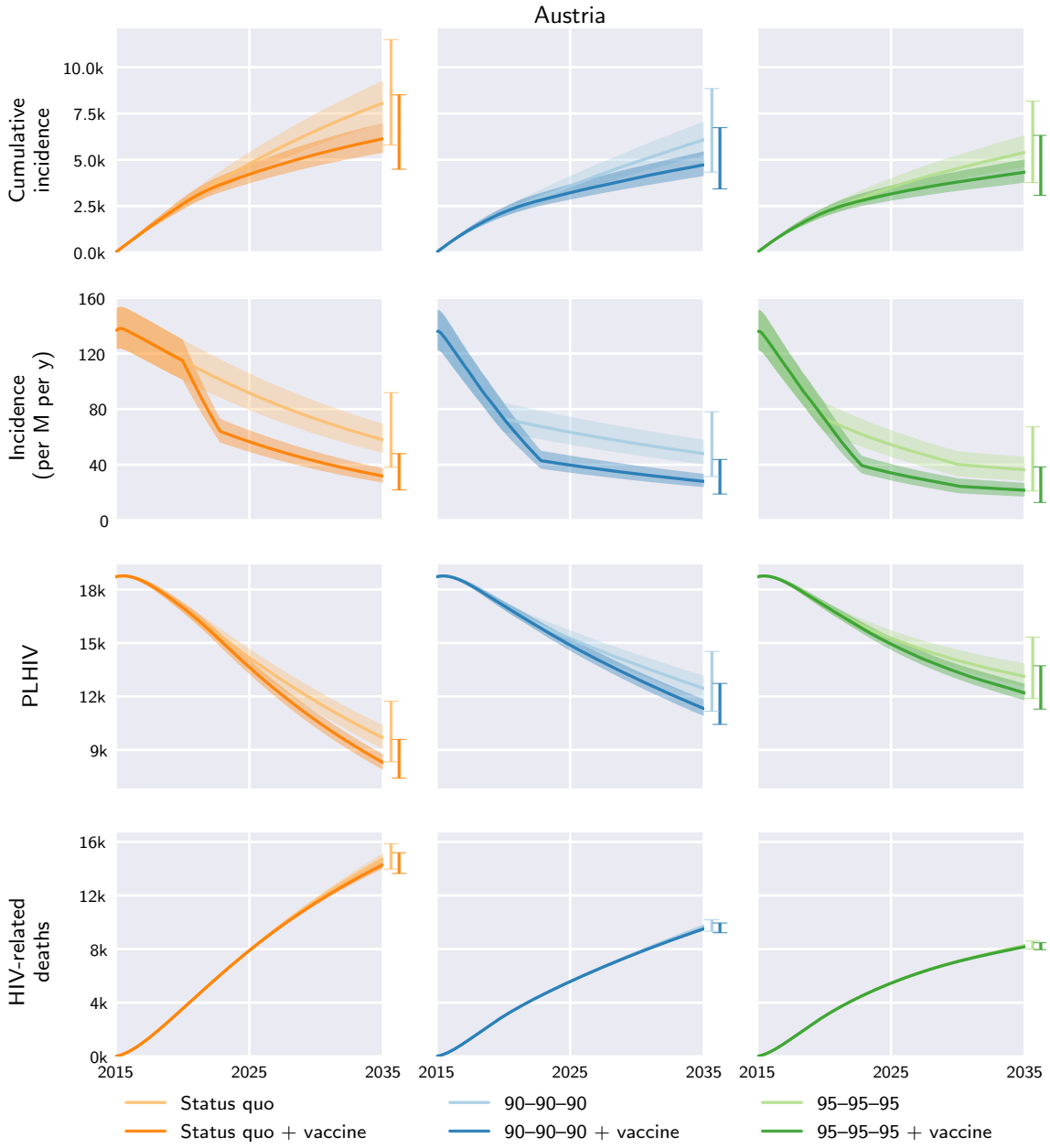

Fig. S20. Austria model outcomes under the different diagnosis, treatment, and vaccination scenarios. Central curves show the medians over model runs with 1000 samples from parameter distributions, shaded regions show the 1st and 3rd quartiles (i.e. 25th and 75th percentiles), and vertical bars to the right of each axis show the 5th and 95th percentiles at the end time, 2035. Regional and global outcomes were aggregated from the country-level model outcomes.

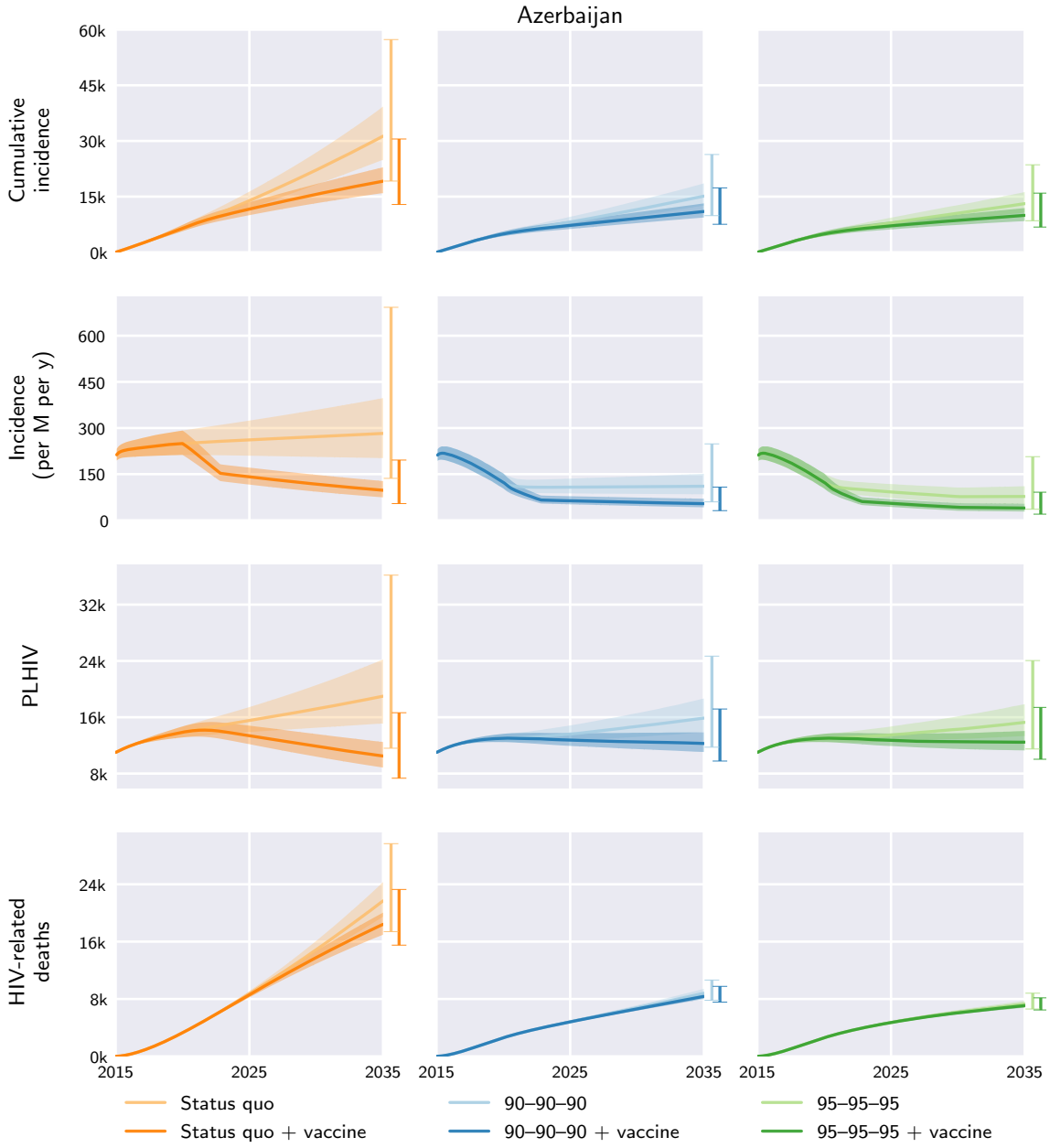

Fig. S21. Azerbaijan model outcomes under the different diagnosis, treatment, and vaccination scenarios. Central curves show the medians over model runs with 1000 samples from parameter distributions, shaded regions show the 1st and 3rd quartiles (i.e. 25th and 75th percentiles), and vertical bars to the right of each axis show the 5th and 95th percentiles at the end time, 2035. Regional and global outcomes were aggregated from the country-level model outcomes.

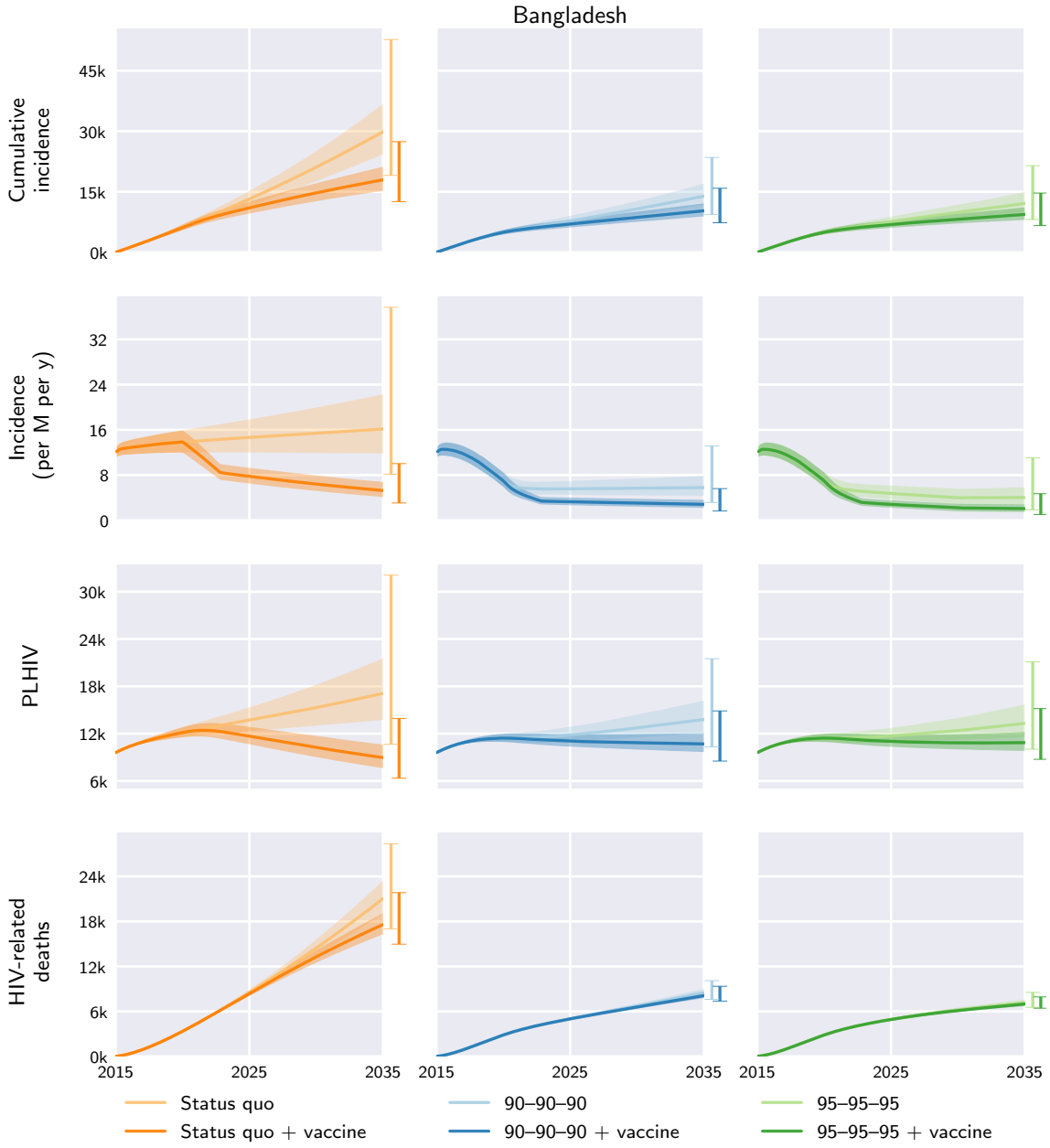

Fig. S22. Bangladesh model outcomes under the different diagnosis, treatment, and vaccination scenarios. Central curves show the medians over model runs with 1000 samples from parameter distributions, shaded regions show the 1st and 3rd quartiles (i.e. 25th and 75th percentiles), and vertical bars to the right of each axis show the 5th and 95th percentiles at the end time, 2035. Regional and global outcomes were aggregated from the country-level model outcomes.

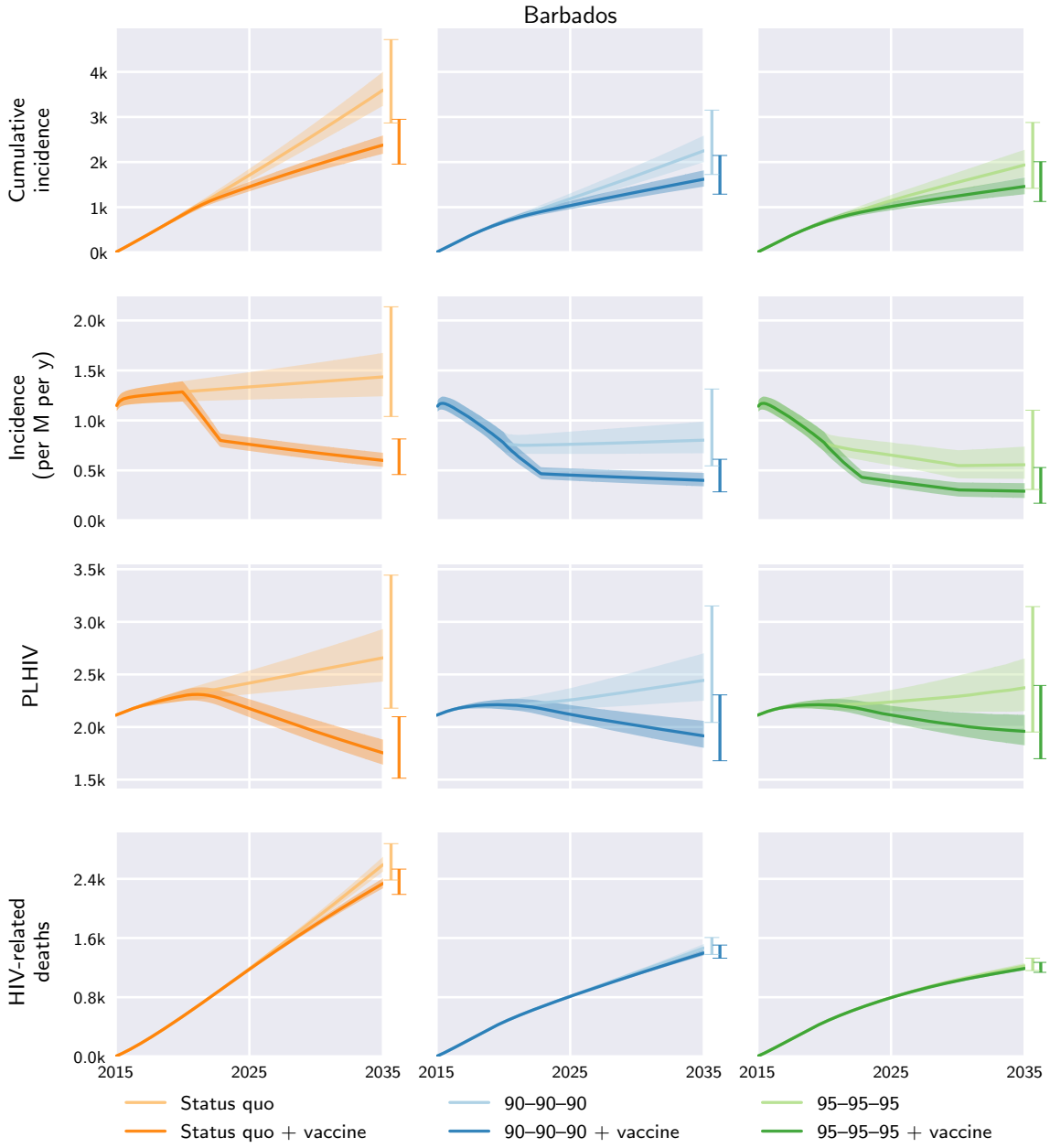

Fig. S23. Barbados model outcomes under the different diagnosis, treatment, and vaccination scenarios. Central curves show the medians over model runs with 1000 samples from parameter distributions, shaded regions show the 1st and 3rd quartiles (i.e. 25th and 75th percentiles), and vertical bars to the right of each axis show the 5th and 95th percentiles at the end time, 2035. Regional and global outcomes were aggregated from the country-level model outcomes.

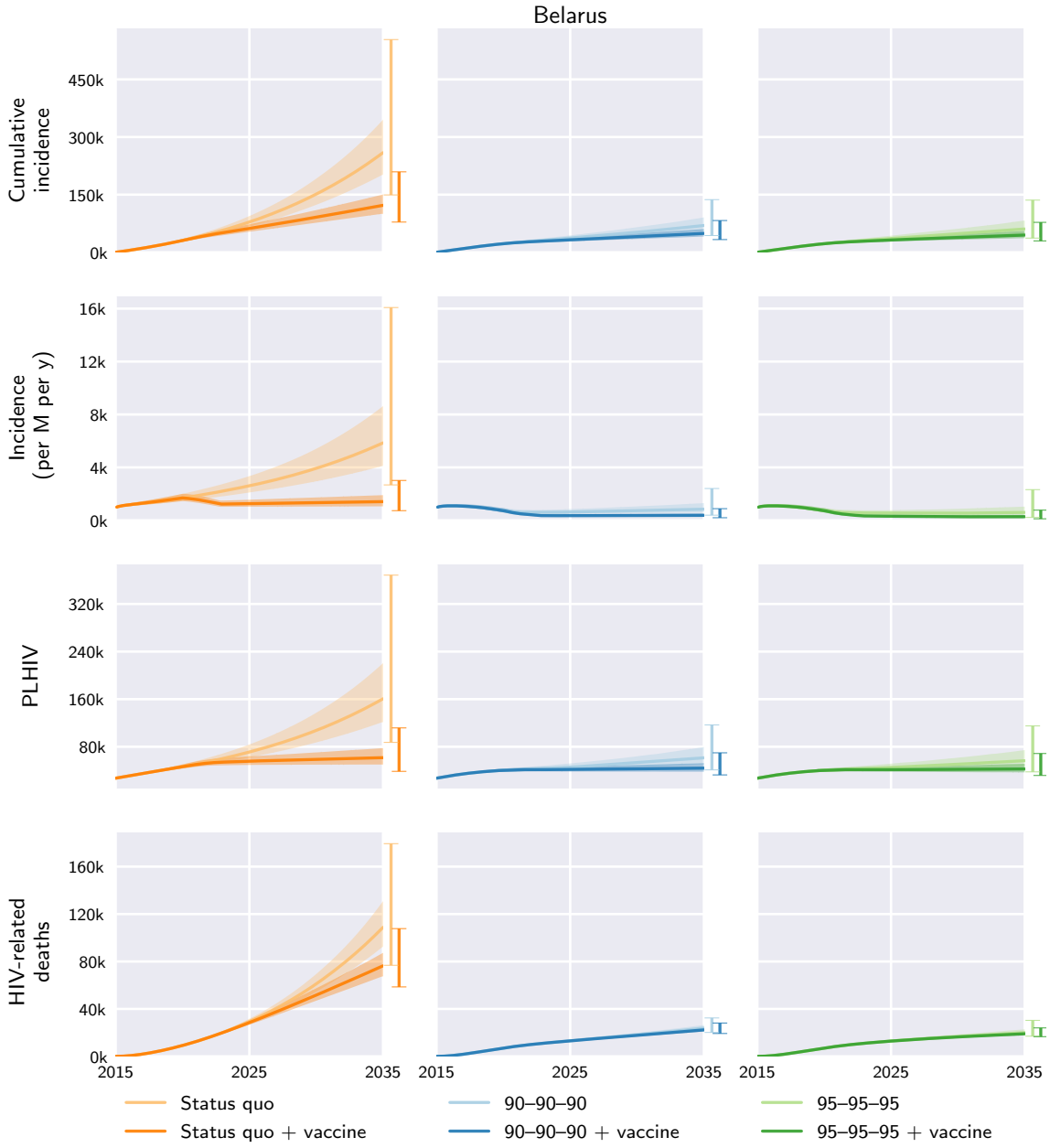

Fig. S24. Belarus model outcomes under the different diagnosis, treatment, and vaccination scenarios. Central curves show the medians over model runs with 1000 samples from parameter distributions, shaded regions show the 1st and 3rd quartiles (i.e. 25th and 75th percentiles), and vertical bars to the right of each axis show the 5th and 95th percentiles at the end time, 2035. Regional and global outcomes were aggregated from the country-level model outcomes.

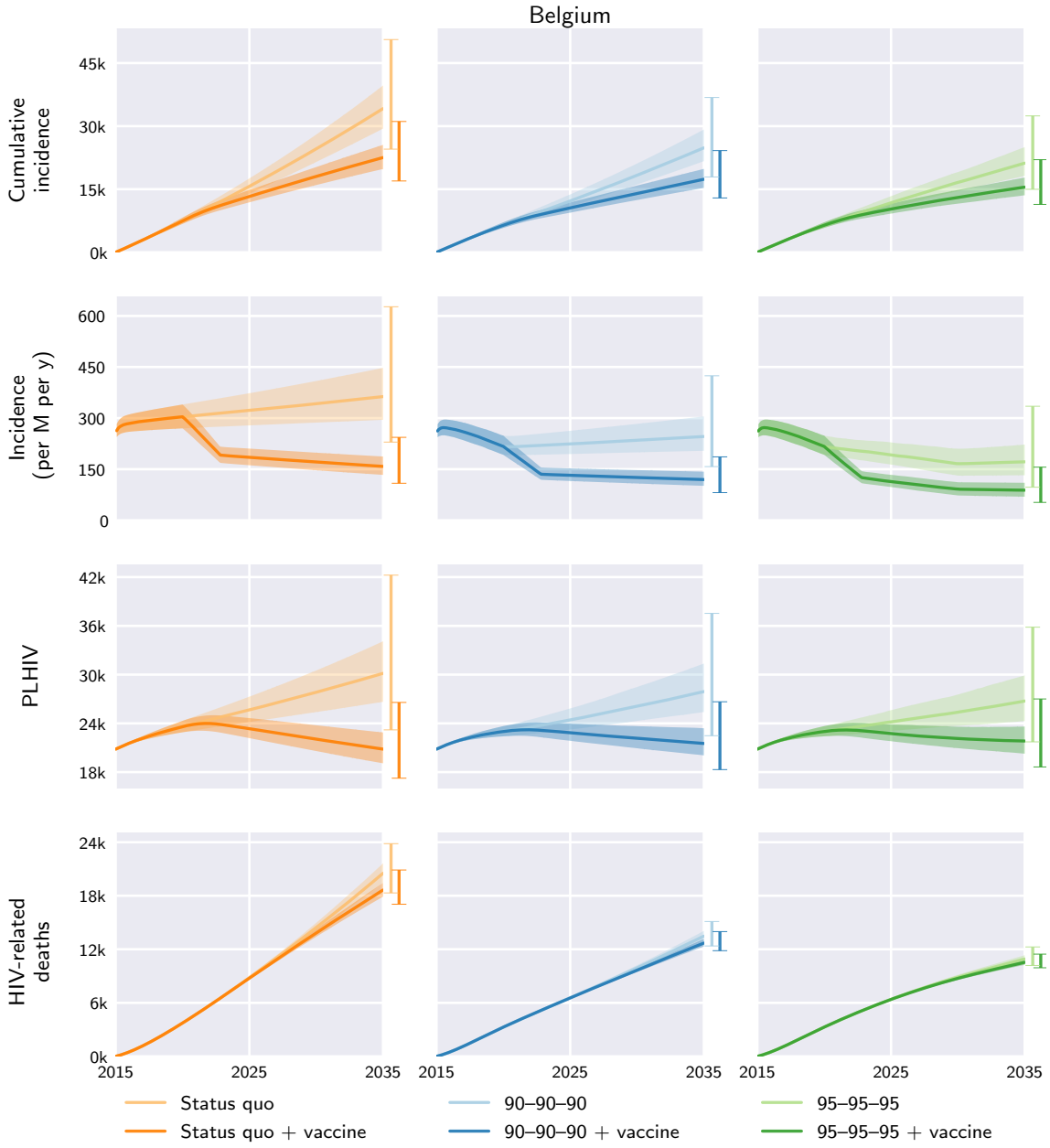

Fig. S25. Belgium model outcomes under the different diagnosis, treatment, and vaccination scenarios. Central curves show the medians over model runs with 1000 samples from parameter distributions, shaded regions show the 1st and 3rd quartiles (i.e. 25th and 75th percentiles), and vertical bars to the right of each axis show the 5th and 95th percentiles at the end time, 2035. Regional and global outcomes were aggregated from the country-level model outcomes.

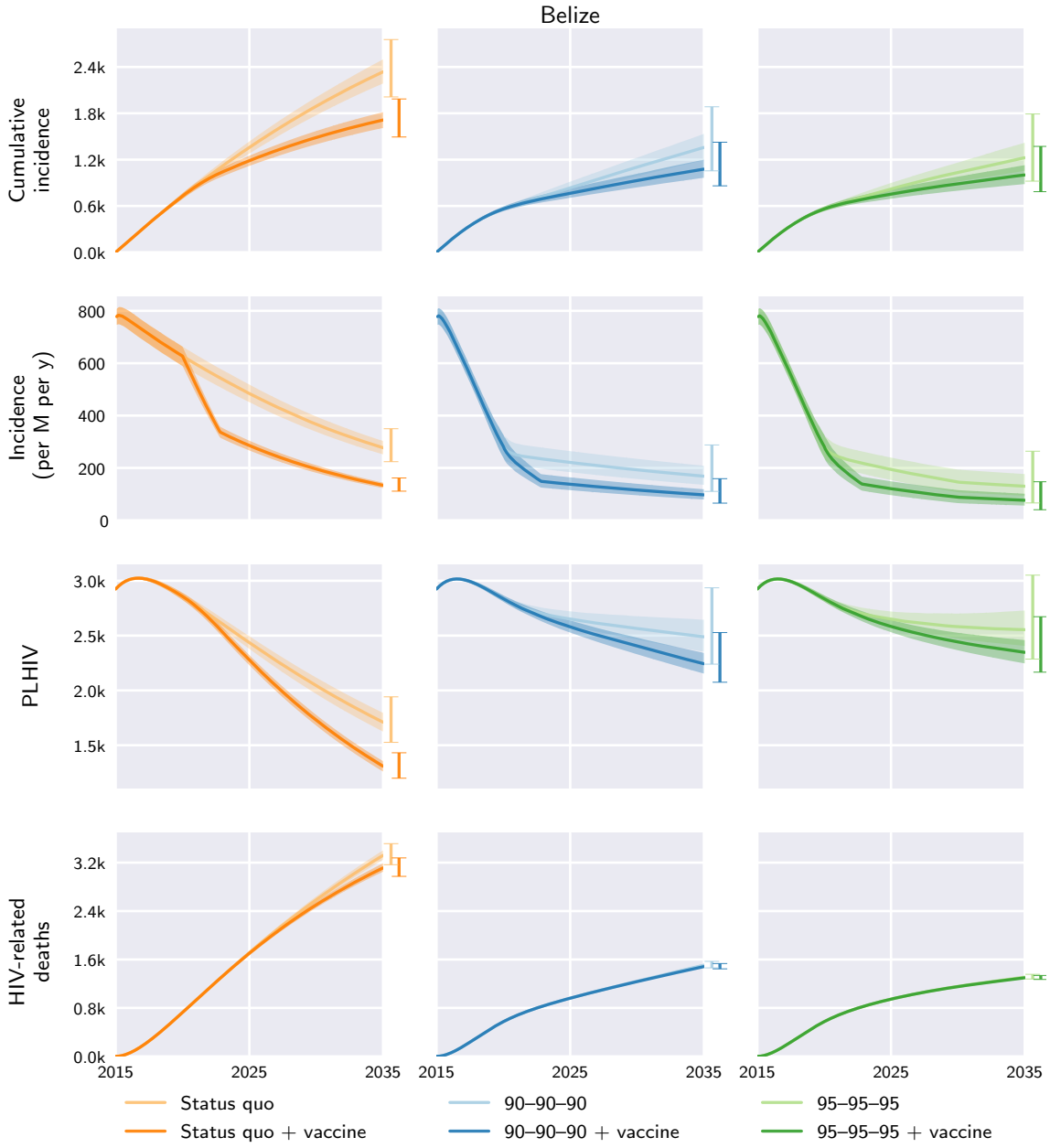

Fig. S26. Belize model outcomes under the different diagnosis, treatment, and vaccination scenarios. Central curves show the medians over model runs with 1000 samples from parameter distributions, shaded regions show the 1st and 3rd quartiles (i.e. 25th and 75th percentiles), and vertical bars to the right of each axis show the 5th and 95th percentiles at the end time, 2035. Regional and global outcomes were aggregated from the country-level model outcomes.

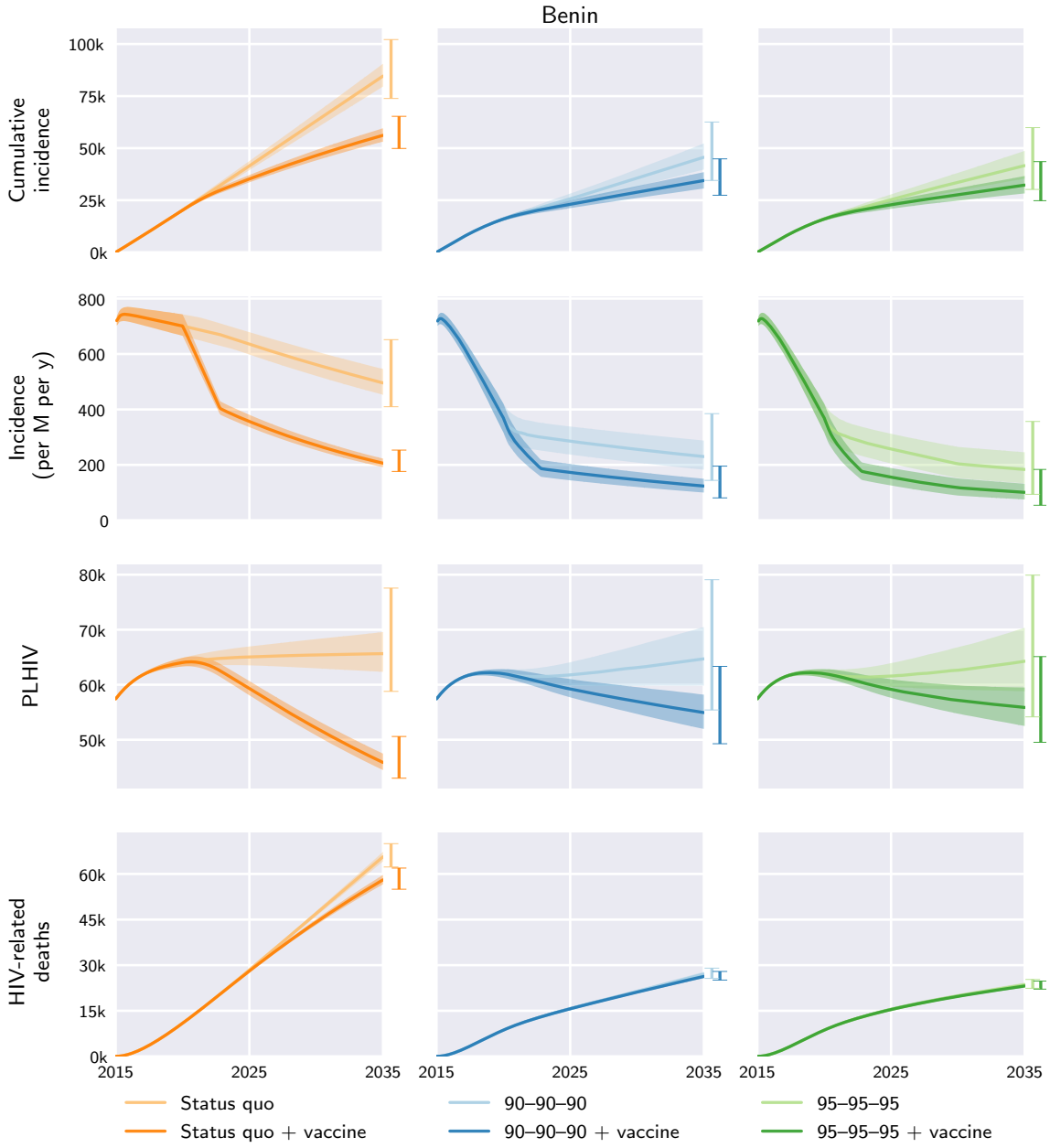

Fig. S27. Benin model outcomes under the different diagnosis, treatment, and vaccination scenarios. Central curves show the medians over model runs with 1000 samples from parameter distributions, shaded regions show the 1st and 3rd quartiles (i.e. 25th and 75th percentiles), and vertical bars to the right of each axis show the 5th and 95th percentiles at the end time, 2035. Regional and global outcomes were aggregated from the country-level model outcomes.

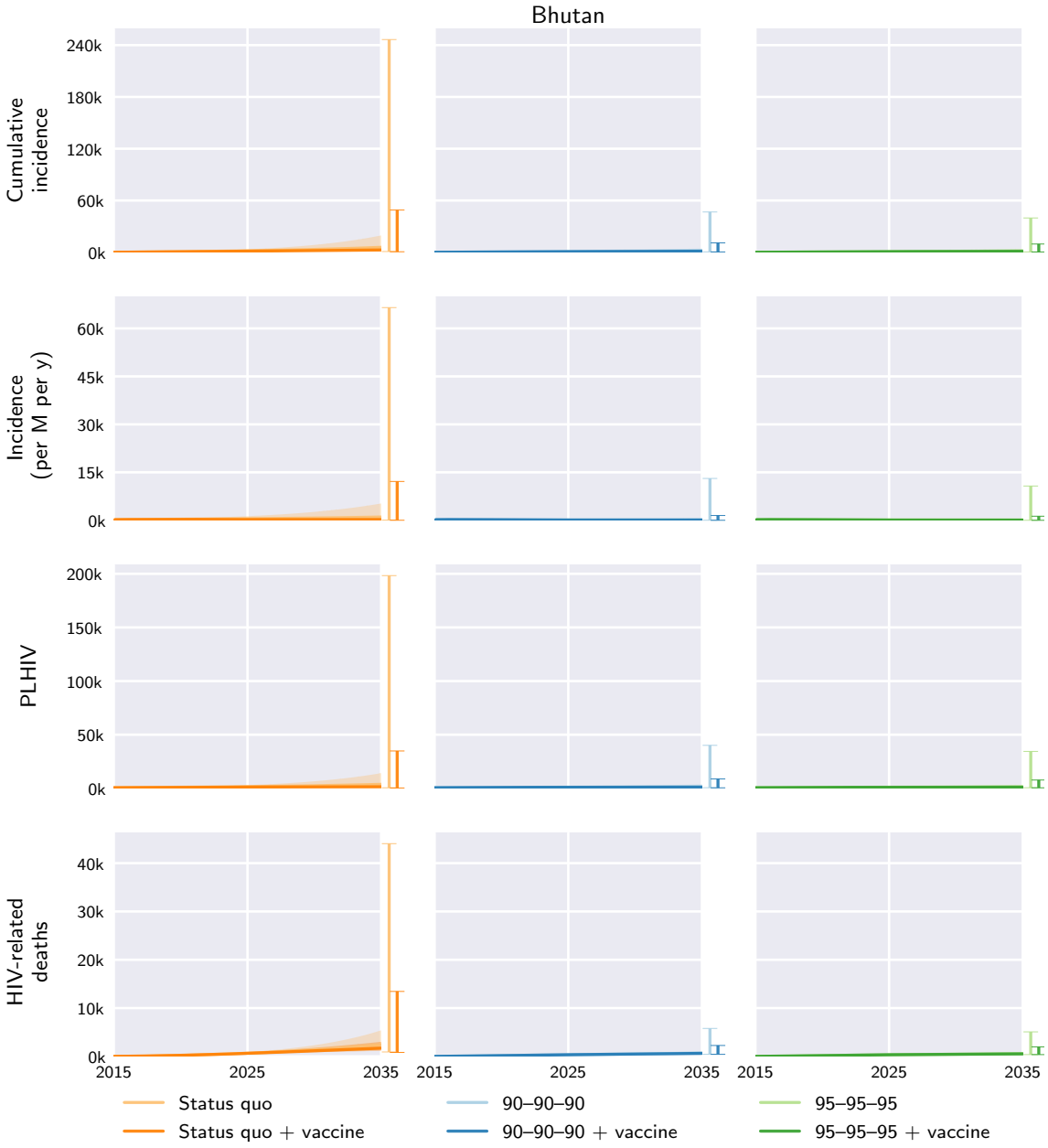

Fig. S28. Bhutan model outcomes under the different diagnosis, treatment, and vaccination scenarios. Central curves show the medians over model runs with 1000 samples from parameter distributions, shaded regions show the 1st and 3rd quartiles (i.e. 25th and 75th percentiles), and vertical bars to the right of each axis show the 5th and 95th percentiles at the end time, 2035. Regional and global outcomes were aggregated from the country-level model outcomes.

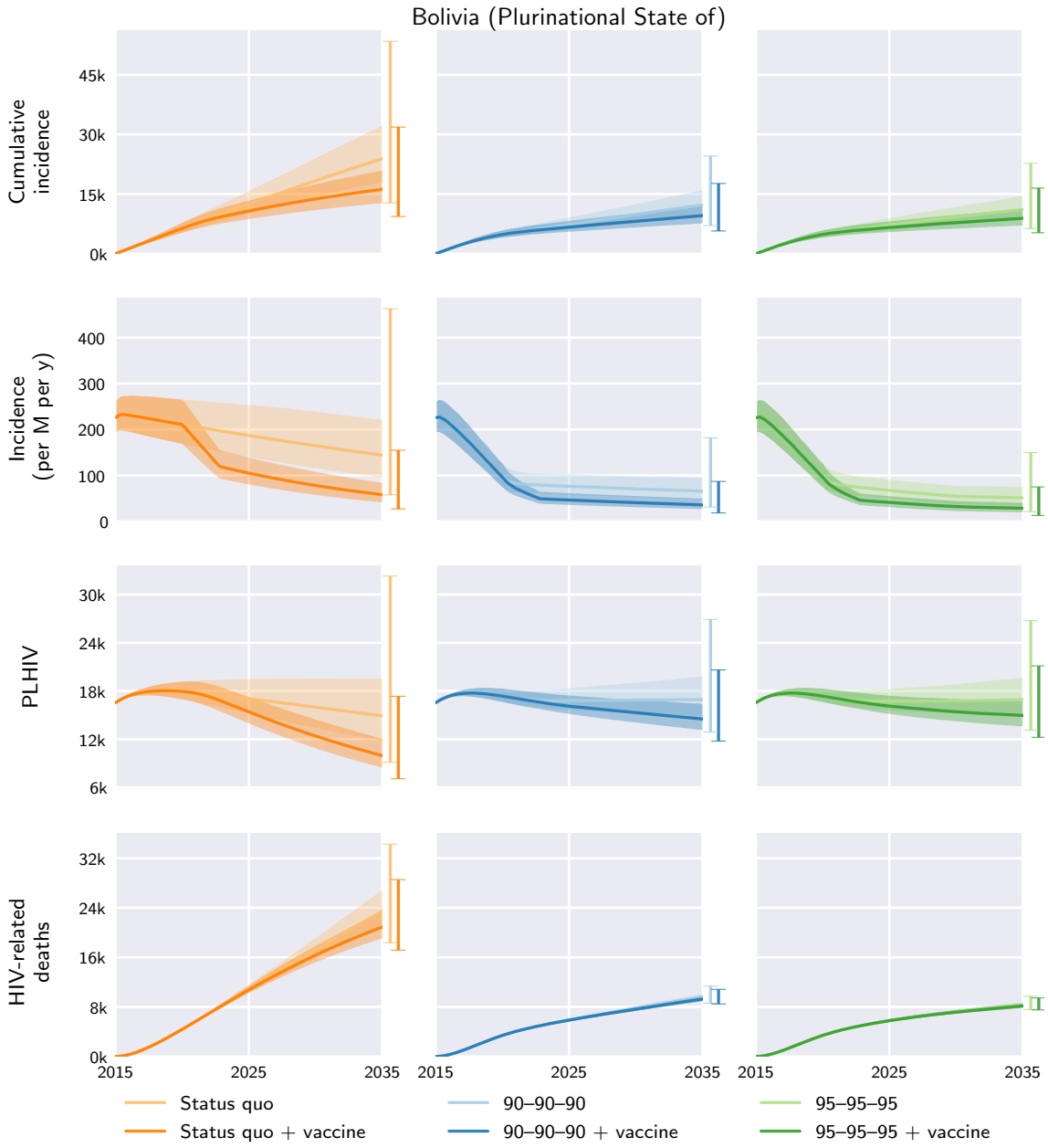

Fig. S29. Bolivia (Plurinational State of) model outcomes under the different diagnosis, treatment, and vaccination scenarios. Central curves show the medians over model runs with 1000 samples from parameter distributions, shaded regions show the 1st and 3rd quartiles (i.e. 25th and 75th percentiles), and vertical bars to the right of each axis show the 5th and 95th percentiles at the end time, 2035. Regional and global outcomes were aggregated from the country-level model outcomes.

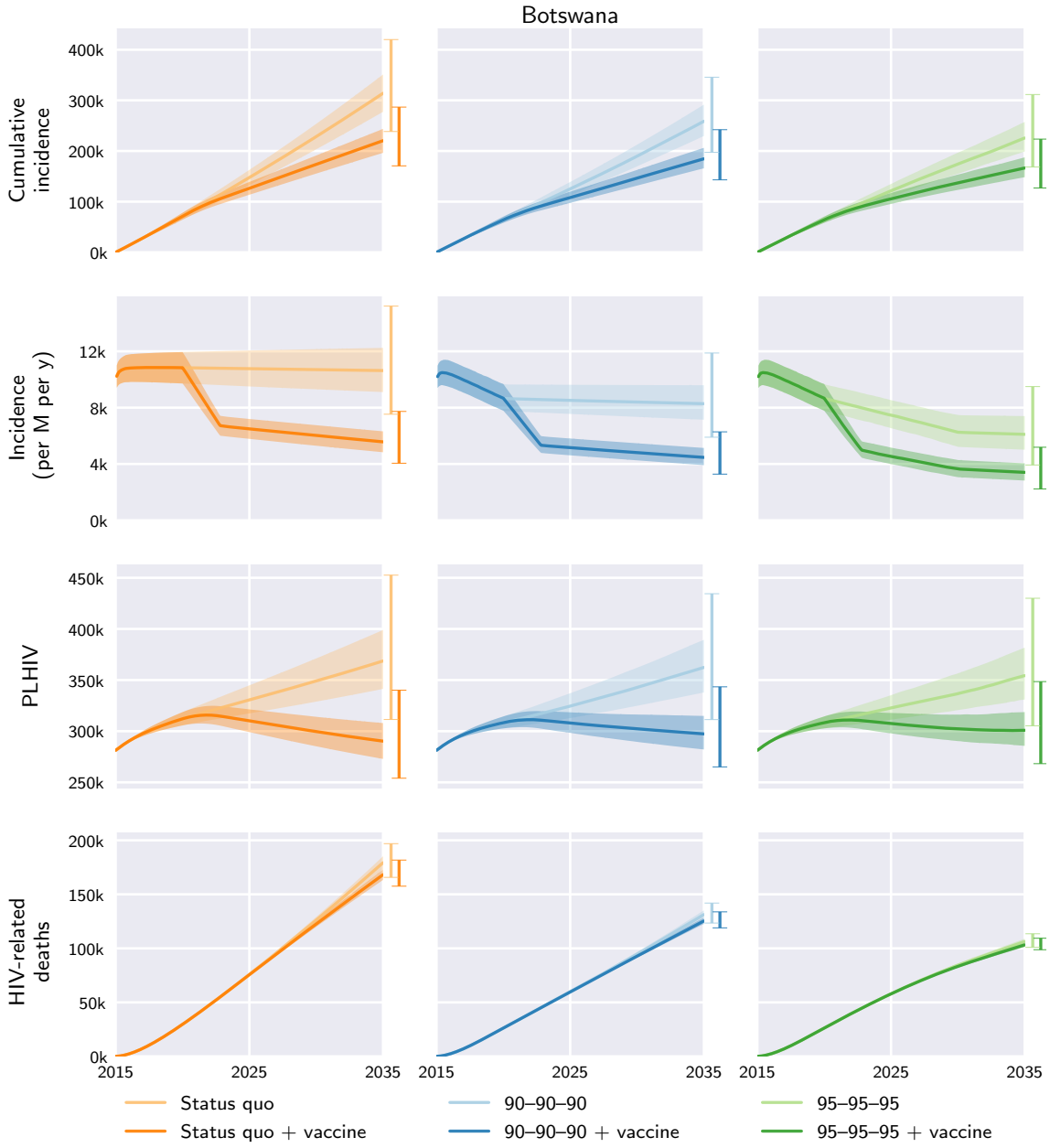

Fig. S30. Botswana model outcomes under the different diagnosis, treatment, and vaccination scenarios. Central curves show the medians over model runs with 1000 samples from parameter distributions, shaded regions show the 1st and 3rd quartiles (i.e. 25th and 75th percentiles), and vertical bars to the right of each axis show the 5th and 95th percentiles at the end time, 2035. Regional and global outcomes were aggregated from the country-level model outcomes.

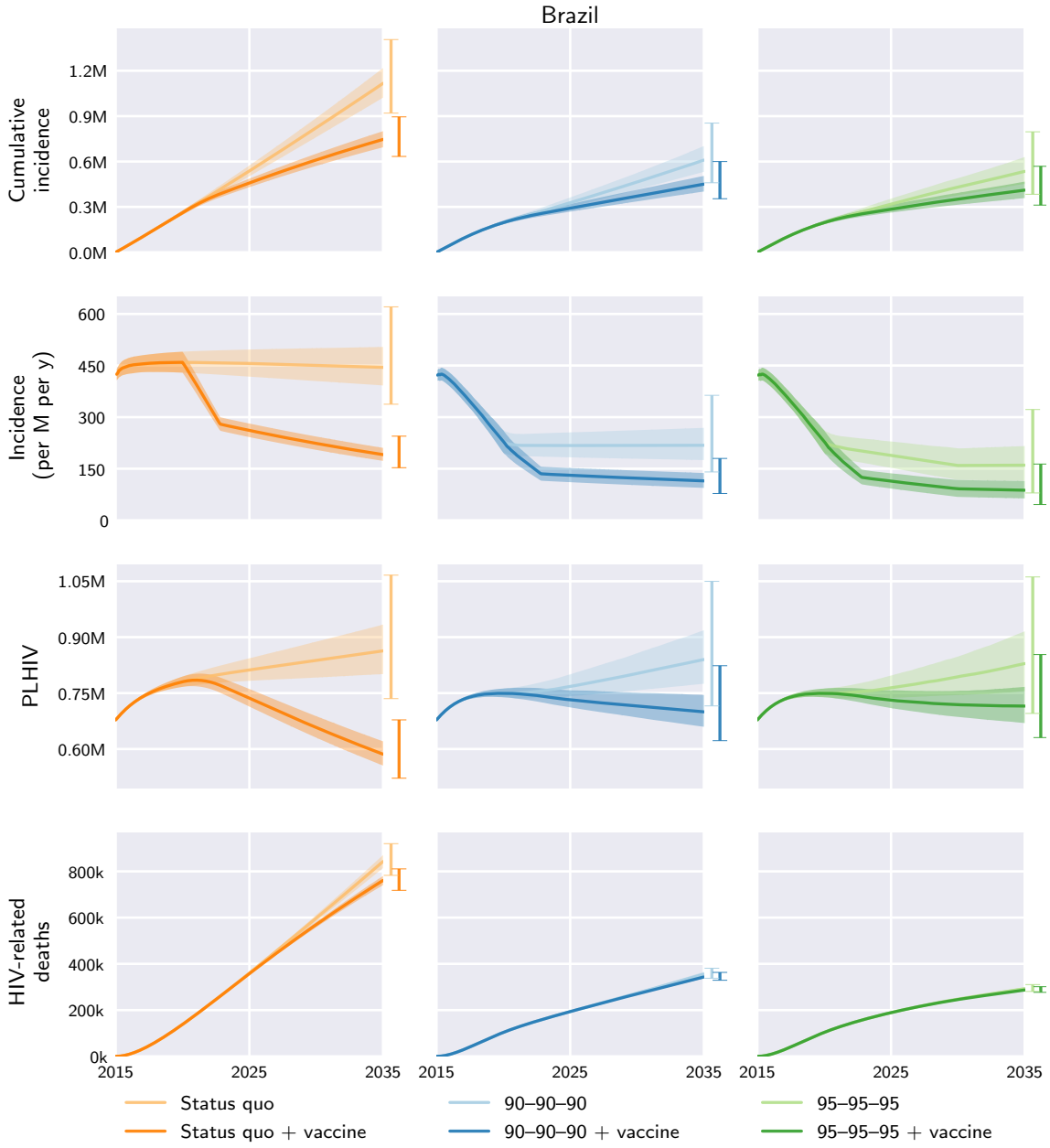

Fig. S31. Brazil model outcomes under the different diagnosis, treatment, and vaccination scenarios. Central curves show the medians over model runs with 1000 samples from parameter distributions, shaded regions show the 1st and 3rd quartiles (i.e. 25th and 75th percentiles), and vertical bars to the right of each axis show the 5th and 95th percentiles at the end time, 2035. Regional and global outcomes were aggregated from the country-level model outcomes.

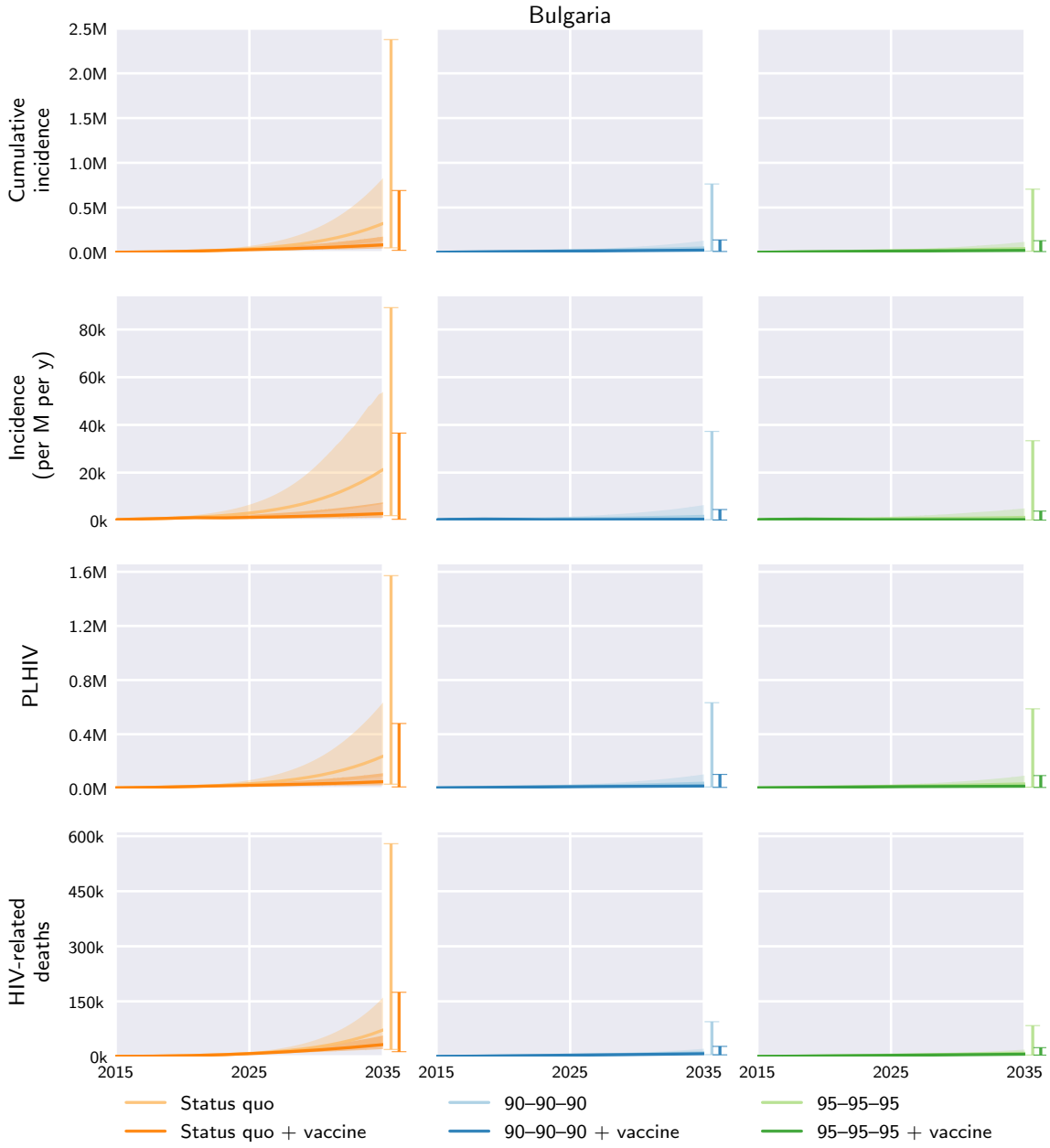

Fig. S32. Bulgaria model outcomes under the different diagnosis, treatment, and vaccination scenarios. Central curves show the medians over model runs with 1000 samples from parameter distributions, shaded regions show the 1st and 3rd quartiles (i.e. 25th and 75th percentiles), and vertical bars to the right of each axis show the 5th and 95th percentiles at the end time, 2035. Regional and global outcomes were aggregated from the country-level model outcomes.

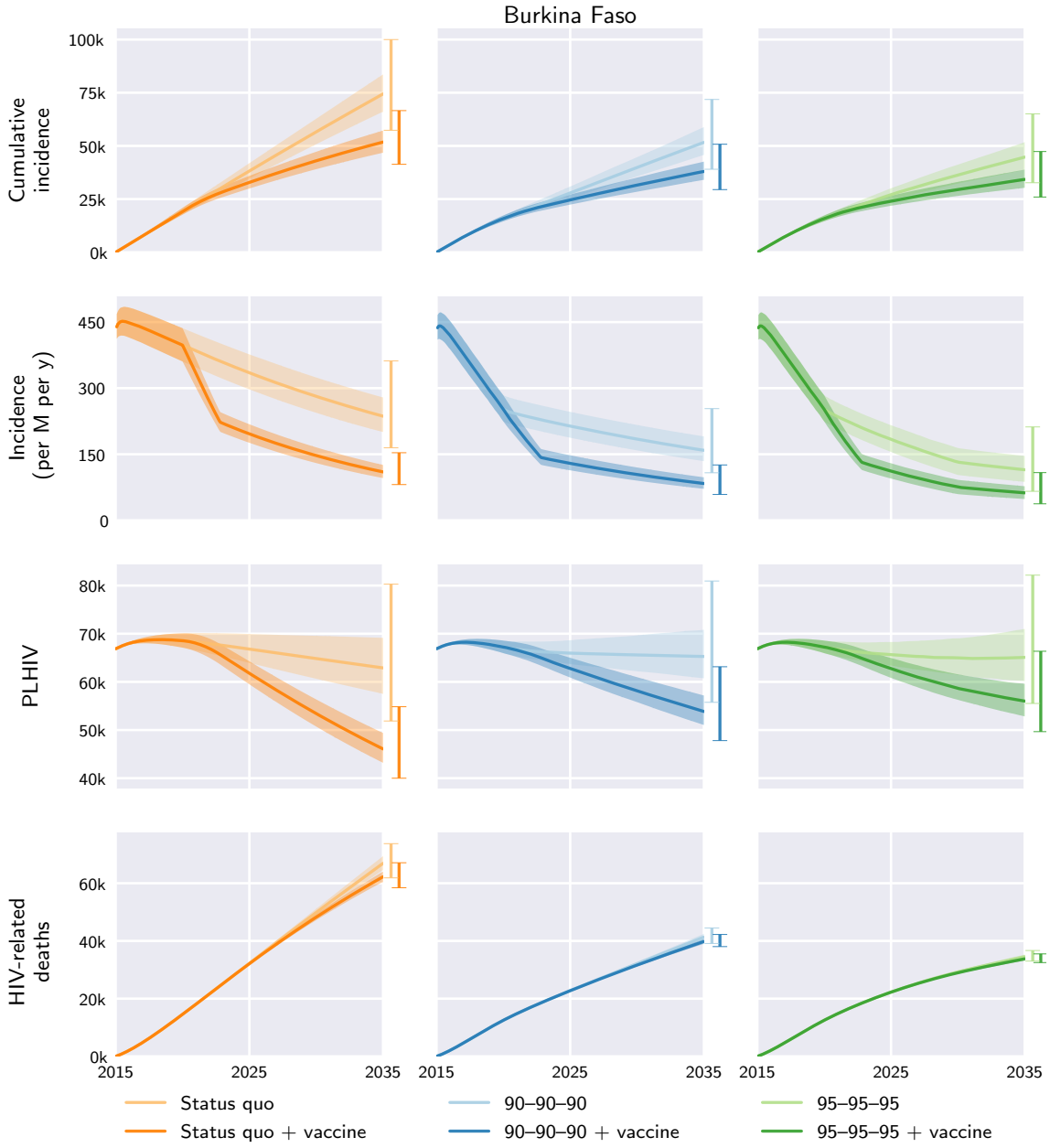

Fig. S33. Burkina Faso model outcomes under the different diagnosis, treatment, and vaccination scenarios. Central curves show the medians over model runs with 1000 samples from parameter distributions, shaded regions show the 1st and 3rd quartiles (i.e. 25th and 75th percentiles), and vertical bars to the right of each axis show the 5th and 95th percentiles at the end time, 2035. Regional and global outcomes were aggregated from the country-level model outcomes.

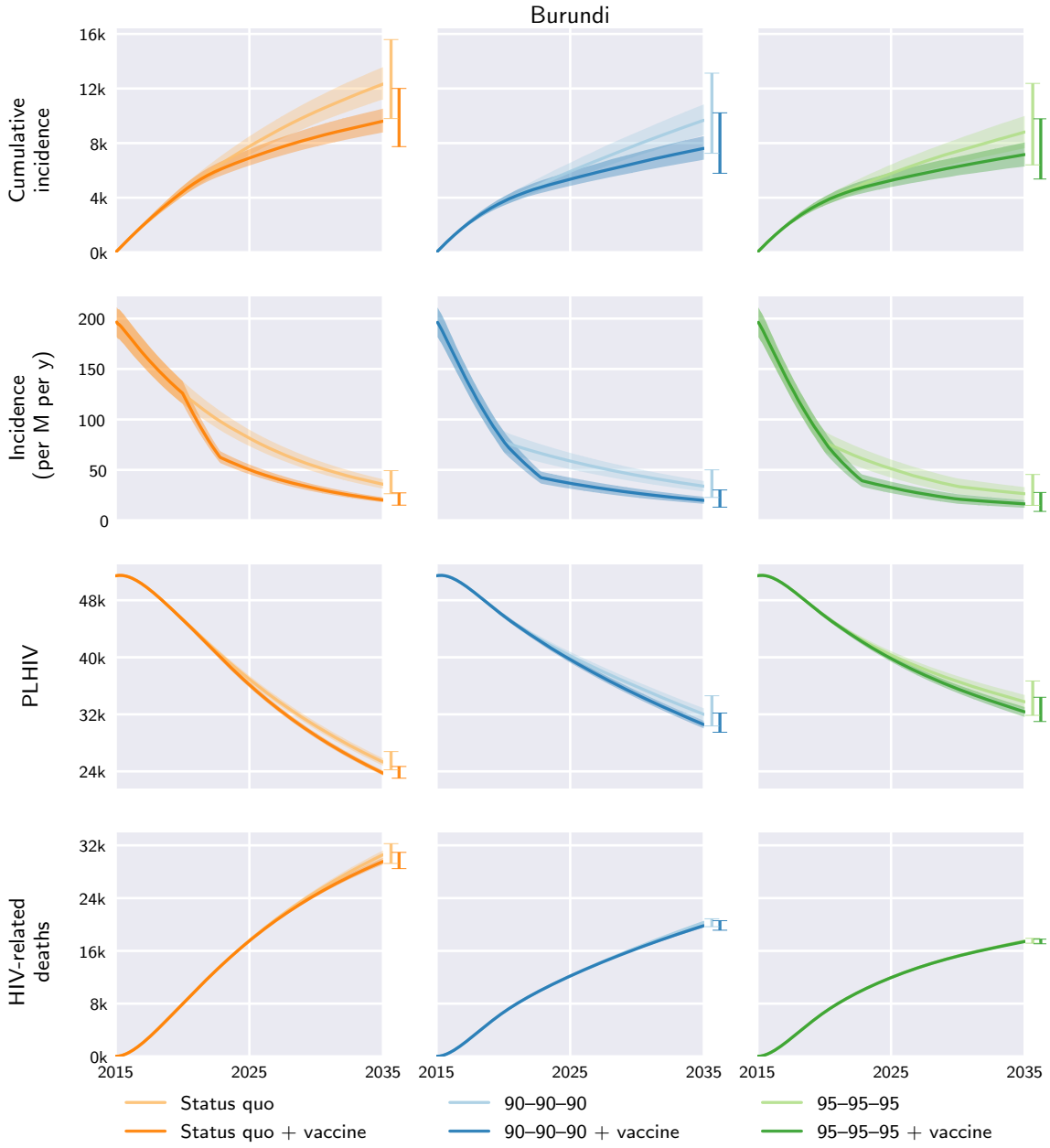

Fig. S34. Burundi model outcomes under the different diagnosis, treatment, and vaccination scenarios. Central curves show the medians over model runs with 1000 samples from parameter distributions, shaded regions show the 1st and 3rd quartiles (i.e. 25th and 75th percentiles), and vertical bars to the right of each axis show the 5th and 95th percentiles at the end time, 2035. Regional and global outcomes were aggregated from the country-level model outcomes.

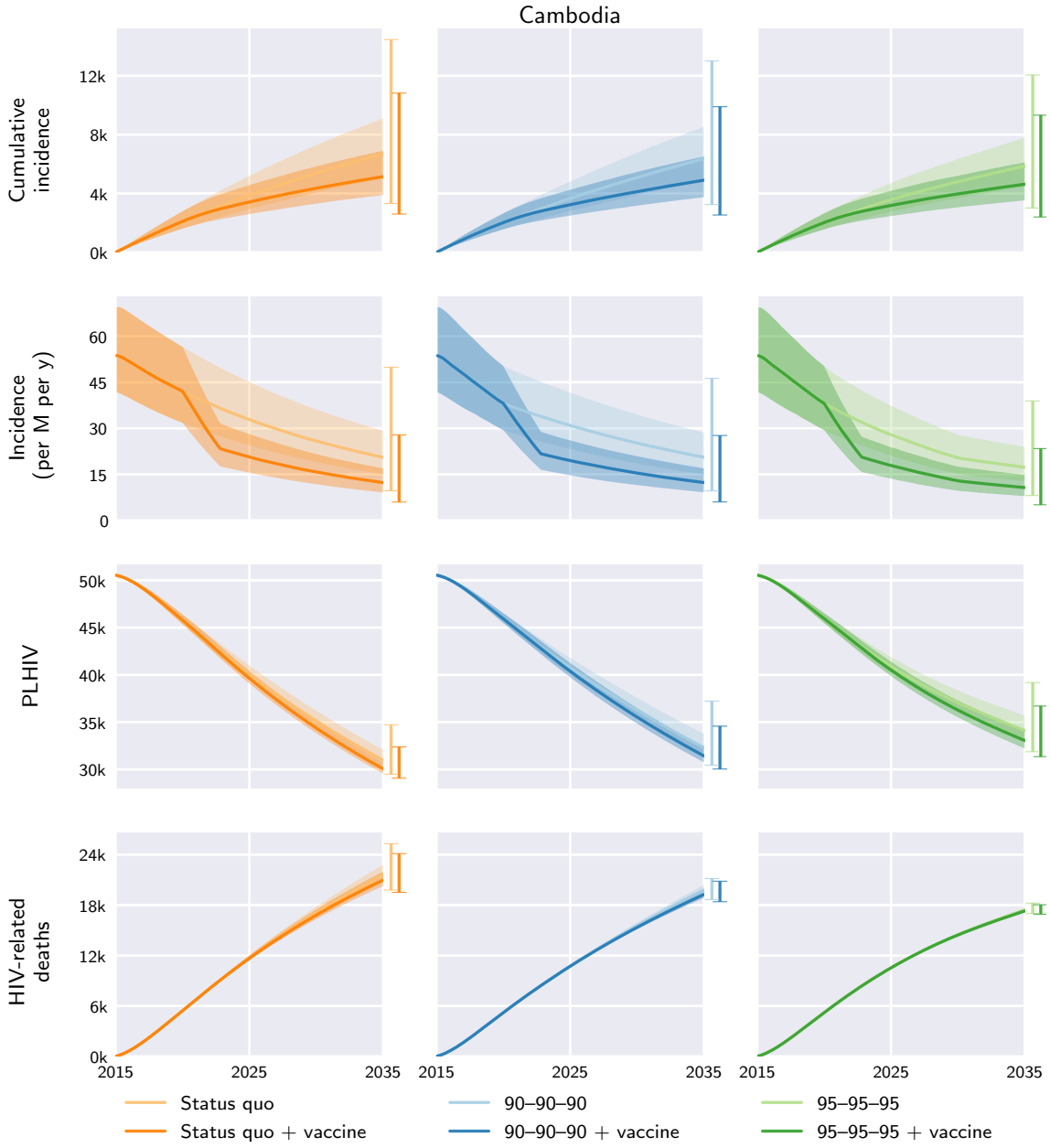

Fig. S35. Cambodia model outcomes under the different diagnosis, treatment, and vaccination scenarios. Central curves show the medians over model runs with 1000 samples from parameter distributions, shaded regions show the 1st and 3rd quartiles (i.e. 25th and 75th percentiles), and vertical bars to the right of each axis show the 5th and 95th percentiles at the end time, 2035. Regional and global outcomes were aggregated from the country-level model outcomes.

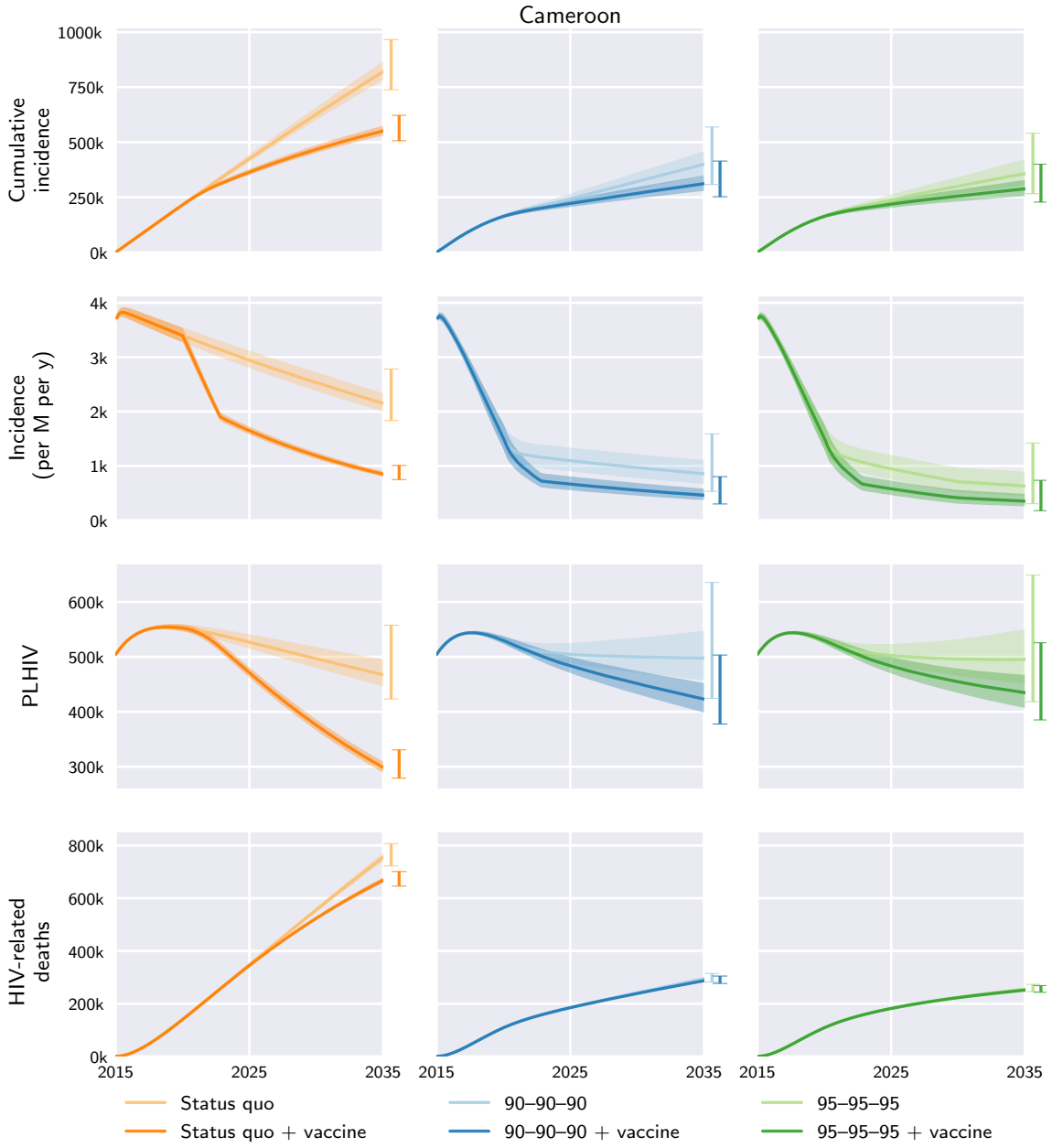

Fig. S36. Cameroon model outcomes under the different diagnosis, treatment, and vaccination scenarios. Central curves show the medians over model runs with 1000 samples from parameter distributions, shaded regions show the 1st and 3rd quartiles (i.e. 25th and 75th percentiles), and vertical bars to the right of each axis show the 5th and 95th percentiles at the end time, 2035. Regional and global outcomes were aggregated from the country-level model outcomes.

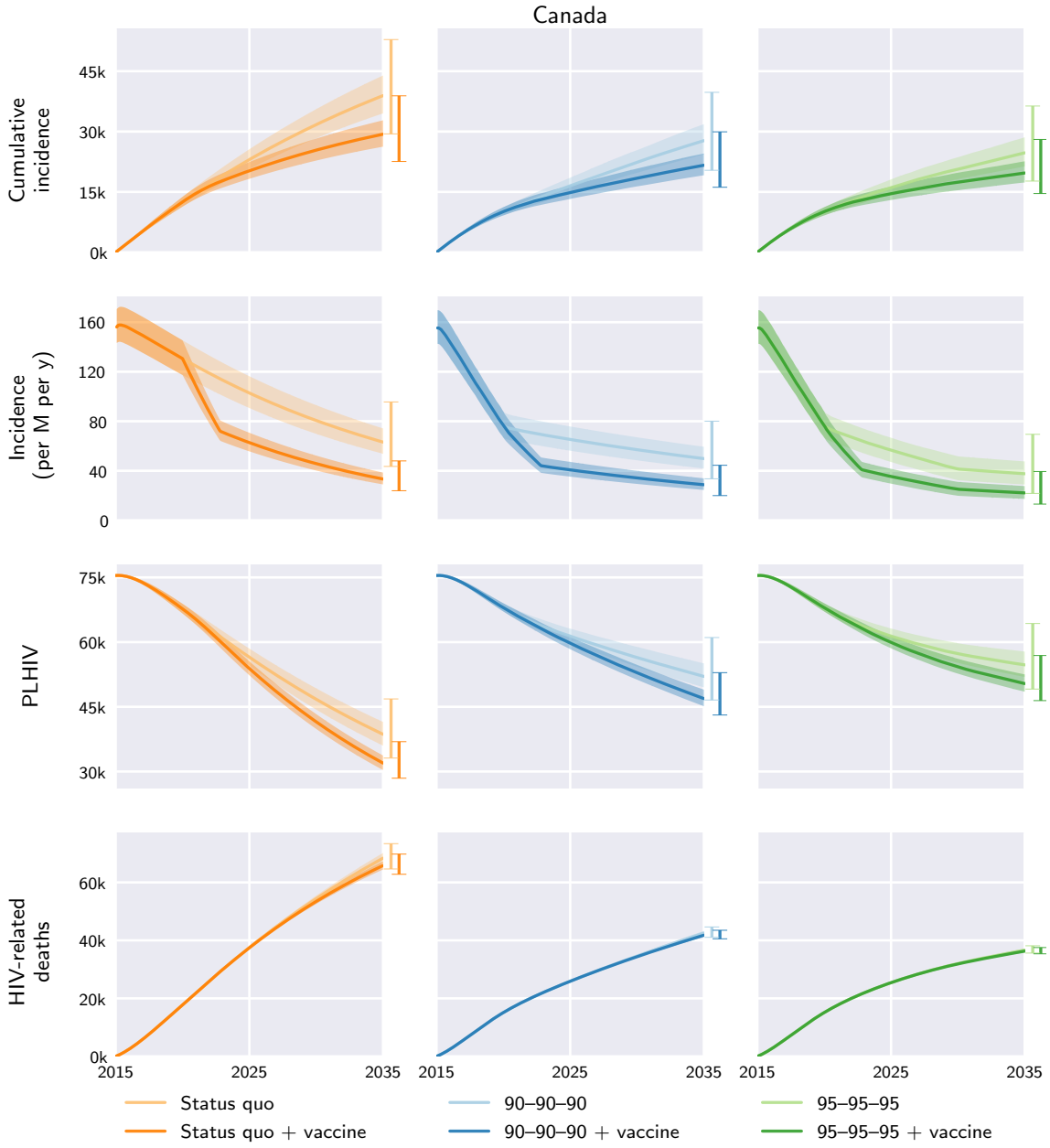

Fig. S37. Canada model outcomes under the different diagnosis, treatment, and vaccination scenarios. Central curves show the medians over model runs with 1000 samples from parameter distributions, shaded regions show the 1st and 3rd quartiles (i.e. 25th and 75th percentiles), and vertical bars to the right of each axis show the 5th and 95th percentiles at the end time, 2035. Regional and global outcomes were aggregated from the country-level model outcomes.

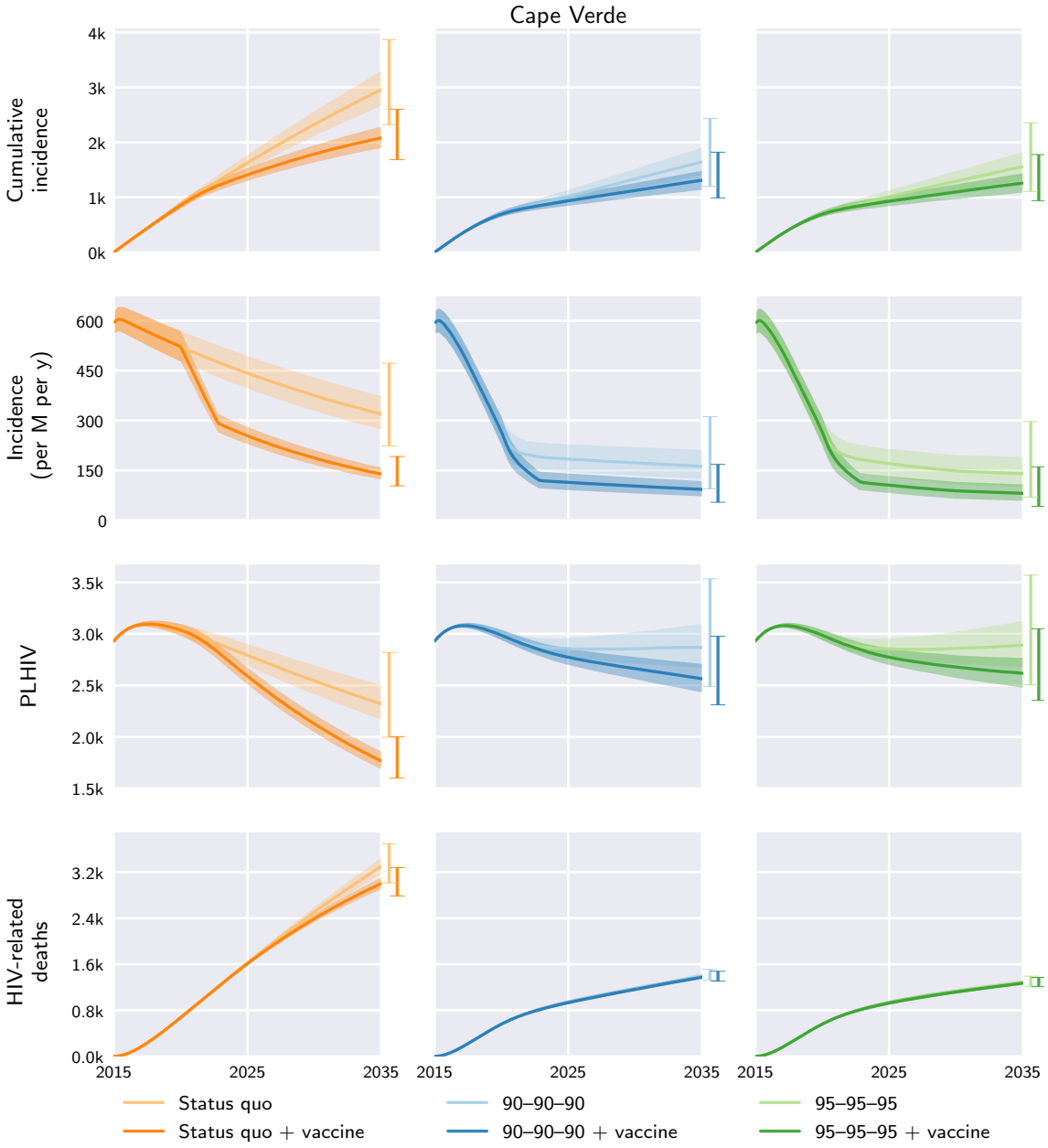

Fig. S38. Cape Verde model outcomes under the different diagnosis, treatment, and vaccination scenarios. Central curves show the medians over model runs with 1000 samples from parameter distributions, shaded regions show the 1st and 3rd quartiles (i.e. 25th and 75th percentiles), and vertical bars to the right of each axis show the 5th and 95th percentiles at the end time, 2035. Regional and global outcomes were aggregated from the country-level model outcomes.

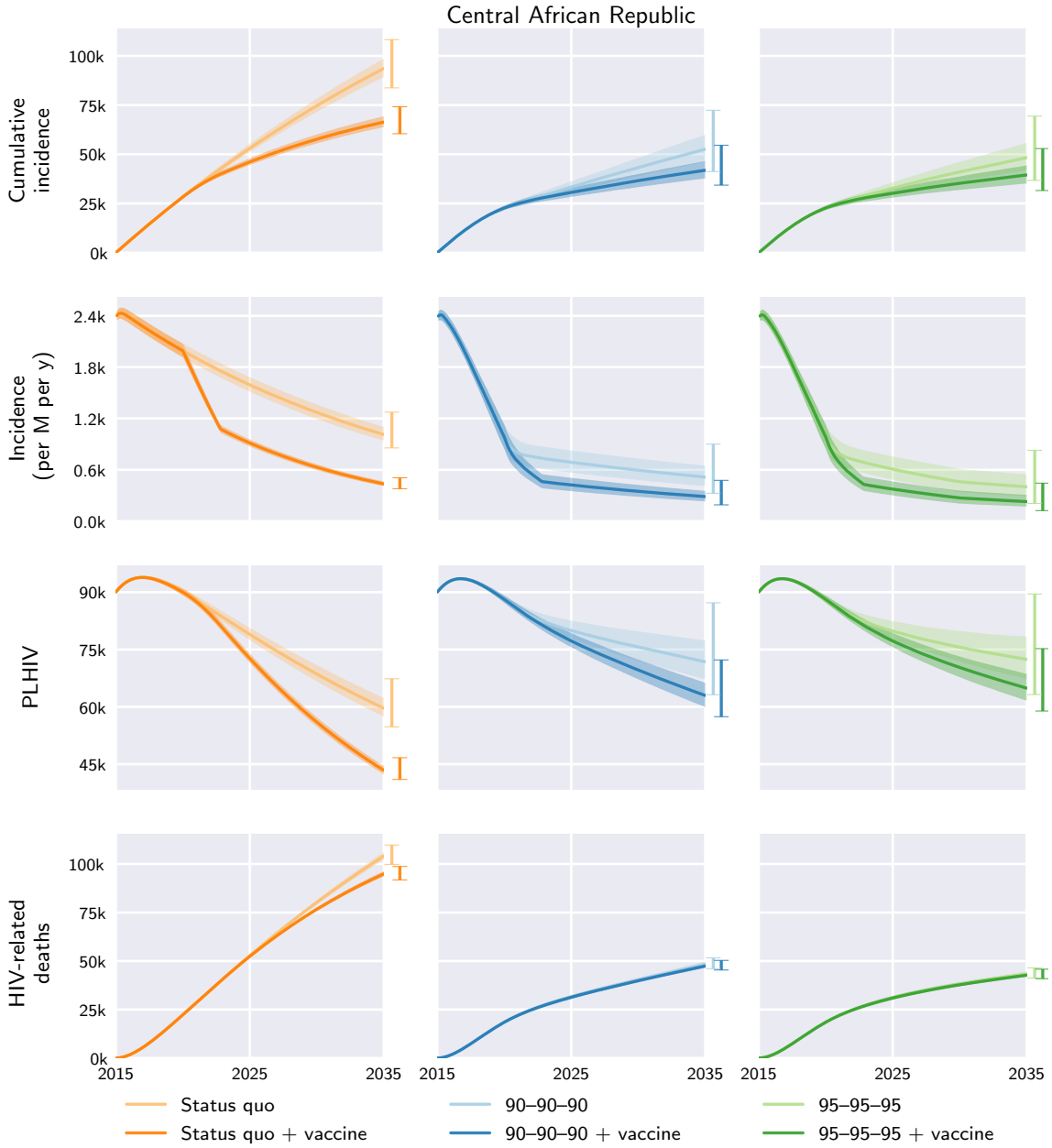

Fig. S39. Central African Republic model outcomes under the different diagnosis, treatment, and vaccination scenarios. Central curves show the medians over model runs with 1000 samples from parameter distributions, shaded regions show the 1st and 3rd quartiles (i.e. 25th and 75th percentiles), and vertical bars to the right of each axis show the 5th and 95th percentiles at the end time, 2035. Regional and global outcomes were aggregated from the country-level model outcomes.

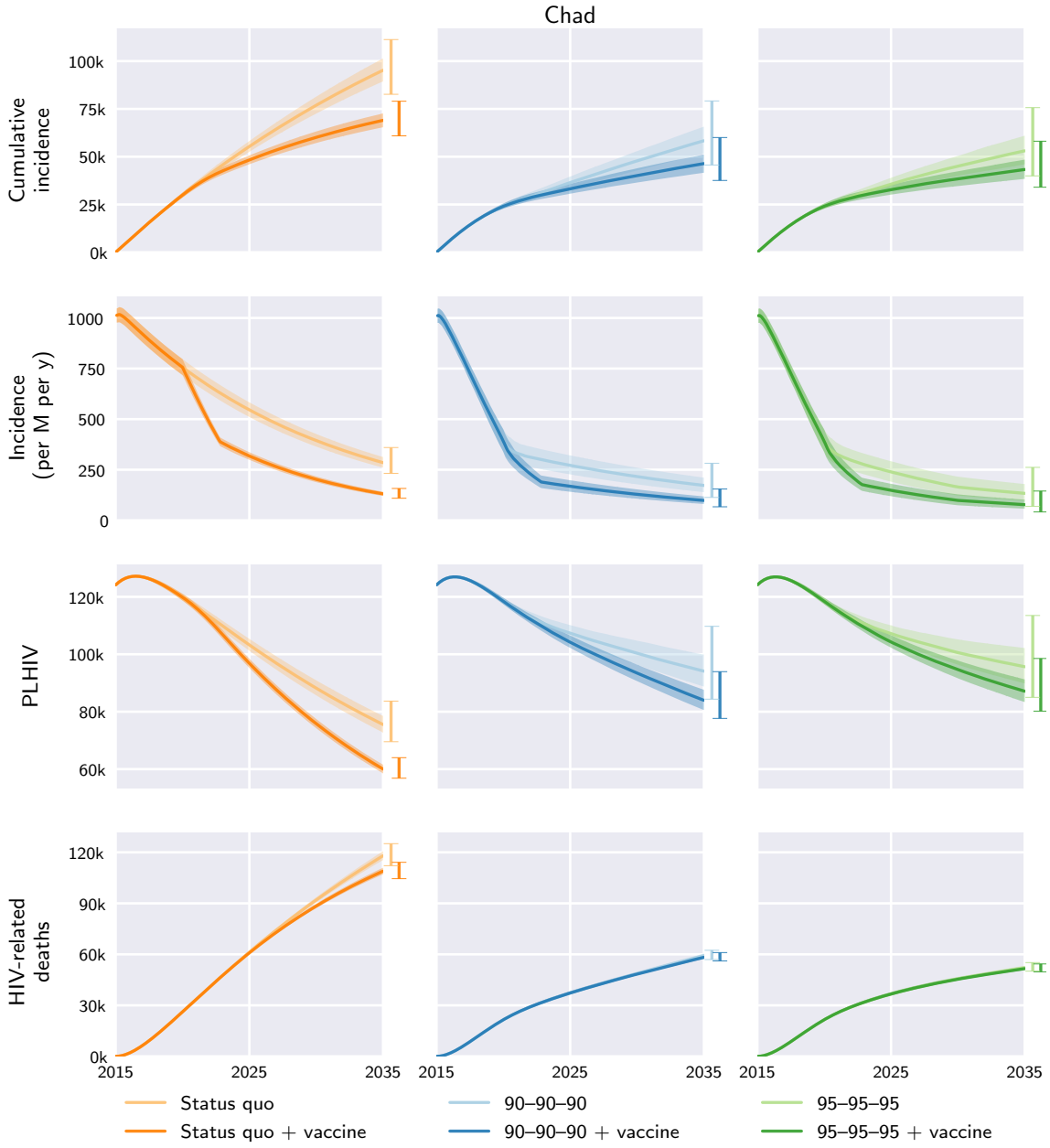

Fig. S40. Chad model outcomes under the different diagnosis, treatment, and vaccination scenarios. Central curves show the medians over model runs with 1000 samples from parameter distributions, shaded regions show the 1st and 3rd quartiles (i.e. 25th and 75th percentiles), and vertical bars to the right of each axis show the 5th and 95th percentiles at the end time, 2035. Regional and global outcomes were aggregated from the country-level model outcomes.

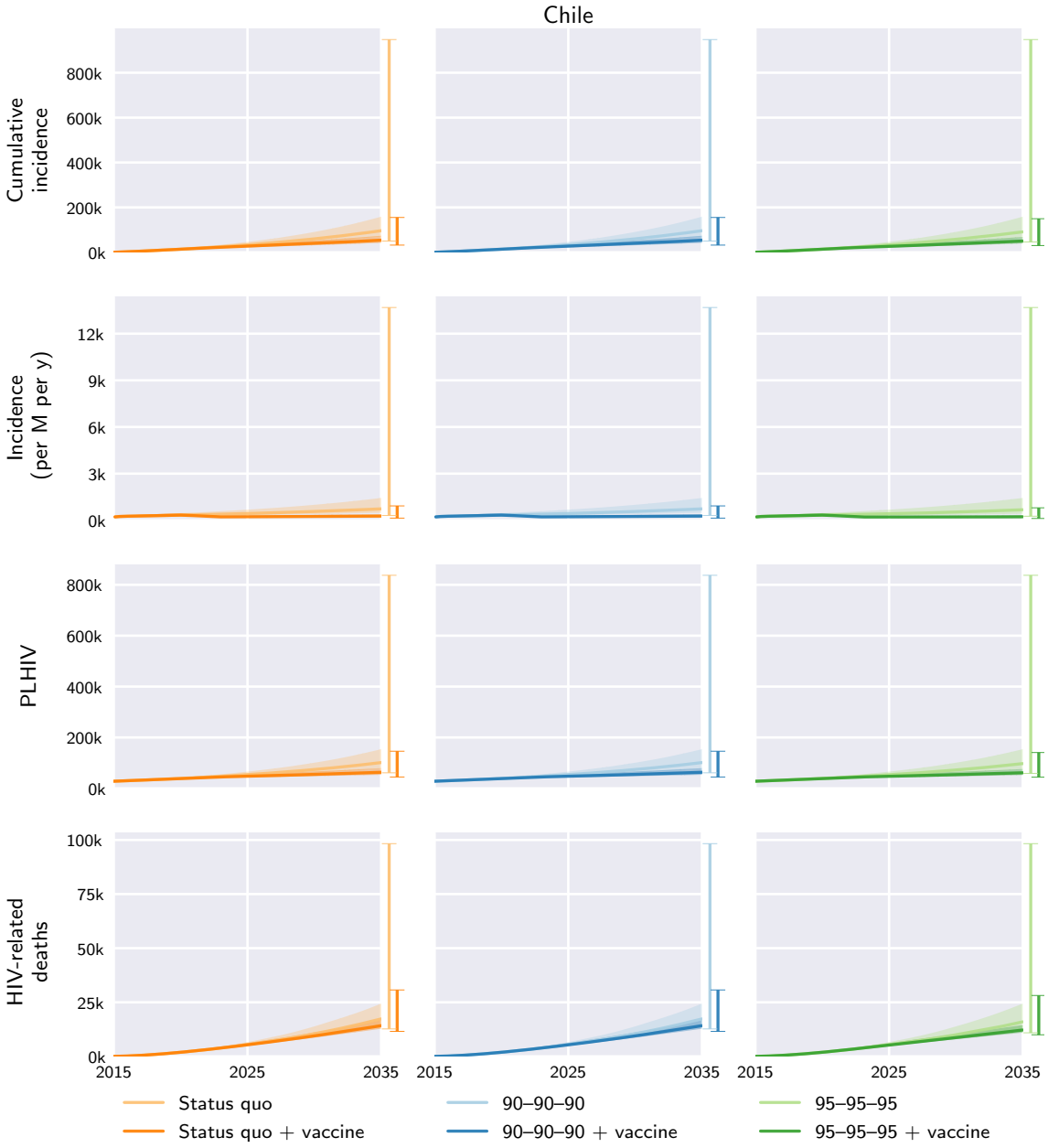

Fig. S41. Chile model outcomes under the different diagnosis, treatment, and vaccination scenarios. Central curves show the medians over model runs with 1000 samples from parameter distributions, shaded regions show the 1st and 3rd quartiles (i.e. 25th and 75th percentiles), and vertical bars to the right of each axis show the 5th and 95th percentiles at the end time, 2035. Regional and global outcomes were aggregated from the country-level model outcomes.

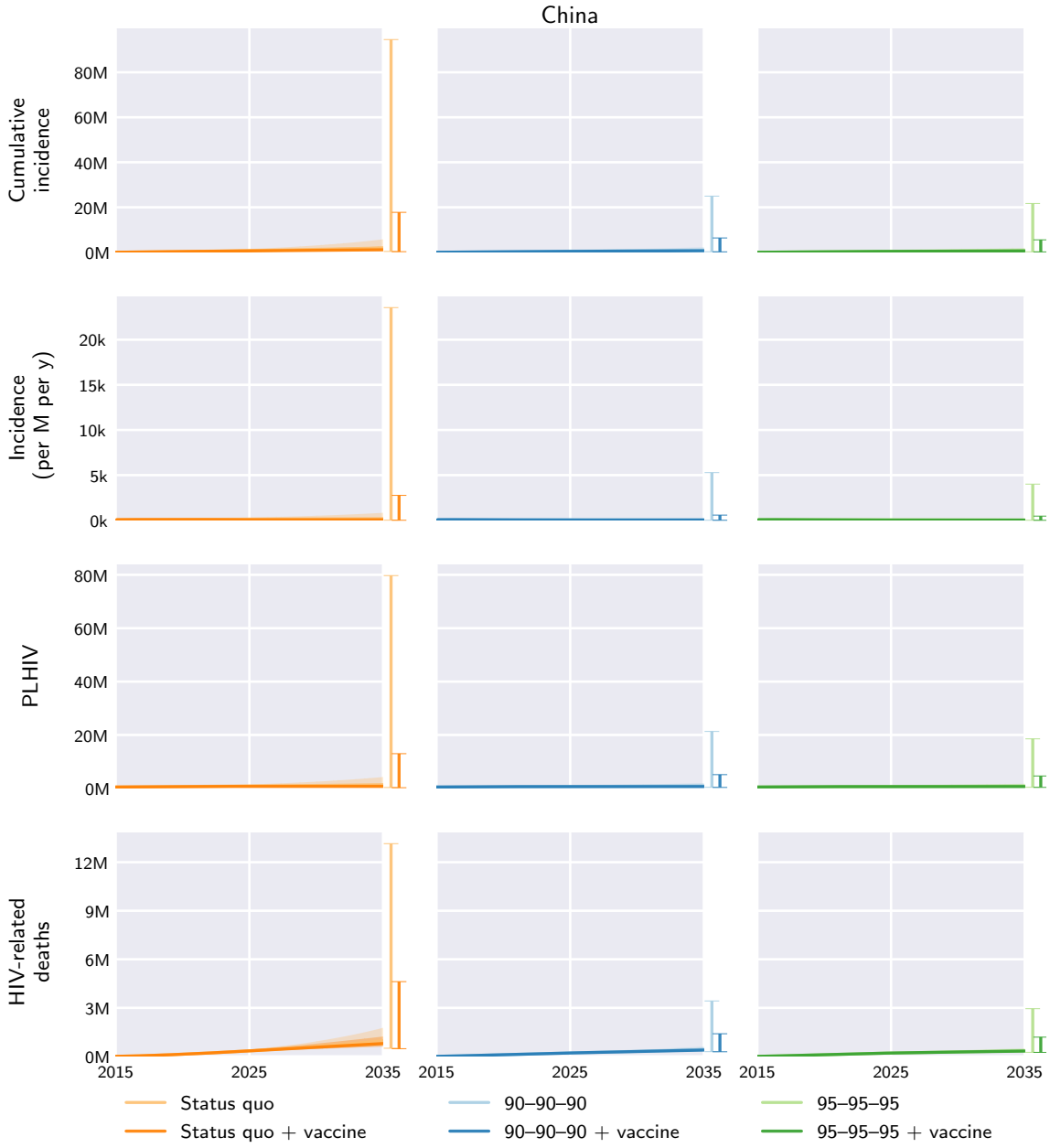

Fig. S42. China model outcomes under the different diagnosis, treatment, and vaccination scenarios. Central curves show the medians over model runs with 1000 samples from parameter distributions, shaded regions show the 1st and 3rd quartiles (i.e. 25th and 75th percentiles), and vertical bars to the right of each axis show the 5th and 95th percentiles at the end time, 2035. Regional and global outcomes were aggregated from the country-level model outcomes.

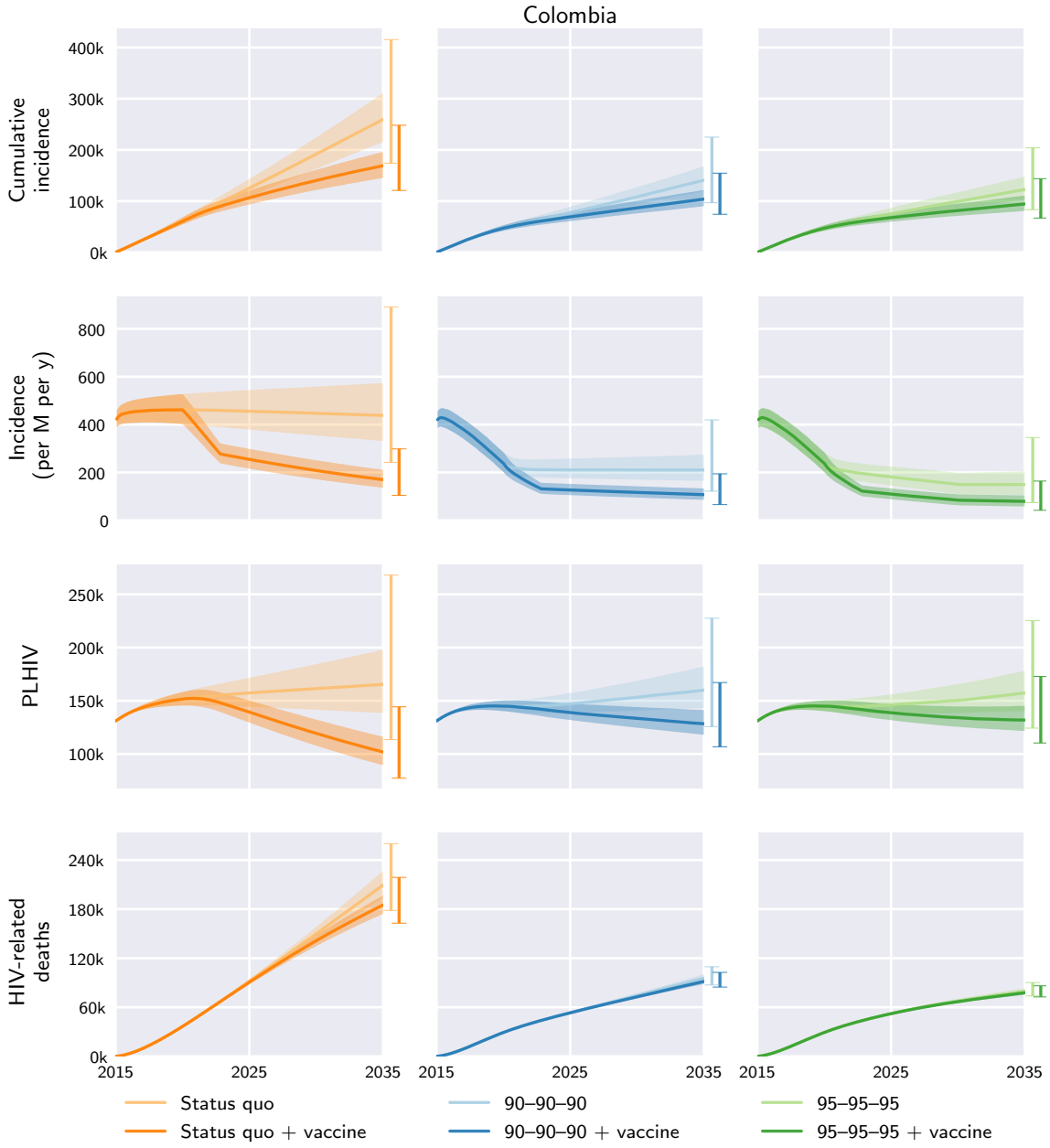

Fig. S43. Colombia model outcomes under the different diagnosis, treatment, and vaccination scenarios. Central curves show the medians over model runs with 1000 samples from parameter distributions, shaded regions show the 1st and 3rd quartiles (i.e. 25th and 75th percentiles), and vertical bars to the right of each axis show the 5th and 95th percentiles at the end time, 2035. Regional and global outcomes were aggregated from the country-level model outcomes.

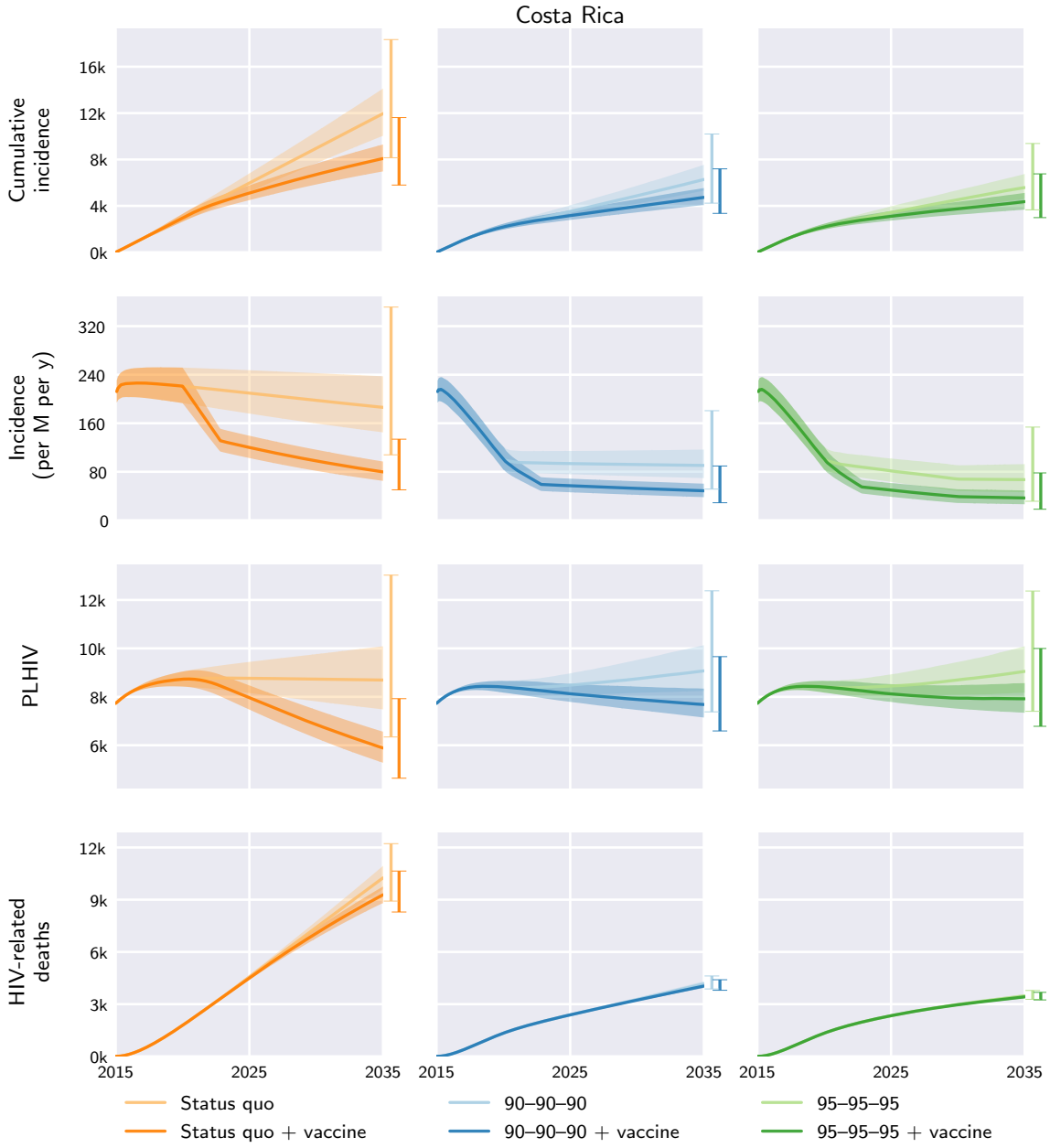

Fig. S44. Costa Rica model outcomes under the different diagnosis, treatment, and vaccination scenarios. Central curves show the medians over model runs with 1000 samples from parameter distributions, shaded regions show the 1st and 3rd quartiles (i.e. 25th and 75th percentiles), and vertical bars to the right of each axis show the 5th and 95th percentiles at the end time, 2035. Regional and global outcomes were aggregated from the country-level model outcomes.

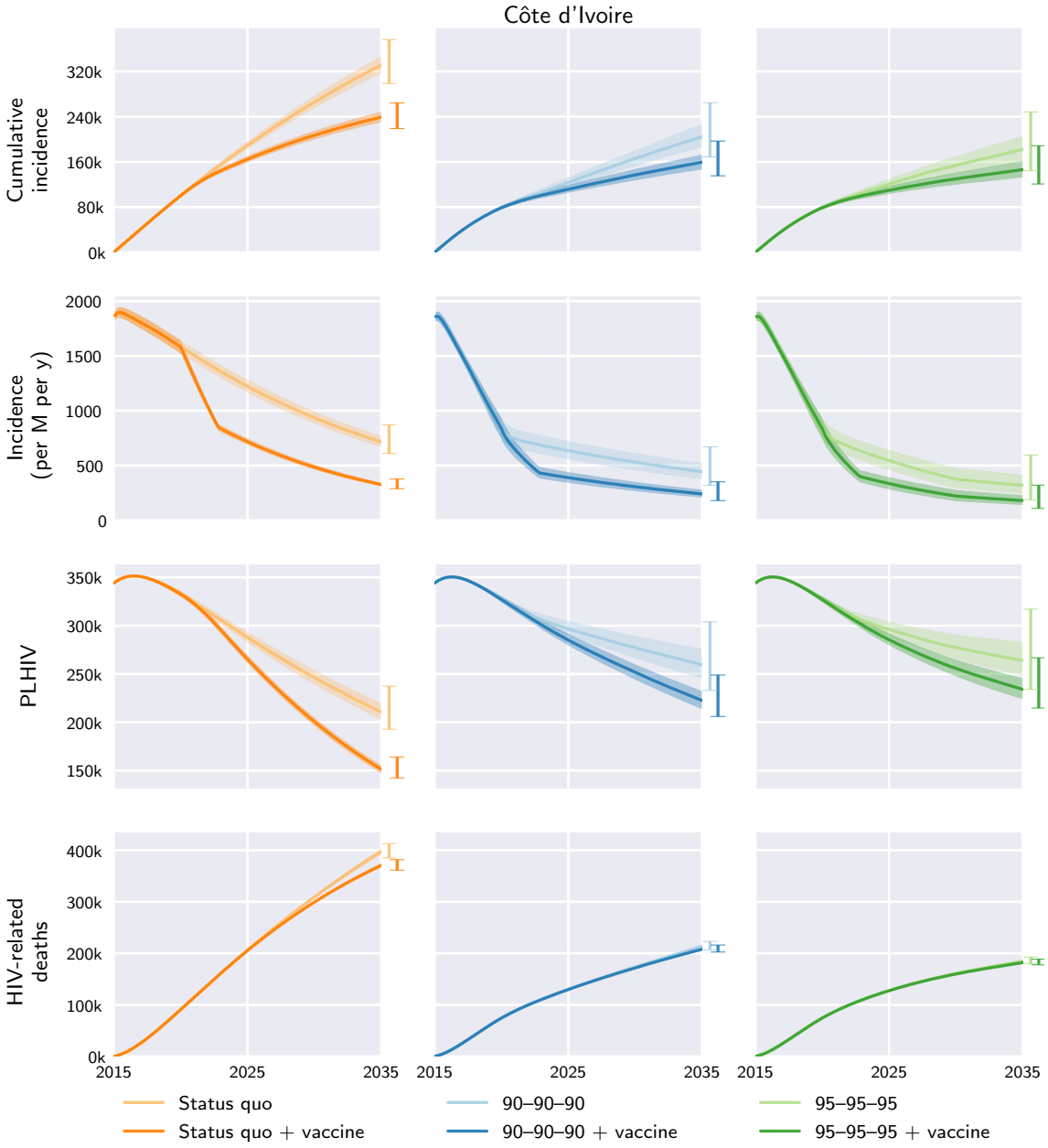

Fig. S45. Côte d'Ivoire model outcomes under the different diagnosis, treatment, and vaccination scenarios. Central curves show the medians over model runs with 1000 samples from parameter distributions, shaded regions show the 1st and 3rd quartiles (i.e. 25th and 75th percentiles), and vertical bars to the right of each axis show the 5th and 95th percentiles at the end time, 2035. Regional and global outcomes were aggregated from the country-level model outcomes.

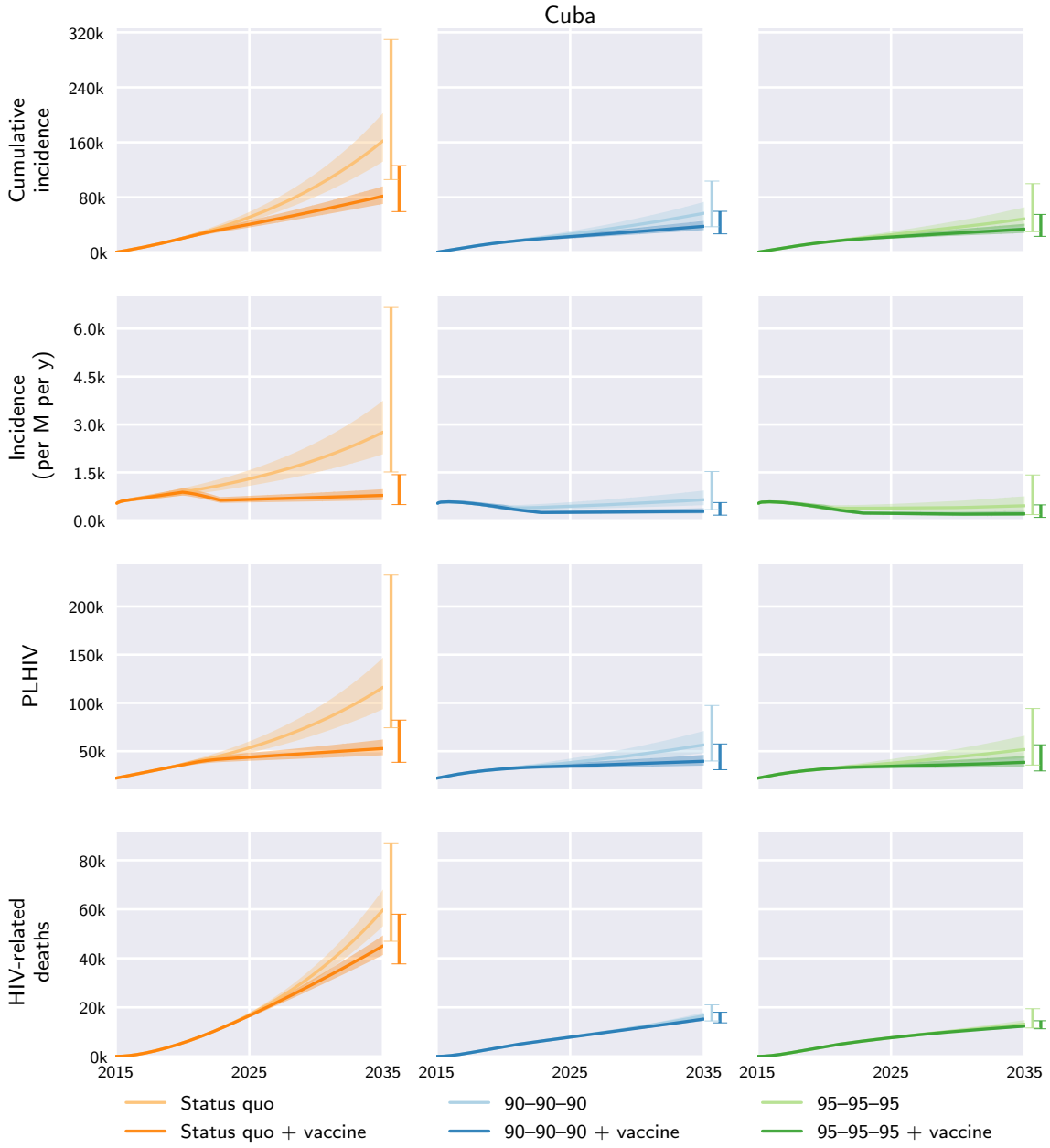

Fig. S46. Cuba model outcomes under the different diagnosis, treatment, and vaccination scenarios. Central curves show the medians over model runs with 1000 samples from parameter distributions, shaded regions show the 1st and 3rd quartiles (i.e. 25th and 75th percentiles), and vertical bars to the right of each axis show the 5th and 95th percentiles at the end time, 2035. Regional and global outcomes were aggregated from the country-level model outcomes.

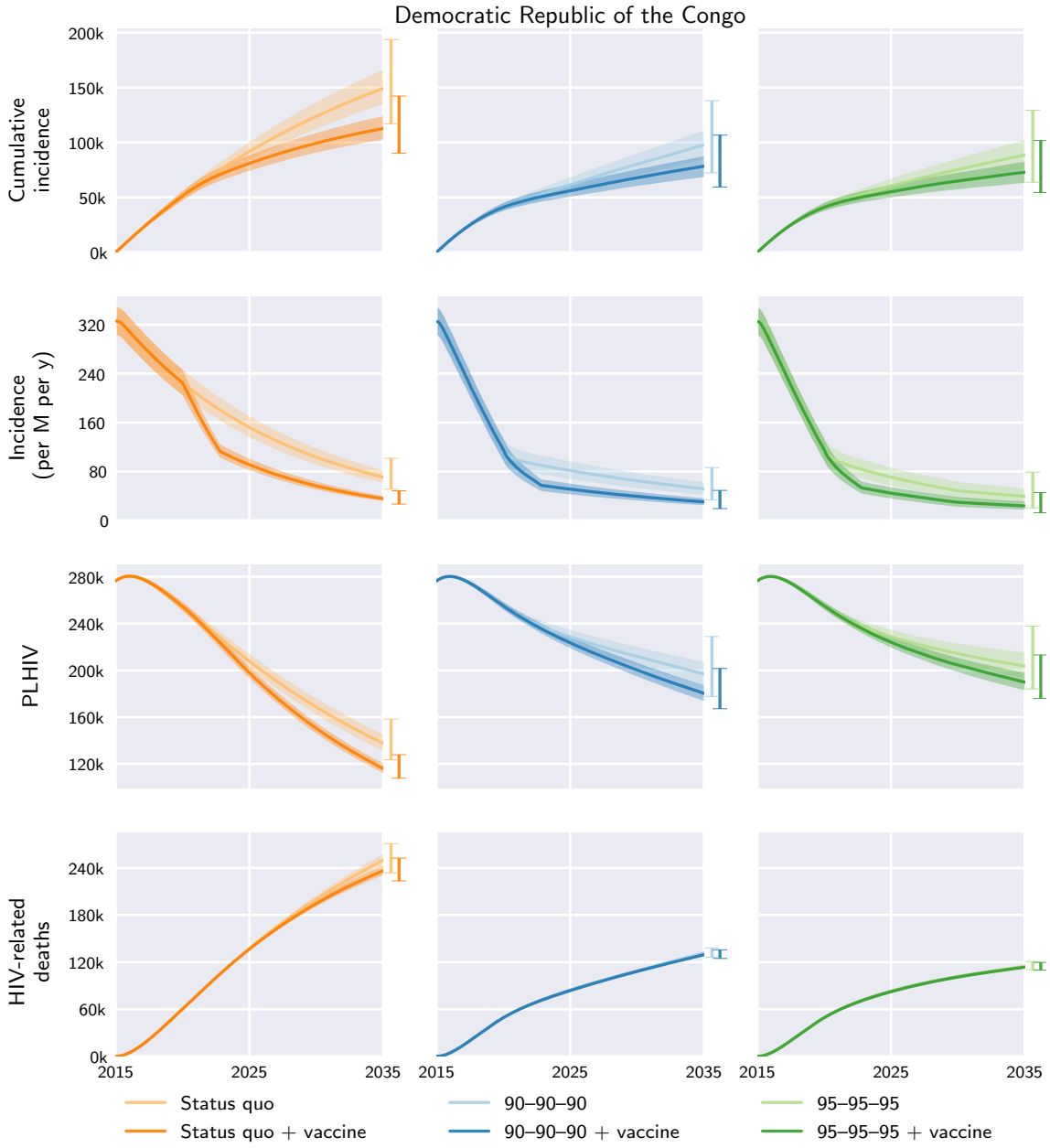

Fig. S47. Democratic Republic of the Congo model outcomes under the different diagnosis, treatment, and vaccination scenarios. Central curves show the medians over model runs with 1000 samples from parameter distributions, shaded regions show the 1st and 3rd quartiles (i.e. 25th and 75th percentiles), and vertical bars to the right of each axis show the 5th and 95th percentiles at the end time, 2035. Regional and global outcomes were aggregated from the country-level model outcomes.

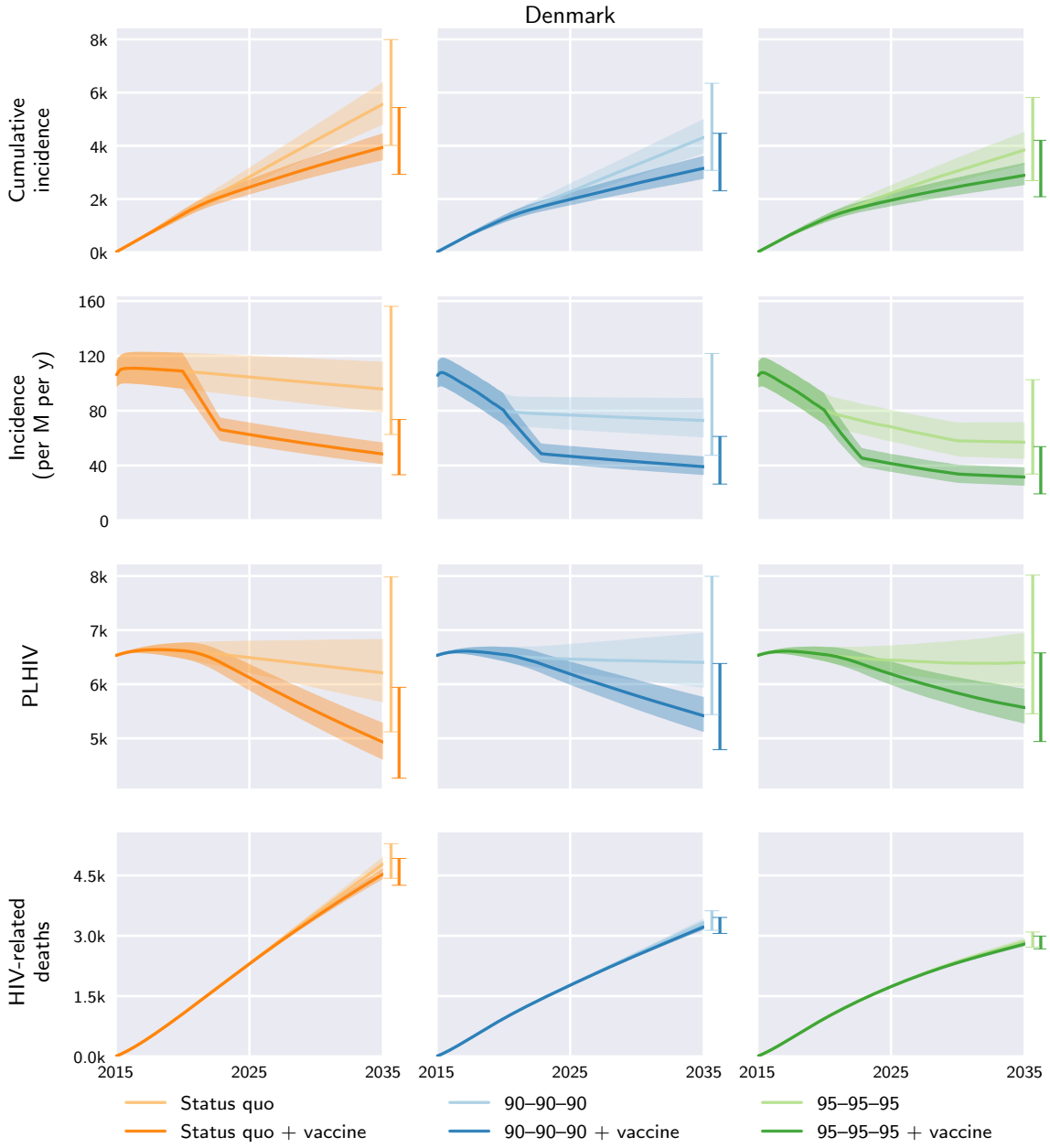

Fig. S48. Denmark model outcomes under the different diagnosis, treatment, and vaccination scenarios. Central curves show the medians over model runs with 1000 samples from parameter distributions, shaded regions show the 1st and 3rd quartiles (i.e. 25th and 75th percentiles), and vertical bars to the right of each axis show the 5th and 95th percentiles at the end time, 2035. Regional and global outcomes were aggregated from the country-level model outcomes.

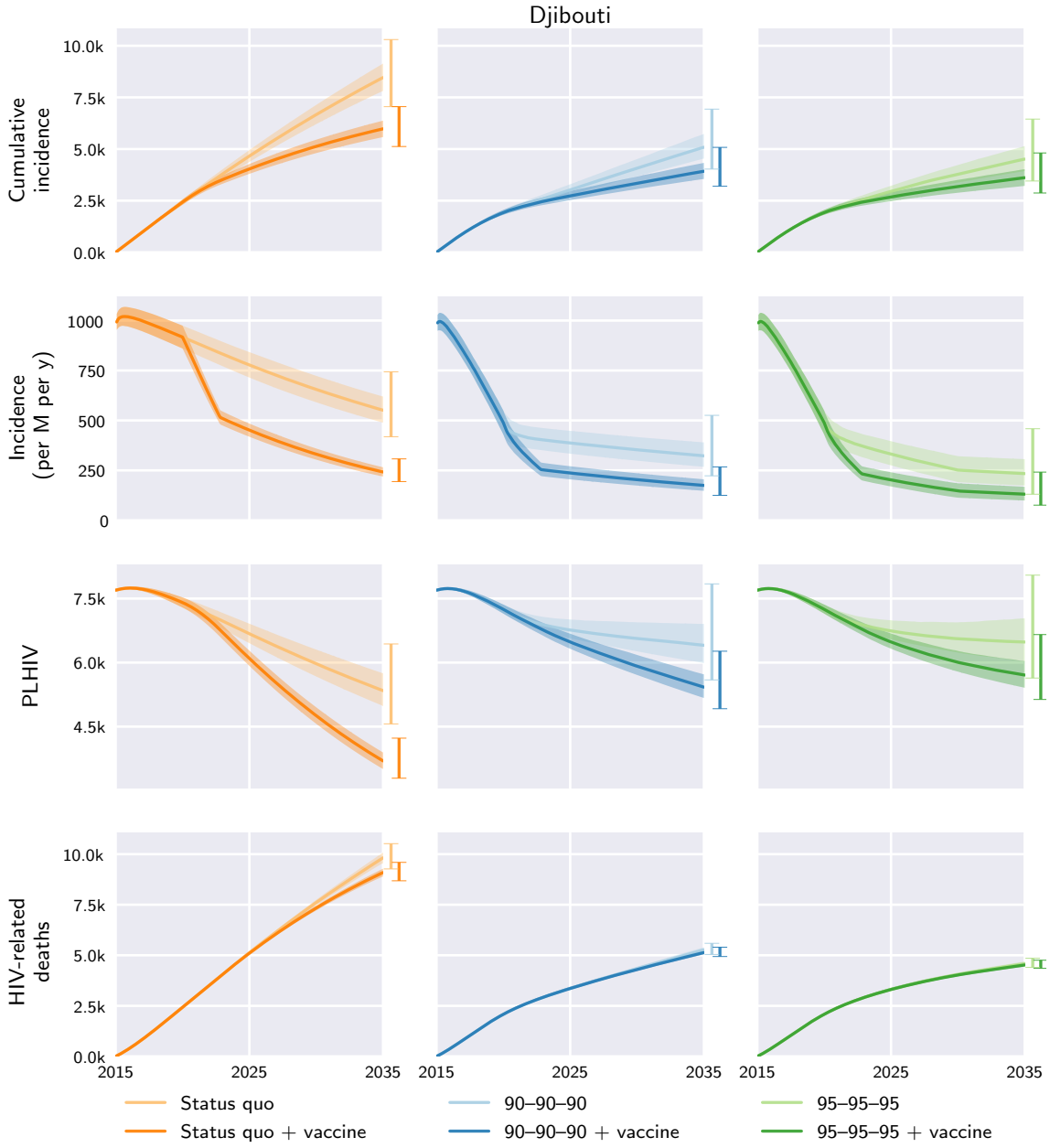

Fig. S49. Djibouti model outcomes under the different diagnosis, treatment, and vaccination scenarios. Central curves show the medians over model runs with 1000 samples from parameter distributions, shaded regions show the 1st and 3rd quartiles (i.e. 25th and 75th percentiles), and vertical bars to the right of each axis show the 5th and 95th percentiles at the end time, 2035. Regional and global outcomes were aggregated from the country-level model outcomes.

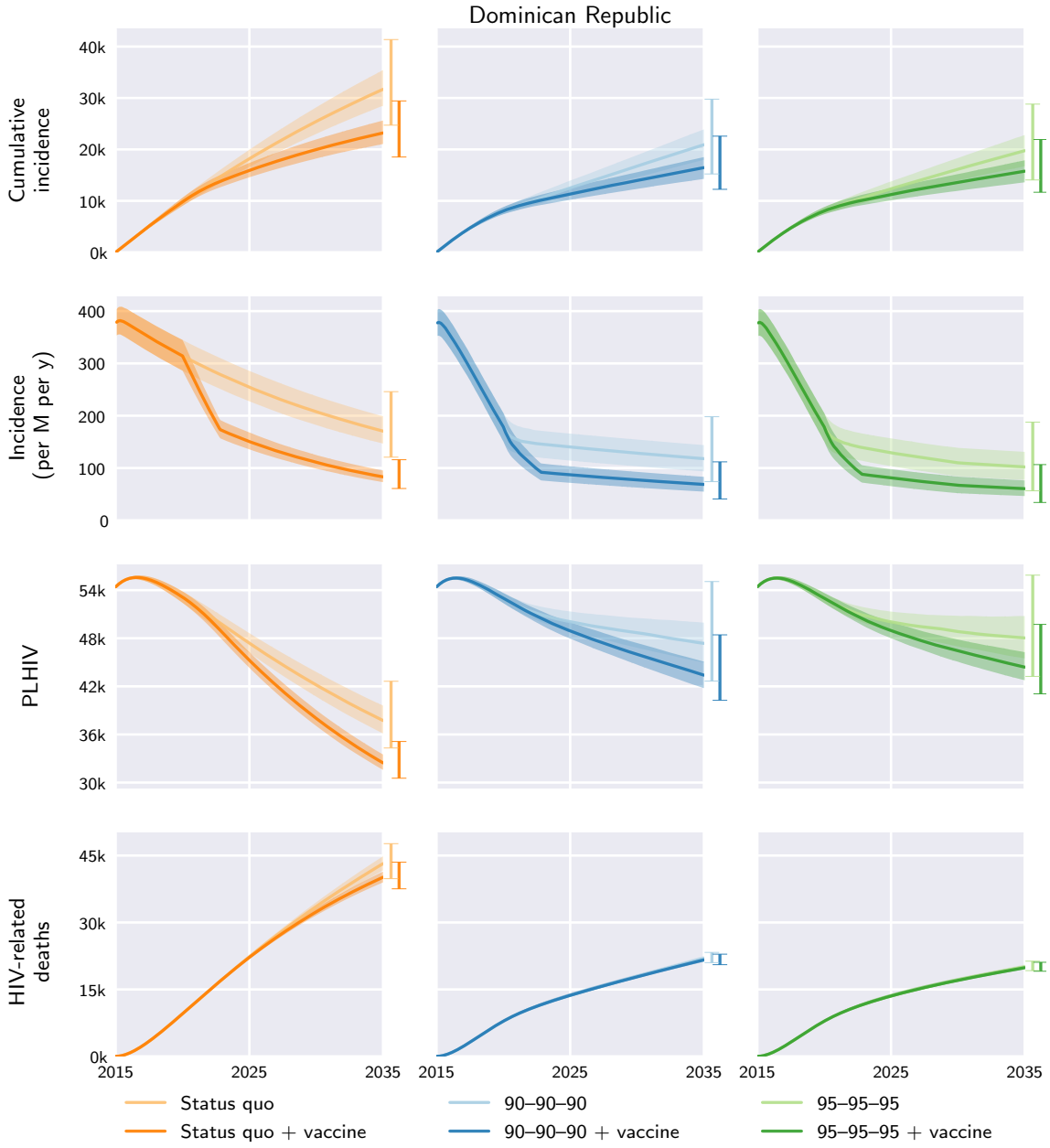

Fig. S50. Dominican Republic model outcomes under the different diagnosis, treatment, and vaccination scenarios. Central curves show the medians over model runs with 1000 samples from parameter distributions, shaded regions show the 1st and 3rd quartiles (i.e. 25th and 75th percentiles), and vertical bars to the right of each axis show the 5th and 95th percentiles at the end time, 2035. Regional and global outcomes were aggregated from the country-level model outcomes.

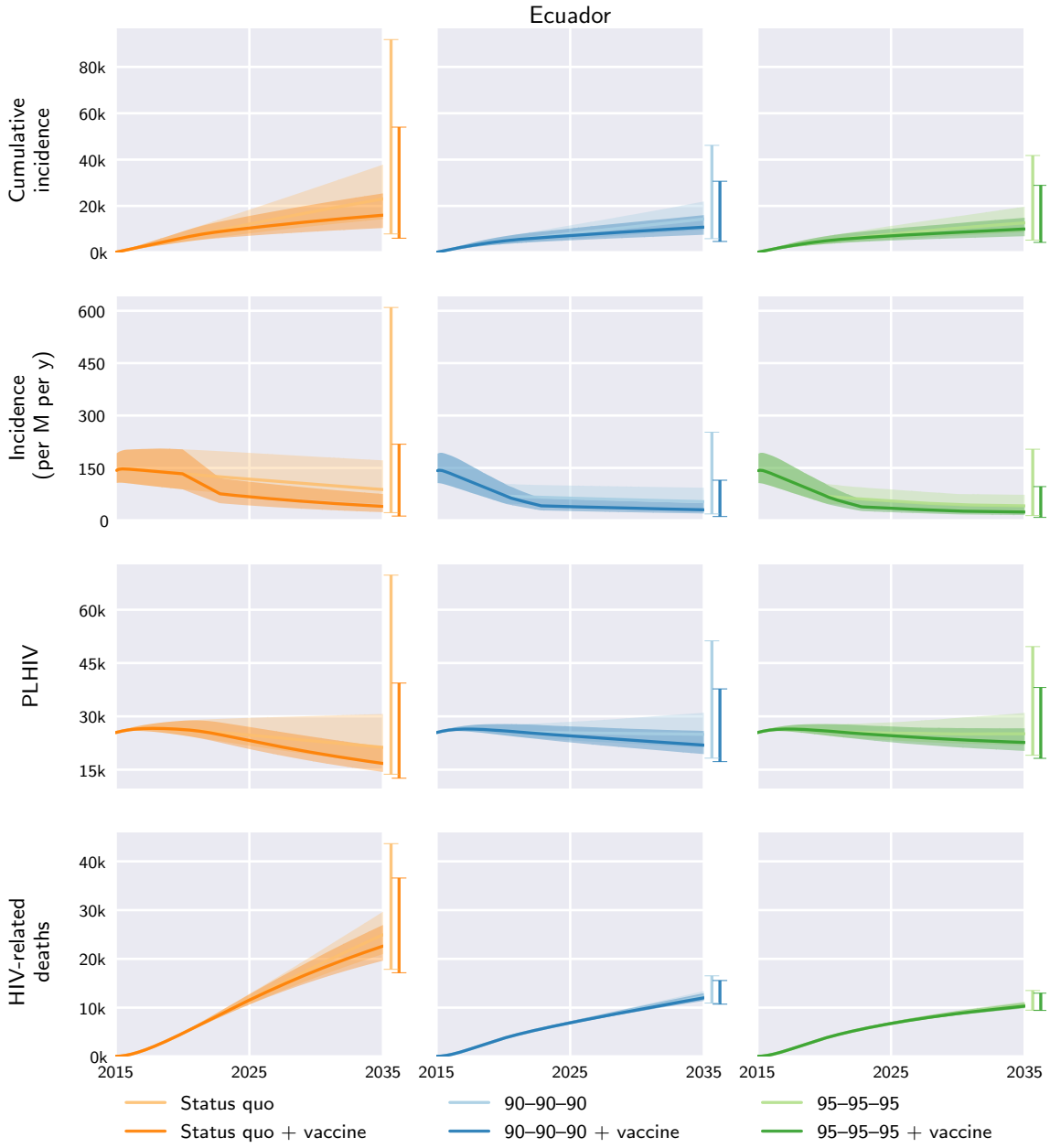

Fig. S51. Ecuador model outcomes under the different diagnosis, treatment, and vaccination scenarios. Central curves show the medians over model runs with 1000 samples from parameter distributions, shaded regions show the 1st and 3rd quartiles (i.e. 25th and 75th percentiles), and vertical bars to the right of each axis show the 5th and 95th percentiles at the end time, 2035. Regional and global outcomes were aggregated from the country-level model outcomes.

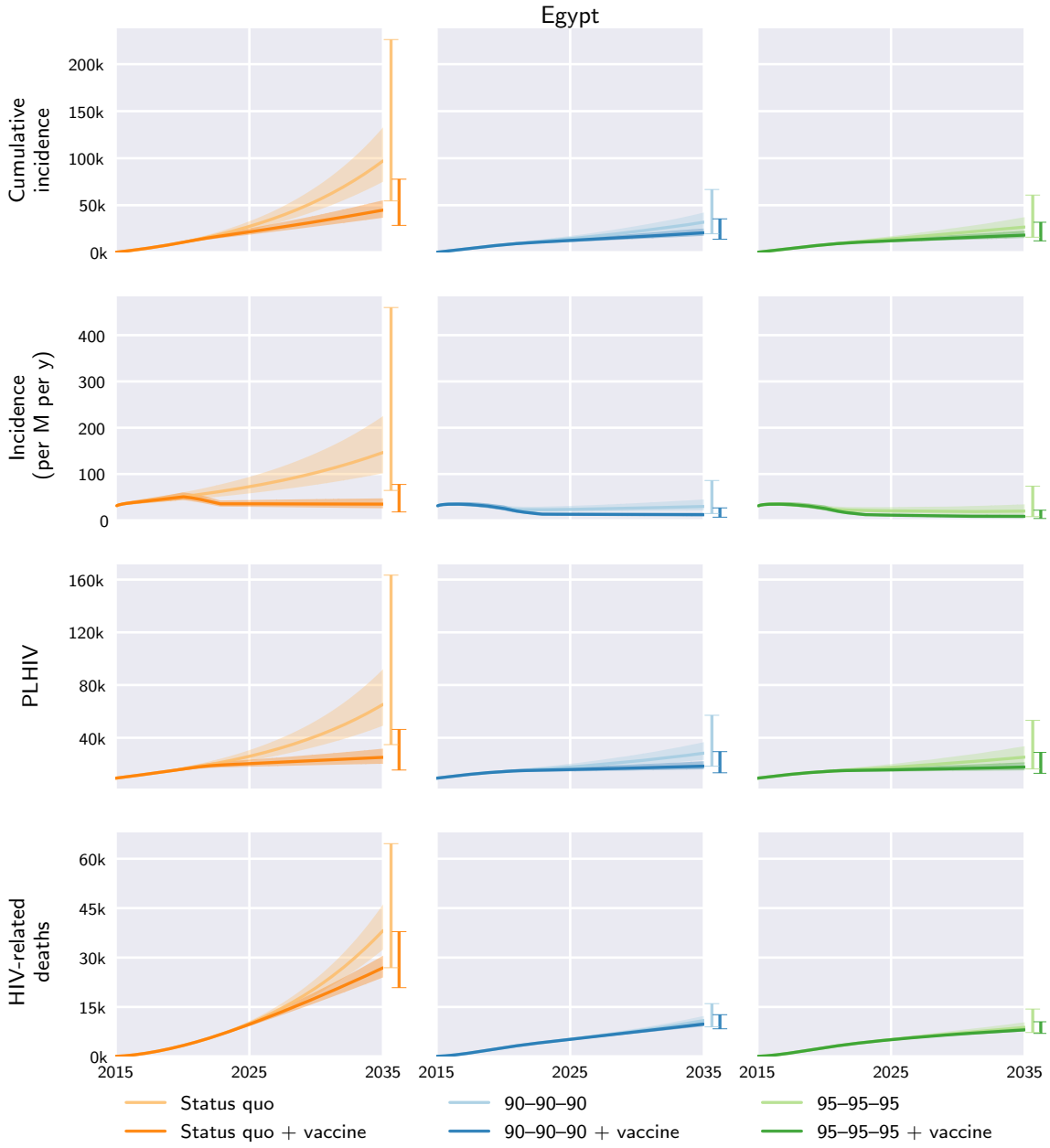

Fig. S52. Egypt model outcomes under the different diagnosis, treatment, and vaccination scenarios. Central curves show the medians over model runs with 1000 samples from parameter distributions, shaded regions show the 1st and 3rd quartiles (i.e. 25th and 75th percentiles), and vertical bars to the right of each axis show the 5th and 95th percentiles at the end time, 2035. Regional and global outcomes were aggregated from the country-level model outcomes.

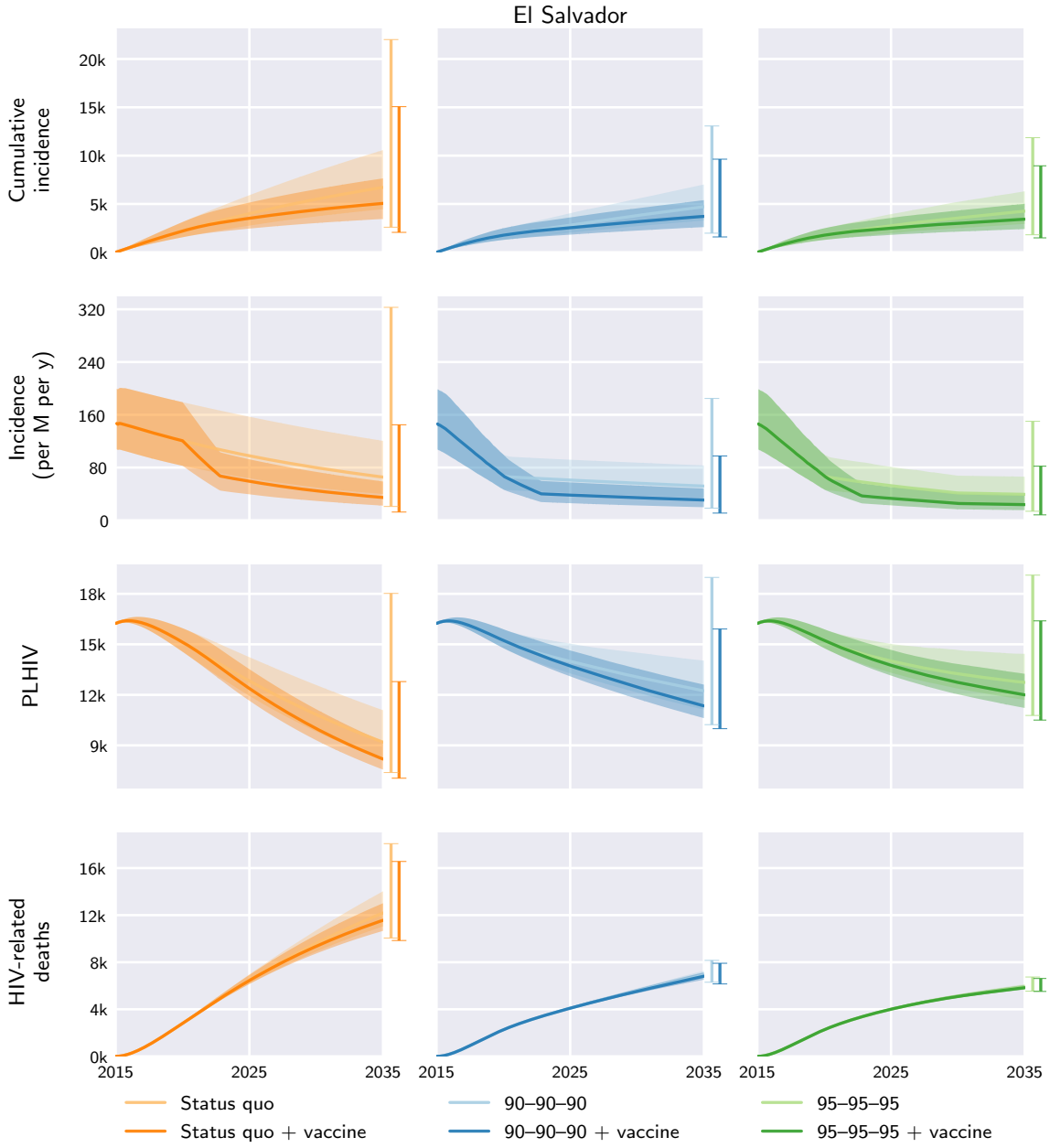

Fig. S53. El Salvador model outcomes under the different diagnosis, treatment, and vaccination scenarios. Central curves show the medians over model runs with 1000 samples from parameter distributions, shaded regions show the 1st and 3rd quartiles (i.e. 25th and 75th percentiles), and vertical bars to the right of each axis show the 5th and 95th percentiles at the end time, 2035. Regional and global outcomes were aggregated from the country-level model outcomes.

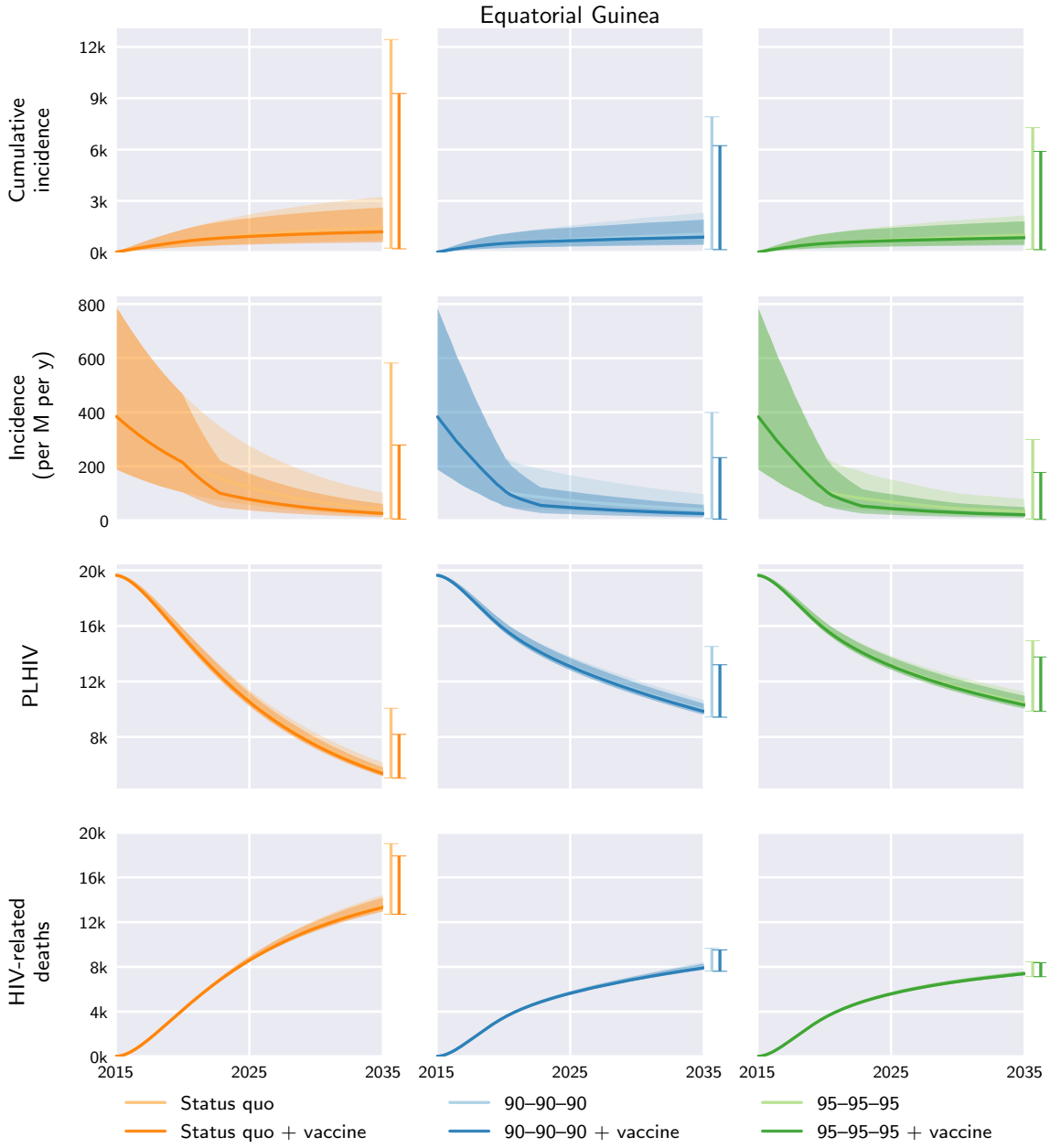

Fig. S54. Equatorial Guinea model outcomes under the different diagnosis, treatment, and vaccination scenarios. Central curves show the medians over model runs with 1000 samples from parameter distributions, shaded regions show the 1st and 3rd quartiles (i.e. 25th and 75th percentiles), and vertical bars to the right of each axis show the 5th and 95th percentiles at the end time, 2035. Regional and global outcomes were aggregated from the country-level model outcomes.

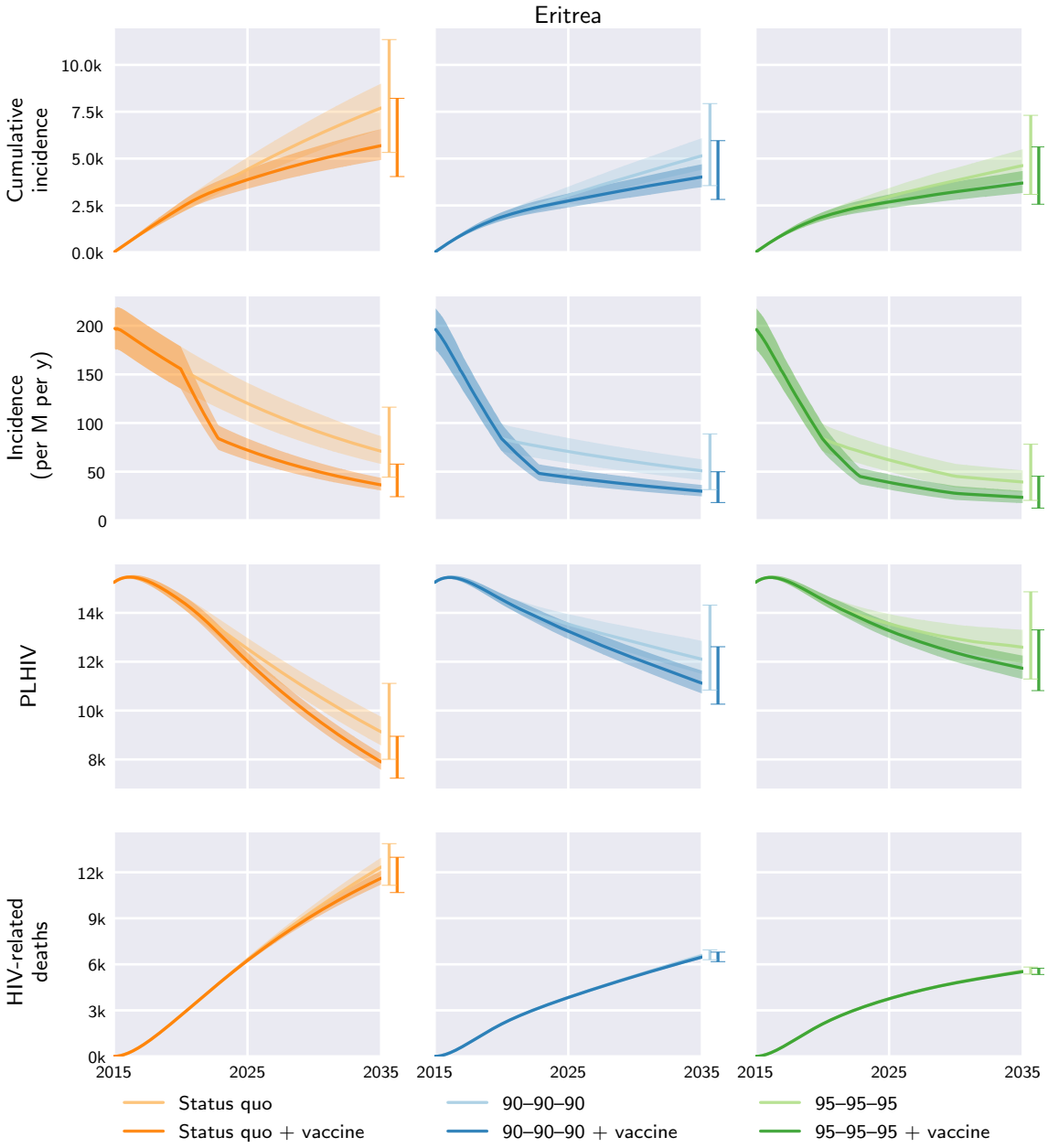

Fig. S55. Eritrea model outcomes under the different diagnosis, treatment, and vaccination scenarios. Central curves show the medians over model runs with 1000 samples from parameter distributions, shaded regions show the 1st and 3rd quartiles (i.e. 25th and 75th percentiles), and vertical bars to the right of each axis show the 5th and 95th percentiles at the end time, 2035. Regional and global outcomes were aggregated from the country-level model outcomes.

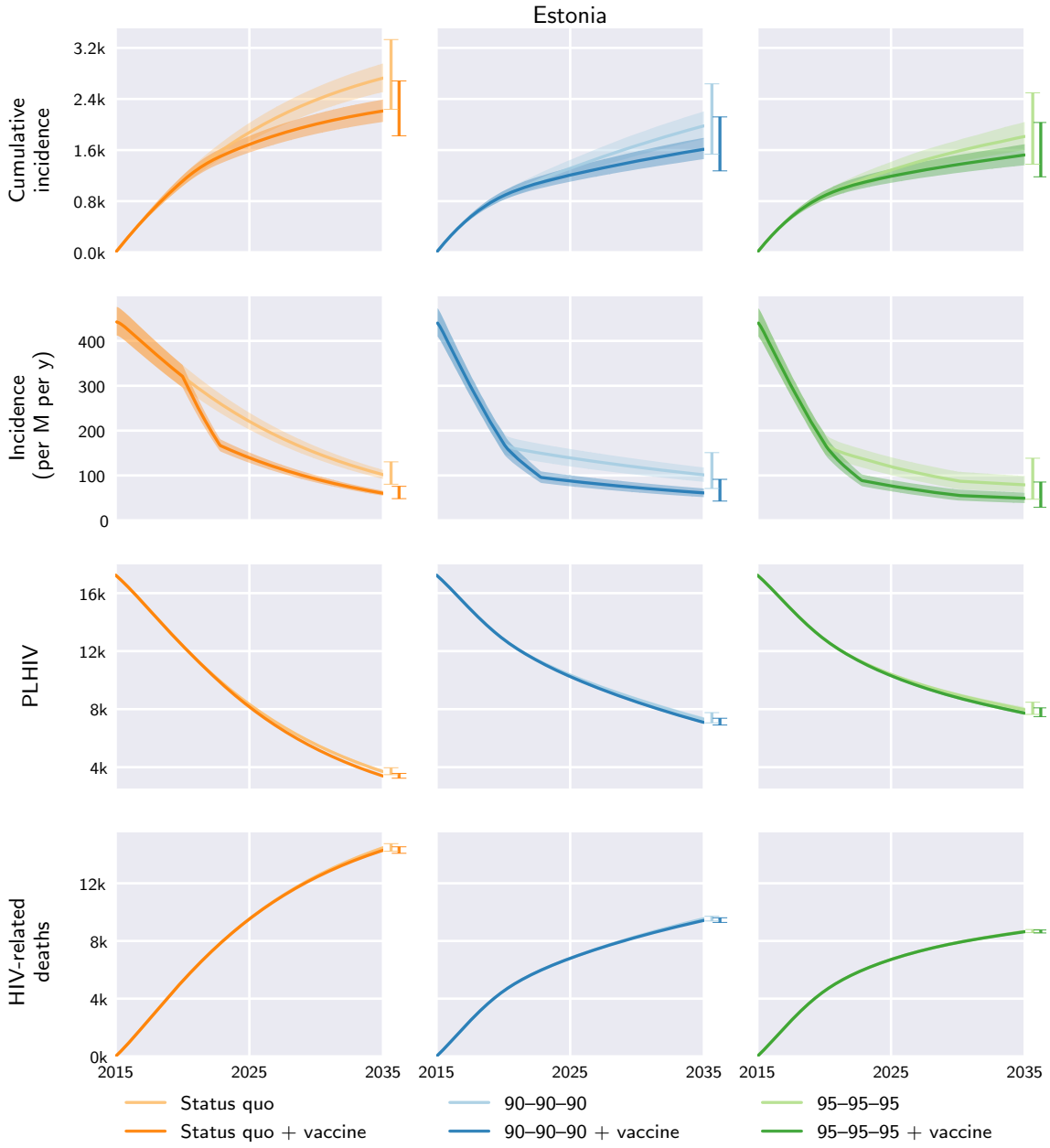

Fig. S56. Estonia model outcomes under the different diagnosis, treatment, and vaccination scenarios. Central curves show the medians over model runs with 1000 samples from parameter distributions, shaded regions show the 1st and 3rd quartiles (i.e. 25th and 75th percentiles), and vertical bars to the right of each axis show the 5th and 95th percentiles at the end time, 2035. Regional and global outcomes were aggregated from the country-level model outcomes.

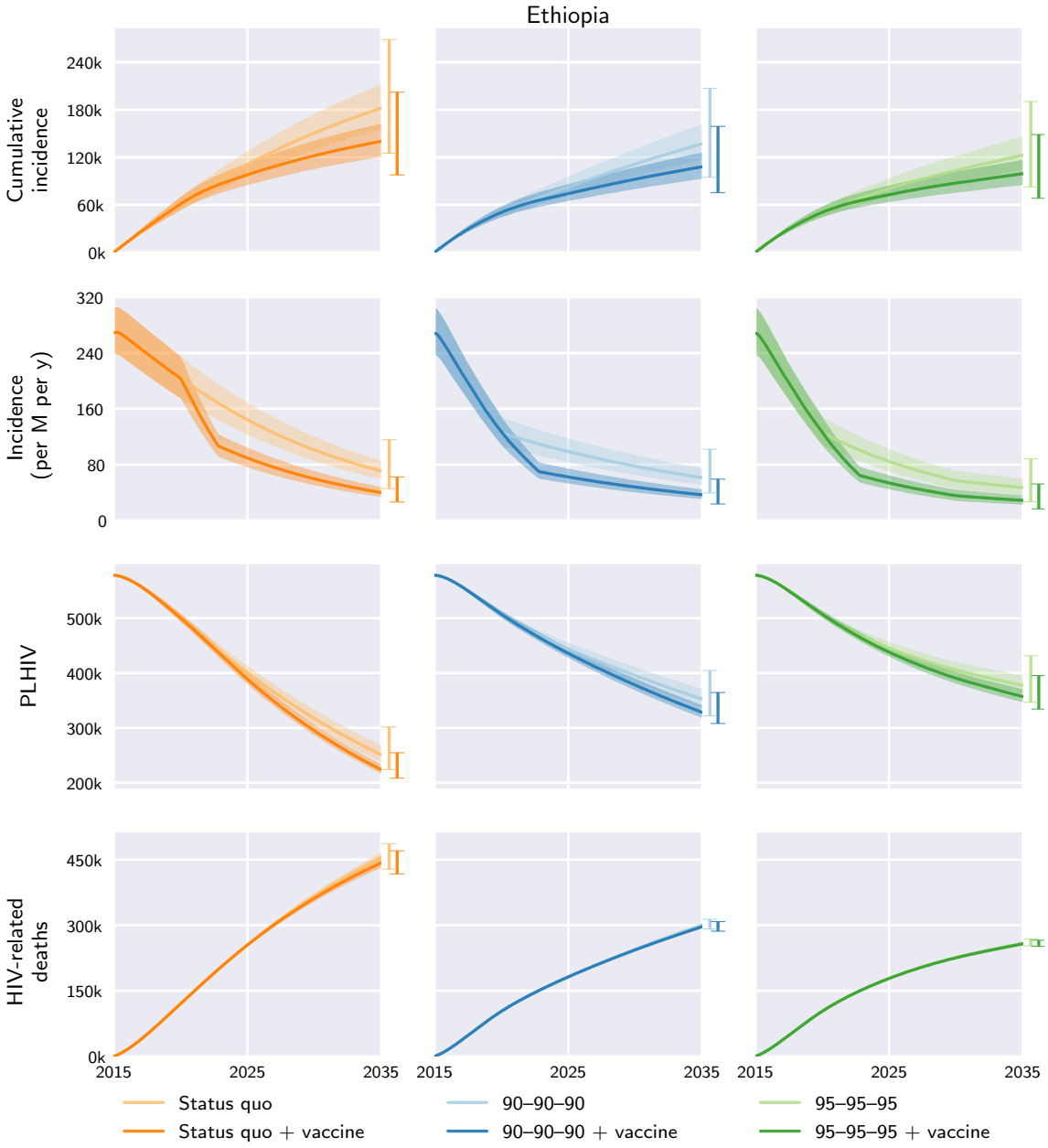

Fig. S57. Ethiopia model outcomes under the different diagnosis, treatment, and vaccination scenarios. Central curves show the medians over model runs with 1000 samples from parameter distributions, shaded regions show the 1st and 3rd quartiles (i.e. 25th and 75th percentiles), and vertical bars to the right of each axis show the 5th and 95th percentiles at the end time, 2035. Regional and global outcomes were aggregated from the country-level model outcomes.

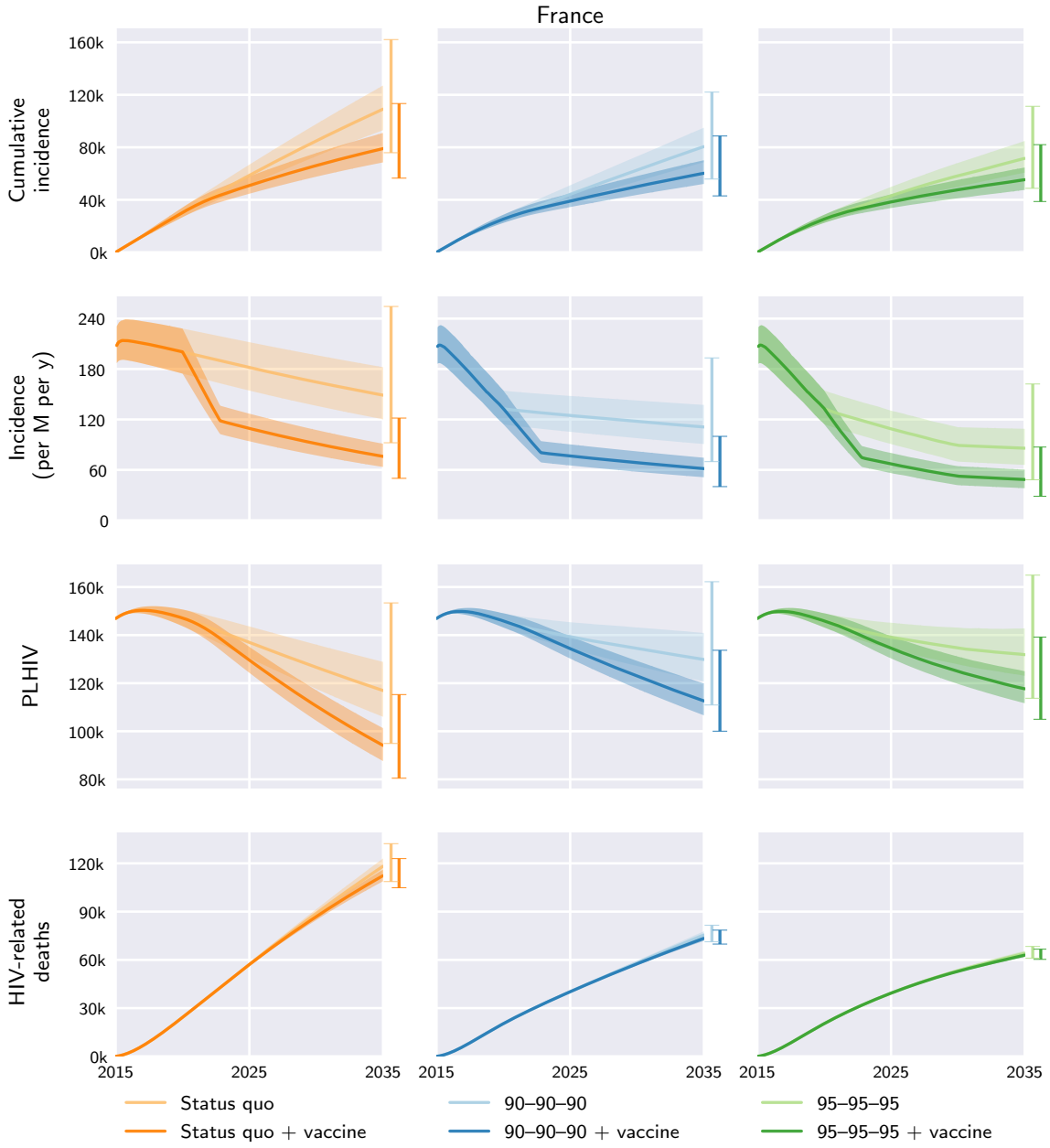

Fig. S58. France model outcomes under the different diagnosis, treatment, and vaccination scenarios. Central curves show the medians over model runs with 1000 samples from parameter distributions, shaded regions show the 1st and 3rd quartiles (i.e. 25th and 75th percentiles), and vertical bars to the right of each axis show the 5th and 95th percentiles at the end time, 2035. Regional and global outcomes were aggregated from the country-level model outcomes.

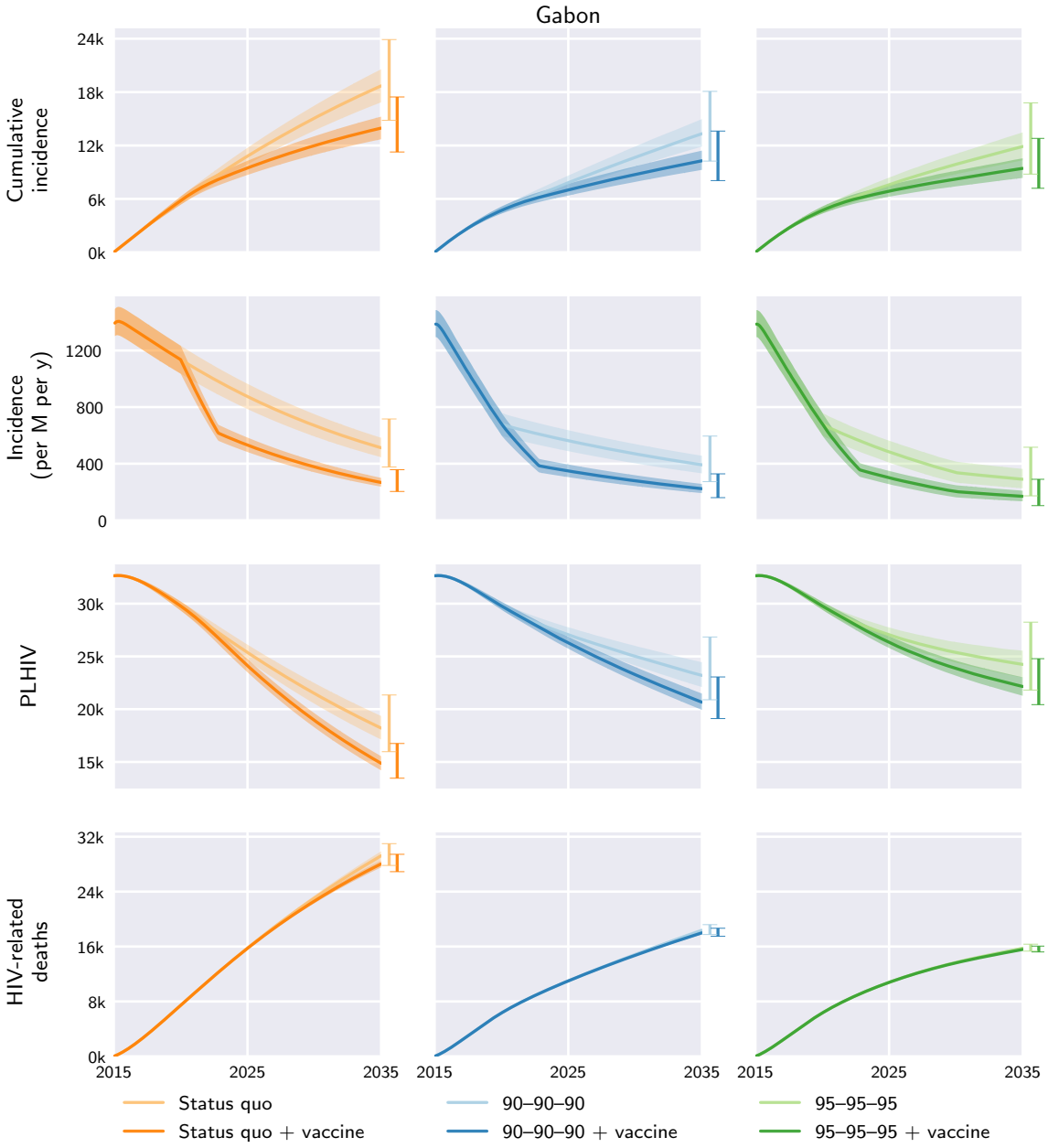

Fig. S59. Gabon model outcomes under the different diagnosis, treatment, and vaccination scenarios. Central curves show the medians over model runs with 1000 samples from parameter distributions, shaded regions show the 1st and 3rd quartiles (i.e. 25th and 75th percentiles), and vertical bars to the right of each axis show the 5th and 95th percentiles at the end time, 2035. Regional and global outcomes were aggregated from the country-level model outcomes.

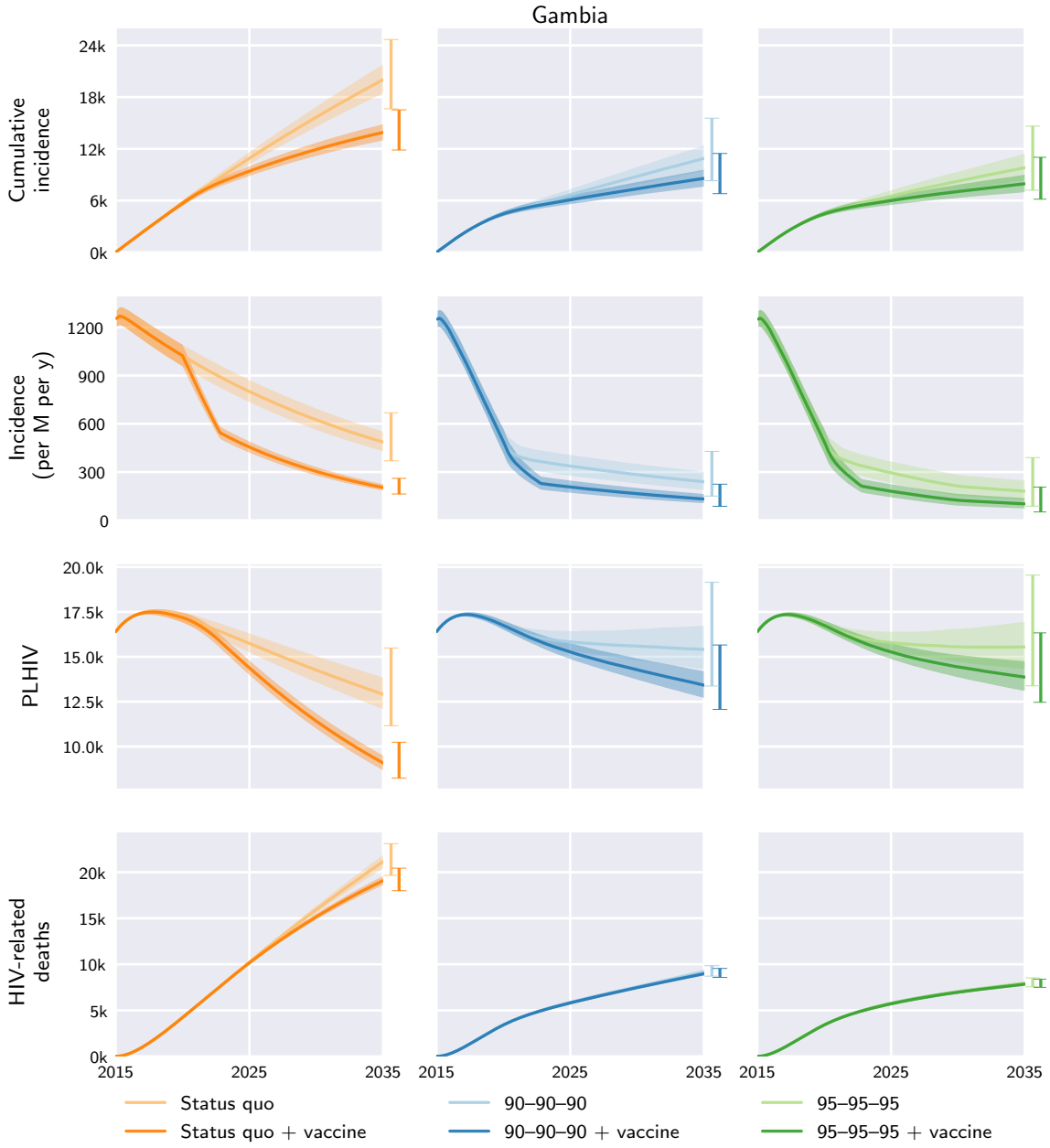

Fig. S60. Gambia model outcomes under the different diagnosis, treatment, and vaccination scenarios. Central curves show the medians over model runs with 1000 samples from parameter distributions, shaded regions show the 1st and 3rd quartiles (i.e. 25th and 75th percentiles), and vertical bars to the right of each axis show the 5th and 95th percentiles at the end time, 2035. Regional and global outcomes were aggregated from the country-level model outcomes.

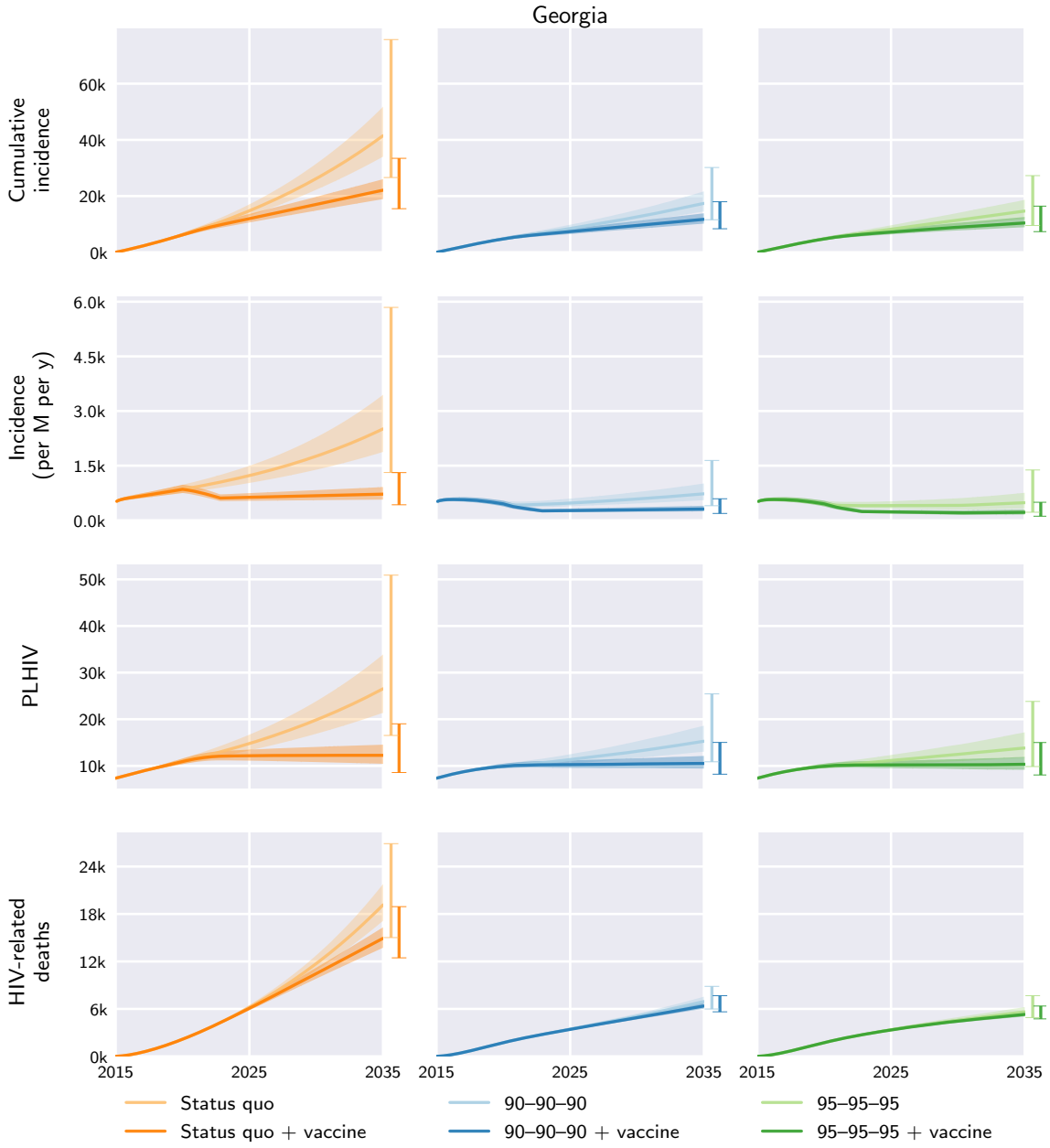

Fig. S61. Georgia model outcomes under the different diagnosis, treatment, and vaccination scenarios. Central curves show the medians over model runs with 1000 samples from parameter distributions, shaded regions show the 1st and 3rd quartiles (i.e. 25th and 75th percentiles), and vertical bars to the right of each axis show the 5th and 95th percentiles at the end time, 2035. Regional and global outcomes were aggregated from the country-level model outcomes.

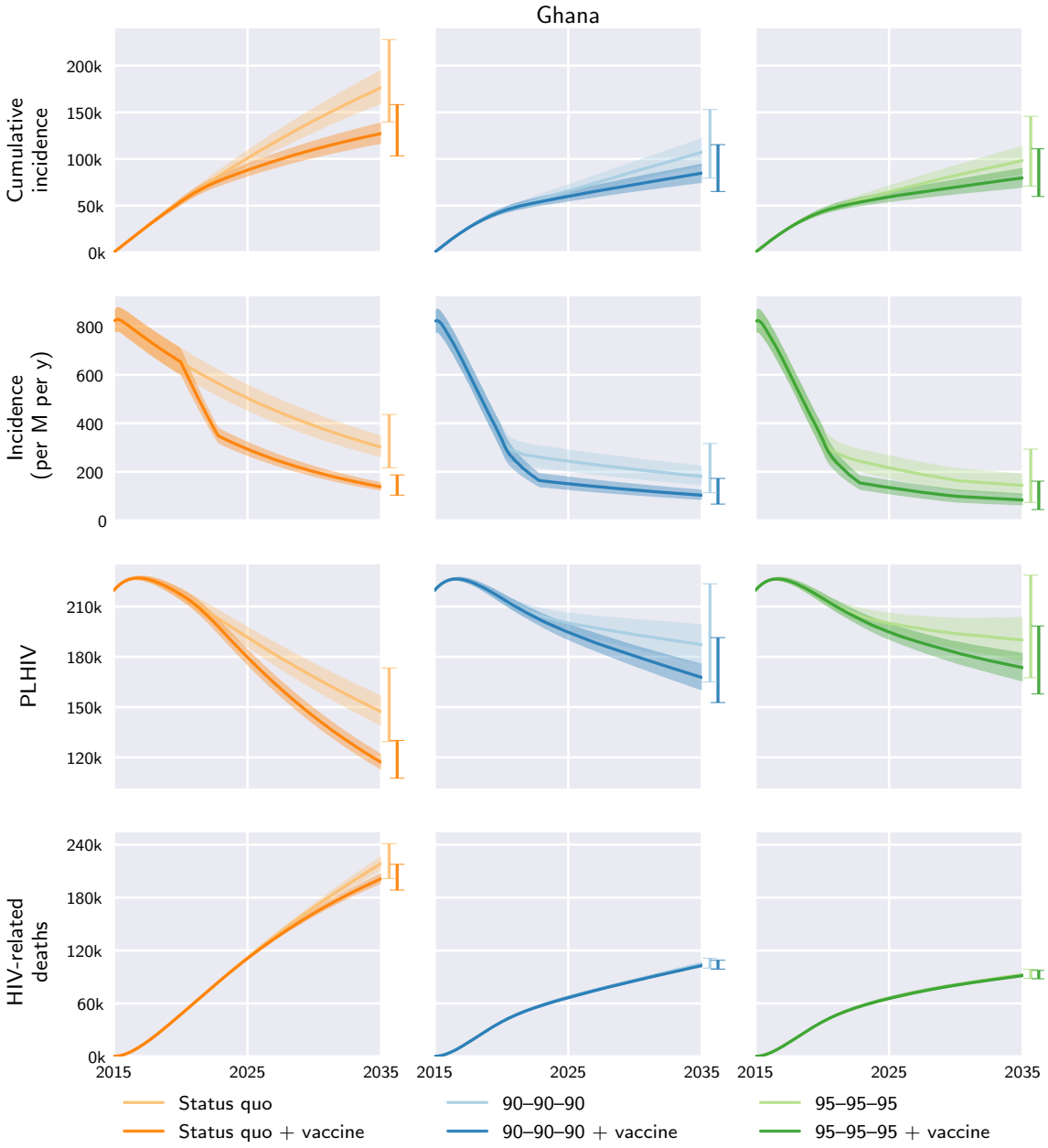

Fig. S62. Ghana model outcomes under the different diagnosis, treatment, and vaccination scenarios. Central curves show the medians over model runs with 1000 samples from parameter distributions, shaded regions show the 1st and 3rd quartiles (i.e. 25th and 75th percentiles), and vertical bars to the right of each axis show the 5th and 95th percentiles at the end time, 2035. Regional and global outcomes were aggregated from the country-level model outcomes.

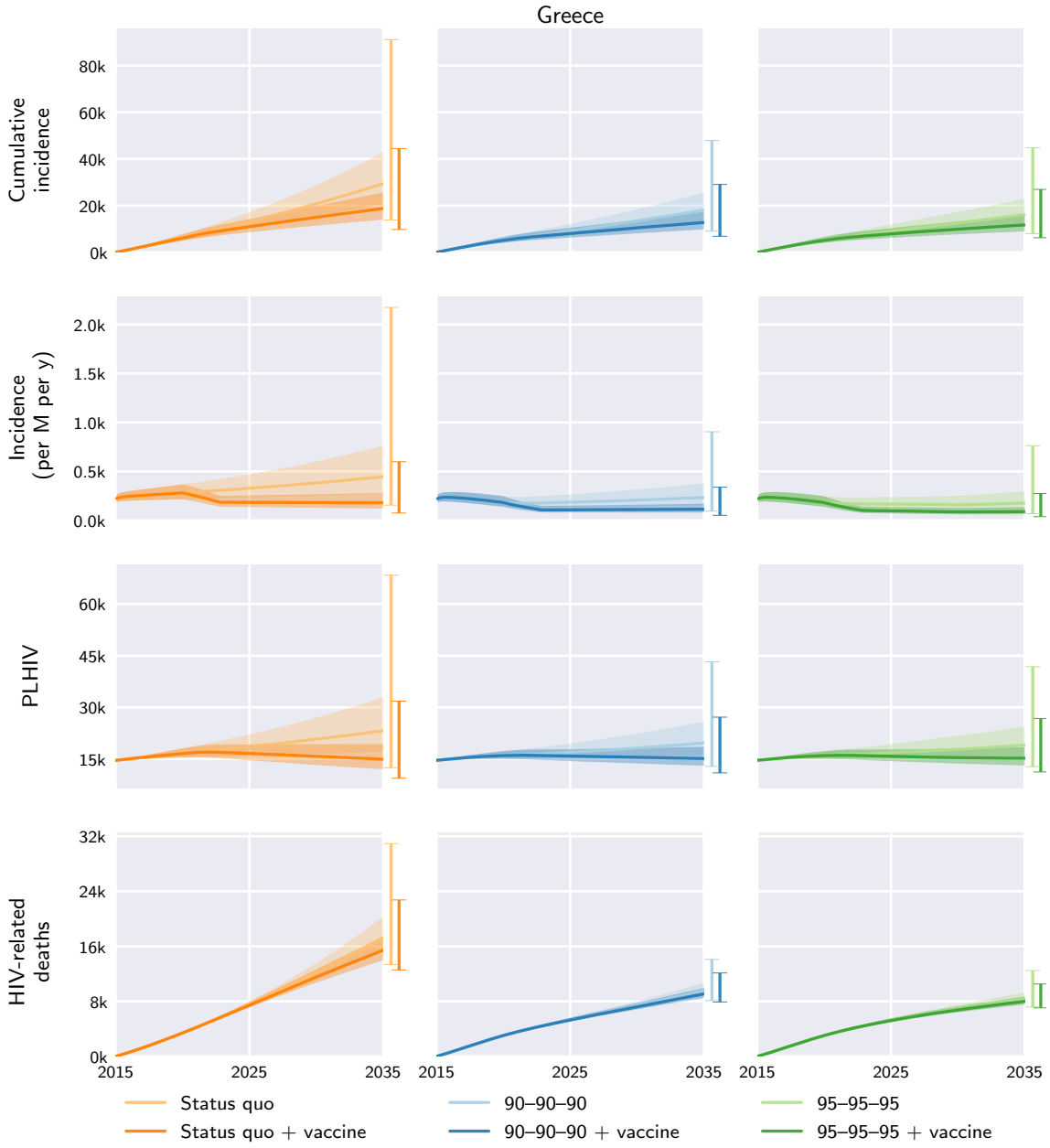

Fig. S63. Greece model outcomes under the different diagnosis, treatment, and vaccination scenarios. Central curves show the medians over model runs with 1000 samples from parameter distributions, shaded regions show the 1st and 3rd quartiles (i.e. 25th and 75th percentiles), and vertical bars to the right of each axis show the 5th and 95th percentiles at the end time, 2035. Regional and global outcomes were aggregated from the country-level model outcomes.

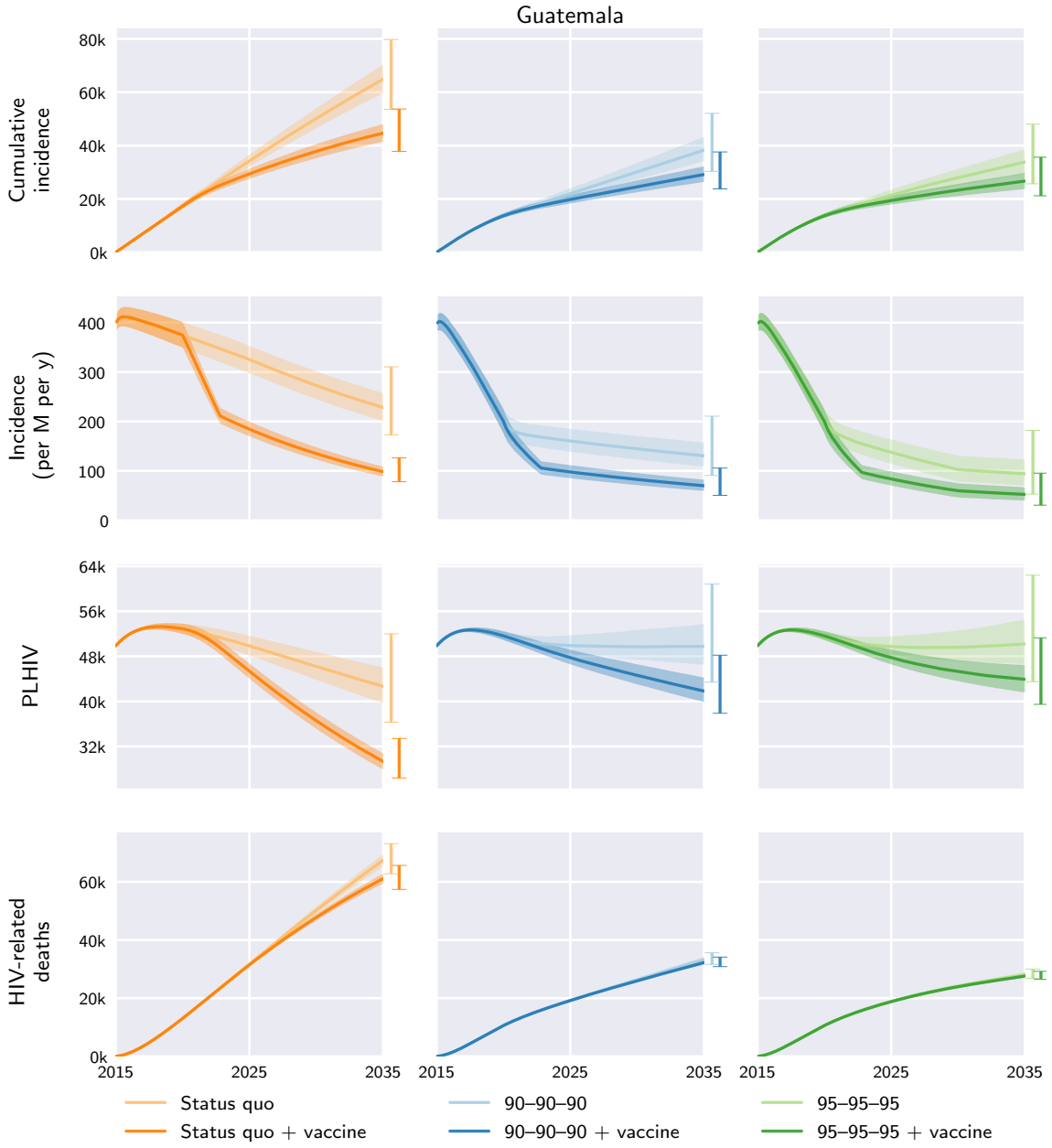

Fig. S64. Guatemala model outcomes under the different diagnosis, treatment, and vaccination scenarios. Central curves show the medians over model runs with 1000 samples from parameter distributions, shaded regions show the 1st and 3rd quartiles (i.e. 25th and 75th percentiles), and vertical bars to the right of each axis show the 5th and 95th percentiles at the end time, 2035. Regional and global outcomes were aggregated from the country-level model outcomes.

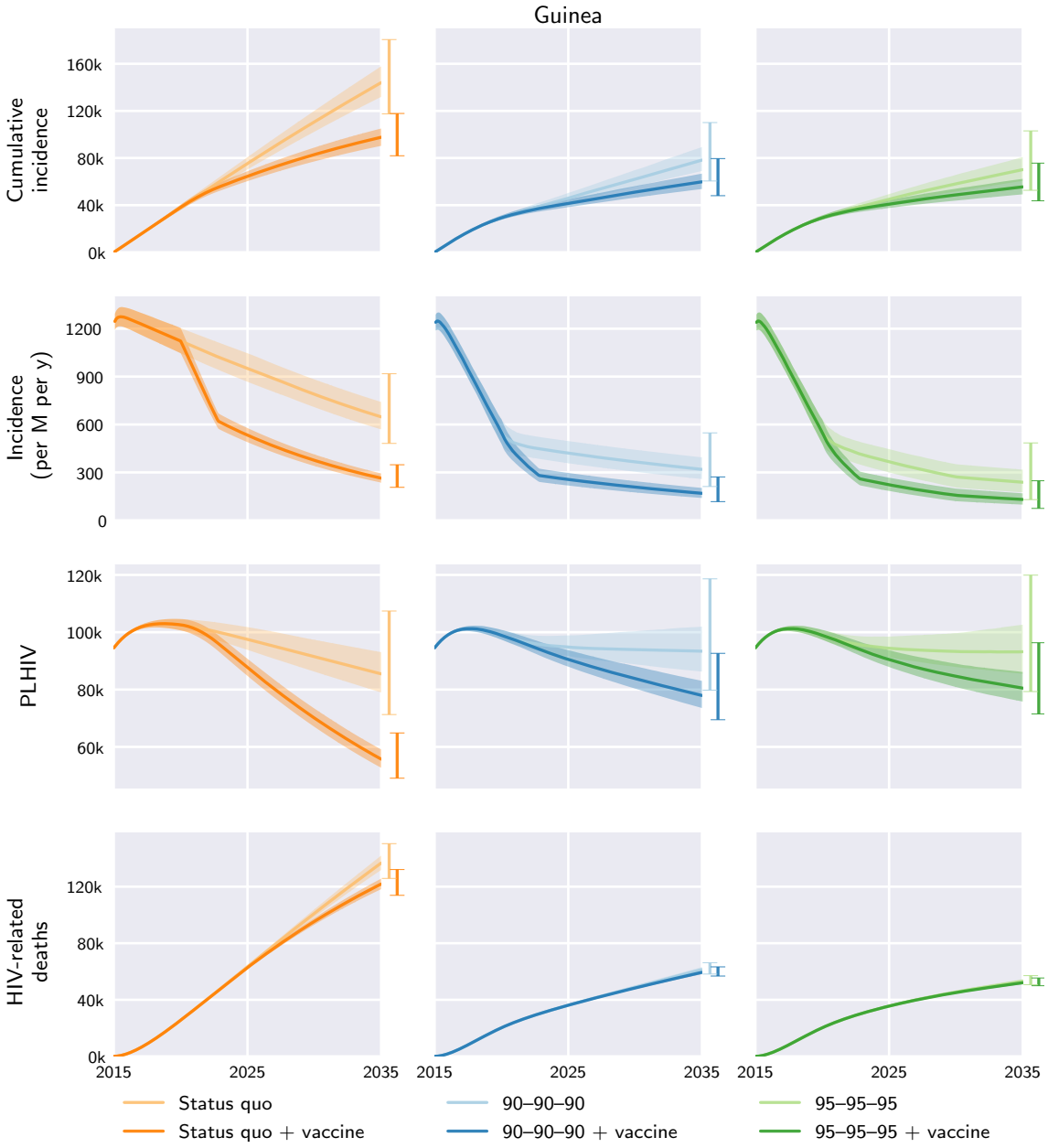

Fig. S65. Guinea model outcomes under the different diagnosis, treatment, and vaccination scenarios. Central curves show the medians over model runs with 1000 samples from parameter distributions, shaded regions show the 1st and 3rd quartiles (i.e. 25th and 75th percentiles), and vertical bars to the right of each axis show the 5th and 95th percentiles at the end time, 2035. Regional and global outcomes were aggregated from the country-level model outcomes.

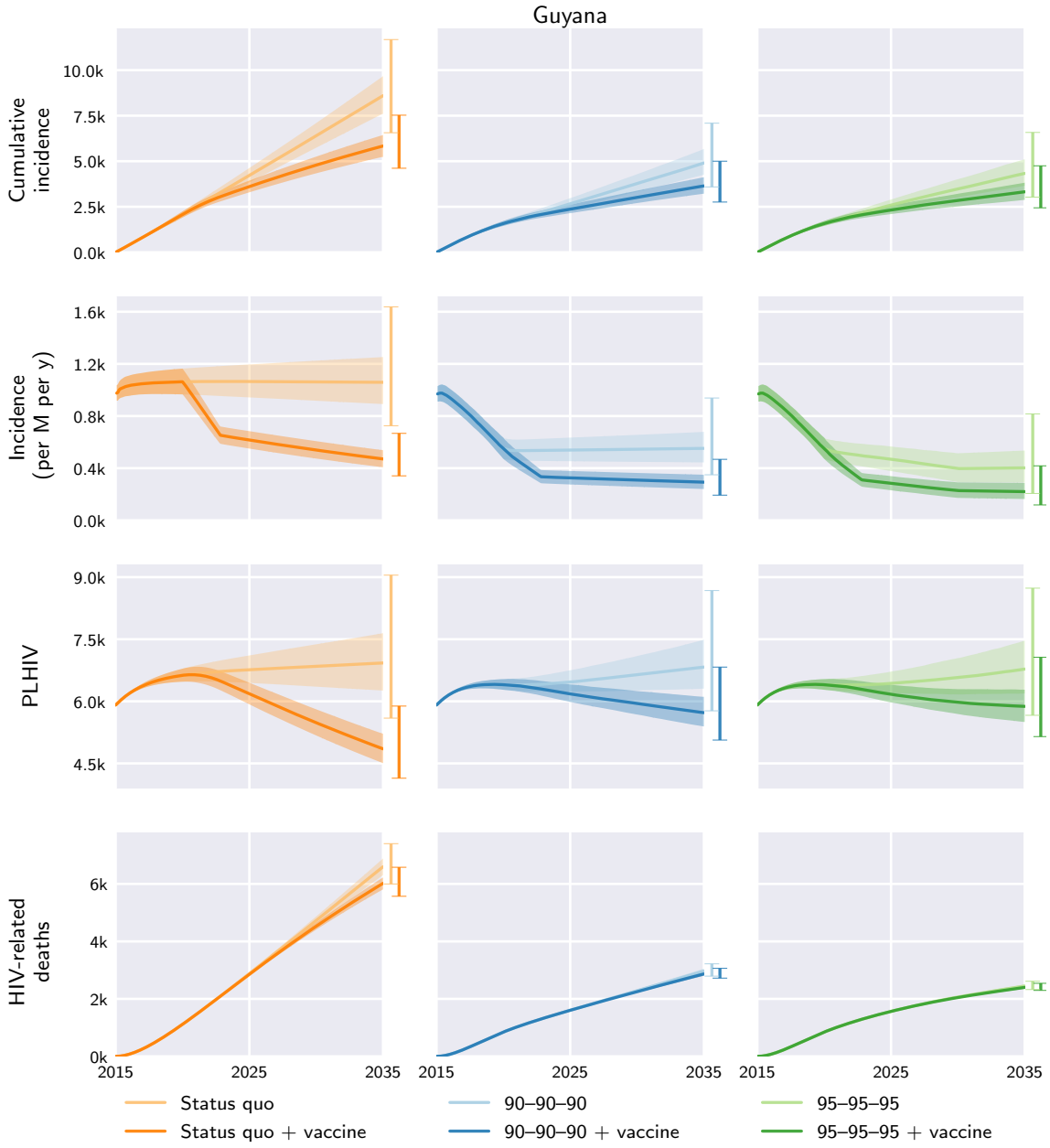

Fig. S66. Guyana model outcomes under the different diagnosis, treatment, and vaccination scenarios. Central curves show the medians over model runs with 1000 samples from parameter distributions, shaded regions show the 1st and 3rd quartiles (i.e. 25th and 75th percentiles), and vertical bars to the right of each axis show the 5th and 95th percentiles at the end time, 2035. Regional and global outcomes were aggregated from the country-level model outcomes.

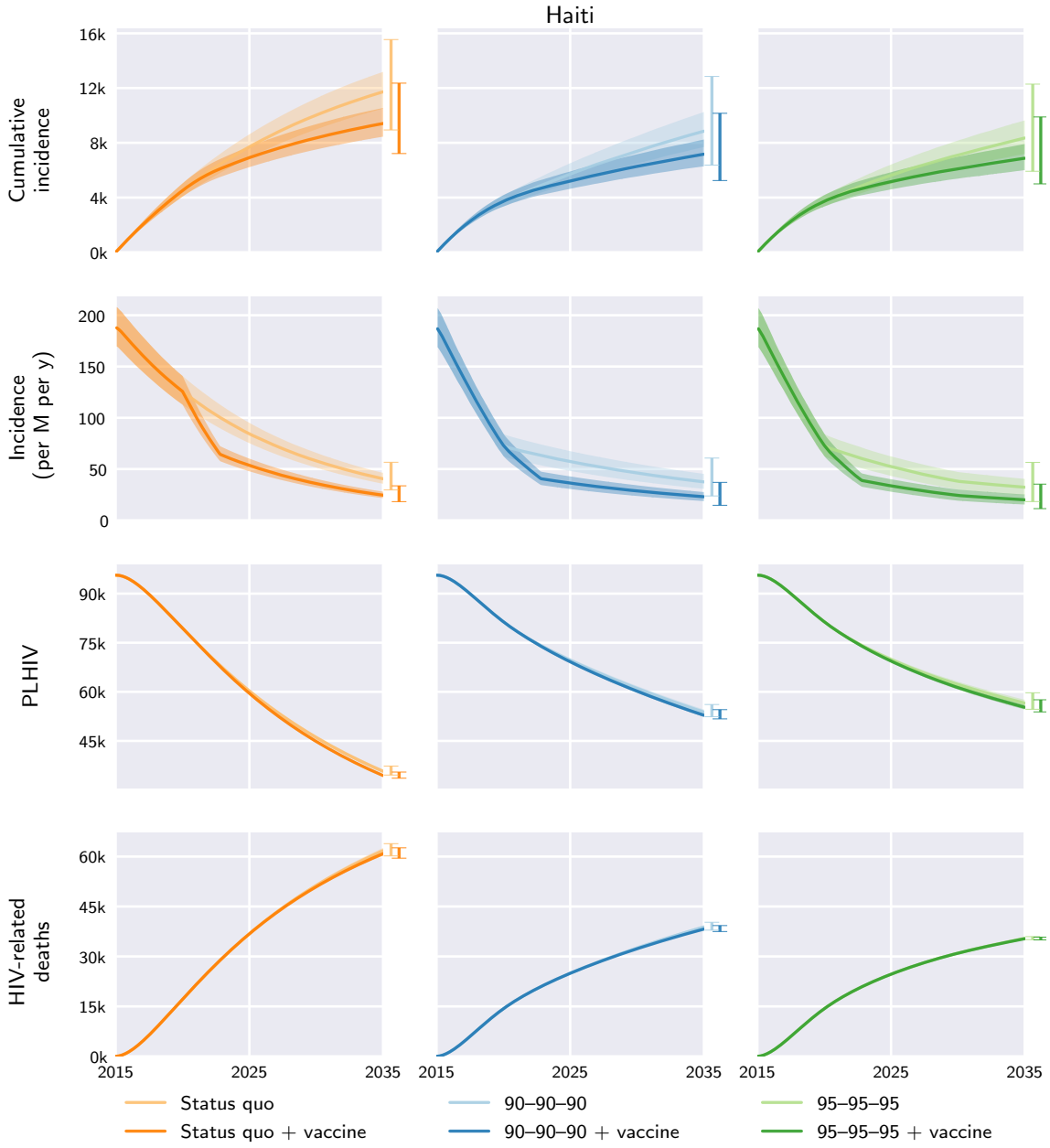

Fig. S67. Haiti model outcomes under the different diagnosis, treatment, and vaccination scenarios. Central curves show the medians over model runs with 1000 samples from parameter distributions, shaded regions show the 1st and 3rd quartiles (i.e. 25th and 75th percentiles), and vertical bars to the right of each axis show the 5th and 95th percentiles at the end time, 2035. Regional and global outcomes were aggregated from the country-level model outcomes.

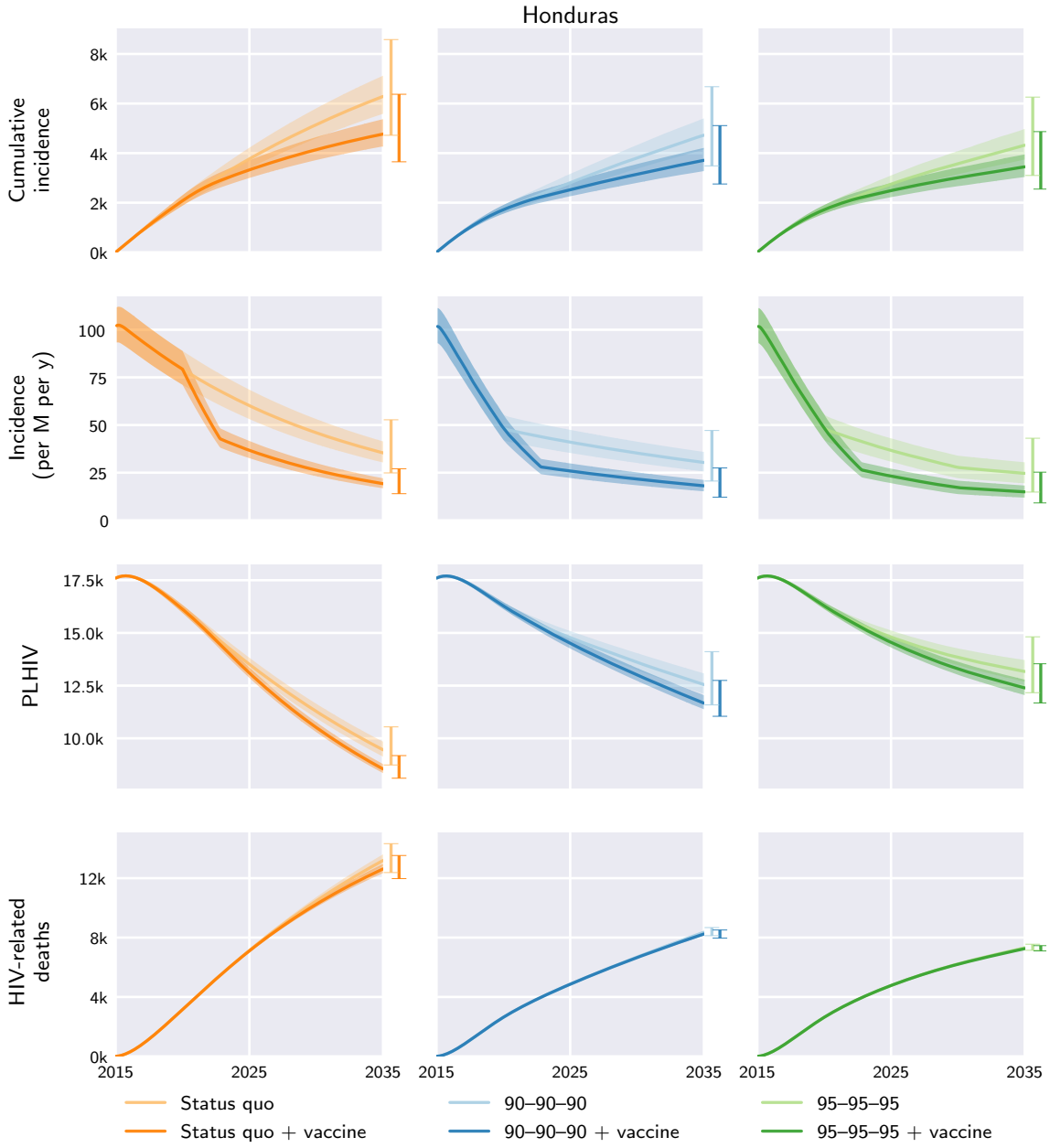

Fig. S68. Honduras model outcomes under the different diagnosis, treatment, and vaccination scenarios. Central curves show the medians over model runs with 1000 samples from parameter distributions, shaded regions show the 1st and 3rd quartiles (i.e. 25th and 75th percentiles), and vertical bars to the right of each axis show the 5th and 95th percentiles at the end time, 2035. Regional and global outcomes were aggregated from the country-level model outcomes.

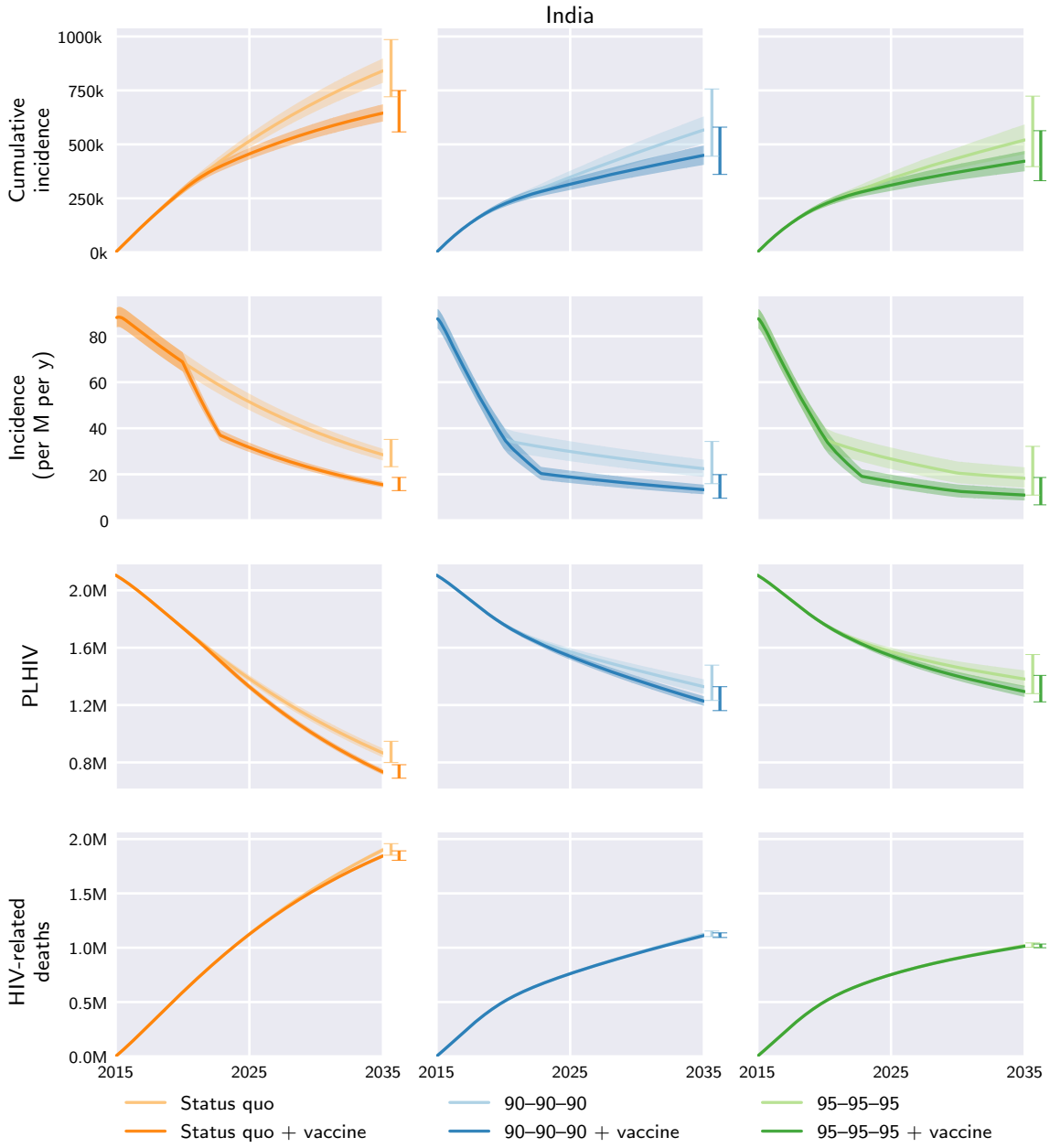

Fig. S69. India model outcomes under the different diagnosis, treatment, and vaccination scenarios. Central curves show the medians over model runs with 1000 samples from parameter distributions, shaded regions show the 1st and 3rd quartiles (i.e. 25th and 75th percentiles), and vertical bars to the right of each axis show the 5th and 95th percentiles at the end time, 2035. Regional and global outcomes were aggregated from the country-level model outcomes.

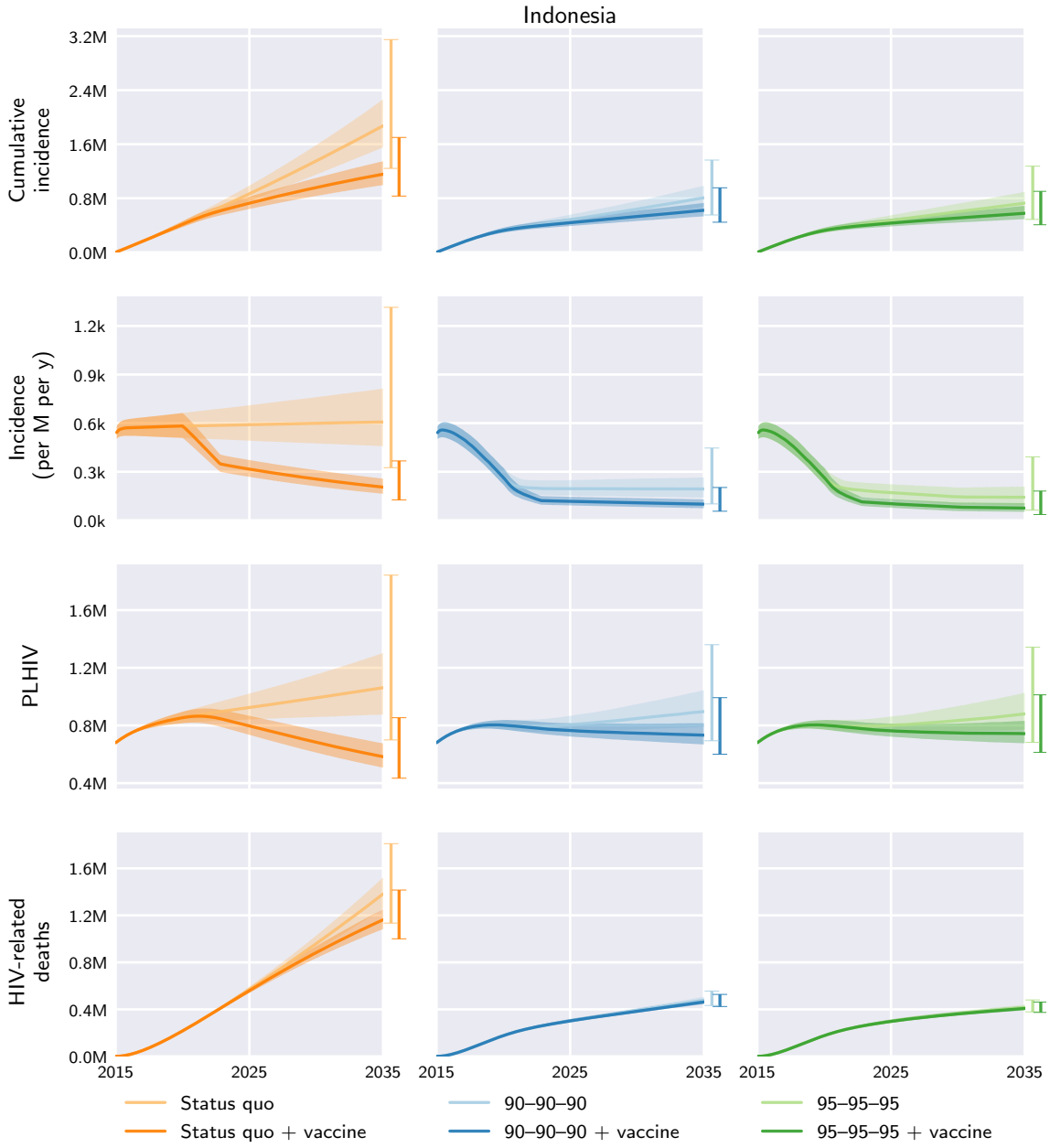

Fig. S70. Indonesia model outcomes under the different diagnosis, treatment, and vaccination scenarios. Central curves show the medians over model runs with 1000 samples from parameter distributions, shaded regions show the 1st and 3rd quartiles (i.e. 25th and 75th percentiles), and vertical bars to the right of each axis show the 5th and 95th percentiles at the end time, 2035. Regional and global outcomes were aggregated from the country-level model outcomes.

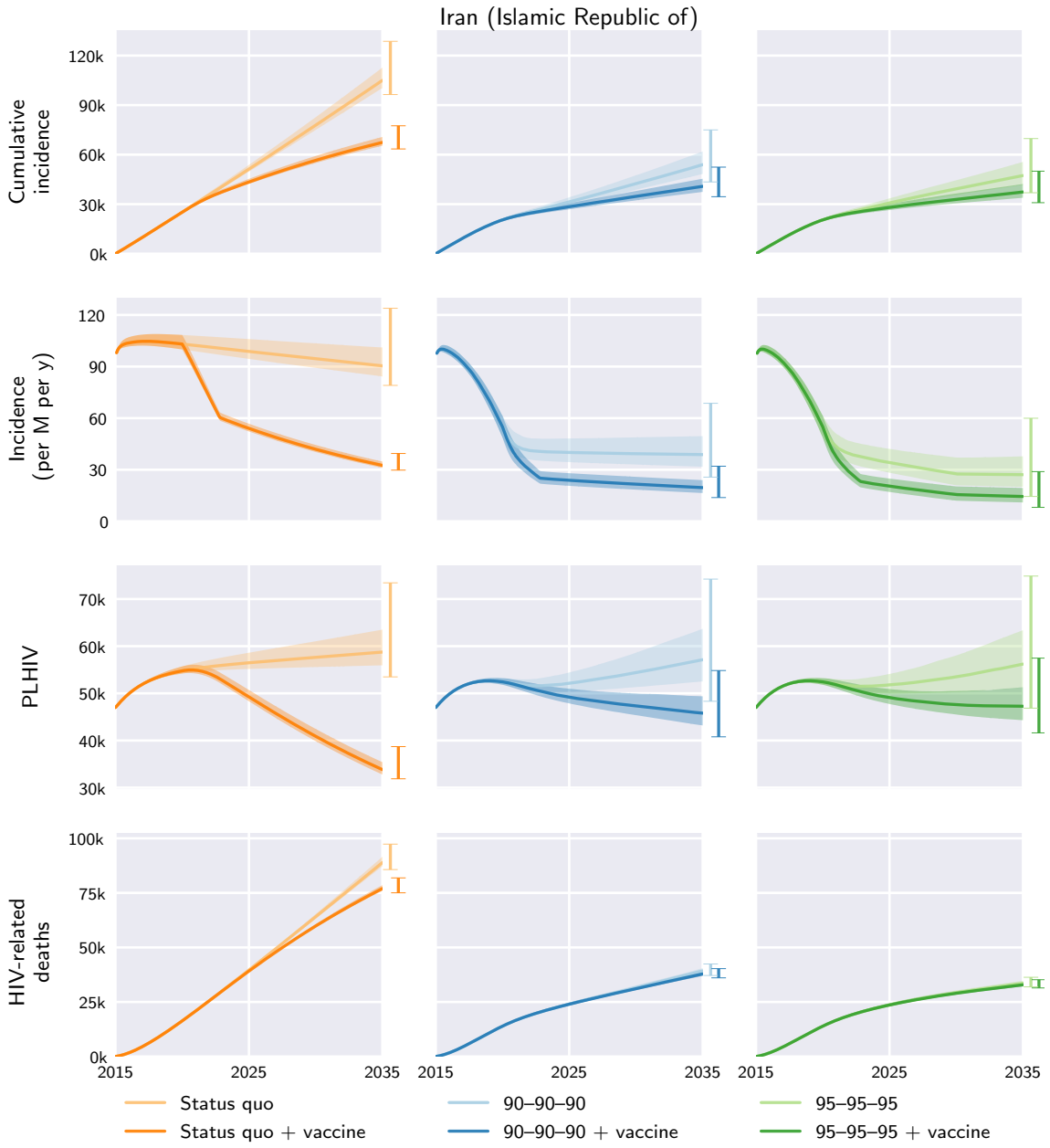

Fig. S71. Iran (Islamic Republic of) model outcomes under the different diagnosis, treatment, and vaccination scenarios. Central curves show the medians over model runs with 1000 samples from parameter distributions, shaded regions show the 1st and 3rd quartiles (i.e. 25th and 75th percentiles), and vertical bars to the right of each axis show the 5th and 95th percentiles at the end time, 2035. Regional and global outcomes were aggregated from the country-level model outcomes.

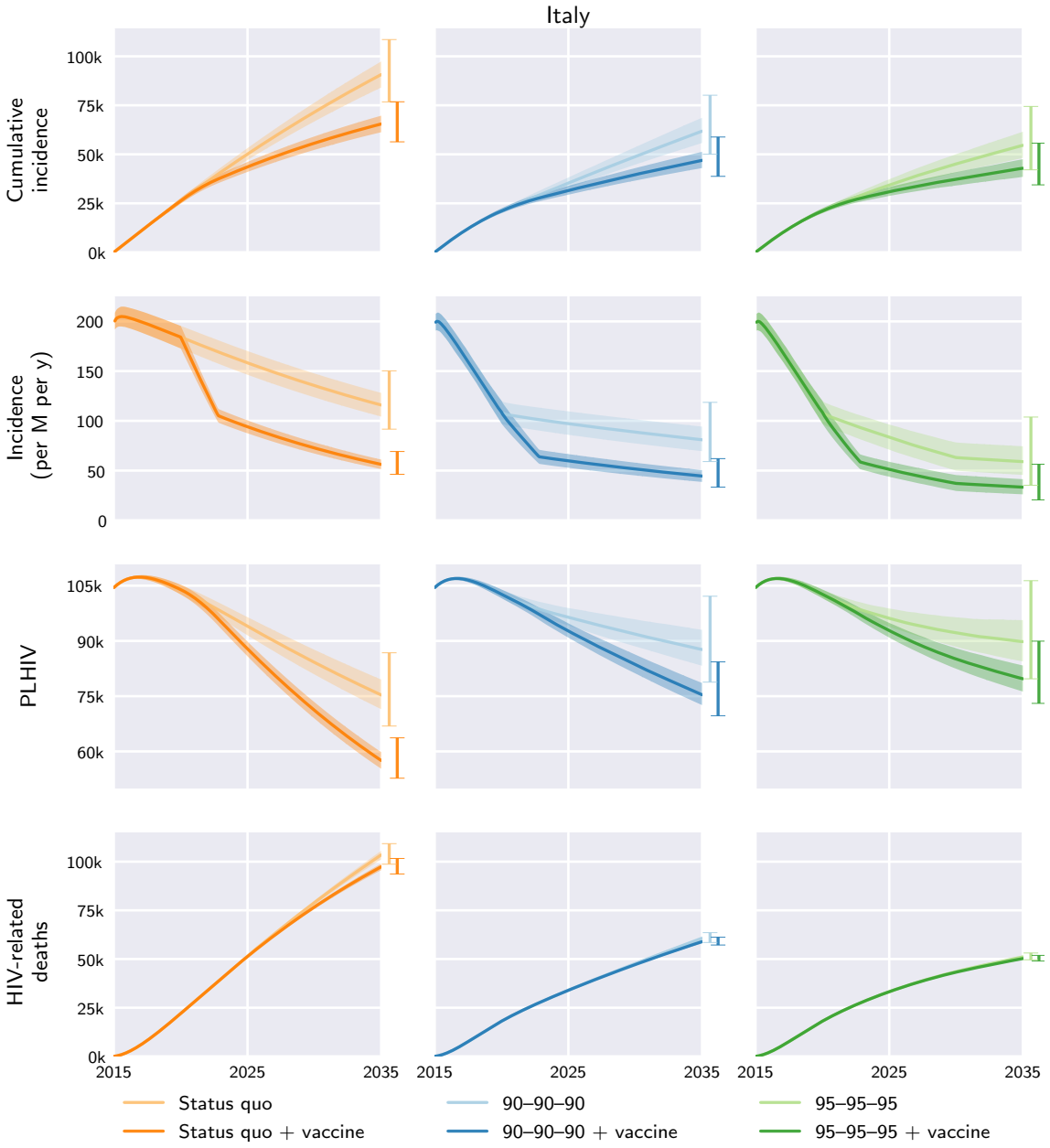

Fig. S72. Italy model outcomes under the different diagnosis, treatment, and vaccination scenarios. Central curves show the medians over model runs with 1000 samples from parameter distributions, shaded regions show the 1st and 3rd quartiles (i.e. 25th and 75th percentiles), and vertical bars to the right of each axis show the 5th and 95th percentiles at the end time, 2035. Regional and global outcomes were aggregated from the country-level model outcomes.

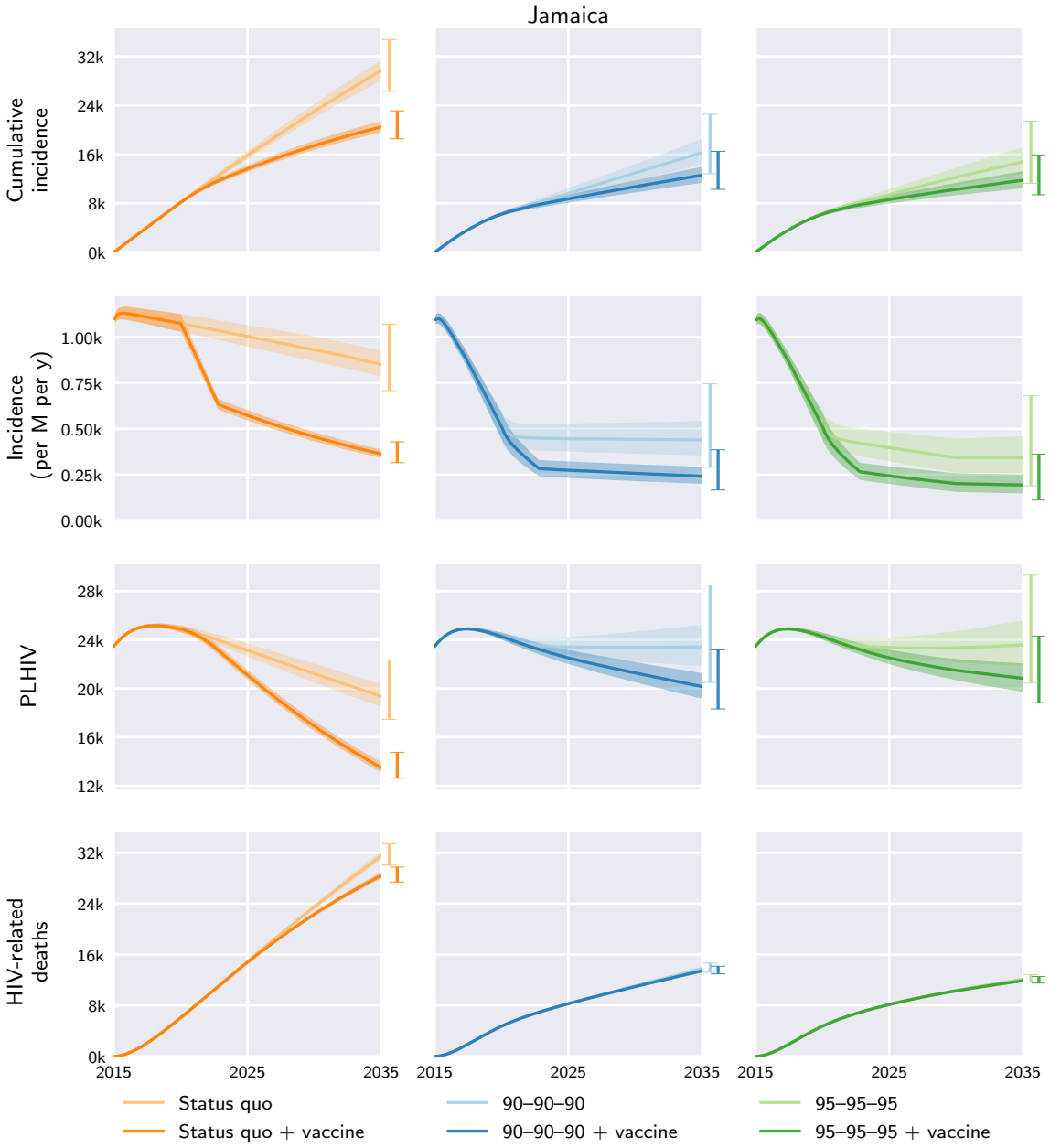

Fig. S73. Jamaica model outcomes under the different diagnosis, treatment, and vaccination scenarios. Central curves show the medians over model runs with 1000 samples from parameter distributions, shaded regions show the 1st and 3rd quartiles (i.e. 25th and 75th percentiles), and vertical bars to the right of each axis show the 5th and 95th percentiles at the end time, 2035. Regional and global outcomes were aggregated from the country-level model outcomes.

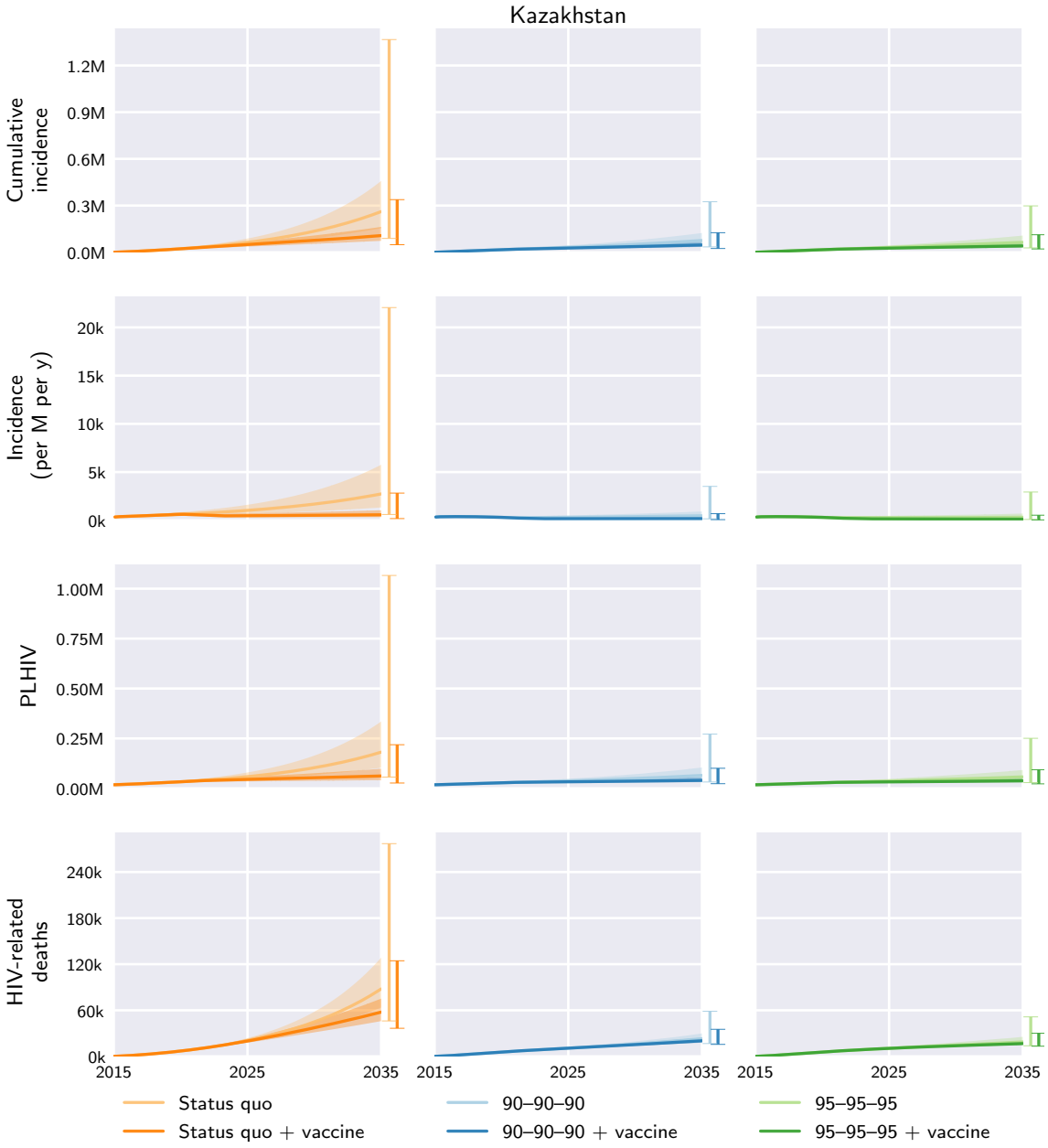

Fig. S74. Kazakhstan model outcomes under the different diagnosis, treatment, and vaccination scenarios. Central curves show the medians over model runs with 1000 samples from parameter distributions, shaded regions show the 1st and 3rd quartiles (i.e. 25th and 75th percentiles), and vertical bars to the right of each axis show the 5th and 95th percentiles at the end time, 2035. Regional and global outcomes were aggregated from the country-level model outcomes.

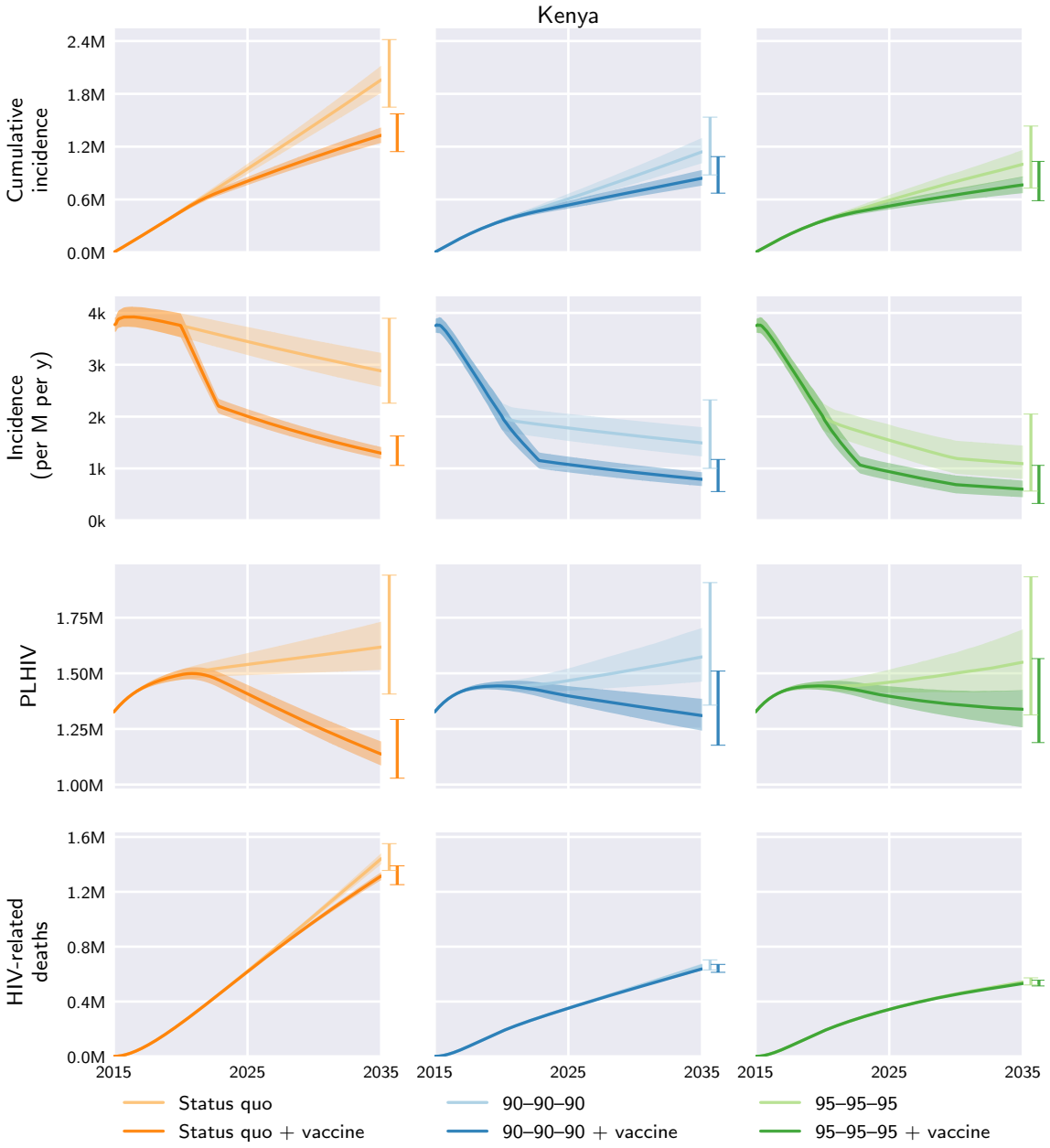

Fig. S75. Kenya model outcomes under the different diagnosis, treatment, and vaccination scenarios. Central curves show the medians over model runs with 1000 samples from parameter distributions, shaded regions show the 1st and 3rd quartiles (i.e. 25th and 75th percentiles), and vertical bars to the right of each axis show the 5th and 95th percentiles at the end time, 2035. Regional and global outcomes were aggregated from the country-level model outcomes.

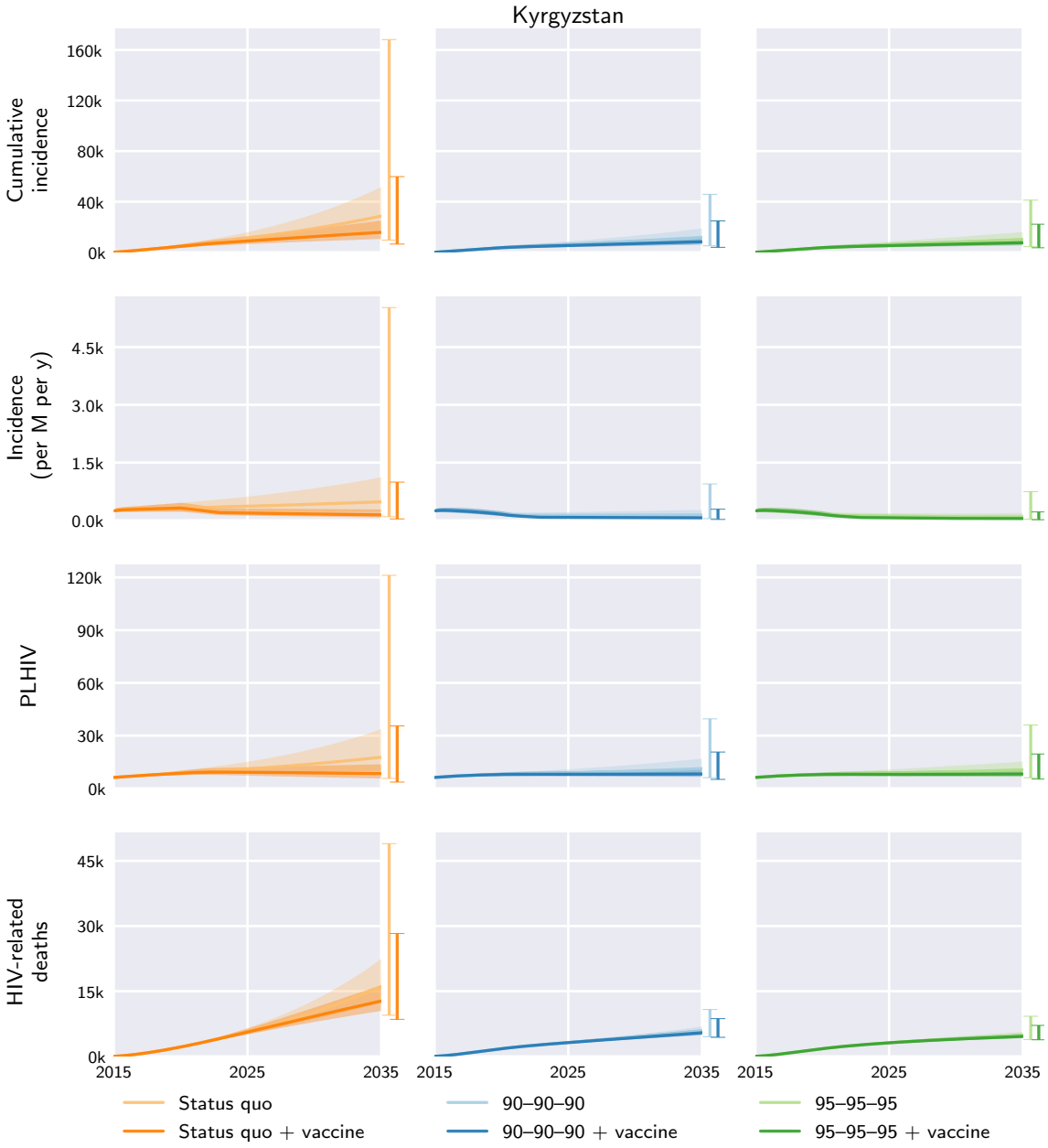

Fig. S76. Kyrgyzstan model outcomes under the different diagnosis, treatment, and vaccination scenarios. Central curves show the medians over model runs with 1000 samples from parameter distributions, shaded regions show the 1st and 3rd quartiles (i.e. 25th and 75th percentiles), and vertical bars to the right of each axis show the 5th and 95th percentiles at the end time, 2035. Regional and global outcomes were aggregated from the country-level model outcomes.

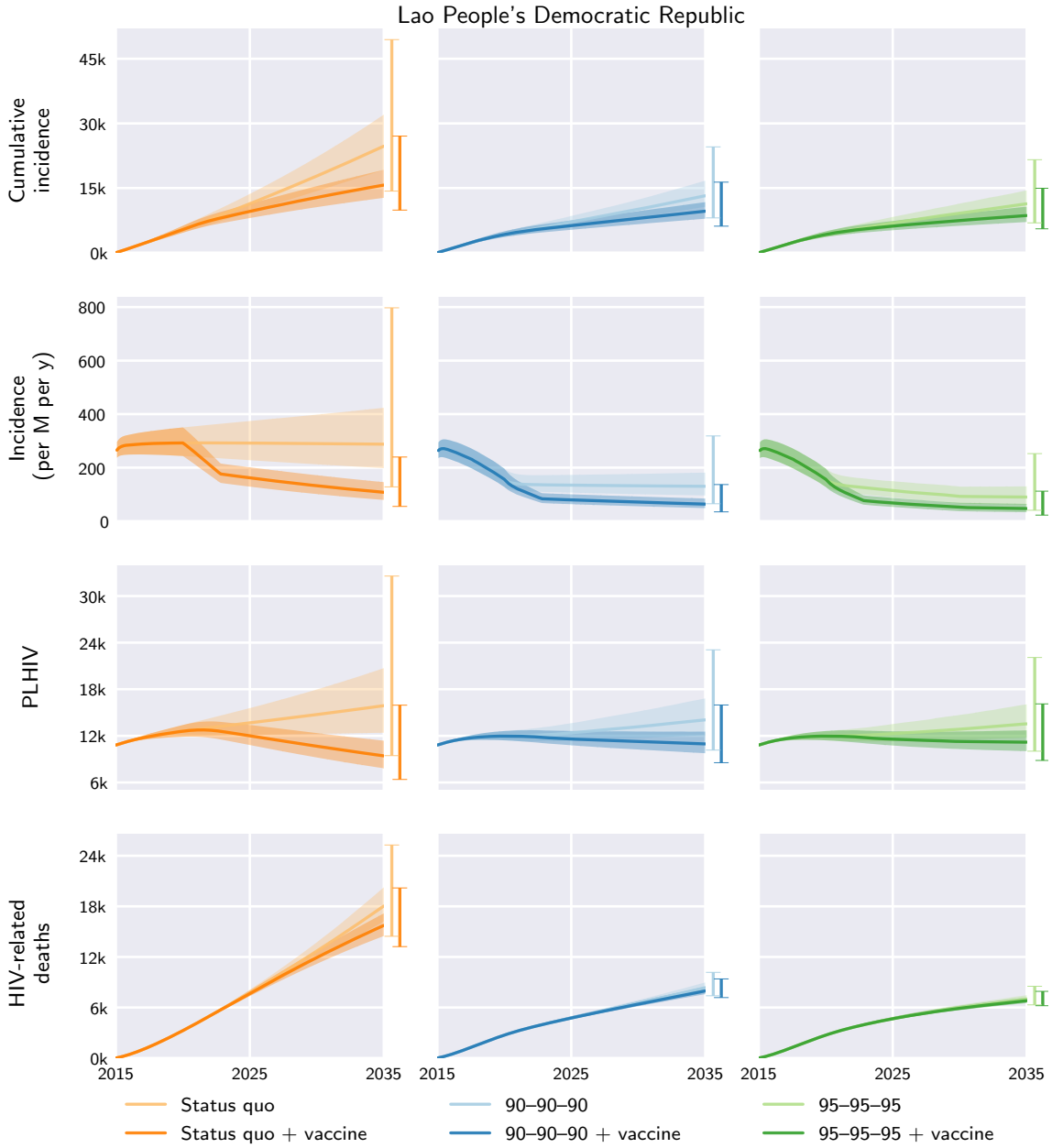

Fig. S77. Lao People's Democratic Republic model outcomes under the different diagnosis, treatment, and vaccination scenarios. Central curves show the medians over model runs with 1000 samples from parameter distributions, shaded regions show the 1st and 3rd quartiles (i.e. 25th and 75th percentiles), and vertical bars to the right of each axis show the 5th and 95th percentiles at the end time, 2035. Regional and global outcomes were aggregated from the country-level model outcomes.

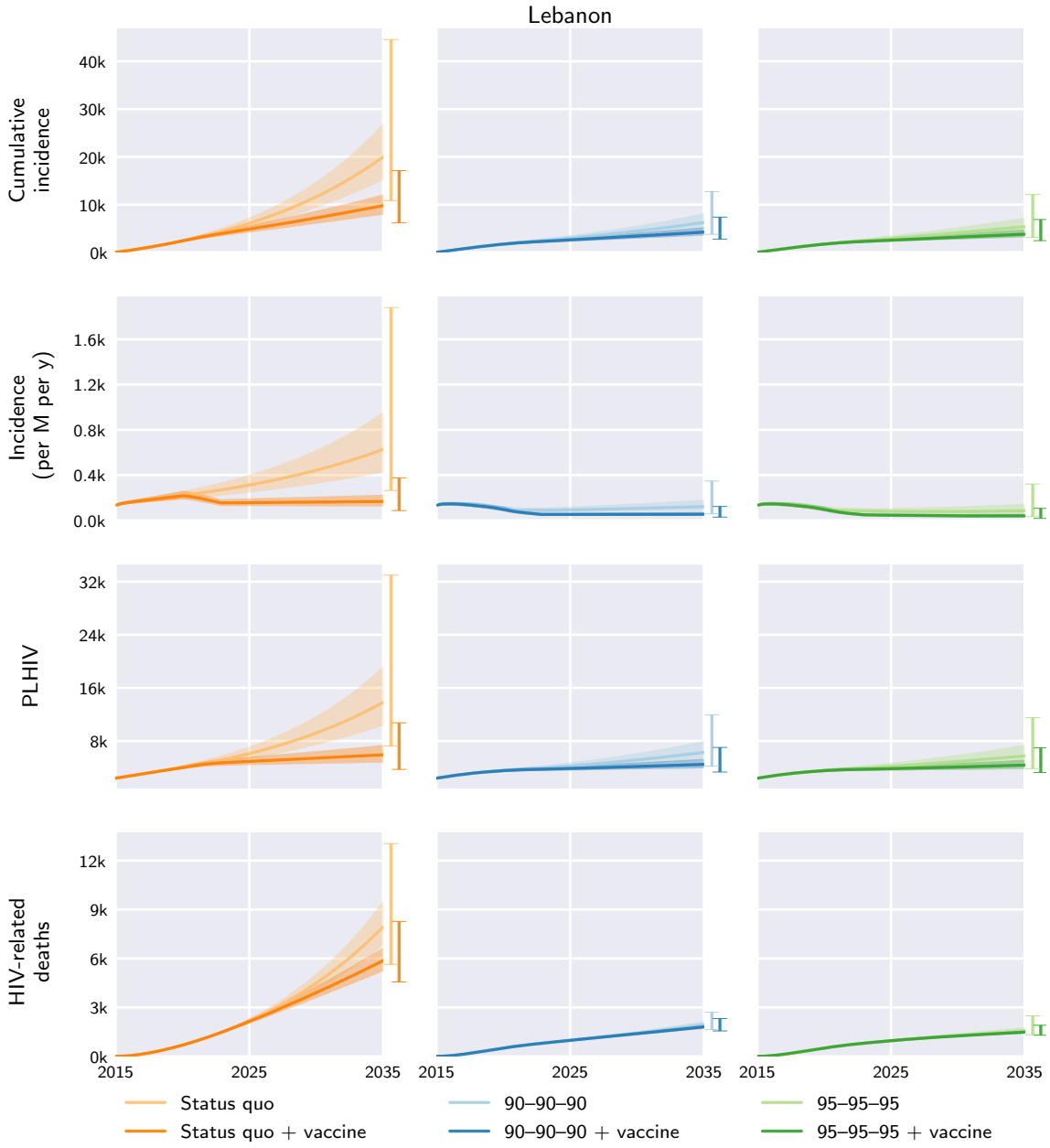

Fig. S78. Lebanon model outcomes under the different diagnosis, treatment, and vaccination scenarios. Central curves show the medians over model runs with 1000 samples from parameter distributions, shaded regions show the 1st and 3rd quartiles (i.e. 25th and 75th percentiles), and vertical bars to the right of each axis show the 5th and 95th percentiles at the end time, 2035. Regional and global outcomes were aggregated from the country-level model outcomes.

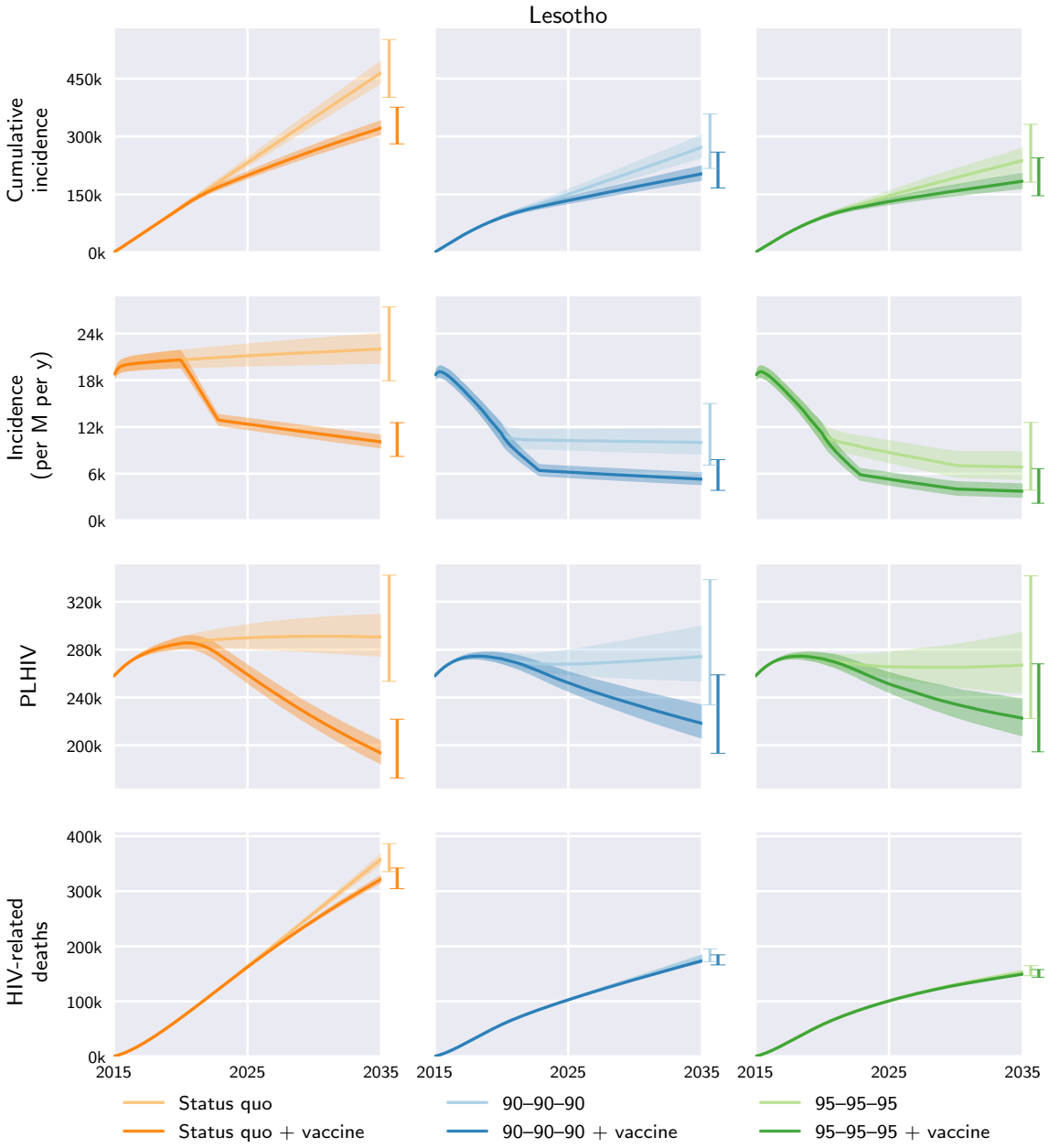

Fig. S79. Lesotho model outcomes under the different diagnosis, treatment, and vaccination scenarios. Central curves show the medians over model runs with 1000 samples from parameter distributions, shaded regions show the 1st and 3rd quartiles (i.e. 25th and 75th percentiles), and vertical bars to the right of each axis show the 5th and 95th percentiles at the end time, 2035. Regional and global outcomes were aggregated from the country-level model outcomes.

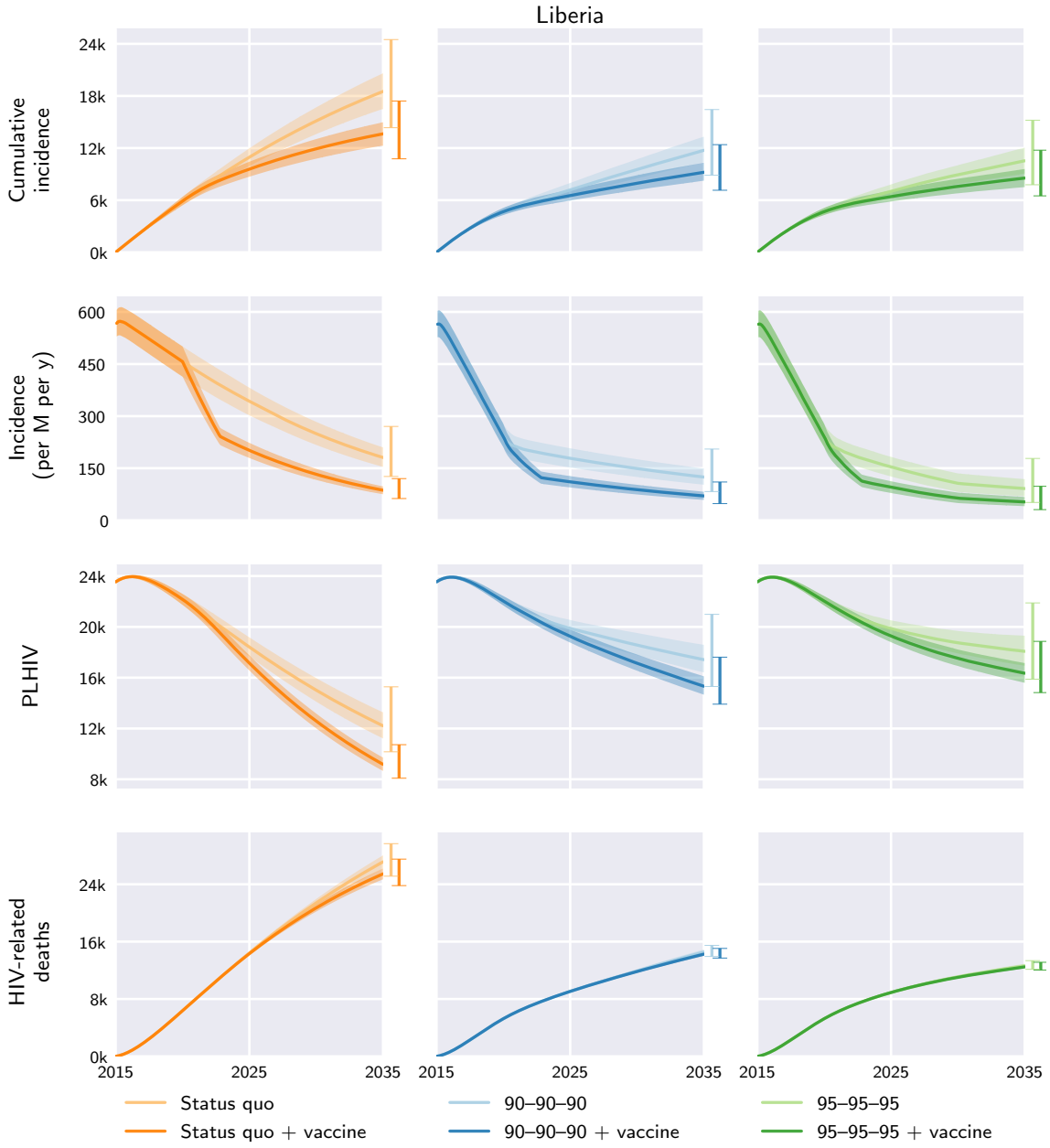

Fig. S80. Liberia model outcomes under the different diagnosis, treatment, and vaccination scenarios. Central curves show the medians over model runs with 1000 samples from parameter distributions, shaded regions show the 1st and 3rd quartiles (i.e. 25th and 75th percentiles), and vertical bars to the right of each axis show the 5th and 95th percentiles at the end time, 2035. Regional and global outcomes were aggregated from the country-level model outcomes.

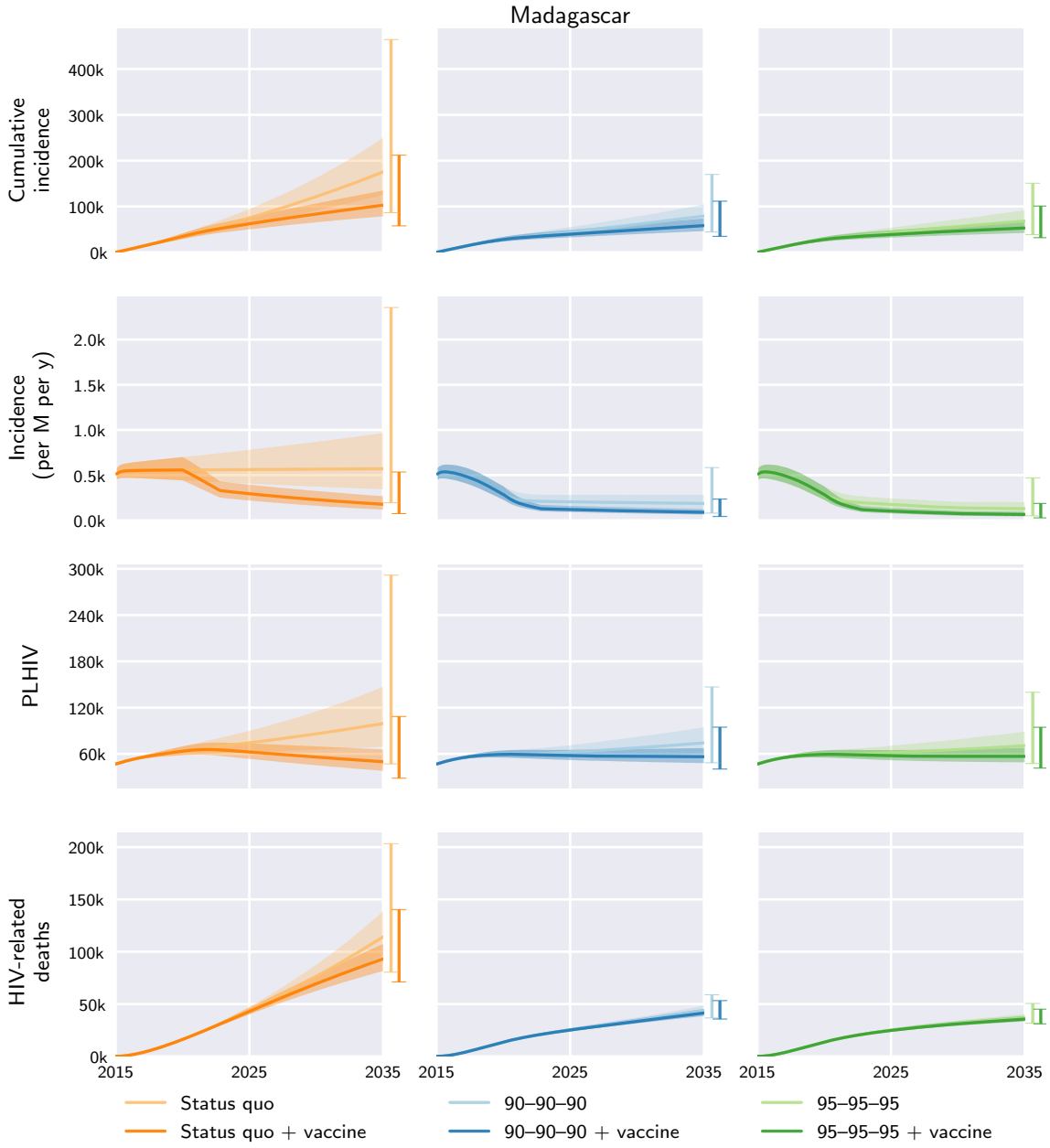

Fig. S81. Madagascar model outcomes under the different diagnosis, treatment, and vaccination scenarios. Central curves show the medians over model runs with 1000 samples from parameter distributions, shaded regions show the 1st and 3rd quartiles (i.e. 25th and 75th percentiles), and vertical bars to the right of each axis show the 5th and 95th percentiles at the end time, 2035. Regional and global outcomes were aggregated from the country-level model outcomes.

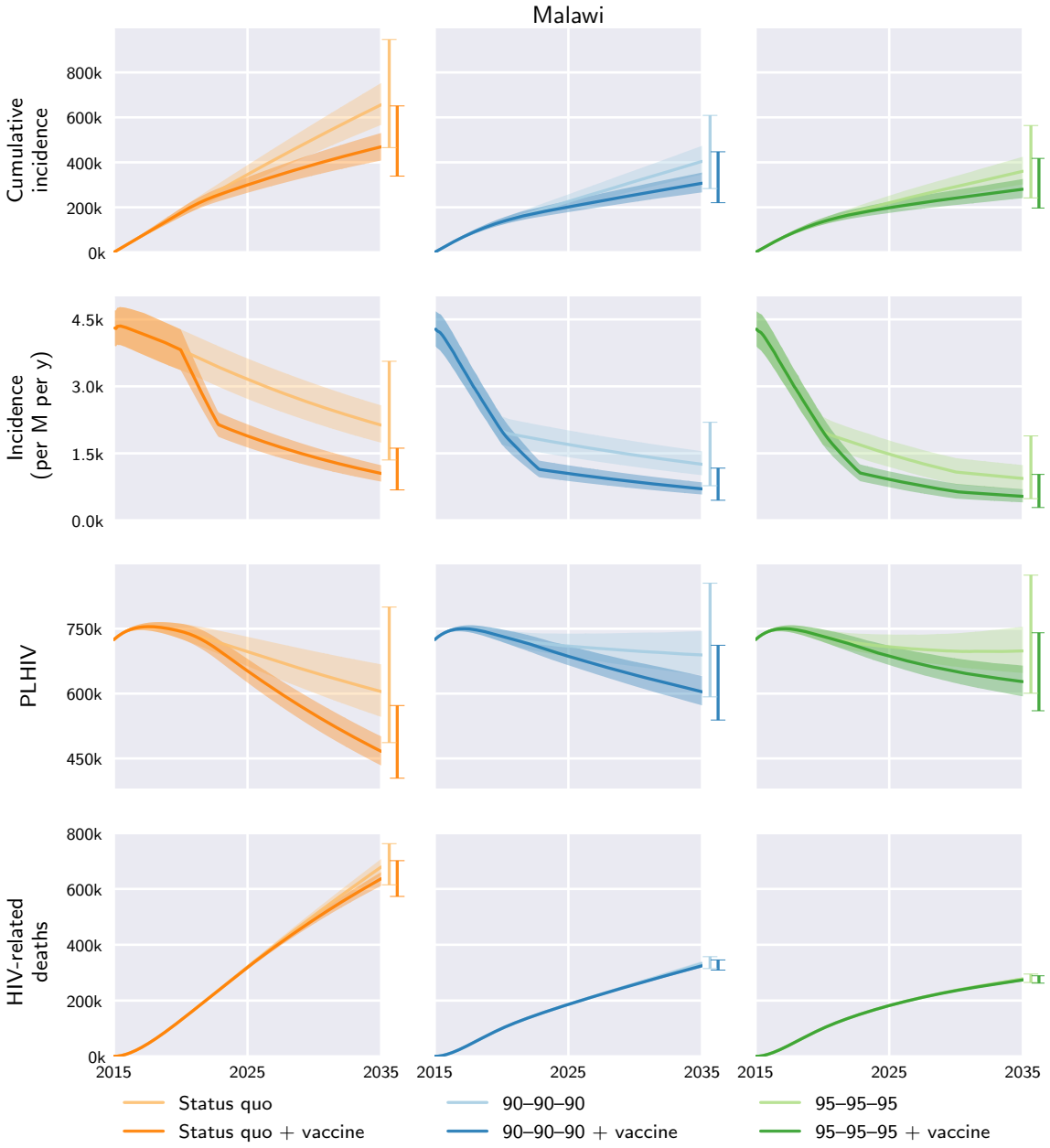

Fig. S82. Malawi model outcomes under the different diagnosis, treatment, and vaccination scenarios. Central curves show the medians over model runs with 1000 samples from parameter distributions, shaded regions show the 1st and 3rd quartiles (i.e. 25th and 75th percentiles), and vertical bars to the right of each axis show the 5th and 95th percentiles at the end time, 2035. Regional and global outcomes were aggregated from the country-level model outcomes.

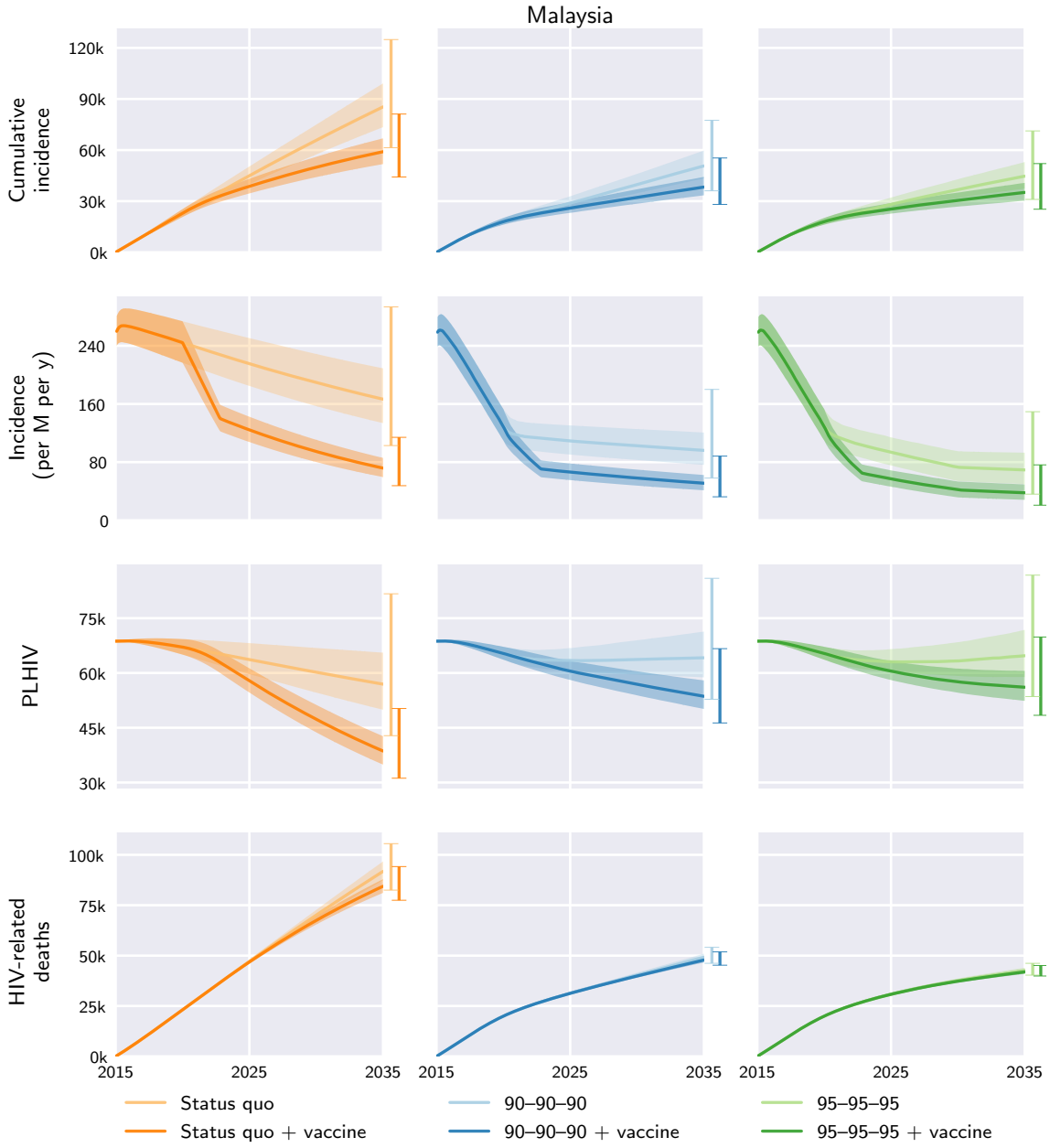

Fig. S83. Malaysia model outcomes under the different diagnosis, treatment, and vaccination scenarios. Central curves show the medians over model runs with 1000 samples from parameter distributions, shaded regions show the 1st and 3rd quartiles (i.e. 25th and 75th percentiles), and vertical bars to the right of each axis show the 5th and 95th percentiles at the end time, 2035. Regional and global outcomes were aggregated from the country-level model outcomes.

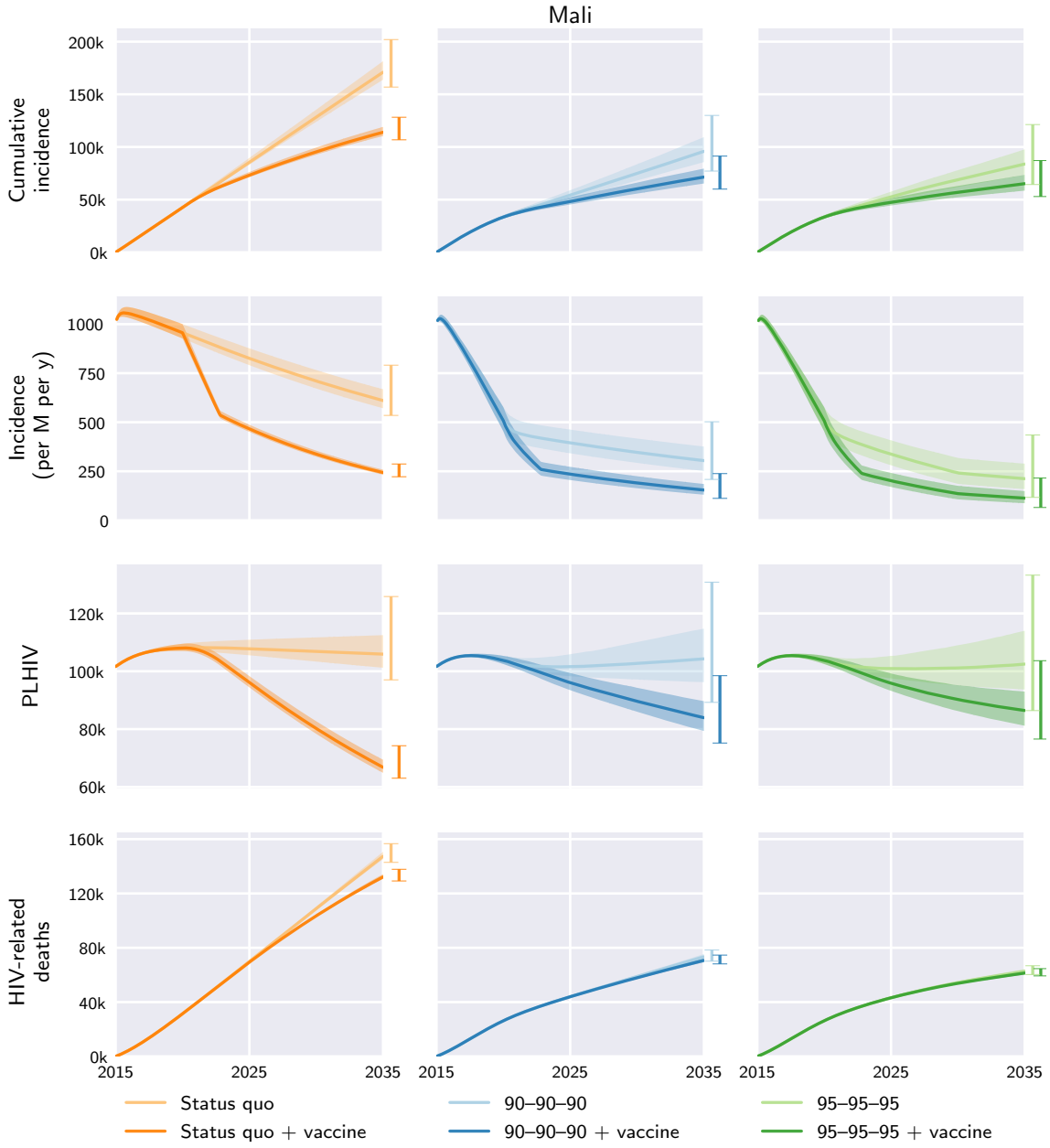

Fig. S84. Mali model outcomes under the different diagnosis, treatment, and vaccination scenarios. Central curves show the medians over model runs with 1000 samples from parameter distributions, shaded regions show the 1st and 3rd quartiles (i.e. 25th and 75th percentiles), and vertical bars to the right of each axis show the 5th and 95th percentiles at the end time, 2035. Regional and global outcomes were aggregated from the country-level model outcomes.

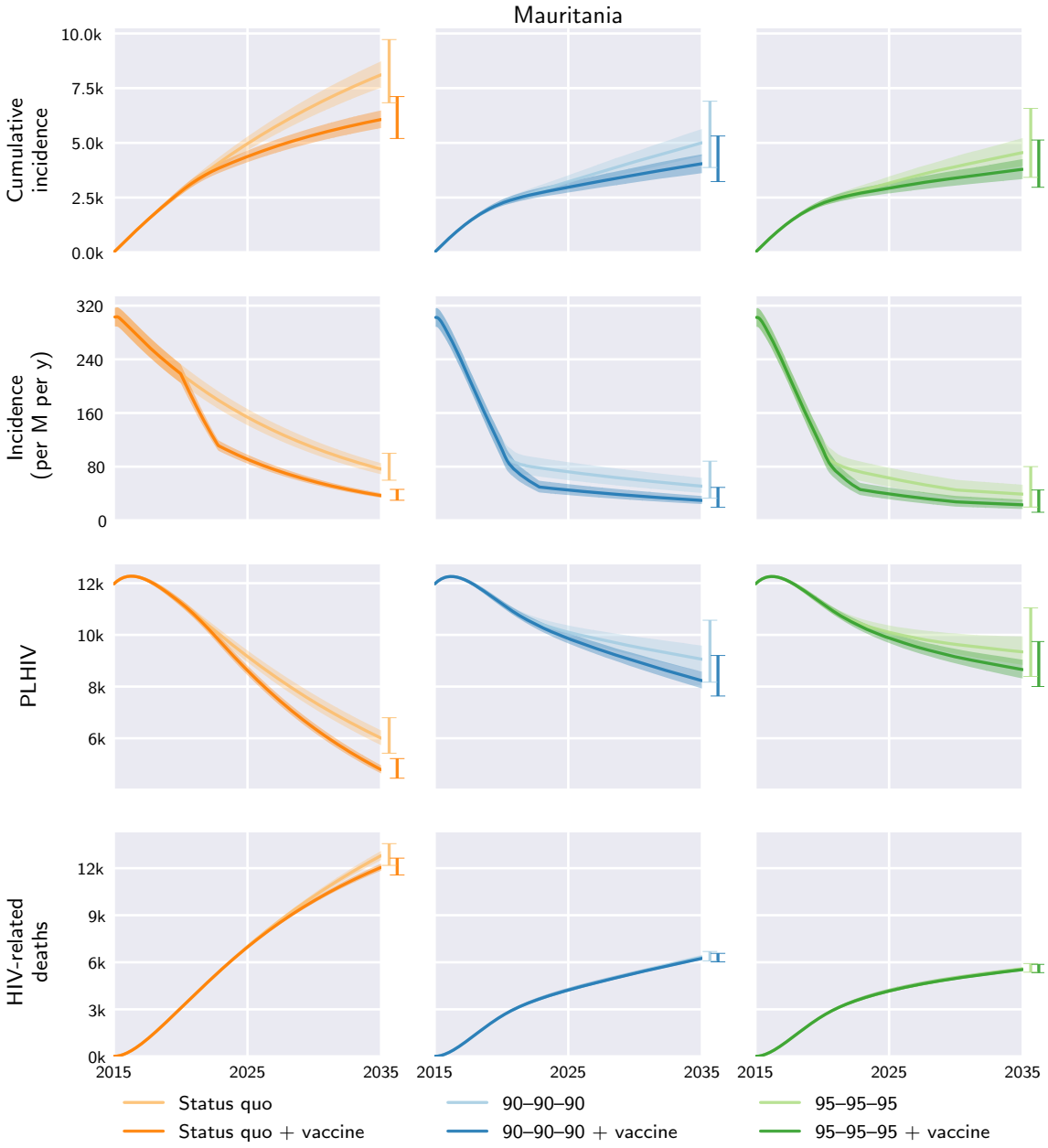

Fig. S85. Mauritania model outcomes under the different diagnosis, treatment, and vaccination scenarios. Central curves show the medians over model runs with 1000 samples from parameter distributions, shaded regions show the 1st and 3rd quartiles (i.e. 25th and 75th percentiles), and vertical bars to the right of each axis show the 5th and 95th percentiles at the end time, 2035. Regional and global outcomes were aggregated from the country-level model outcomes.

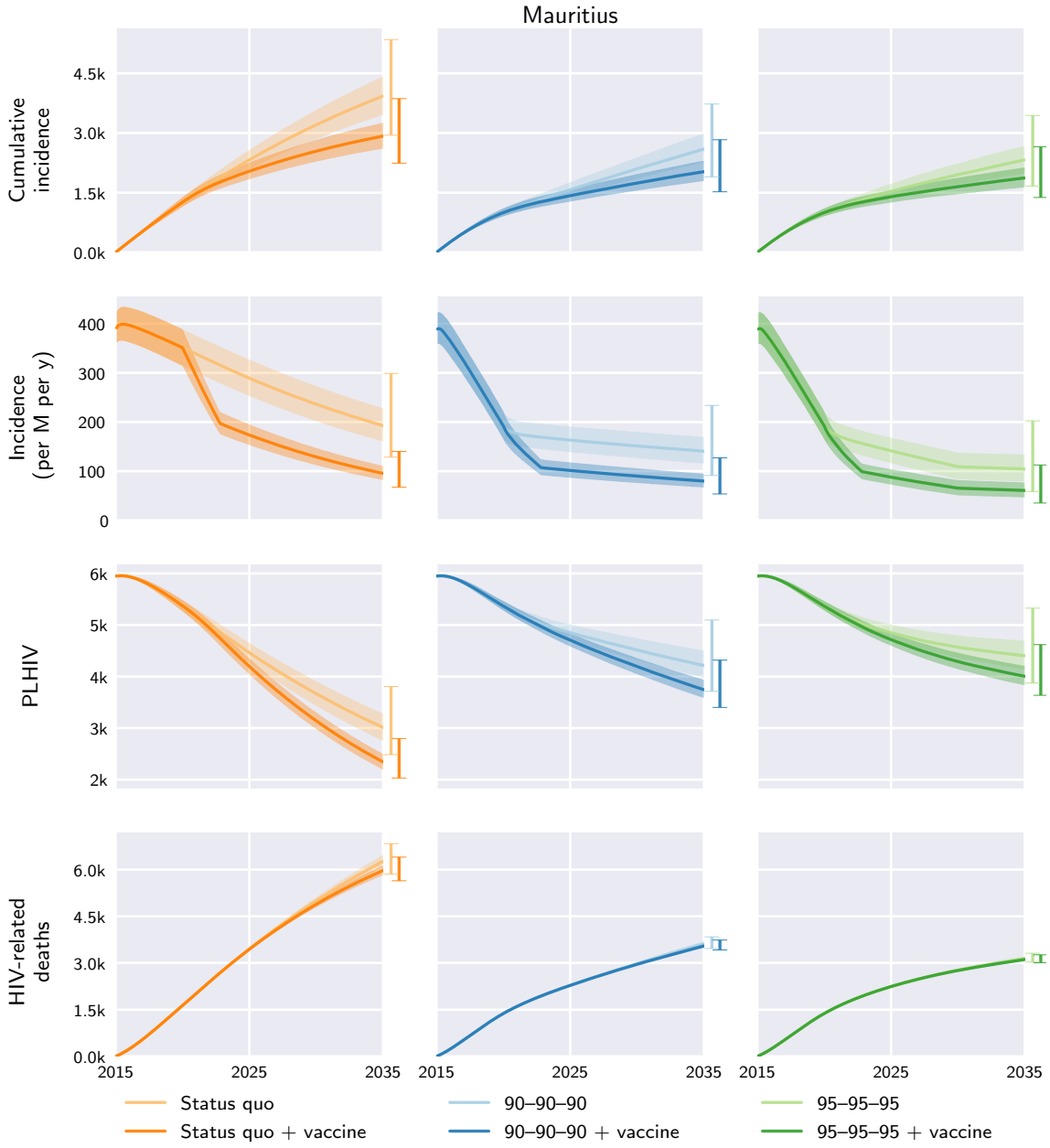

Fig. S86. Mauritius model outcomes under the different diagnosis, treatment, and vaccination scenarios. Central curves show the medians over model runs with 1000 samples from parameter distributions, shaded regions show the 1st and 3rd quartiles (i.e. 25th and 75th percentiles), and vertical bars to the right of each axis show the 5th and 95th percentiles at the end time, 2035. Regional and global outcomes were aggregated from the country-level model outcomes.

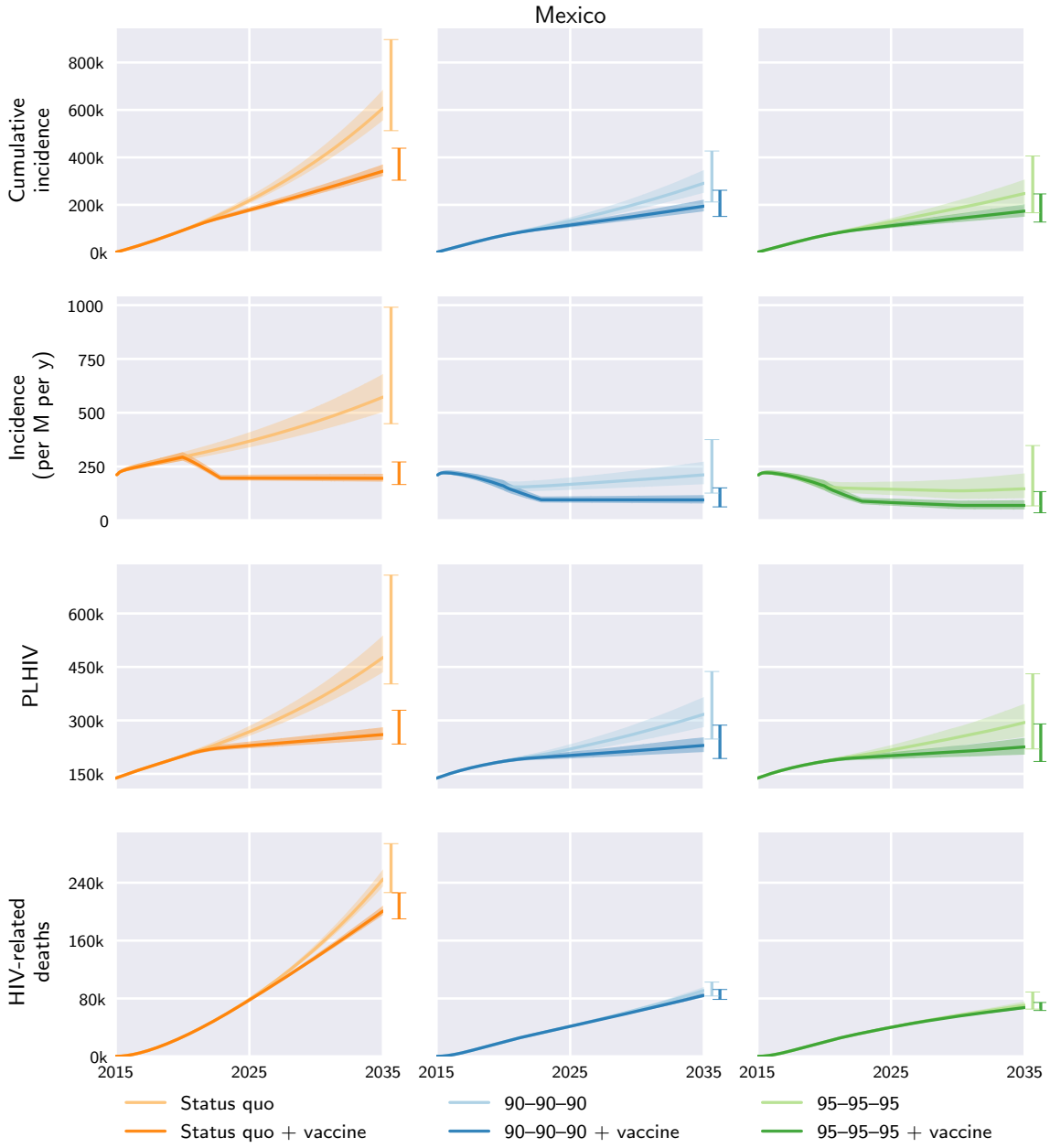

Fig. S87. Mexico model outcomes under the different diagnosis, treatment, and vaccination scenarios. Central curves show the medians over model runs with 1000 samples from parameter distributions, shaded regions show the 1st and 3rd quartiles (i.e. 25th and 75th percentiles), and vertical bars to the right of each axis show the 5th and 95th percentiles at the end time, 2035. Regional and global outcomes were aggregated from the country-level model outcomes.

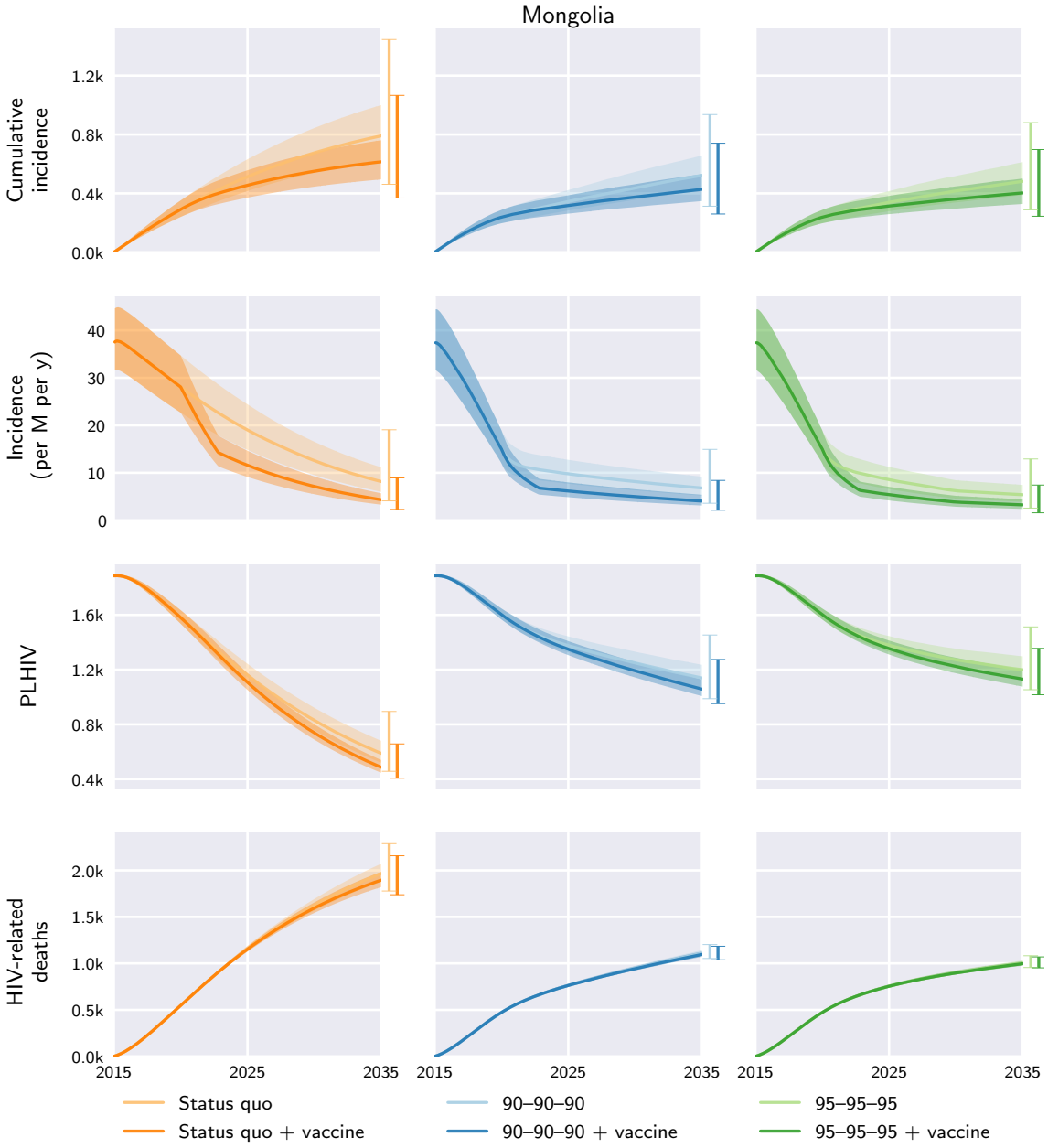

Fig. S88. Mongolia model outcomes under the different diagnosis, treatment, and vaccination scenarios. Central curves show the medians over model runs with 1000 samples from parameter distributions, shaded regions show the 1st and 3rd quartiles (i.e. 25th and 75th percentiles), and vertical bars to the right of each axis show the 5th and 95th percentiles at the end time, 2035. Regional and global outcomes were aggregated from the country-level model outcomes.

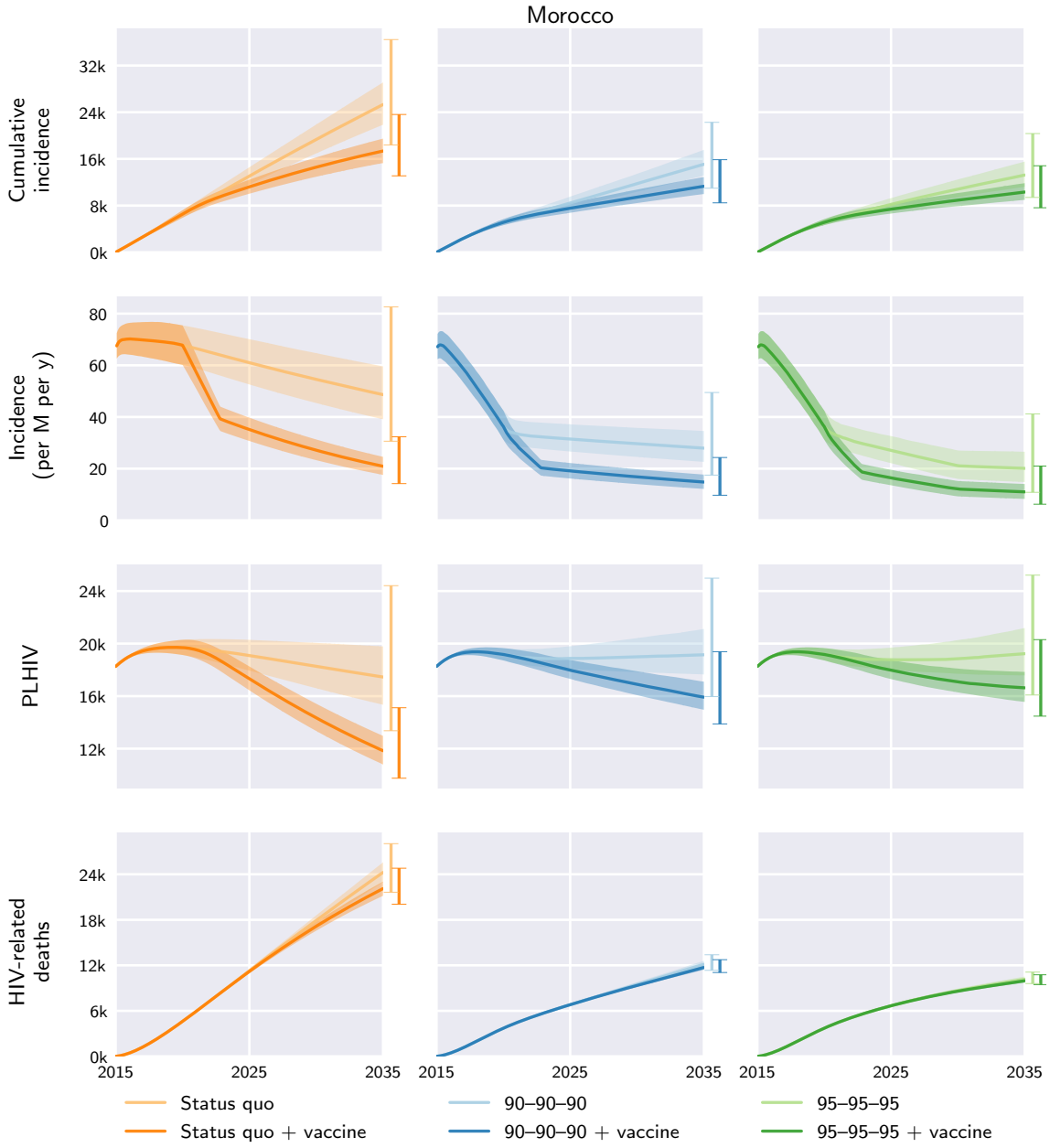

Fig. S89. Morocco model outcomes under the different diagnosis, treatment, and vaccination scenarios. Central curves show the medians over model runs with 1000 samples from parameter distributions, shaded regions show the 1st and 3rd quartiles (i.e. 25th and 75th percentiles), and vertical bars to the right of each axis show the 5th and 95th percentiles at the end time, 2035. Regional and global outcomes were aggregated from the country-level model outcomes.

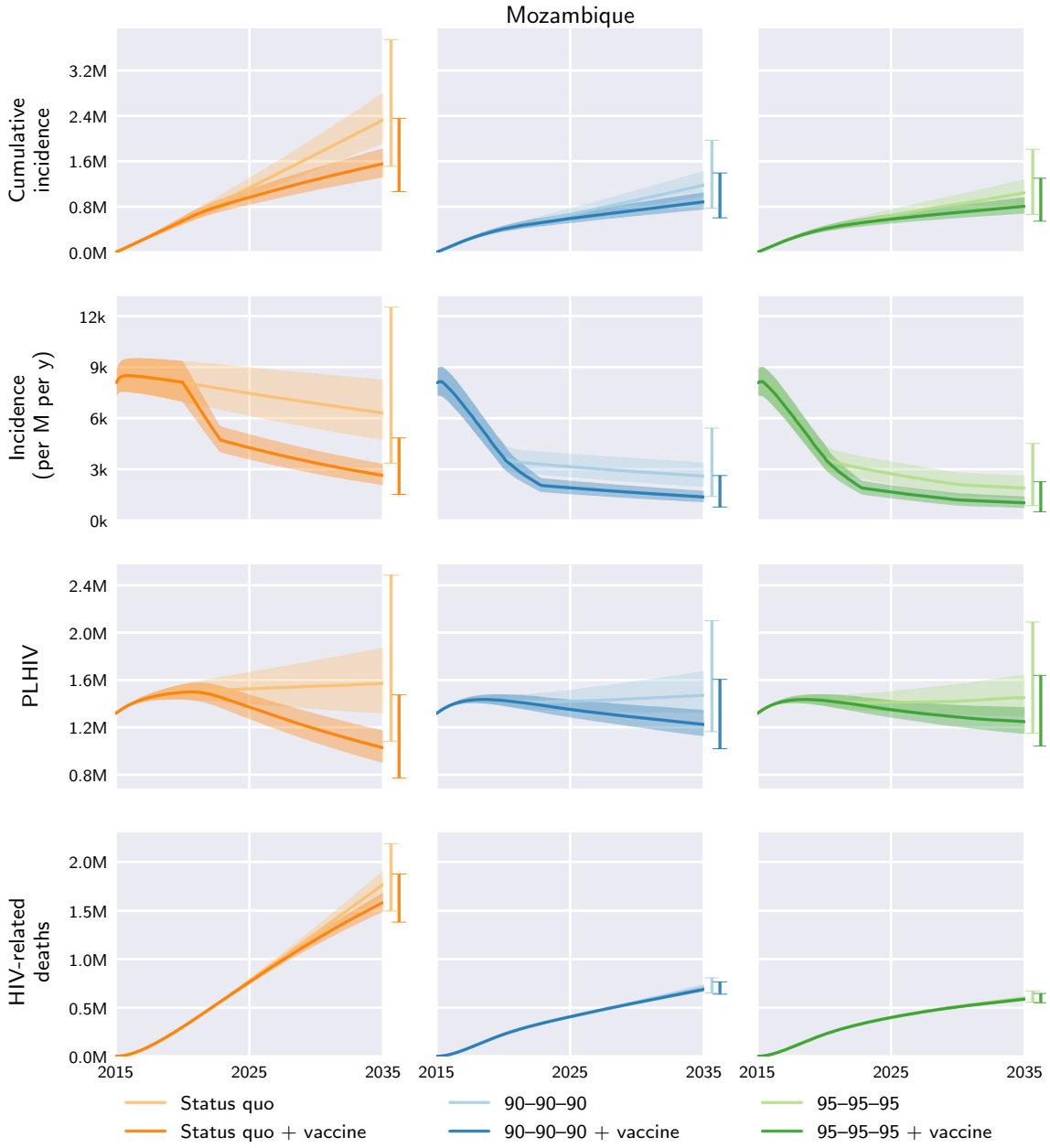

Fig. S90. Mozambique model outcomes under the different diagnosis, treatment, and vaccination scenarios. Central curves show the medians over model runs with 1000 samples from parameter distributions, shaded regions show the 1st and 3rd quartiles (i.e. 25th and 75th percentiles), and vertical bars to the right of each axis show the 5th and 95th percentiles at the end time, 2035. Regional and global outcomes were aggregated from the country-level model outcomes.

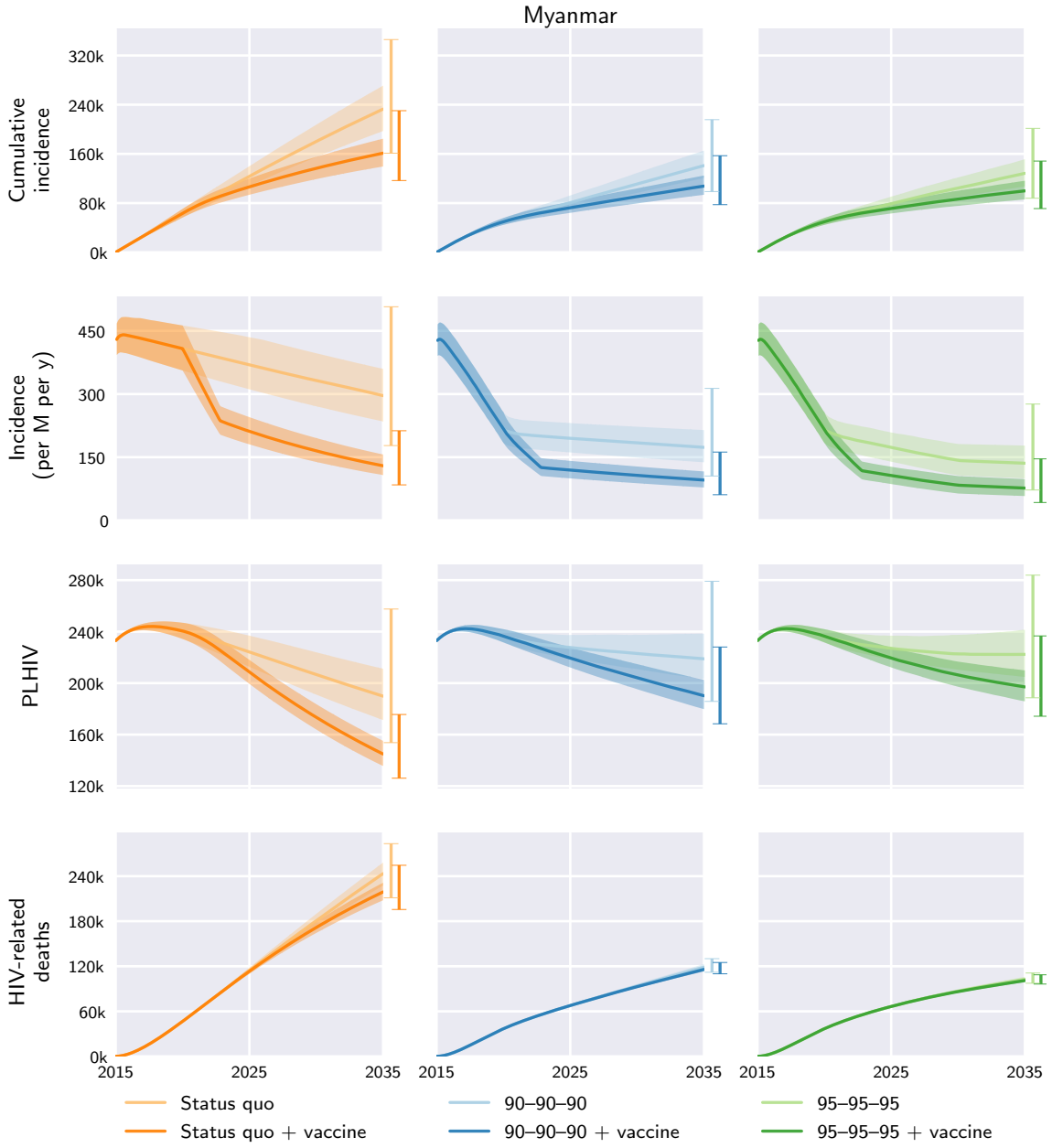

Fig. S91. Myanmar model outcomes under the different diagnosis, treatment, and vaccination scenarios. Central curves show the medians over model runs with 1000 samples from parameter distributions, shaded regions show the 1st and 3rd quartiles (i.e. 25th and 75th percentiles), and vertical bars to the right of each axis show the 5th and 95th percentiles at the end time, 2035. Regional and global outcomes were aggregated from the country-level model outcomes.

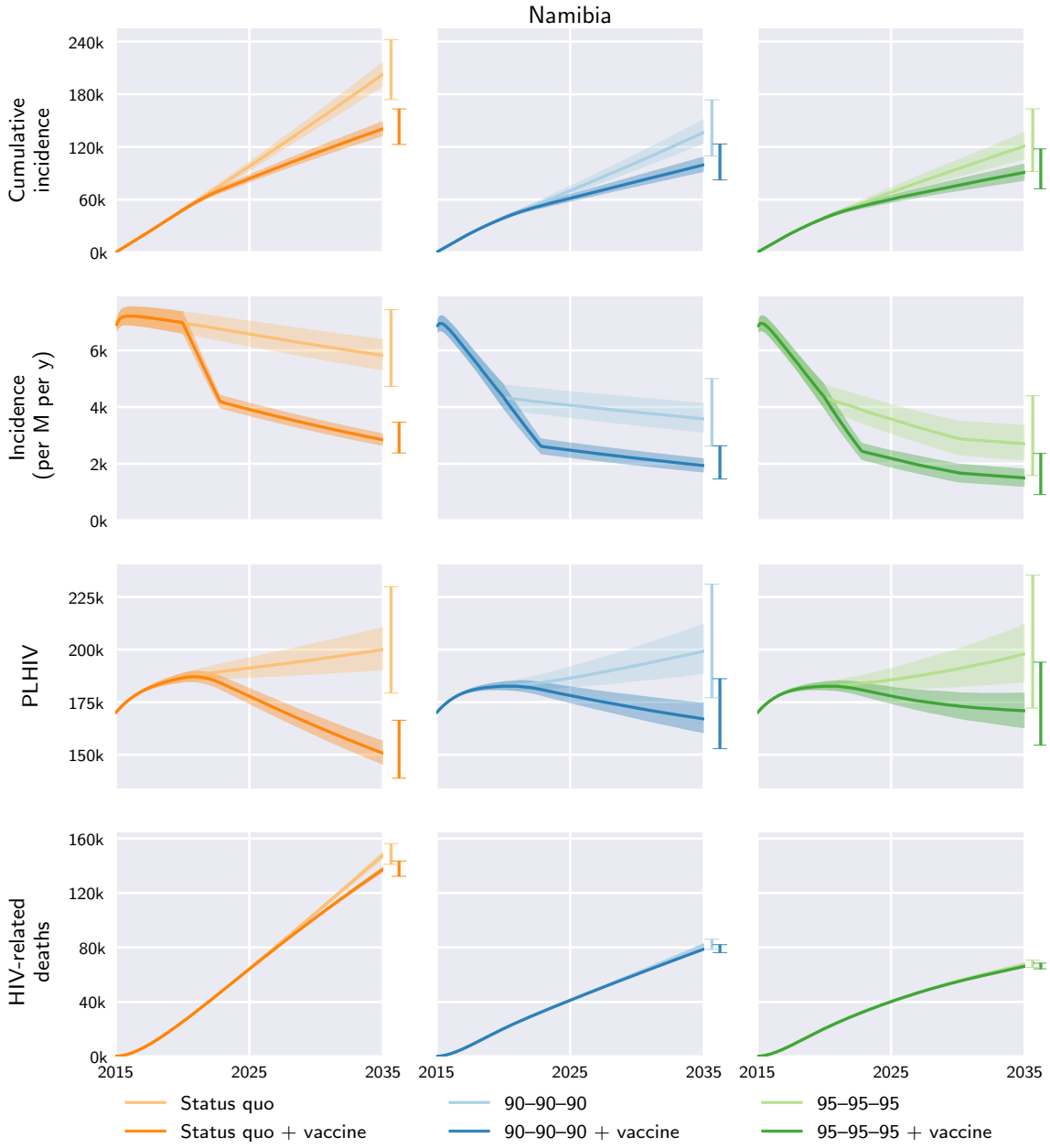

Fig. S92. Namibia model outcomes under the different diagnosis, treatment, and vaccination scenarios. Central curves show the medians over model runs with 1000 samples from parameter distributions, shaded regions show the 1st and 3rd quartiles (i.e. 25th and 75th percentiles), and vertical bars to the right of each axis show the 5th and 95th percentiles at the end time, 2035. Regional and global outcomes were aggregated from the country-level model outcomes.

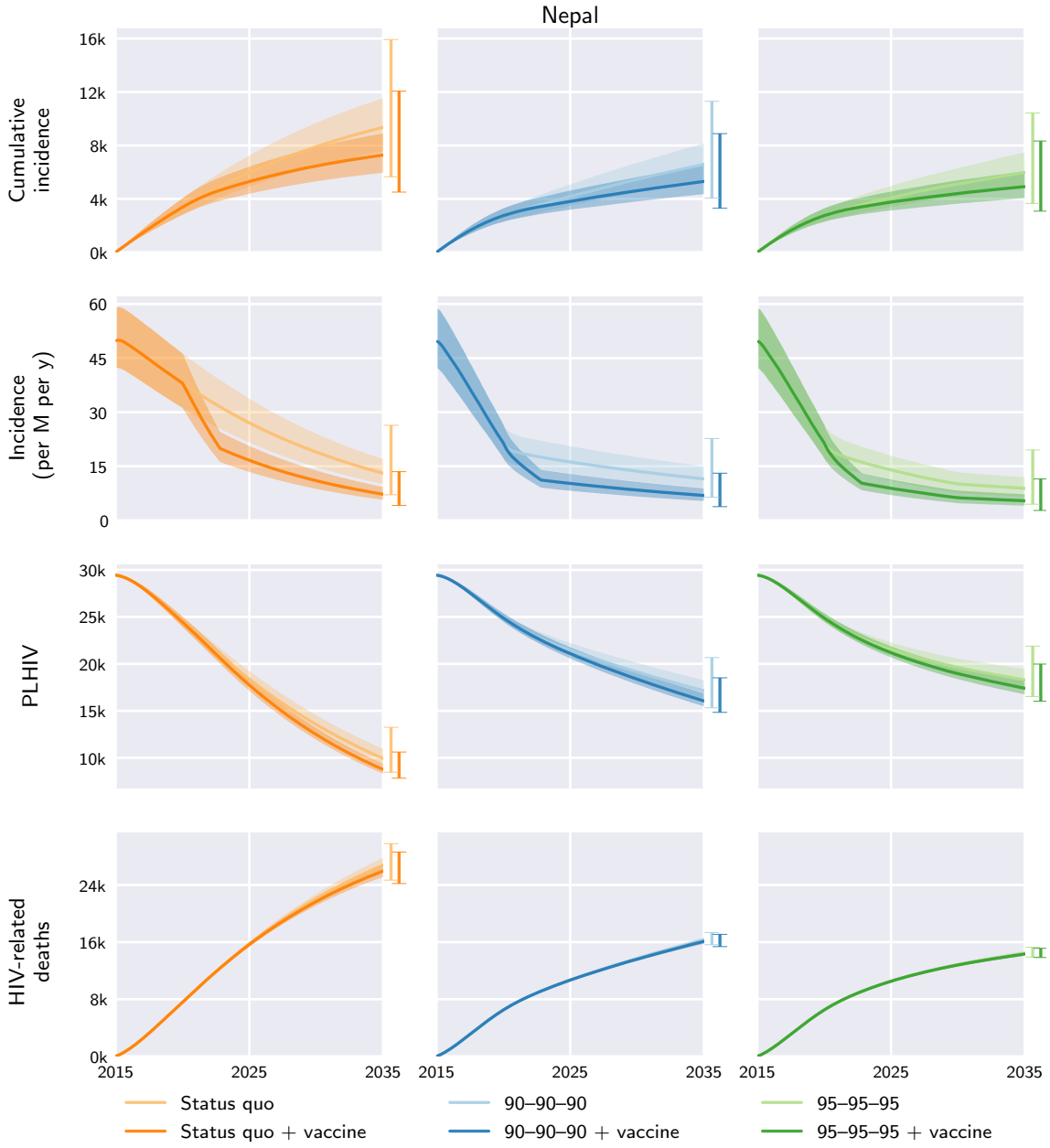

Fig. S93. Nepal model outcomes under the different diagnosis, treatment, and vaccination scenarios. Central curves show the medians over model runs with 1000 samples from parameter distributions, shaded regions show the 1st and 3rd quartiles (i.e. 25th and 75th percentiles), and vertical bars to the right of each axis show the 5th and 95th percentiles at the end time, 2035. Regional and global outcomes were aggregated from the country-level model outcomes.

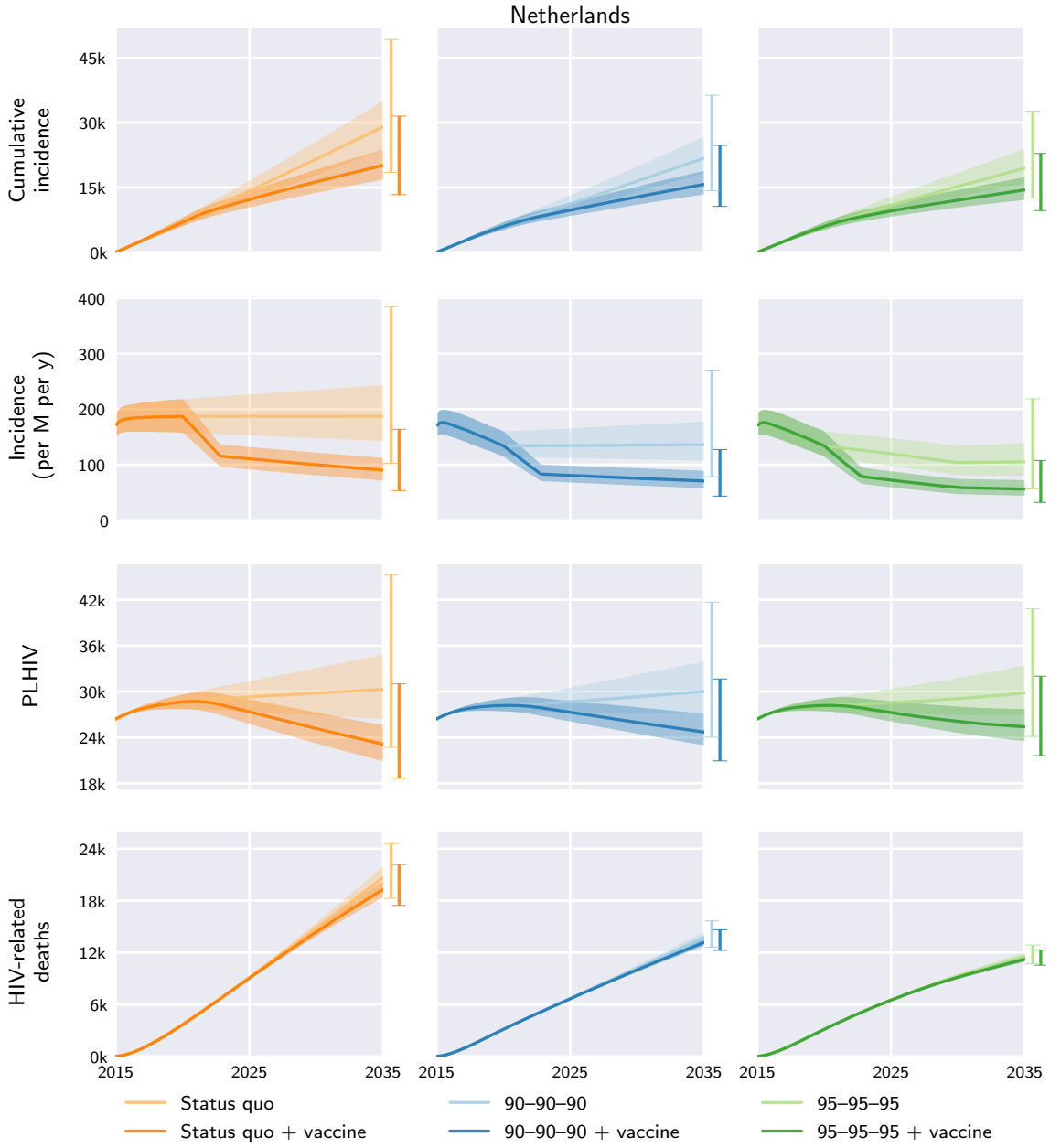

Fig. S94. Netherlands model outcomes under the different diagnosis, treatment, and vaccination scenarios. Central curves show the medians over model runs with 1000 samples from parameter distributions, shaded regions show the 1st and 3rd quartiles (i.e. 25th and 75th percentiles), and vertical bars to the right of each axis show the 5th and 95th percentiles at the end time, 2035. Regional and global outcomes were aggregated from the country-level model outcomes.

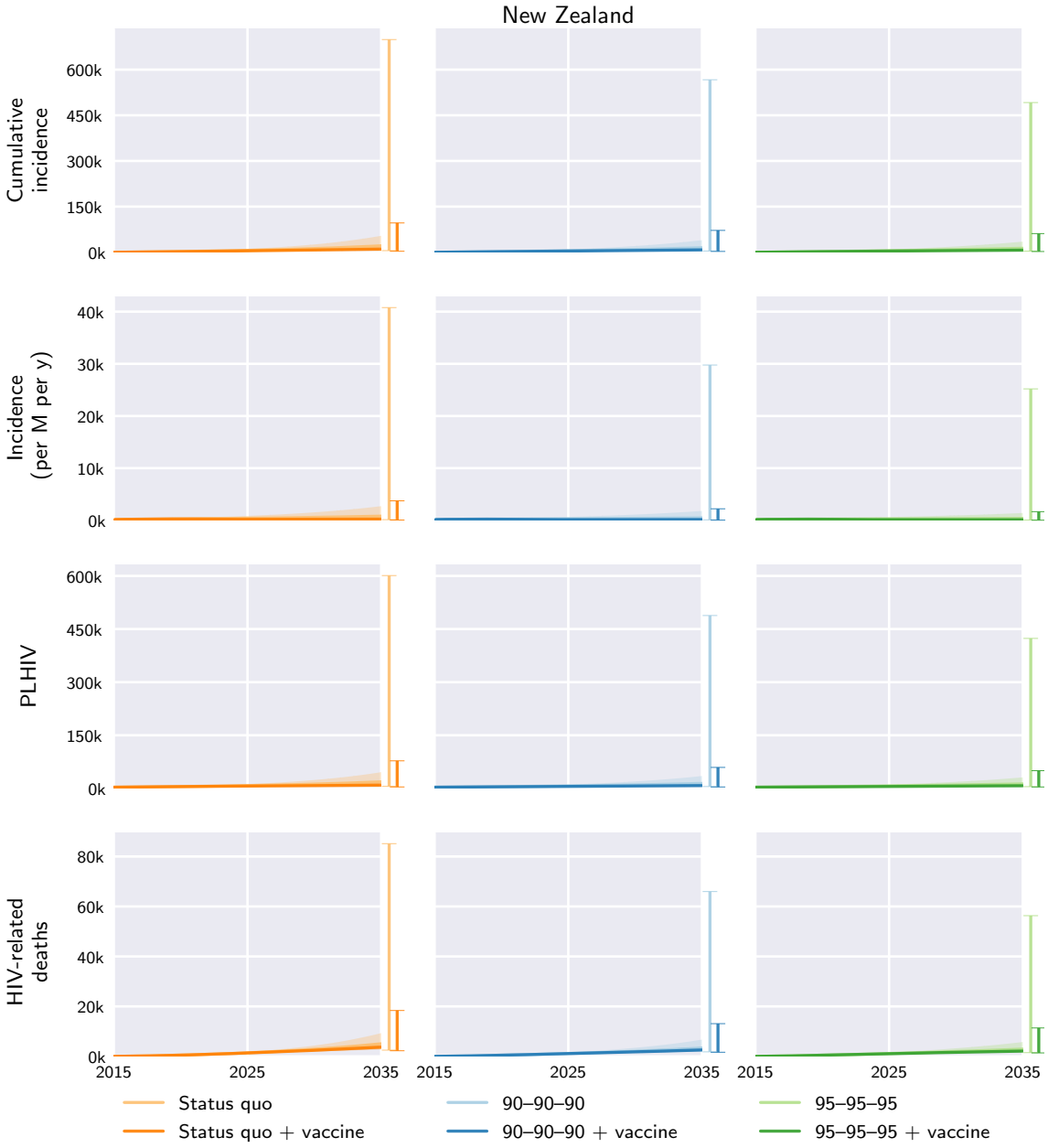

Fig. S95. New Zealand model outcomes under the different diagnosis, treatment, and vaccination scenarios. Central curves show the medians over model runs with 1000 samples from parameter distributions, shaded regions show the 1st and 3rd quartiles (i.e. 25th and 75th percentiles), and vertical bars to the right of each axis show the 5th and 95th percentiles at the end time, 2035. Regional and global outcomes were aggregated from the country-level model outcomes.

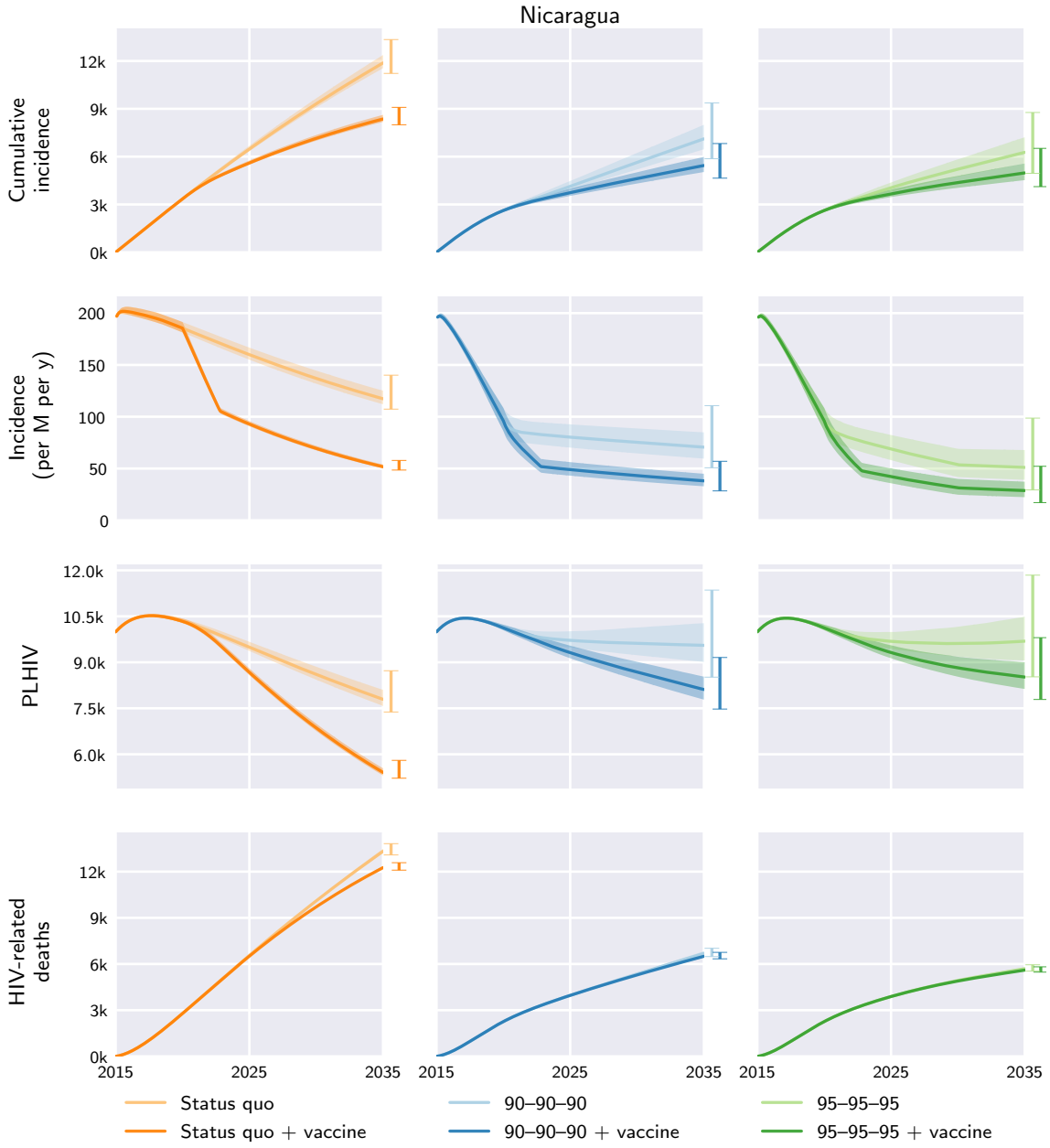

Fig. S96. Nicaragua model outcomes under the different diagnosis, treatment, and vaccination scenarios. Central curves show the medians over model runs with 1000 samples from parameter distributions, shaded regions show the 1st and 3rd quartiles (i.e. 25th and 75th percentiles), and vertical bars to the right of each axis show the 5th and 95th percentiles at the end time, 2035. Regional and global outcomes were aggregated from the country-level model outcomes.

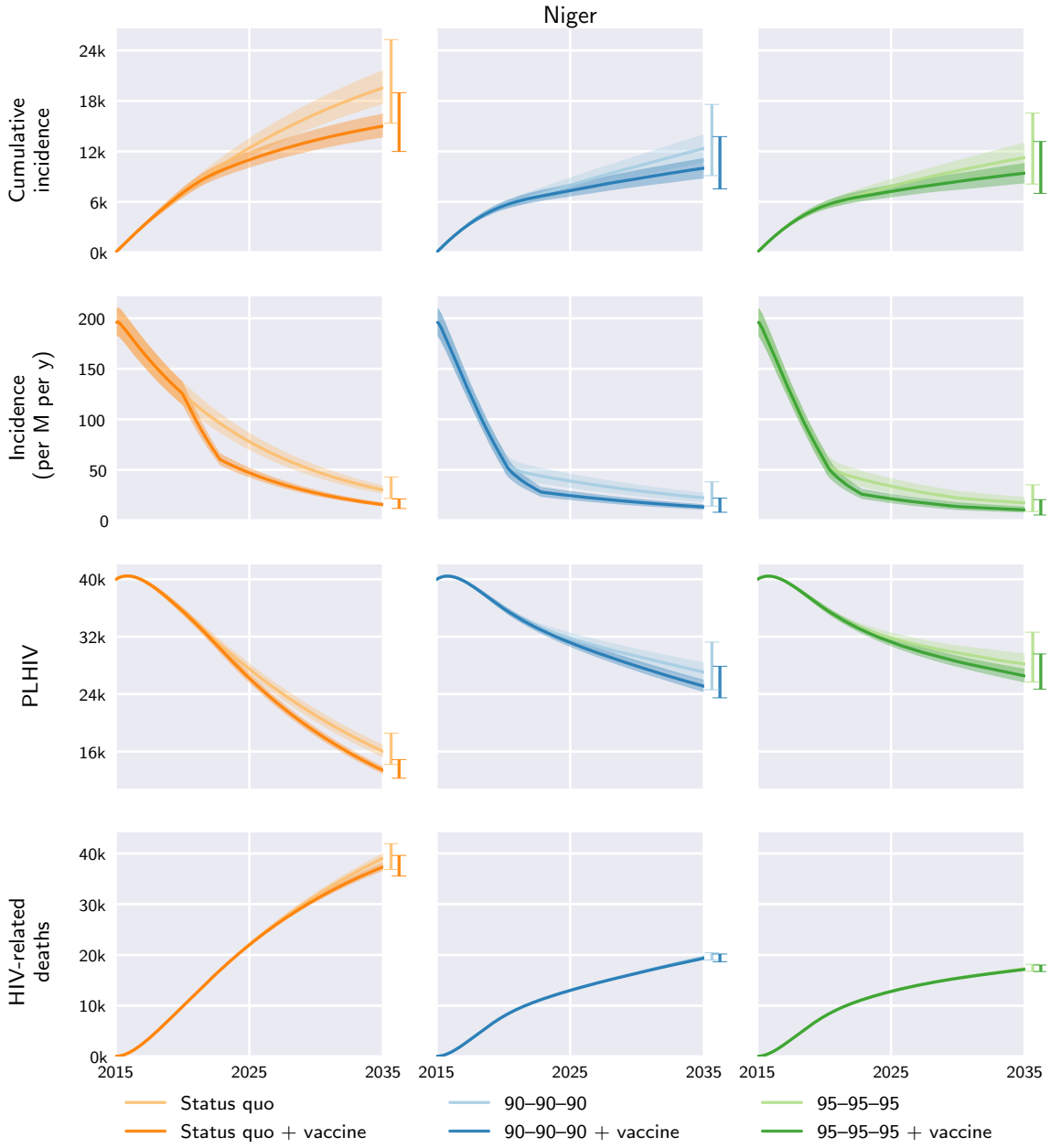

Fig. S97. Niger model outcomes under the different diagnosis, treatment, and vaccination scenarios. Central curves show the medians over model runs with 1000 samples from parameter distributions, shaded regions show the 1st and 3rd quartiles (i.e. 25th and 75th percentiles), and vertical bars to the right of each axis show the 5th and 95th percentiles at the end time, 2035. Regional and global outcomes were aggregated from the country-level model outcomes.

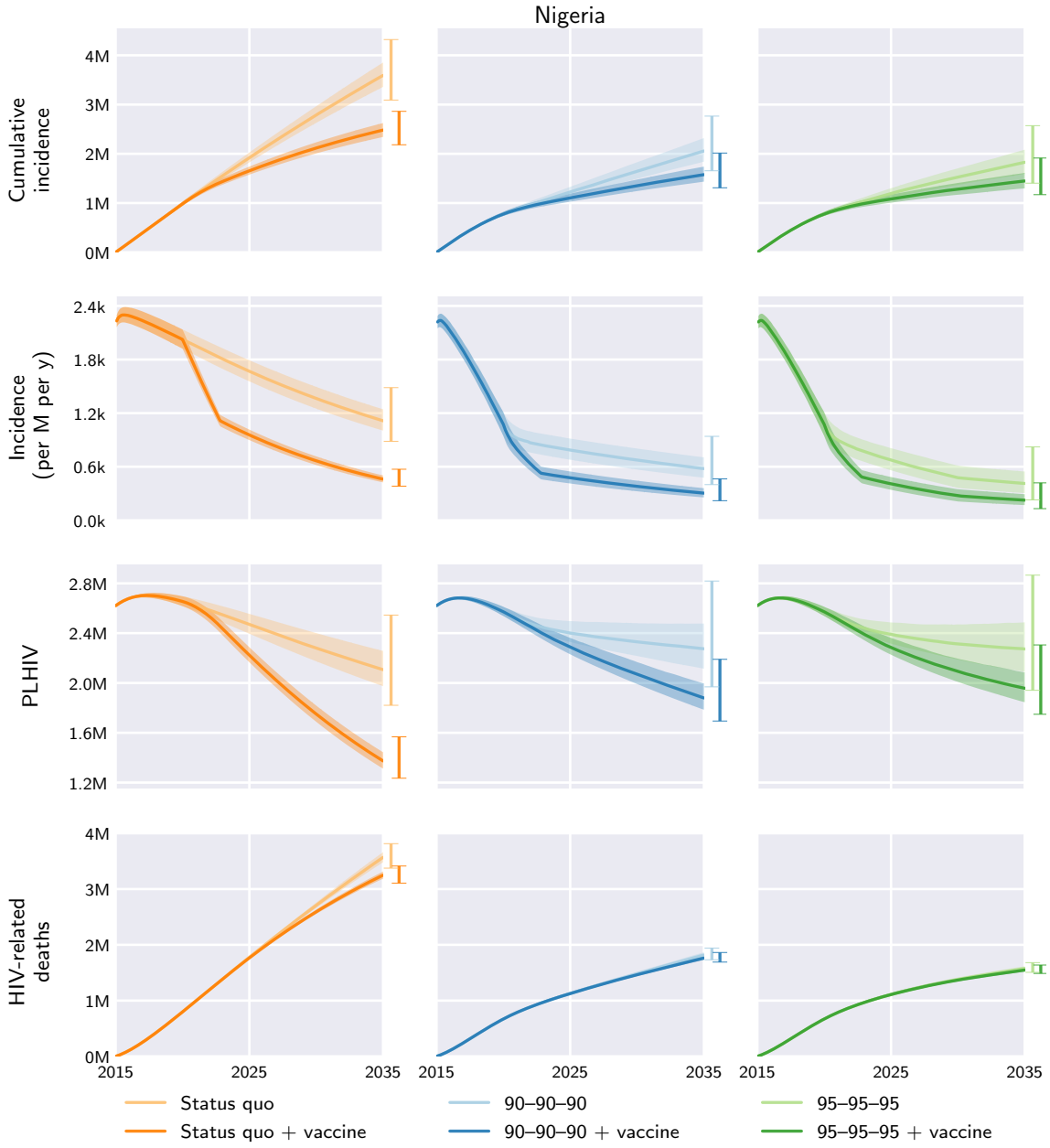

Fig. S98. Nigeria model outcomes under the different diagnosis, treatment, and vaccination scenarios. Central curves show the medians over model runs with 1000 samples from parameter distributions, shaded regions show the 1st and 3rd quartiles (i.e. 25th and 75th percentiles), and vertical bars to the right of each axis show the 5th and 95th percentiles at the end time, 2035. Regional and global outcomes were aggregated from the country-level model outcomes.

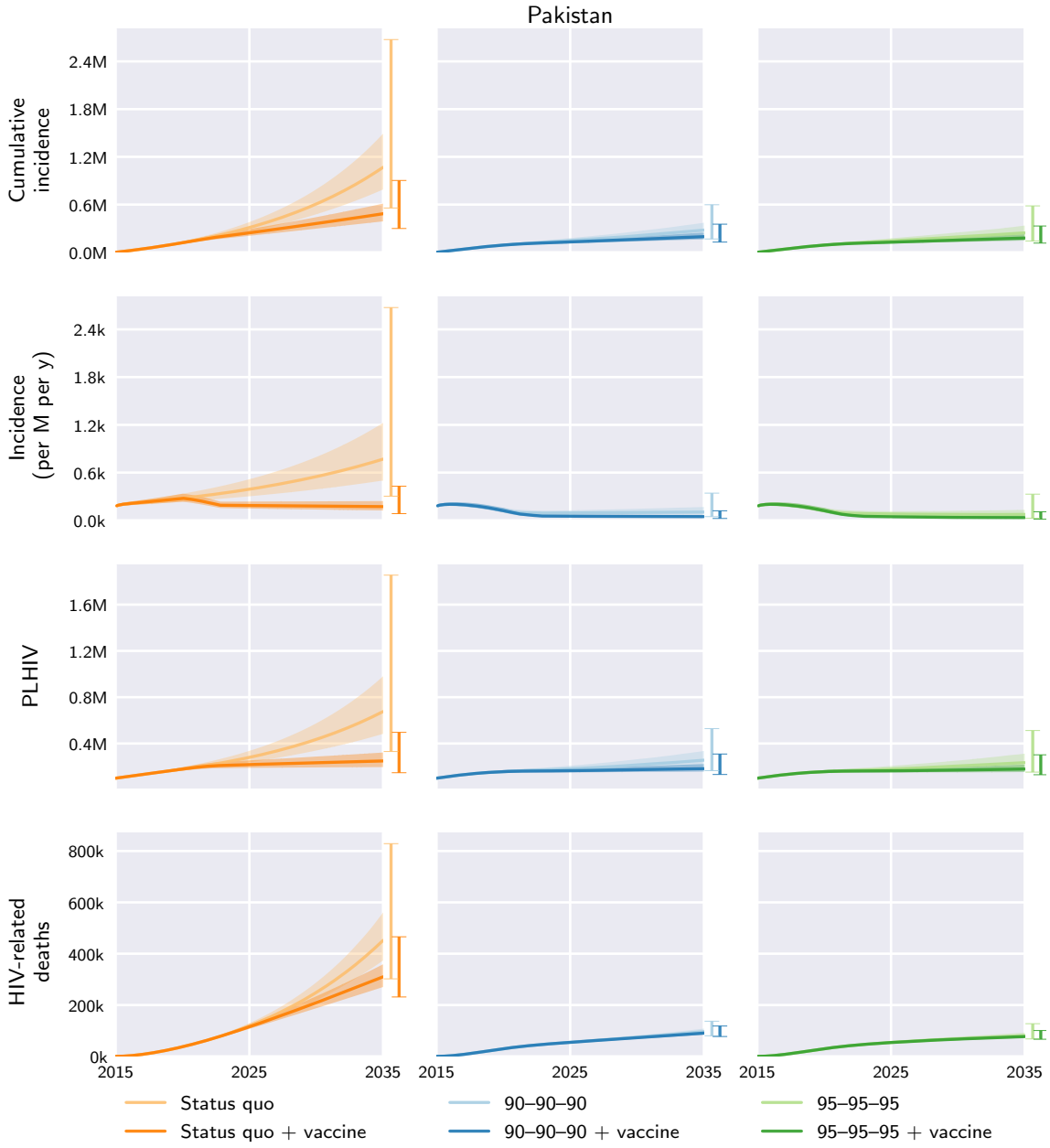

Fig. S99. Pakistan model outcomes under the different diagnosis, treatment, and vaccination scenarios. Central curves show the medians over model runs with 1000 samples from parameter distributions, shaded regions show the 1st and 3rd quartiles (i.e. 25th and 75th percentiles), and vertical bars to the right of each axis show the 5th and 95th percentiles at the end time, 2035. Regional and global outcomes were aggregated from the country-level model outcomes.

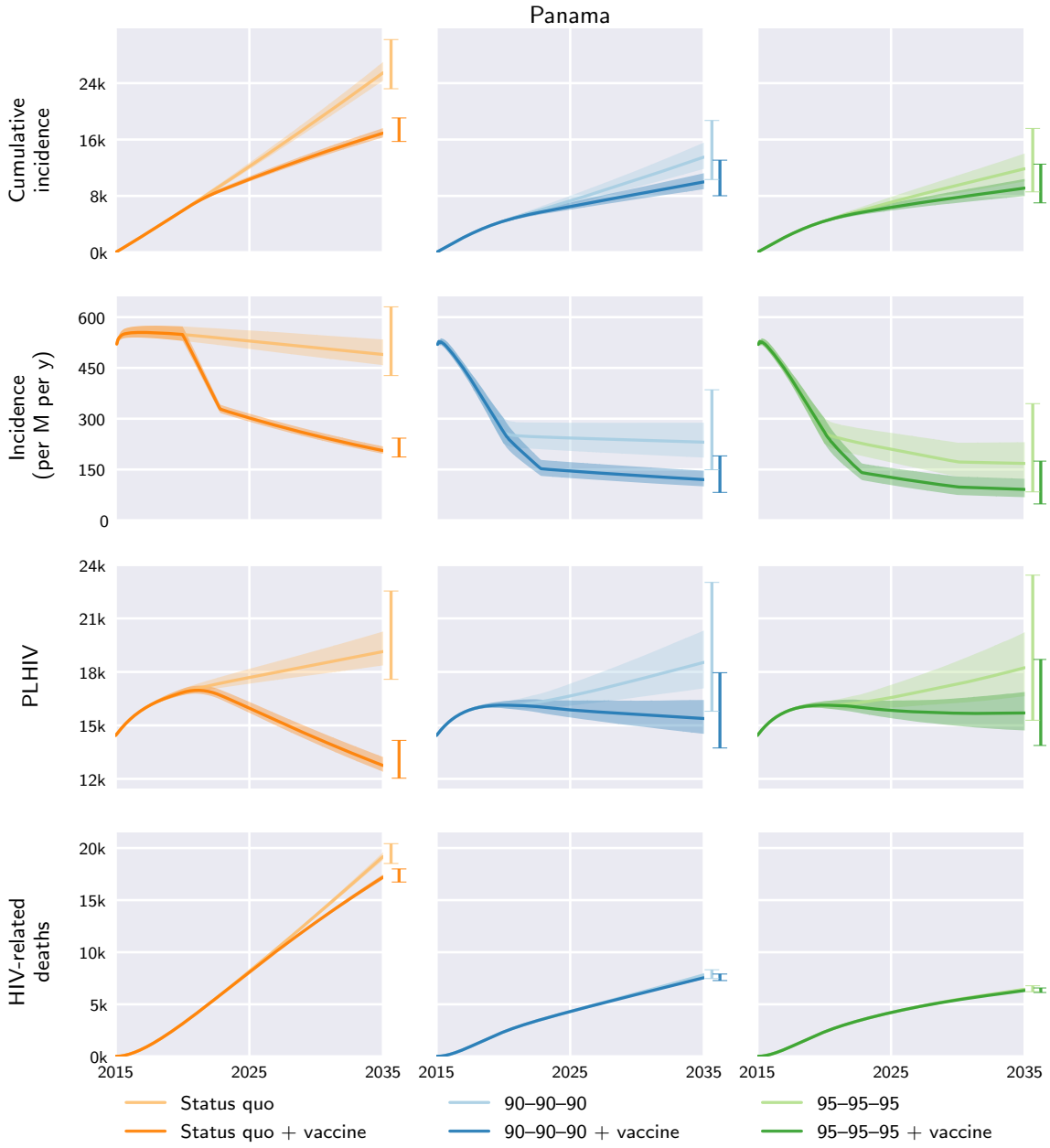

Fig. S100. Panama model outcomes under the different diagnosis, treatment, and vaccination scenarios. Central curves show the medians over model runs with 1000 samples from parameter distributions, shaded regions show the 1st and 3rd quartiles (i.e. 25th and 75th percentiles), and vertical bars to the right of each axis show the 5th and 95th percentiles at the end time, 2035. Regional and global outcomes were aggregated from the country-level model outcomes.

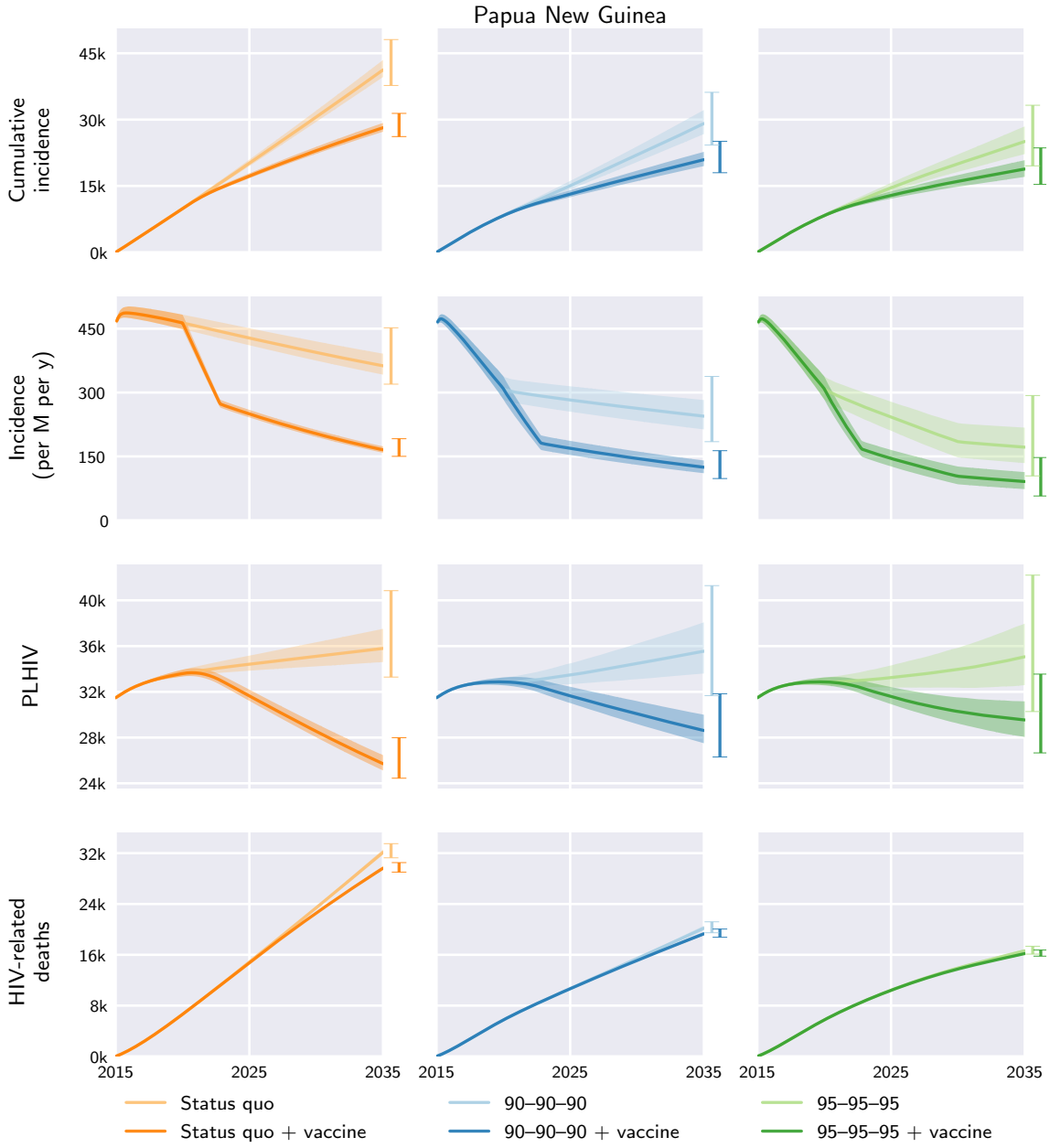

Fig. S101. Papua New Guinea model outcomes under the different diagnosis, treatment, and vaccination scenarios. Central curves show the medians over model runs with 1000 samples from parameter distributions, shaded regions show the 1st and 3rd quartiles (i.e. 25th and 75th percentiles), and vertical bars to the right of each axis show the 5th and 95th percentiles at the end time, 2035. Regional and global outcomes were aggregated from the country-level model outcomes.

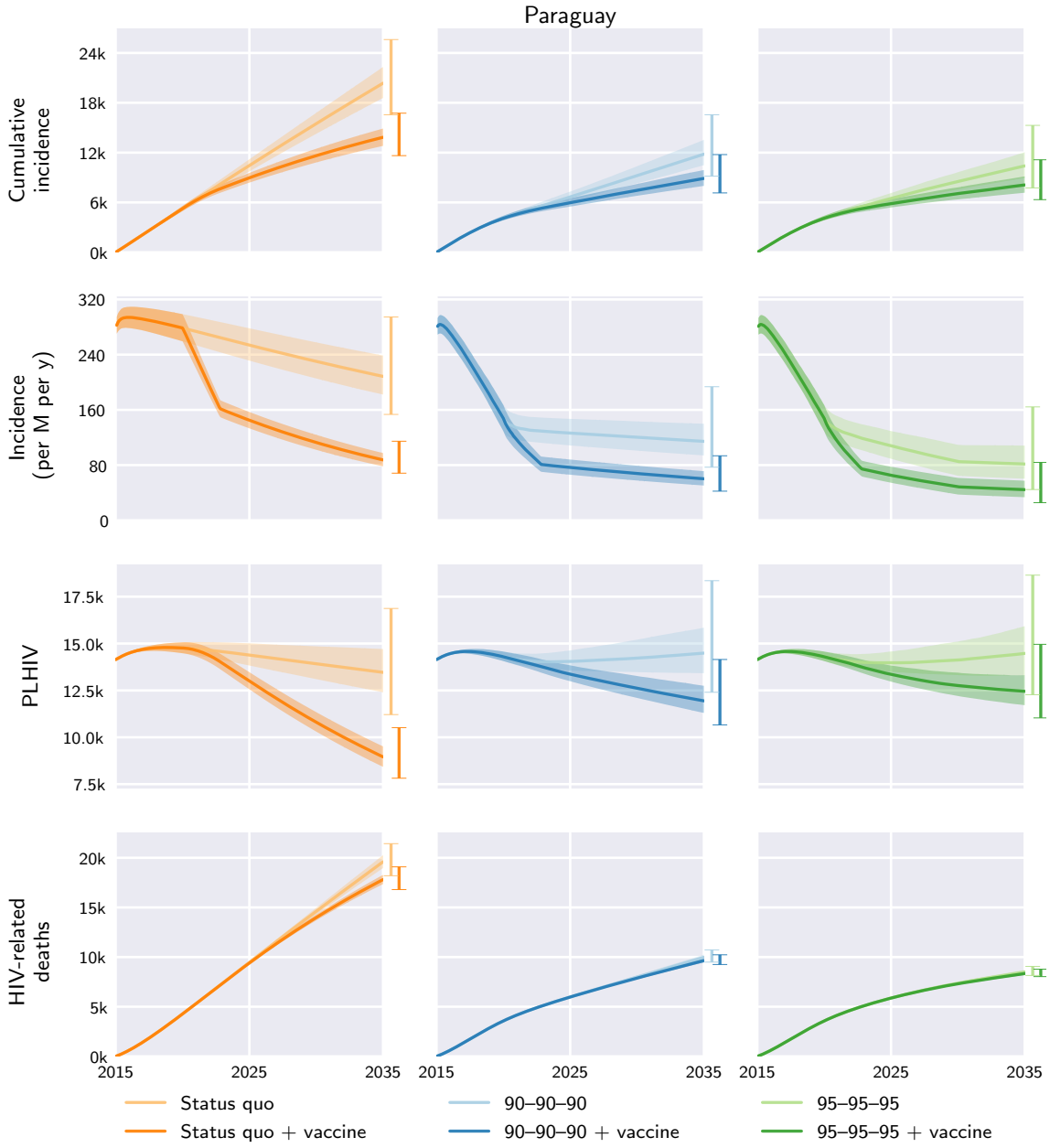

Fig. S102. Paraguay model outcomes under the different diagnosis, treatment, and vaccination scenarios. Central curves show the medians over model runs with 1000 samples from parameter distributions, shaded regions show the 1st and 3rd quartiles (i.e. 25th and 75th percentiles), and vertical bars to the right of each axis show the 5th and 95th percentiles at the end time, 2035. Regional and global outcomes were aggregated from the country-level model outcomes.

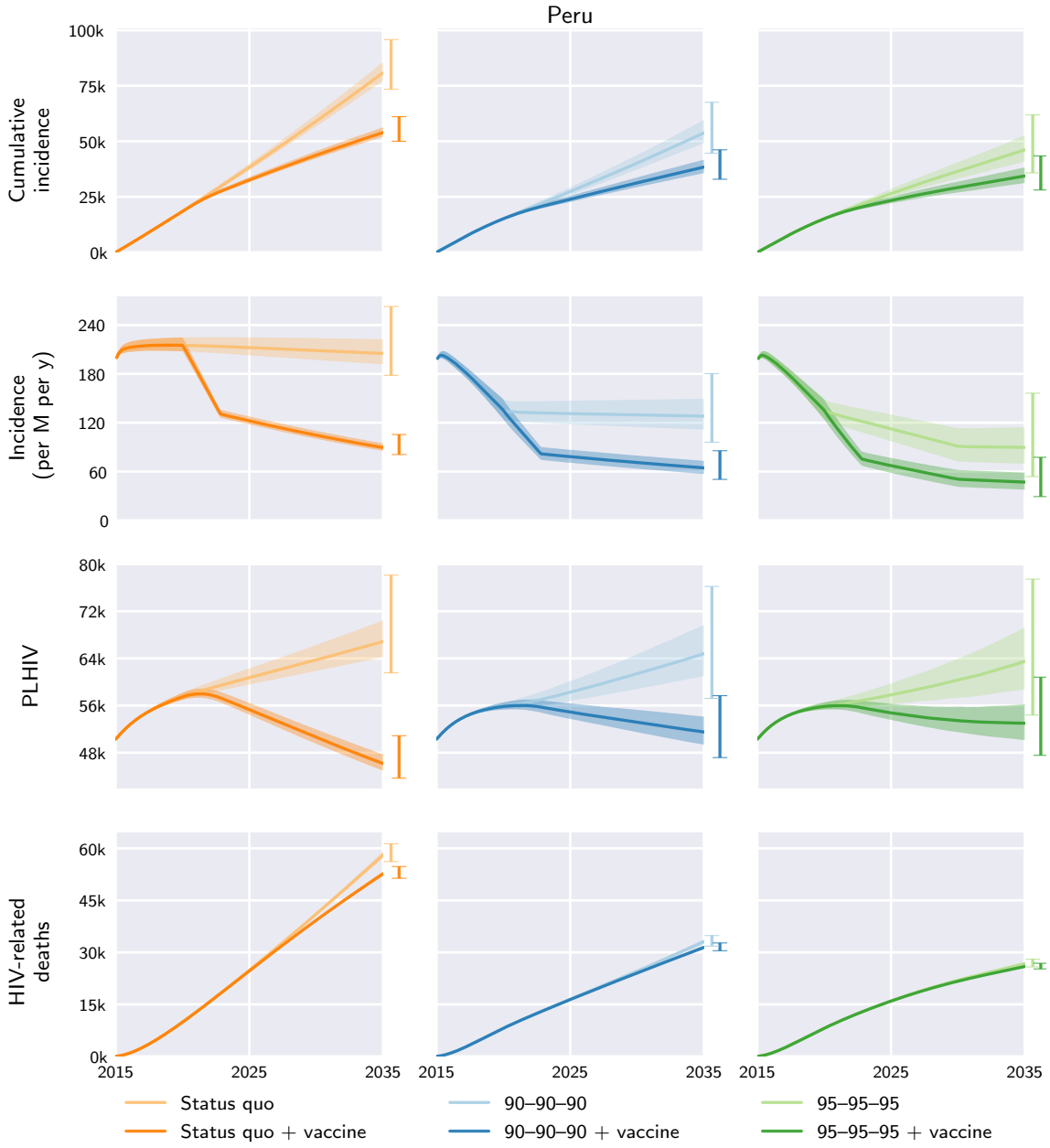

Fig. S103. Peru model outcomes under the different diagnosis, treatment, and vaccination scenarios. Central curves show the medians over model runs with 1000 samples from parameter distributions, shaded regions show the 1st and 3rd quartiles (i.e. 25th and 75th percentiles), and vertical bars to the right of each axis show the 5th and 95th percentiles at the end time, 2035. Regional and global outcomes were aggregated from the country-level model outcomes.

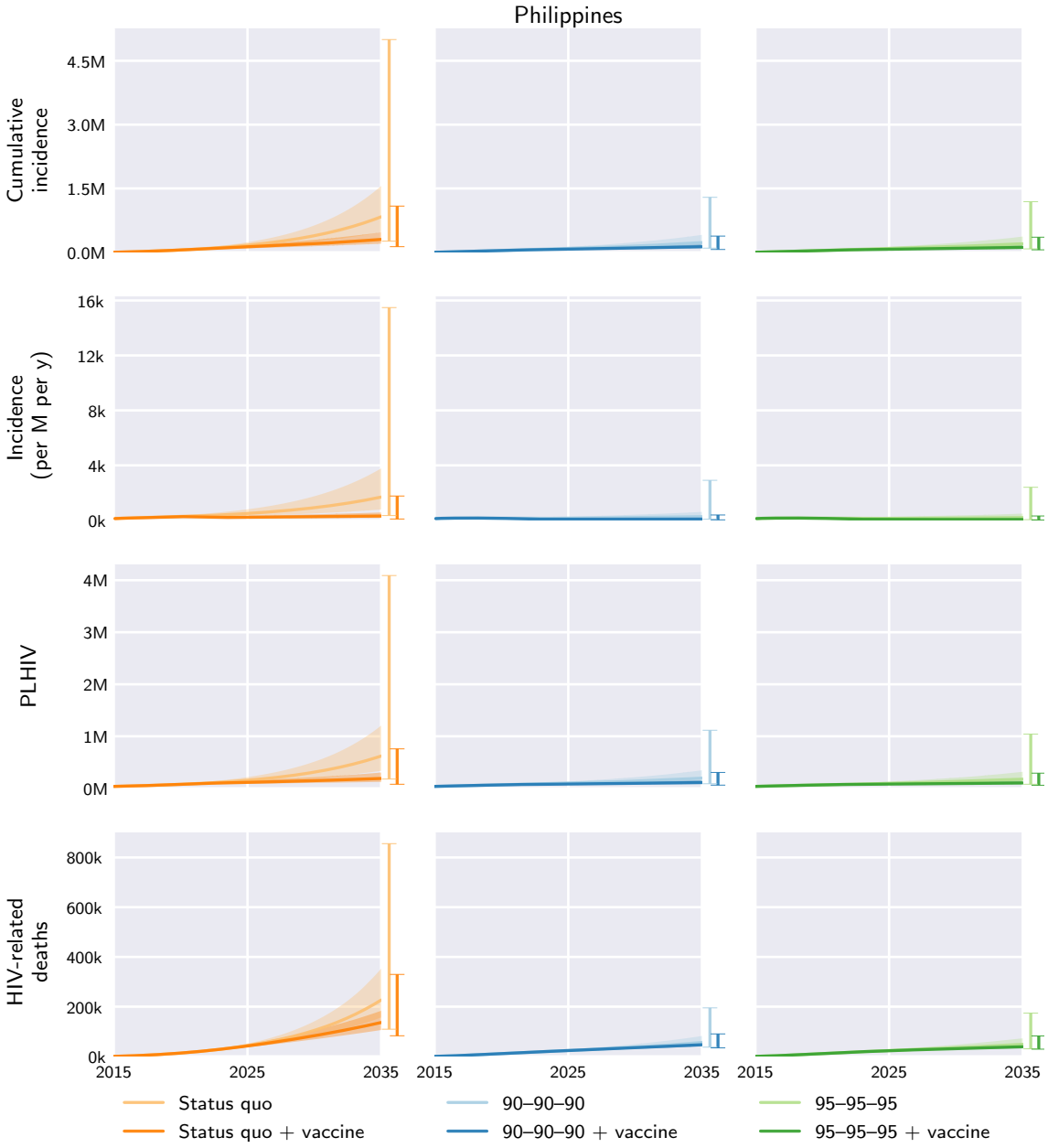

Fig. S104. Philippines model outcomes under the different diagnosis, treatment, and vaccination scenarios. Central curves show the medians over model runs with 1000 samples from parameter distributions, shaded regions show the 1st and 3rd quartiles (i.e. 25th and 75th percentiles), and vertical bars to the right of each axis show the 5th and 95th percentiles at the end time, 2035. Regional and global outcomes were aggregated from the country-level model outcomes.

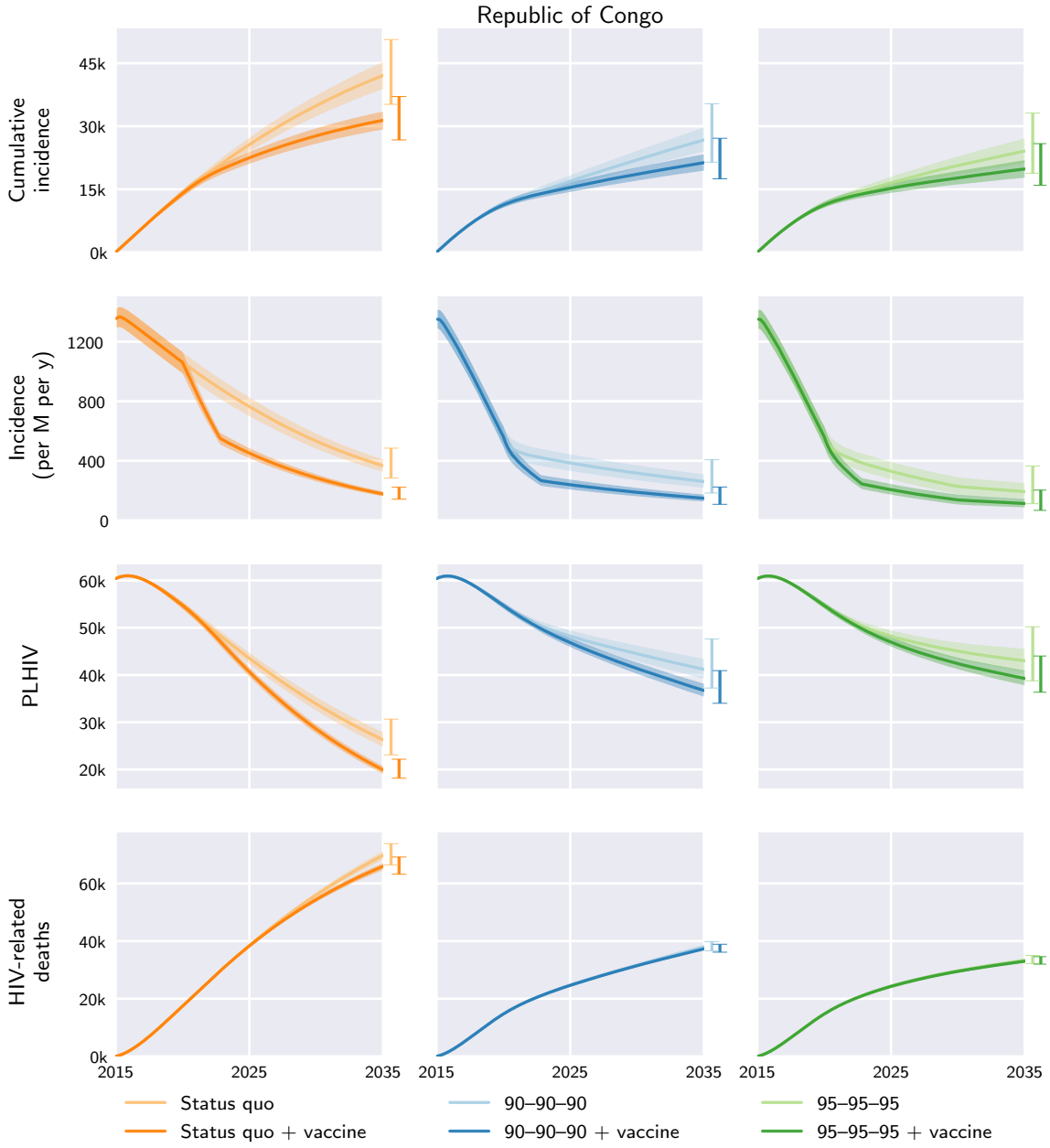

Fig. S105. Republic of Congo model outcomes under the different diagnosis, treatment, and vaccination scenarios. Central curves show the medians over model runs with 1000 samples from parameter distributions, shaded regions show the 1st and 3rd quartiles (i.e. 25th and 75th percentiles), and vertical bars to the right of each axis show the 5th and 95th percentiles at the end time, 2035. Regional and global outcomes were aggregated from the country-level model outcomes.

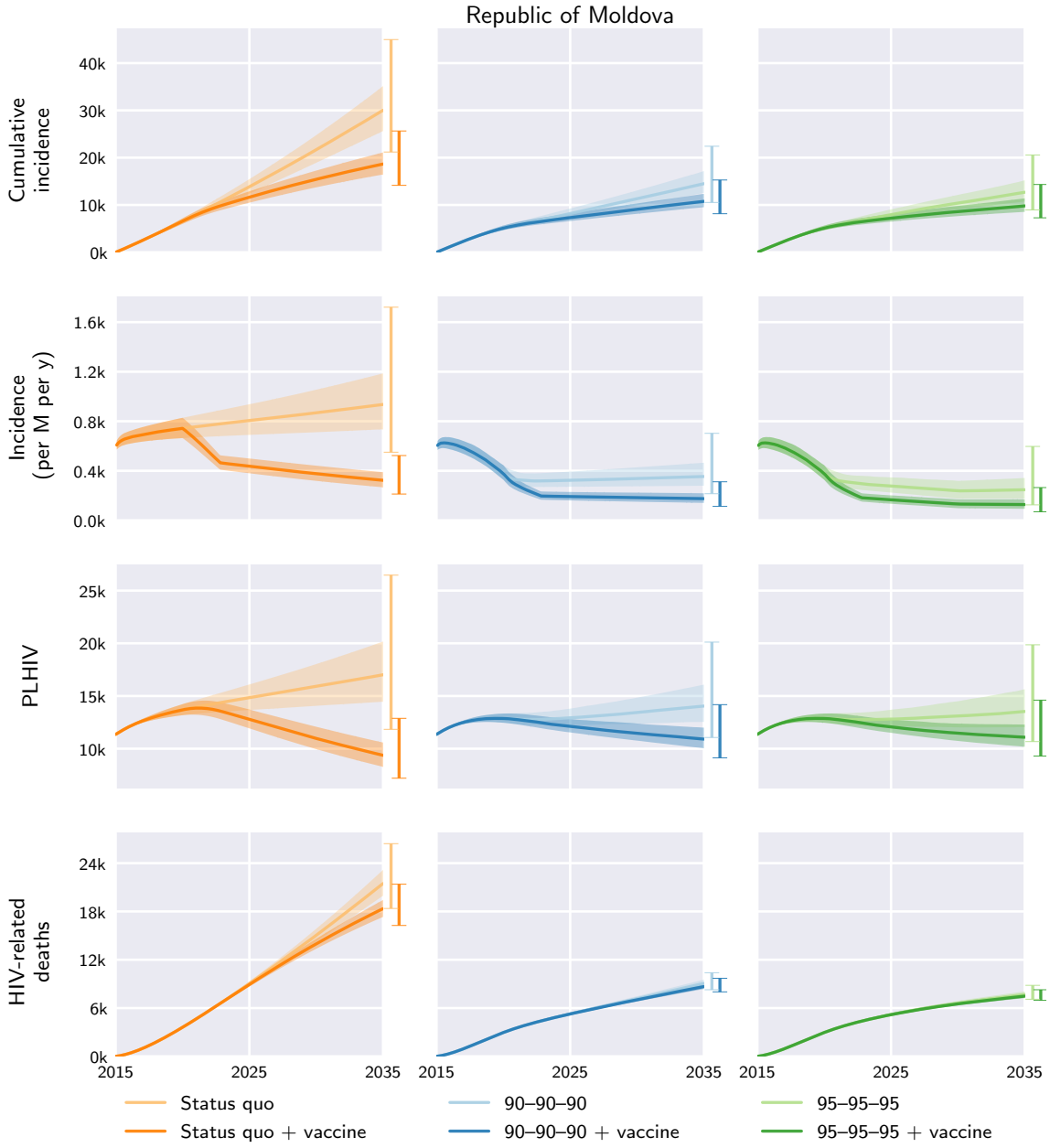

Fig. S106. Republic of Moldova model outcomes under the different diagnosis, treatment, and vaccination scenarios. Central curves show the medians over model runs with 1000 samples from parameter distributions, shaded regions show the 1st and 3rd quartiles (i.e. 25th and 75th percentiles), and vertical bars to the right of each axis show the 5th and 95th percentiles at the end time, 2035. Regional and global outcomes were aggregated from the country-level model outcomes.

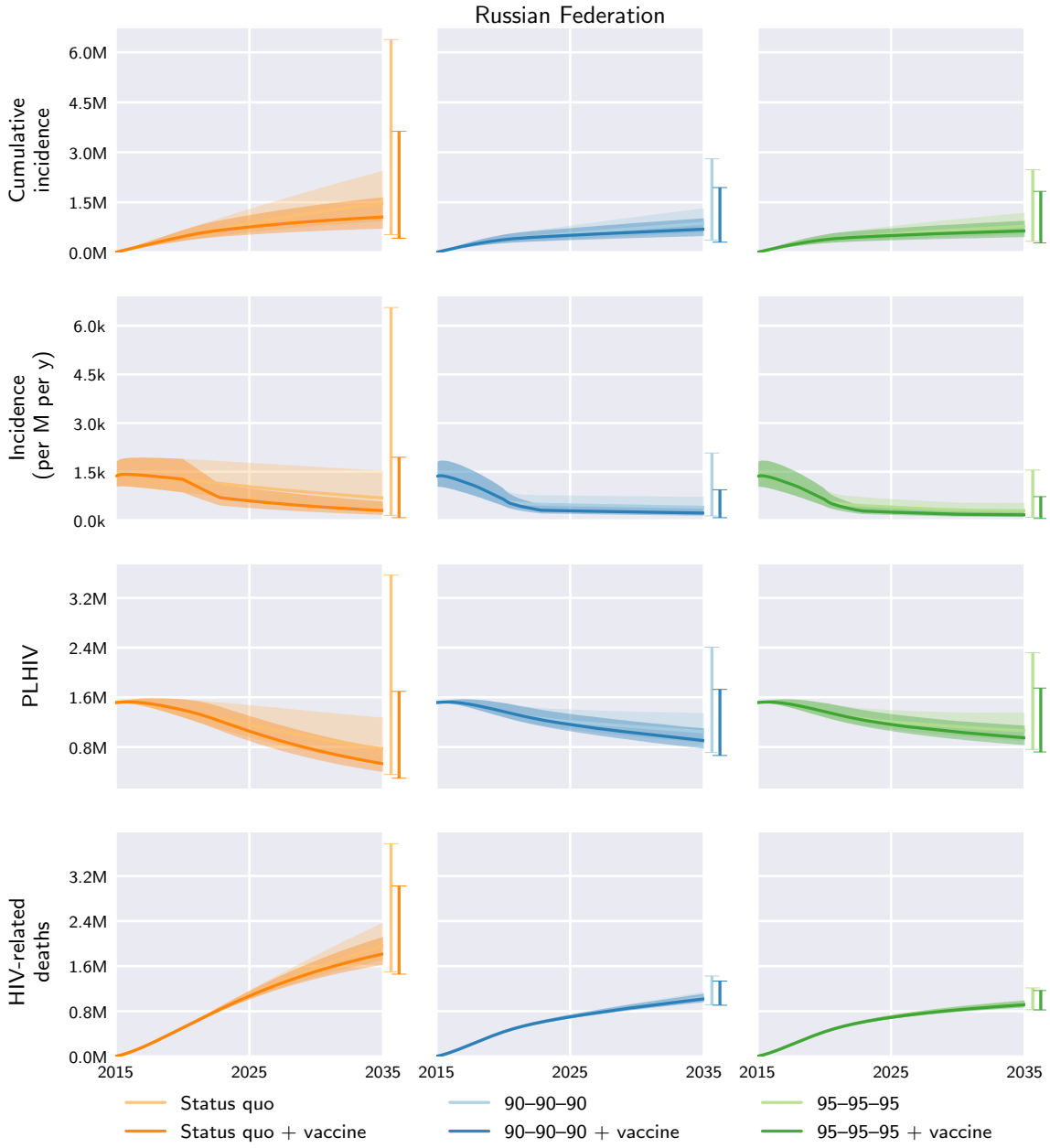

Fig. S107. Russian Federation model outcomes under the different diagnosis, treatment, and vaccination scenarios. Central curves show the medians over model runs with 1000 samples from parameter distributions, shaded regions show the 1st and 3rd quartiles (i.e. 25th and 75th percentiles), and vertical bars to the right of each axis show the 5th and 95th percentiles at the end time, 2035. Regional and global outcomes were aggregated from the country-level model outcomes.

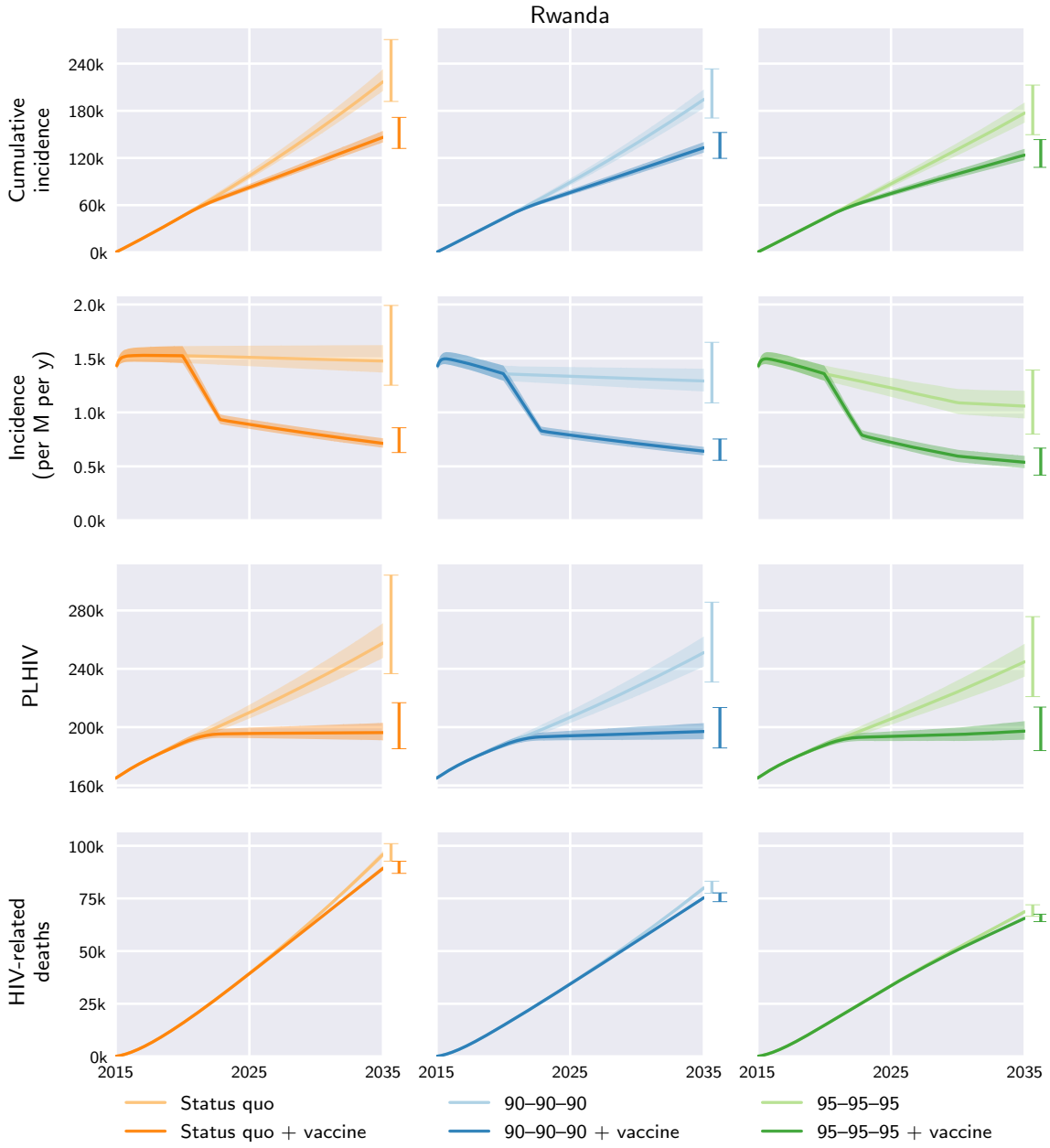

Fig. S108. Rwanda model outcomes under the different diagnosis, treatment, and vaccination scenarios. Central curves show the medians over model runs with 1000 samples from parameter distributions, shaded regions show the 1st and 3rd quartiles (i.e. 25th and 75th percentiles), and vertical bars to the right of each axis show the 5th and 95th percentiles at the end time, 2035. Regional and global outcomes were aggregated from the country-level model outcomes.

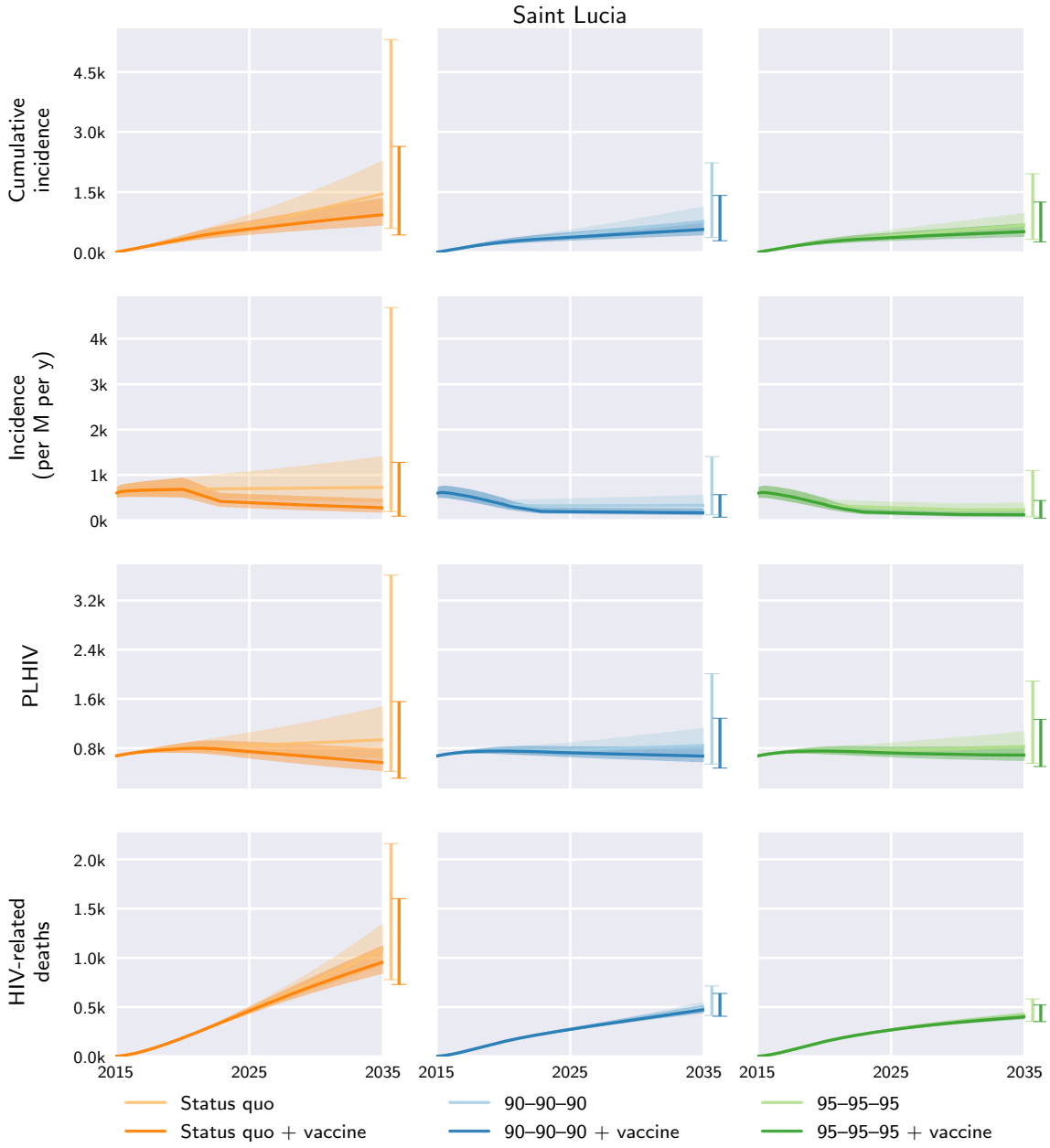

Fig. S109. Saint Lucia model outcomes under the different diagnosis, treatment, and vaccination scenarios. Central curves show the medians over model runs with 1000 samples from parameter distributions, shaded regions show the 1st and 3rd quartiles (i.e. 25th and 75th percentiles), and vertical bars to the right of each axis show the 5th and 95th percentiles at the end time, 2035. Regional and global outcomes were aggregated from the country-level model outcomes.

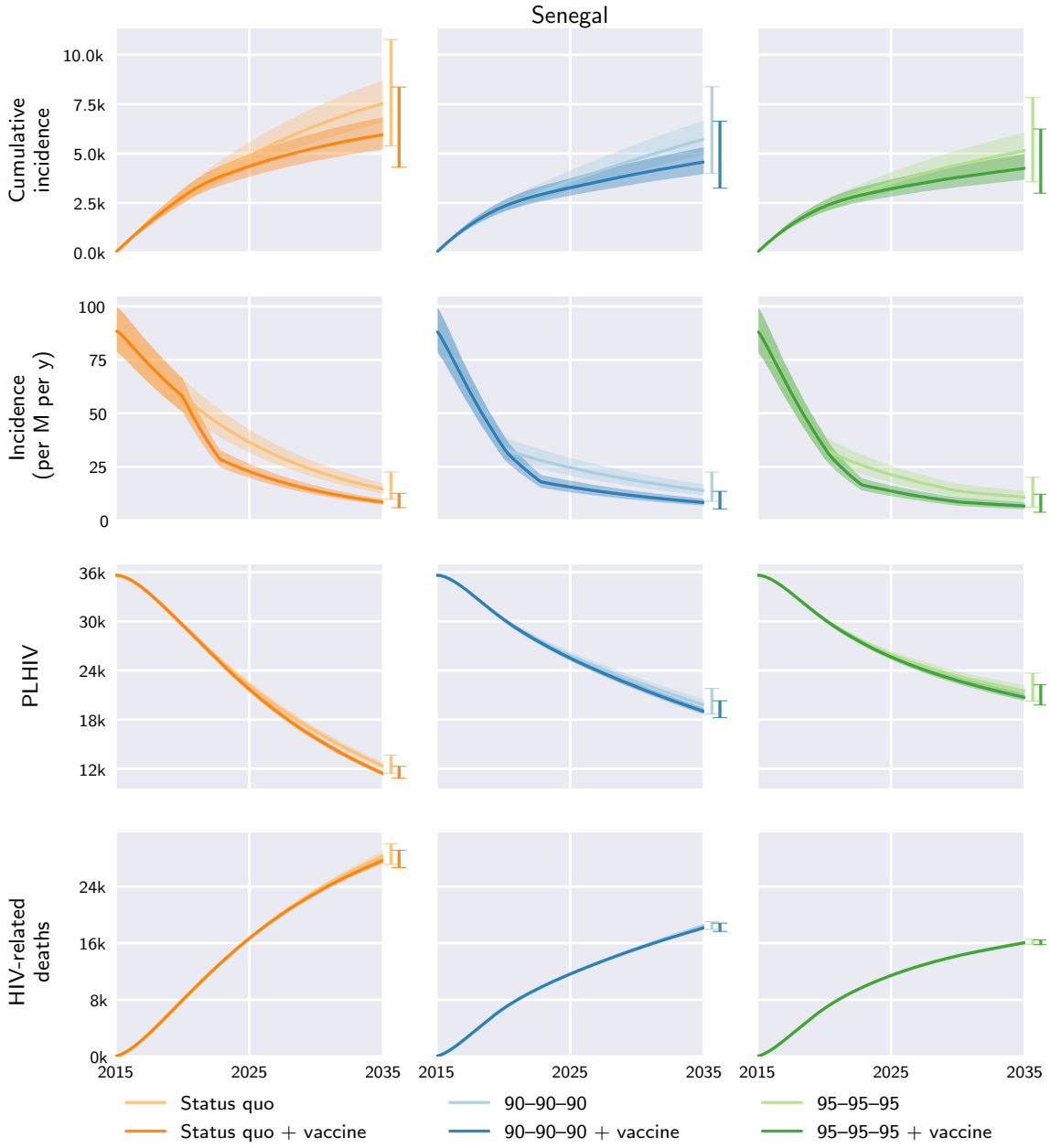

Fig. S110. Senegal model outcomes under the different diagnosis, treatment, and vaccination scenarios. Central curves show the medians over model runs with 1000 samples from parameter distributions, shaded regions show the 1st and 3rd quartiles (i.e. 25th and 75th percentiles), and vertical bars to the right of each axis show the 5th and 95th percentiles at the end time, 2035. Regional and global outcomes were aggregated from the country-level model outcomes.

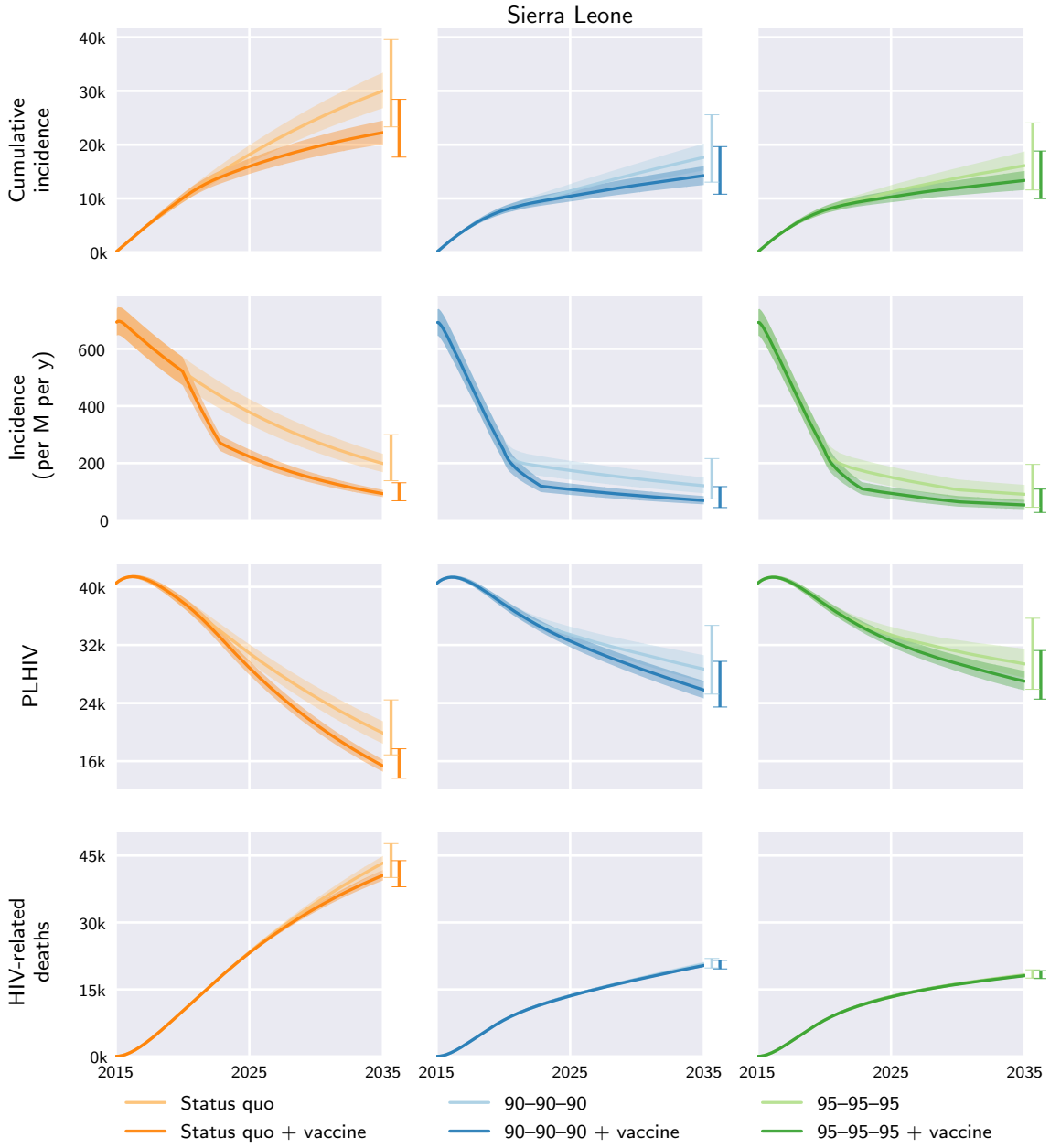

Fig. S111. Sierra Leone model outcomes under the different diagnosis, treatment, and vaccination scenarios. Central curves show the medians over model runs with 1000 samples from parameter distributions, shaded regions show the 1st and 3rd quartiles (i.e. 25th and 75th percentiles), and vertical bars to the right of each axis show the 5th and 95th percentiles at the end time, 2035. Regional and global outcomes were aggregated from the country-level model outcomes.

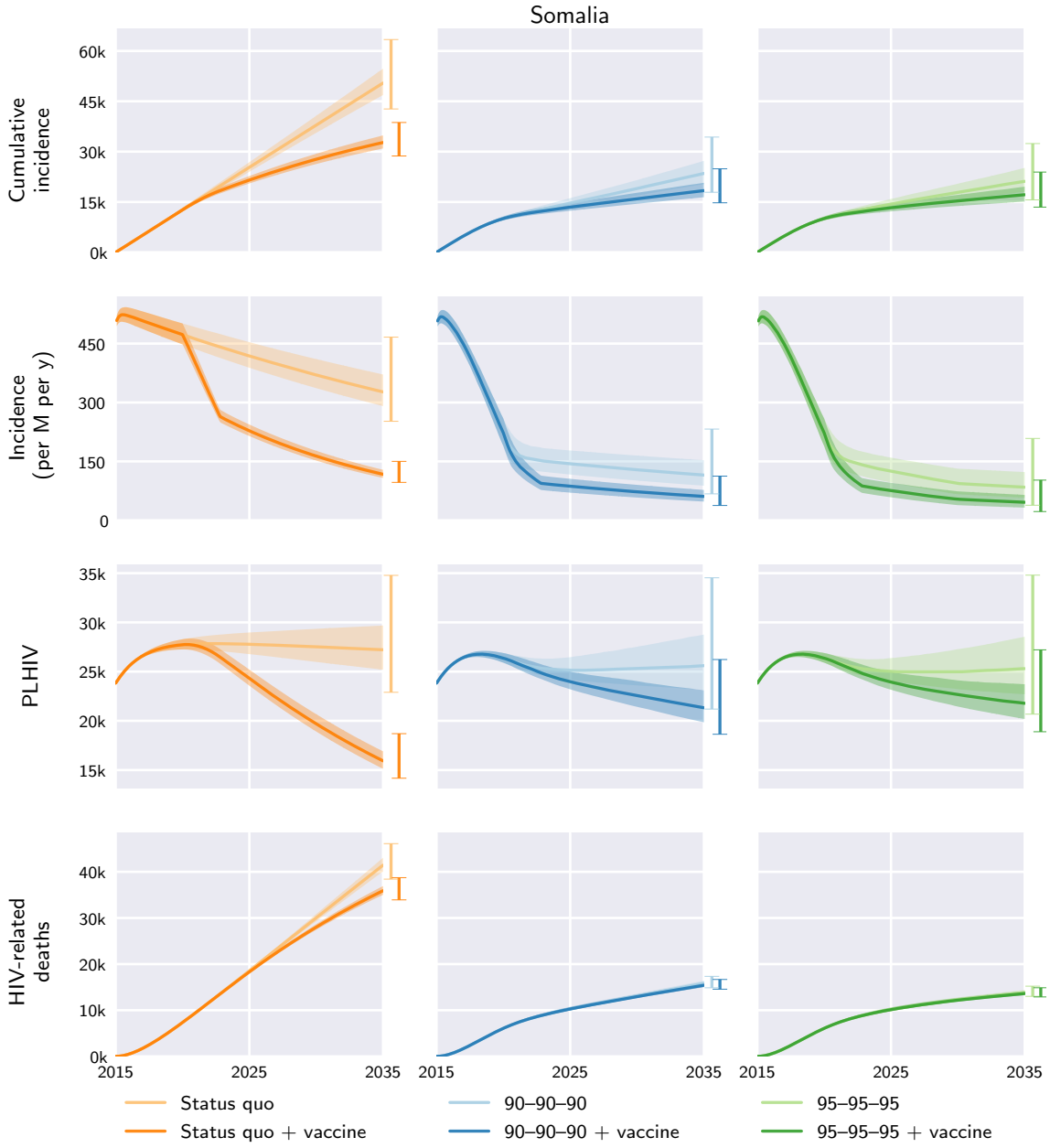

Fig. S112. Somalia model outcomes under the different diagnosis, treatment, and vaccination scenarios. Central curves show the medians over model runs with 1000 samples from parameter distributions, shaded regions show the 1st and 3rd quartiles (i.e. 25th and 75th percentiles), and vertical bars to the right of each axis show the 5th and 95th percentiles at the end time, 2035. Regional and global outcomes were aggregated from the country-level model outcomes.

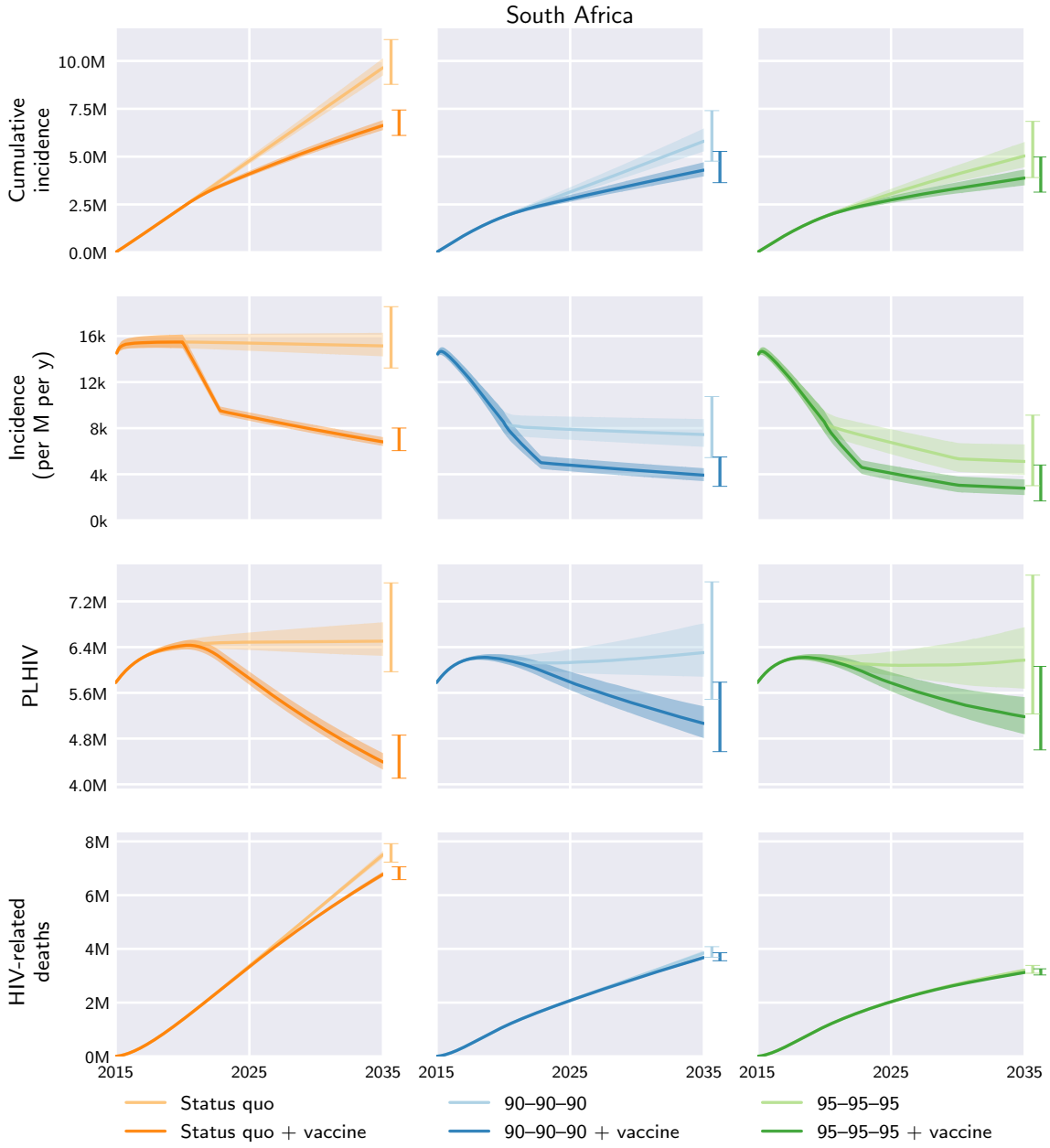

Fig. S113. South Africa model outcomes under the different diagnosis, treatment, and vaccination scenarios. Central curves show the medians over model runs with 1000 samples from parameter distributions, shaded regions show the 1st and 3rd quartiles (i.e. 25th and 75th percentiles), and vertical bars to the right of each axis show the 5th and 95th percentiles at the end time, 2035. Regional and global outcomes were aggregated from the country-level model outcomes.

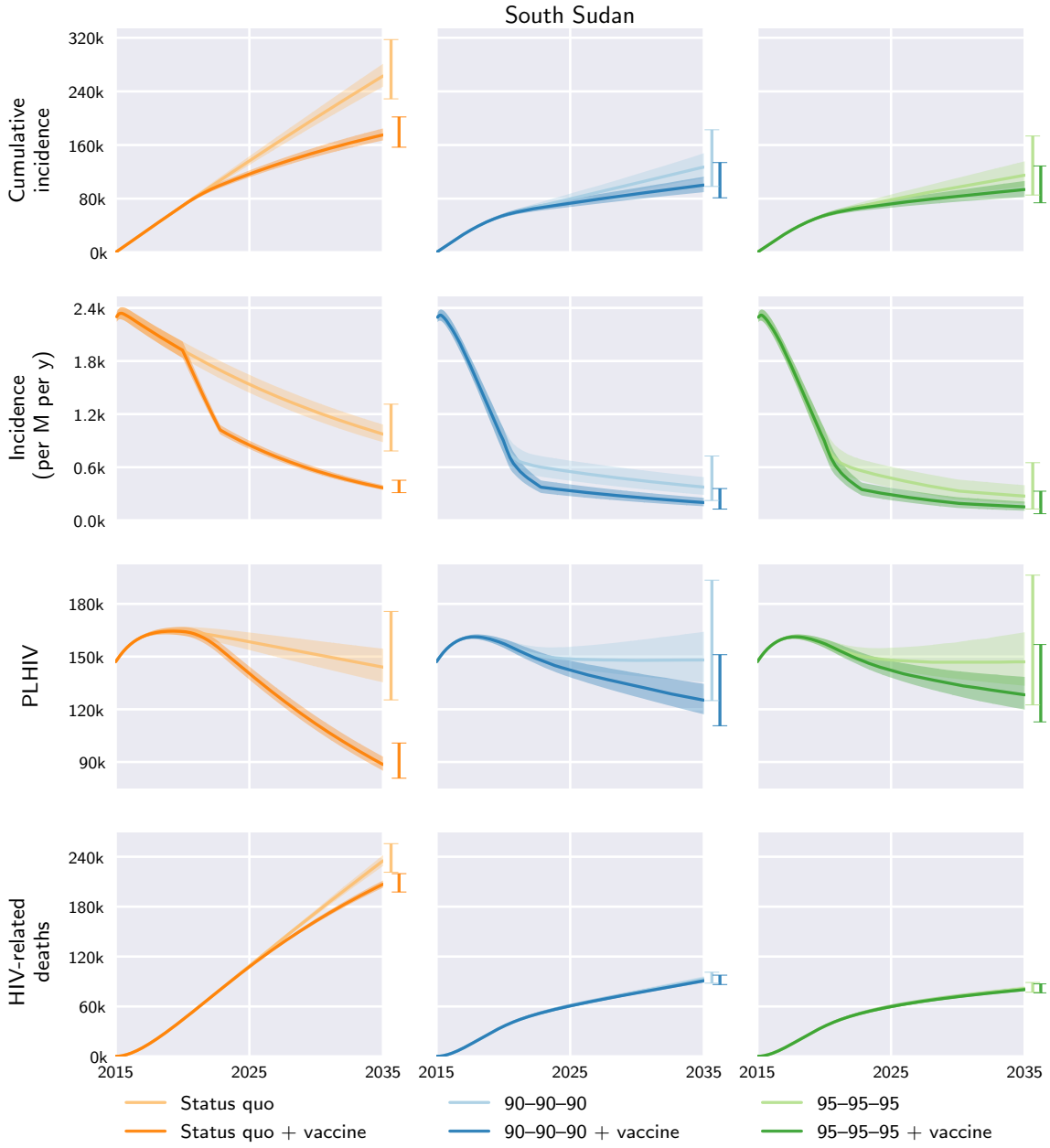

Fig. S114. South Sudan model outcomes under the different diagnosis, treatment, and vaccination scenarios. Central curves show the medians over model runs with 1000 samples from parameter distributions, shaded regions show the 1st and 3rd quartiles (i.e. 25th and 75th percentiles), and vertical bars to the right of each axis show the 5th and 95th percentiles at the end time, 2035. Regional and global outcomes were aggregated from the country-level model outcomes.

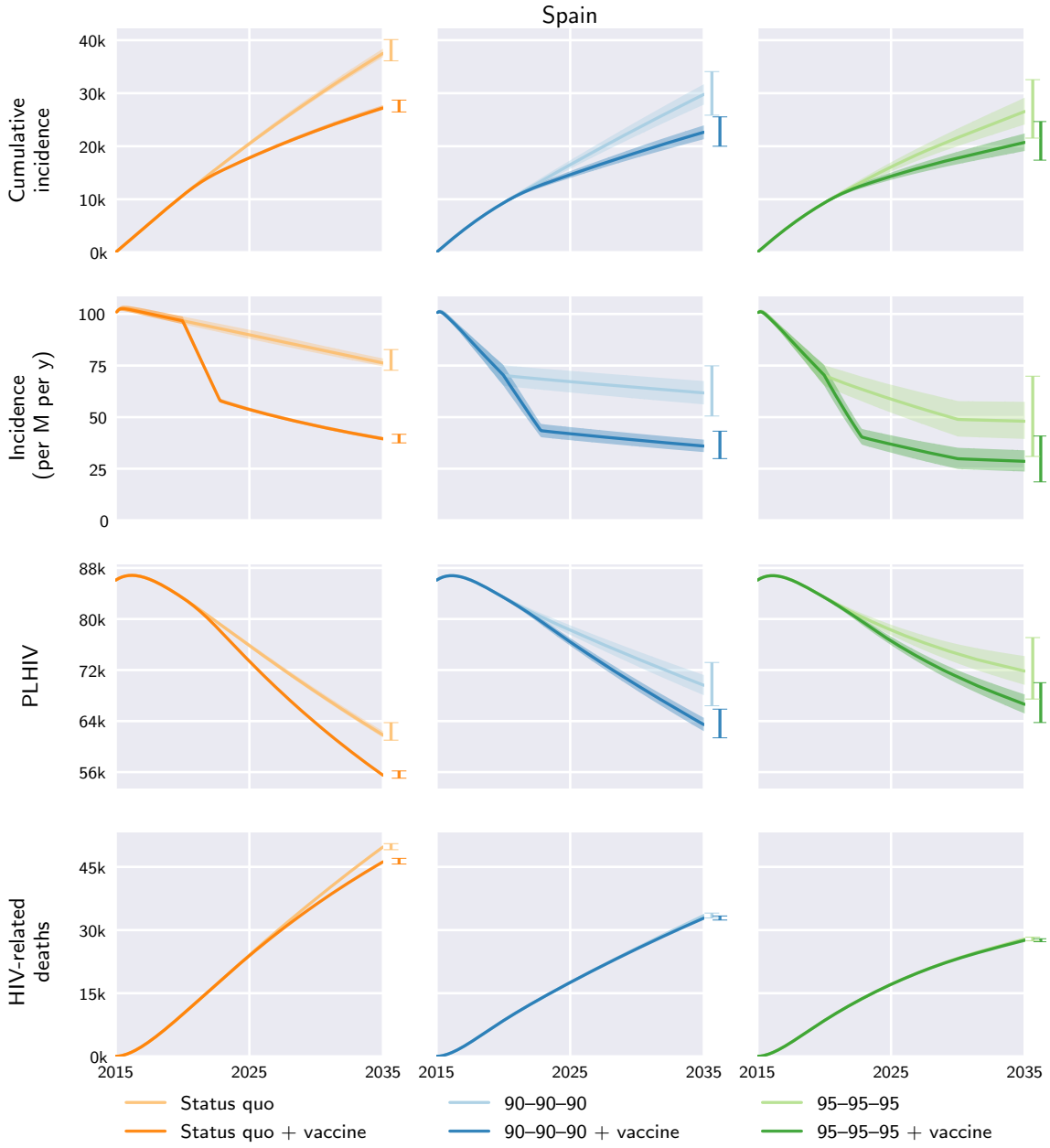

Fig. S115. Spain model outcomes under the different diagnosis, treatment, and vaccination scenarios. Central curves show the medians over model runs with 1000 samples from parameter distributions, shaded regions show the 1st and 3rd quartiles (i.e. 25th and 75th percentiles), and vertical bars to the right of each axis show the 5th and 95th percentiles at the end time, 2035. Regional and global outcomes were aggregated from the country-level model outcomes.

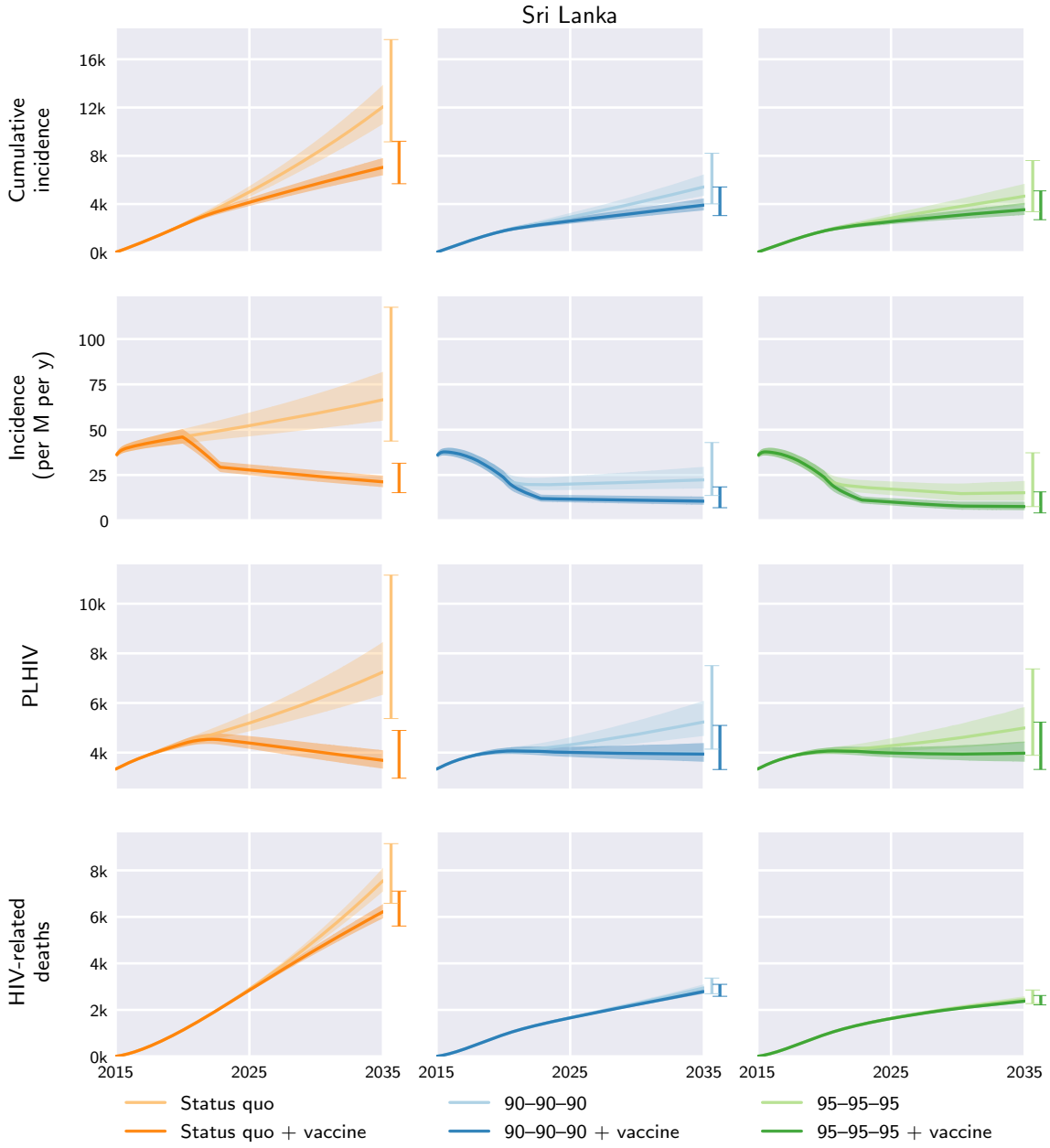

Fig. S116. Sri Lanka model outcomes under the different diagnosis, treatment, and vaccination scenarios. Central curves show the medians over model runs with 1000 samples from parameter distributions, shaded regions show the 1st and 3rd quartiles (i.e. 25th and 75th percentiles), and vertical bars to the right of each axis show the 5th and 95th percentiles at the end time, 2035. Regional and global outcomes were aggregated from the country-level model outcomes.

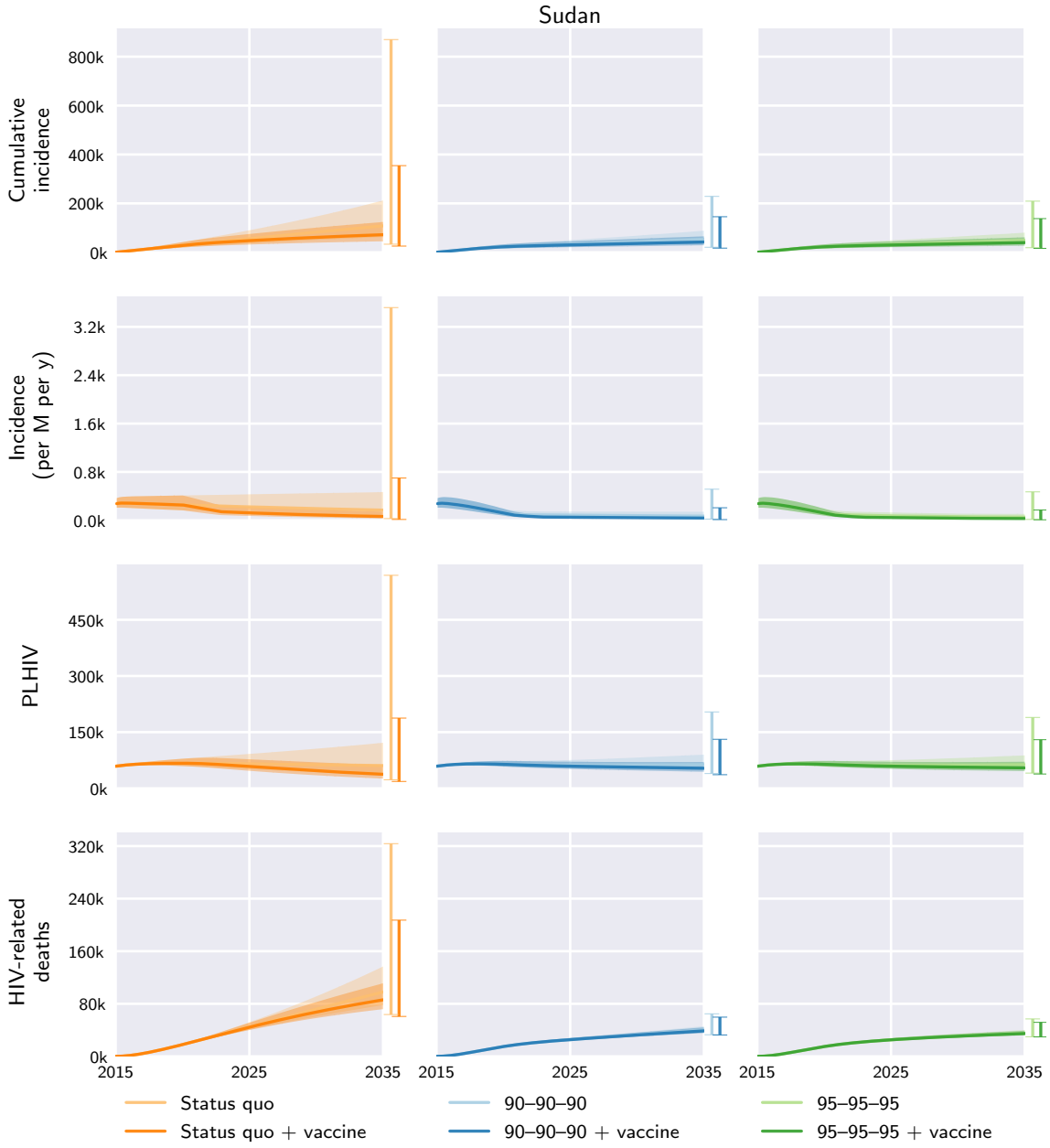

Fig. S117. Sudan model outcomes under the different diagnosis, treatment, and vaccination scenarios. Central curves show the medians over model runs with 1000 samples from parameter distributions, shaded regions show the 1st and 3rd quartiles (i.e. 25th and 75th percentiles), and vertical bars to the right of each axis show the 5th and 95th percentiles at the end time, 2035. Regional and global outcomes were aggregated from the country-level model outcomes.

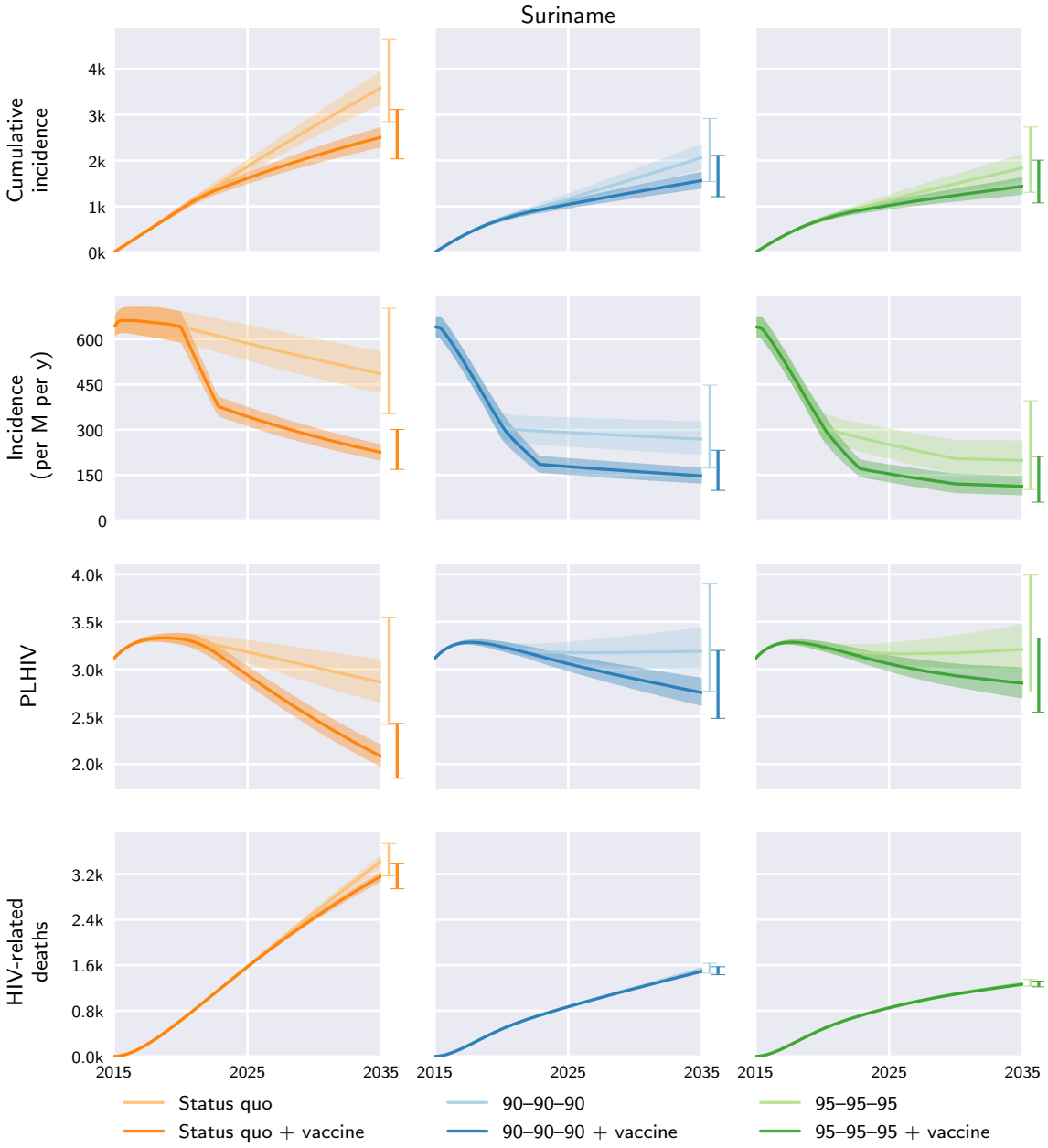

Fig. S118. Suriname model outcomes under the different diagnosis, treatment, and vaccination scenarios. Central curves show the medians over model runs with 1000 samples from parameter distributions, shaded regions show the 1st and 3rd quartiles (i.e. 25th and 75th percentiles), and vertical bars to the right of each axis show the 5th and 95th percentiles at the end time, 2035. Regional and global outcomes were aggregated from the country-level model outcomes.

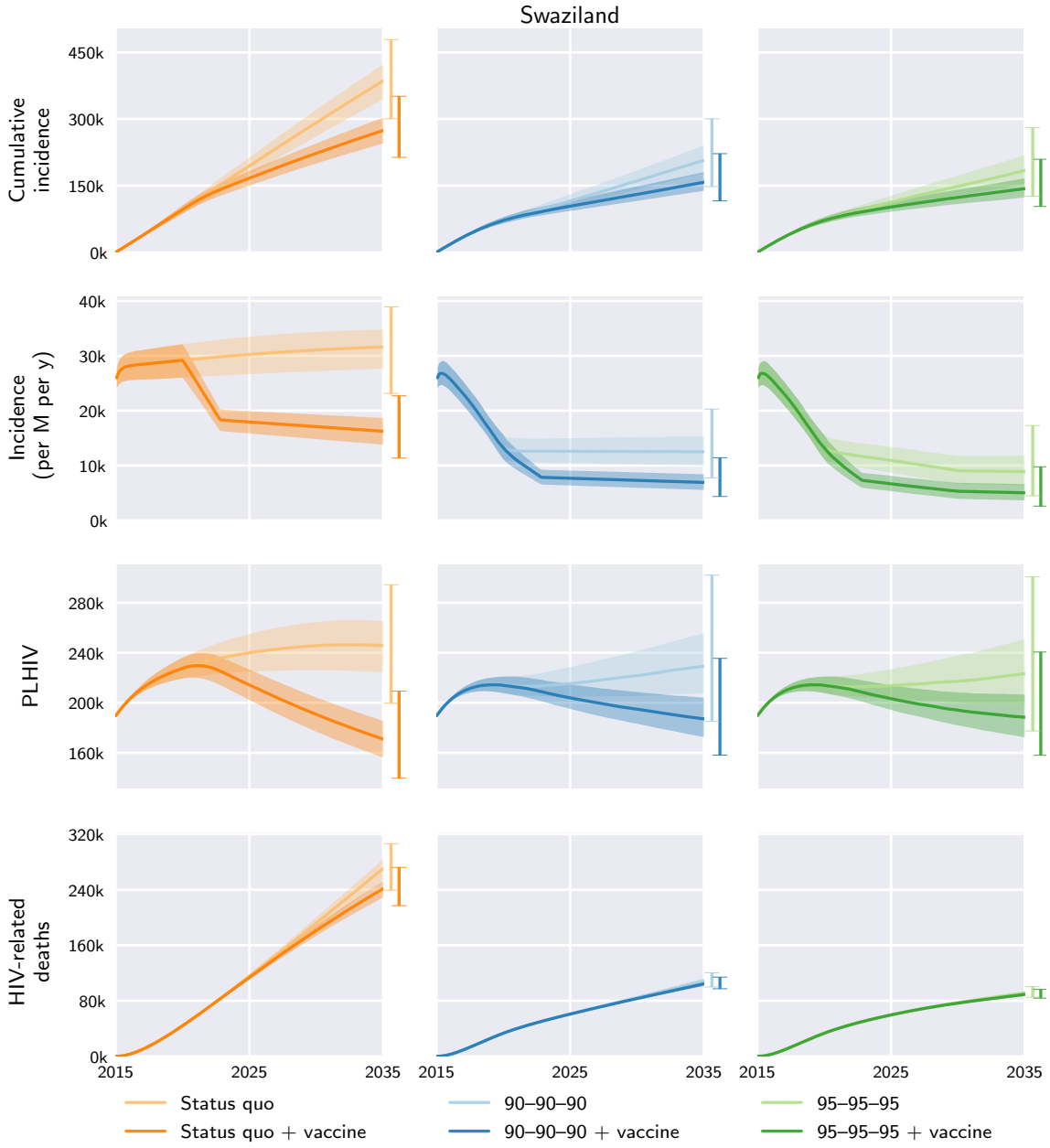

Fig. S119. Swaziland model outcomes under the different diagnosis, treatment, and vaccination scenarios. Central curves show the medians over model runs with 1000 samples from parameter distributions, shaded regions show the 1st and 3rd quartiles (i.e. 25th and 75th percentiles), and vertical bars to the right of each axis show the 5th and 95th percentiles at the end time, 2035. Regional and global outcomes were aggregated from the country-level model outcomes.

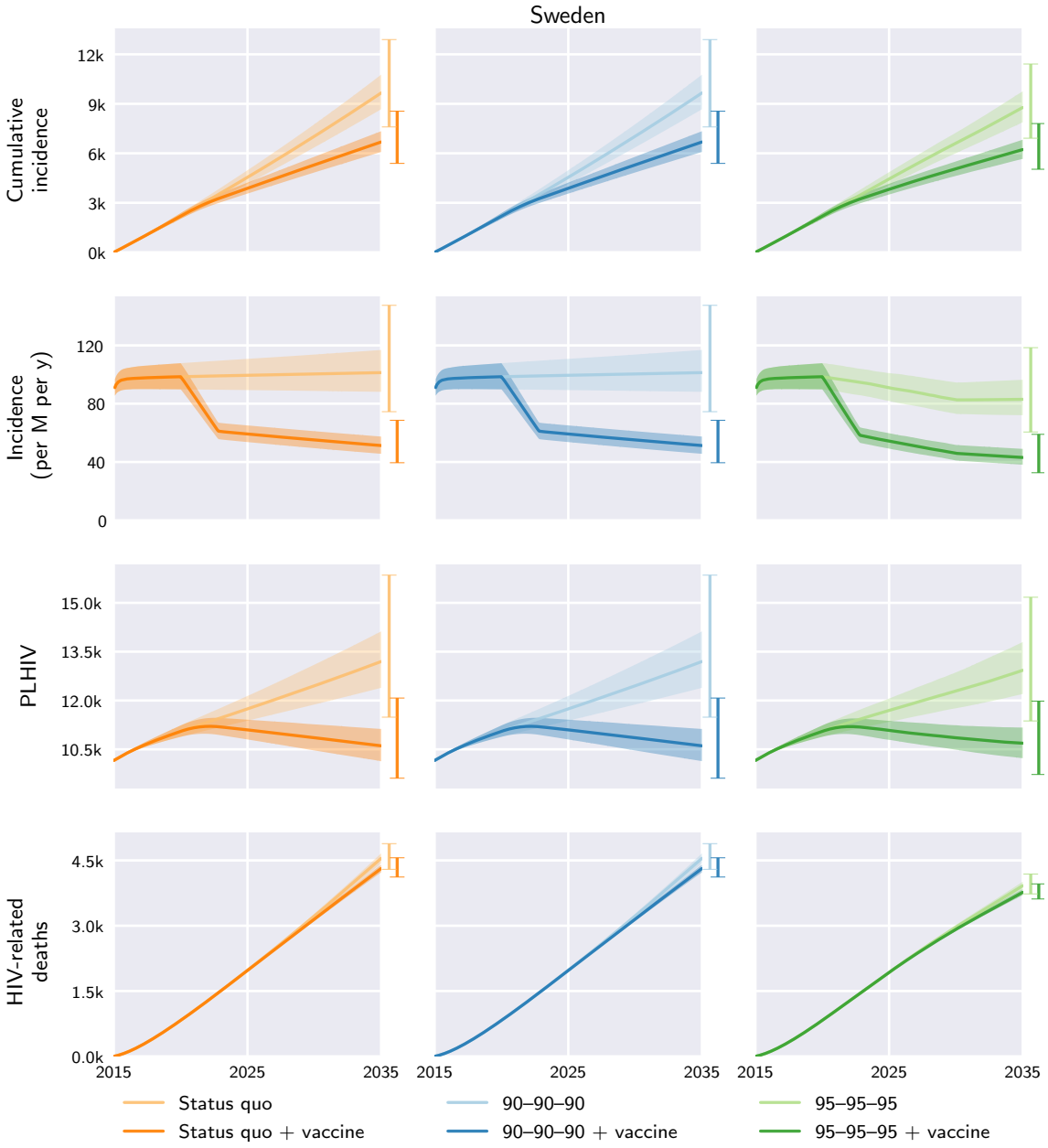

Fig. S120. Sweden model outcomes under the different diagnosis, treatment, and vaccination scenarios. Central curves show the medians over model runs with 1000 samples from parameter distributions, shaded regions show the 1st and 3rd quartiles (i.e. 25th and 75th percentiles), and vertical bars to the right of each axis show the 5th and 95th percentiles at the end time, 2035. Regional and global outcomes were aggregated from the country-level model outcomes.

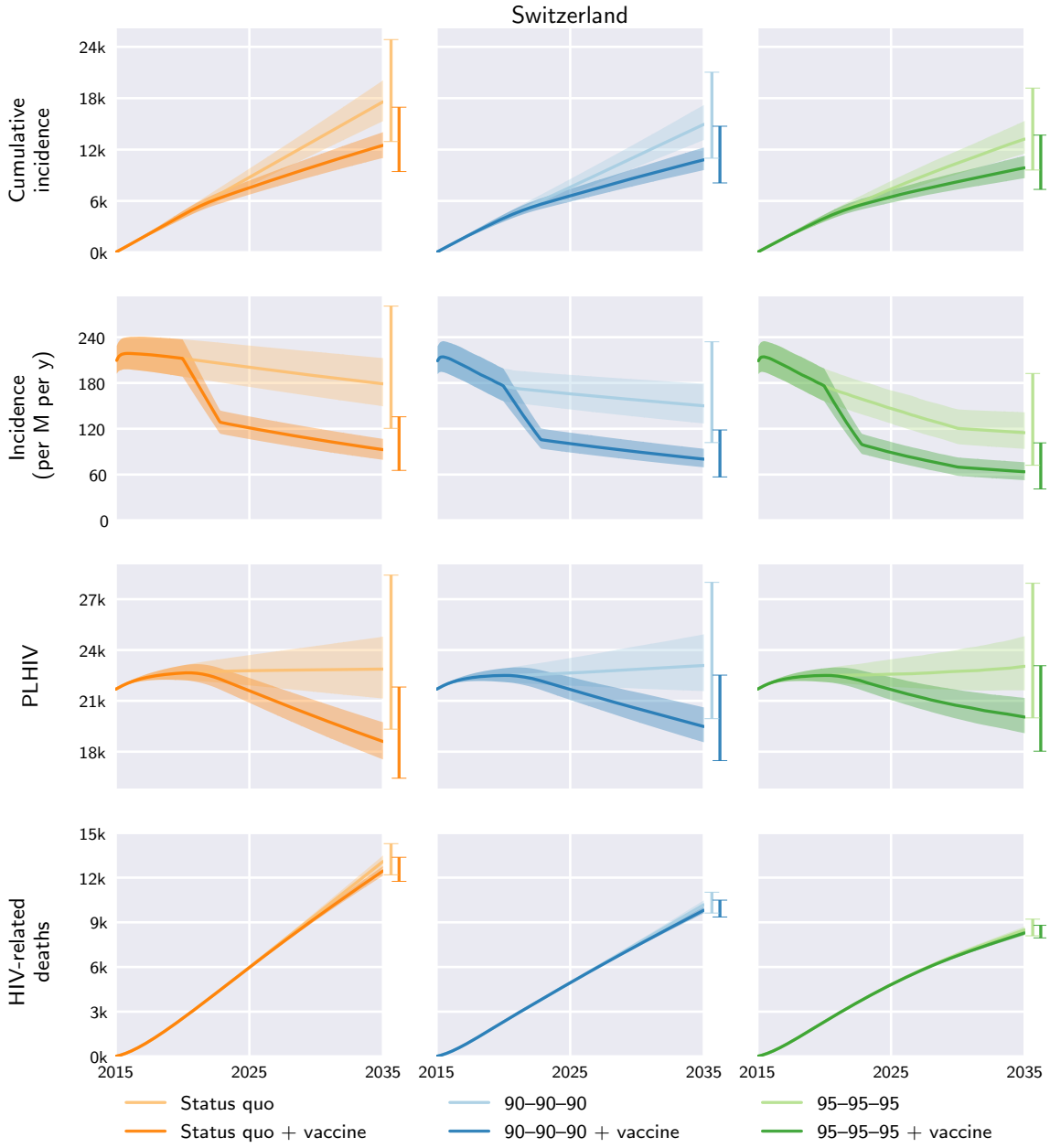

Fig. S121. Switzerland model outcomes under the different diagnosis, treatment, and vaccination scenarios. Central curves show the medians over model runs with 1000 samples from parameter distributions, shaded regions show the 1st and 3rd quartiles (i.e. 25th and 75th percentiles), and vertical bars to the right of each axis show the 5th and 95th percentiles at the end time, 2035. Regional and global outcomes were aggregated from the country-level model outcomes.

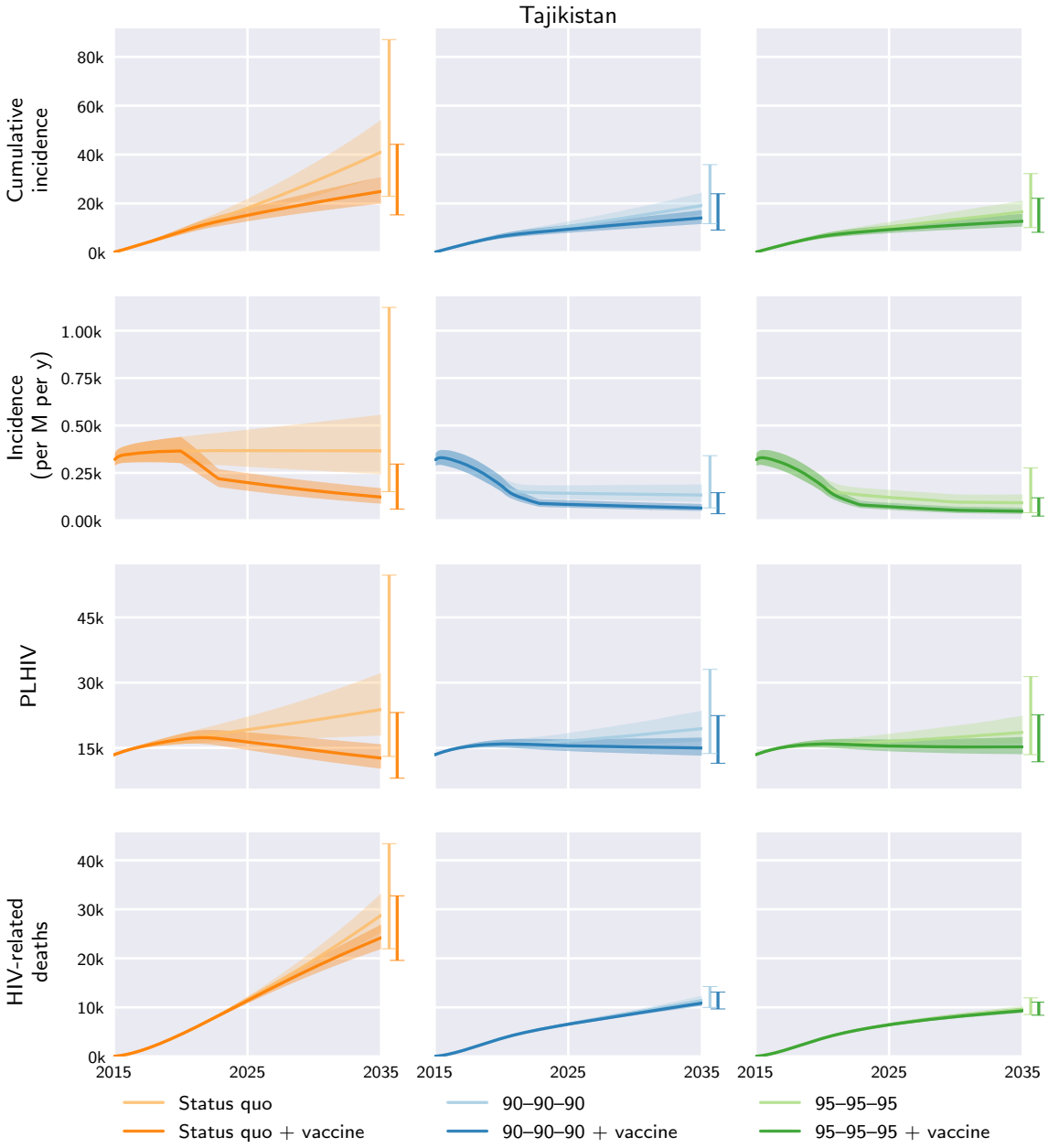

Fig. S122. Tajikistan model outcomes under the different diagnosis, treatment, and vaccination scenarios. Central curves show the medians over model runs with 1000 samples from parameter distributions, shaded regions show the 1st and 3rd quartiles (i.e. 25th and 75th percentiles), and vertical bars to the right of each axis show the 5th and 95th percentiles at the end time, 2035. Regional and global outcomes were aggregated from the country-level model outcomes.

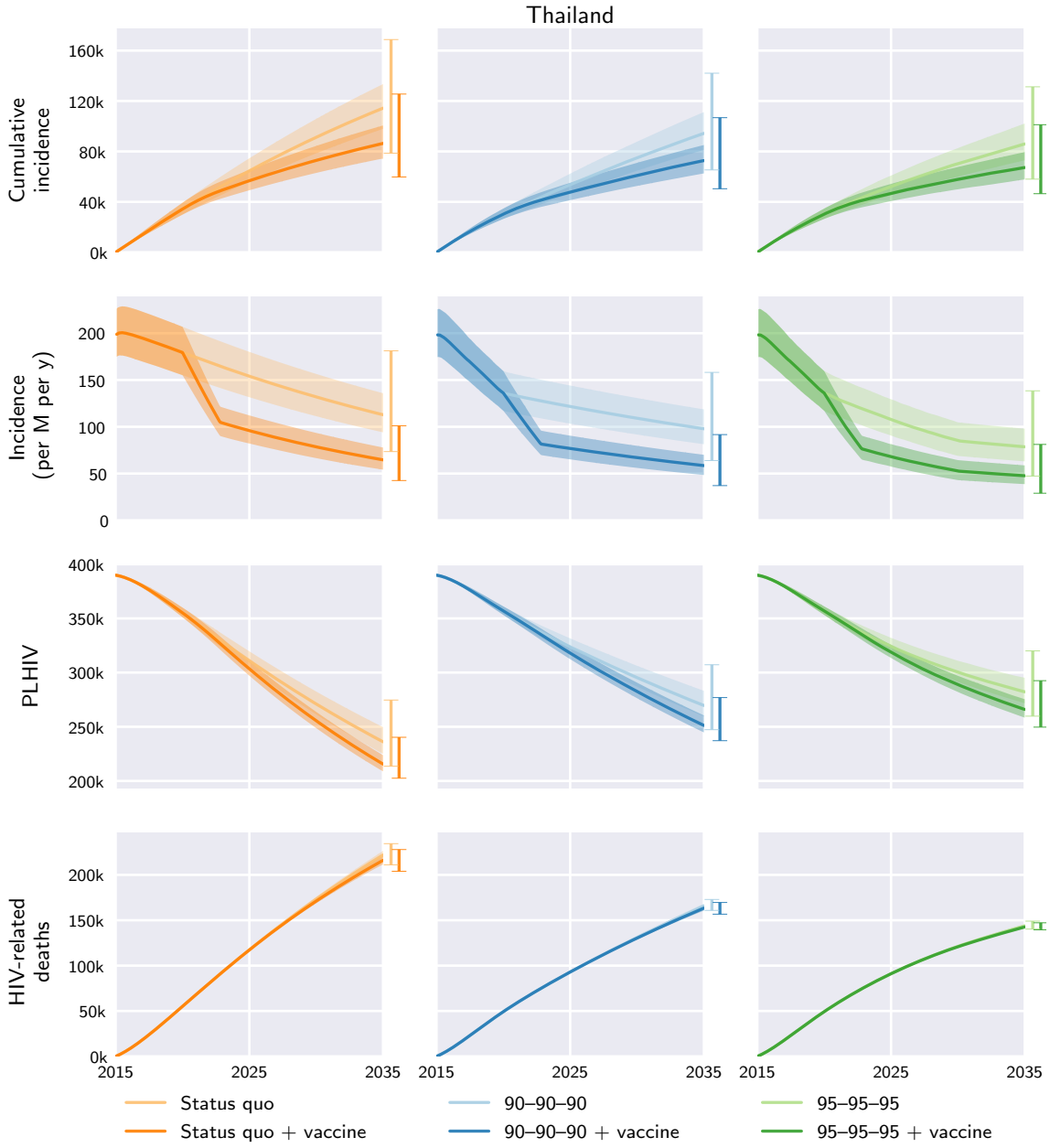

Fig. S123. Thailand model outcomes under the different diagnosis, treatment, and vaccination scenarios. Central curves show the medians over model runs with 1000 samples from parameter distributions, shaded regions show the 1st and 3rd quartiles (i.e. 25th and 75th percentiles), and vertical bars to the right of each axis show the 5th and 95th percentiles at the end time, 2035. Regional and global outcomes were aggregated from the country-level model outcomes.

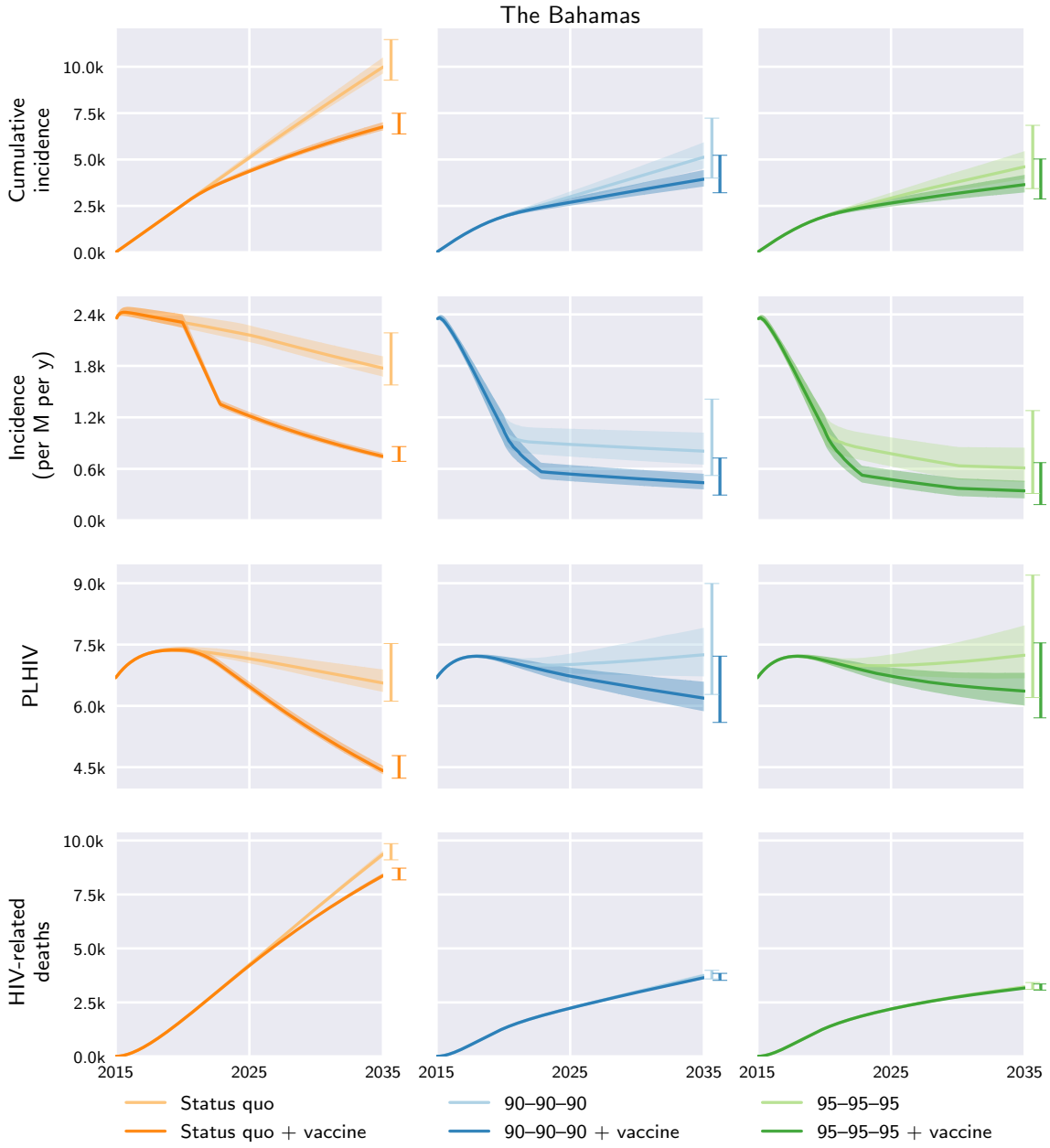

Fig. S124. The Bahamas model outcomes under the different diagnosis, treatment, and vaccination scenarios. Central curves show the medians over model runs with 1000 samples from parameter distributions, shaded regions show the 1st and 3rd quartiles (i.e. 25th and 75th percentiles), and vertical bars to the right of each axis show the 5th and 95th percentiles at the end time, 2035. Regional and global outcomes were aggregated from the country-level model outcomes.

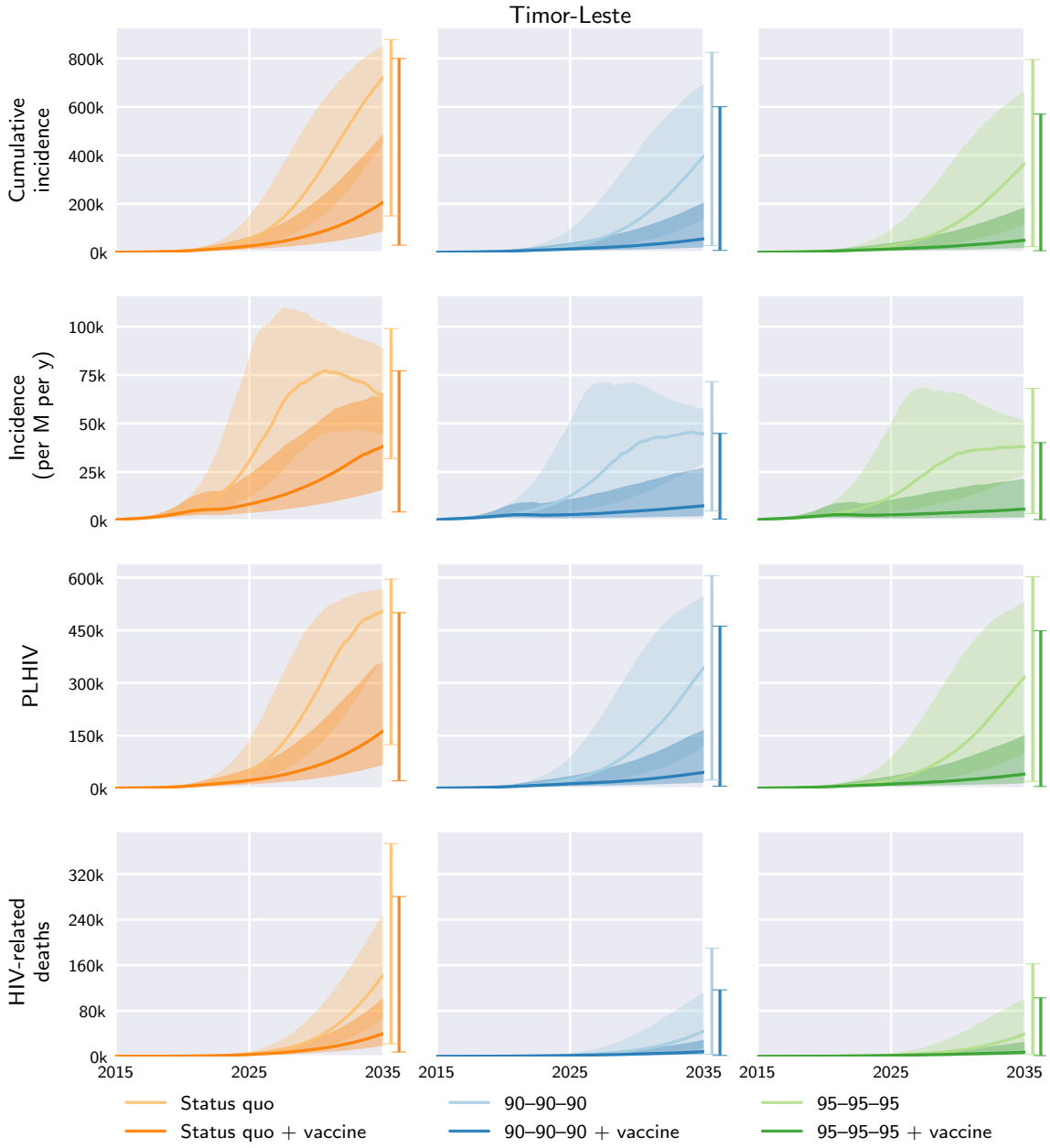

Fig. S125. Timor-Leste model outcomes under the different diagnosis, treatment, and vaccination scenarios. Central curves show the medians over model runs with 1000 samples from parameter distributions, shaded regions show the 1st and 3rd quartiles (i.e. 25th and 75th percentiles), and vertical bars to the right of each axis show the 5th and 95th percentiles at the end time, 2035. Regional and global outcomes were aggregated from the country-level model outcomes.

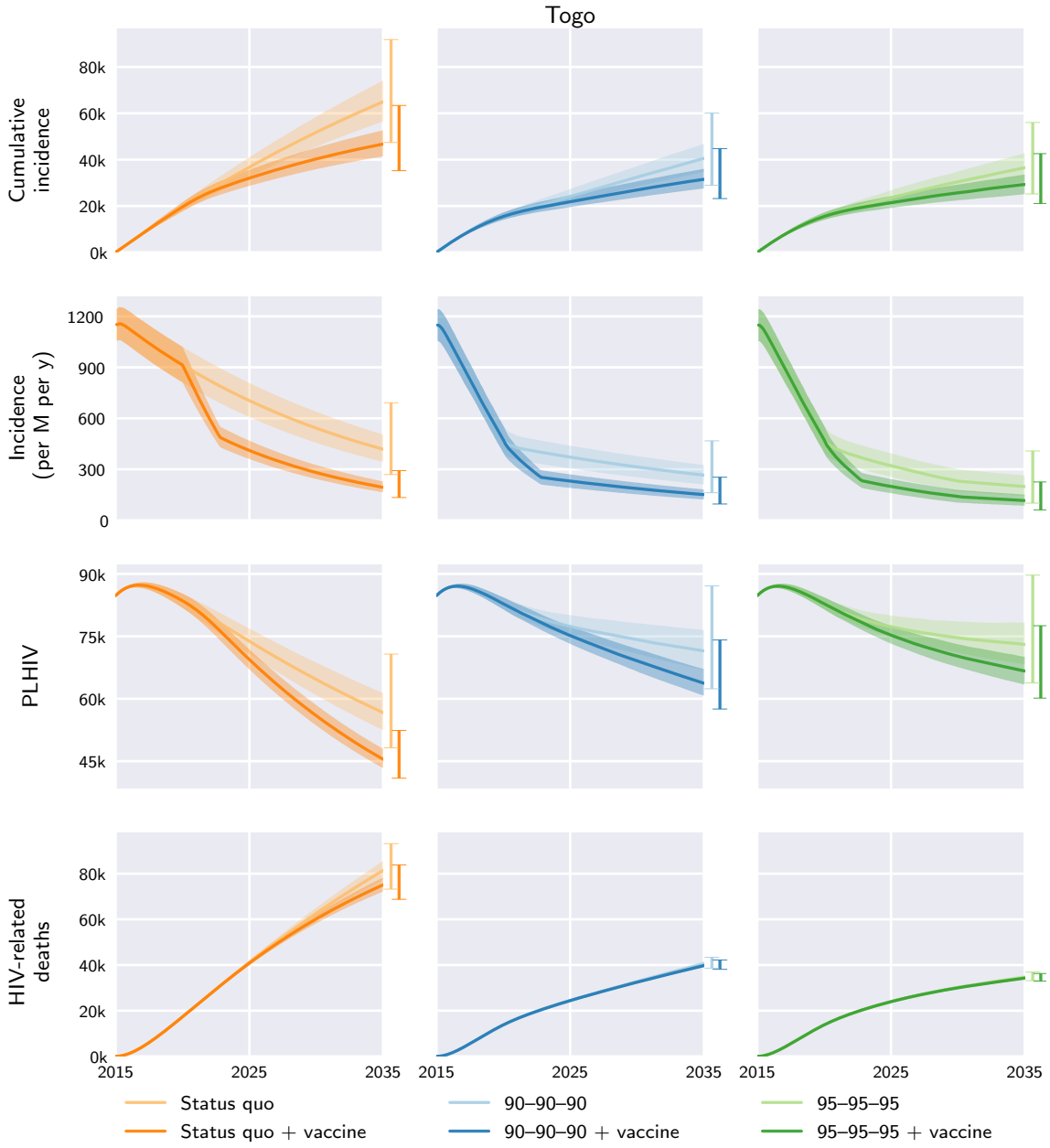

Fig. S126. Togo model outcomes under the different diagnosis, treatment, and vaccination scenarios. Central curves show the medians over model runs with 1000 samples from parameter distributions, shaded regions show the 1st and 3rd quartiles (i.e. 25th and 75th percentiles), and vertical bars to the right of each axis show the 5th and 95th percentiles at the end time, 2035. Regional and global outcomes were aggregated from the country-level model outcomes.

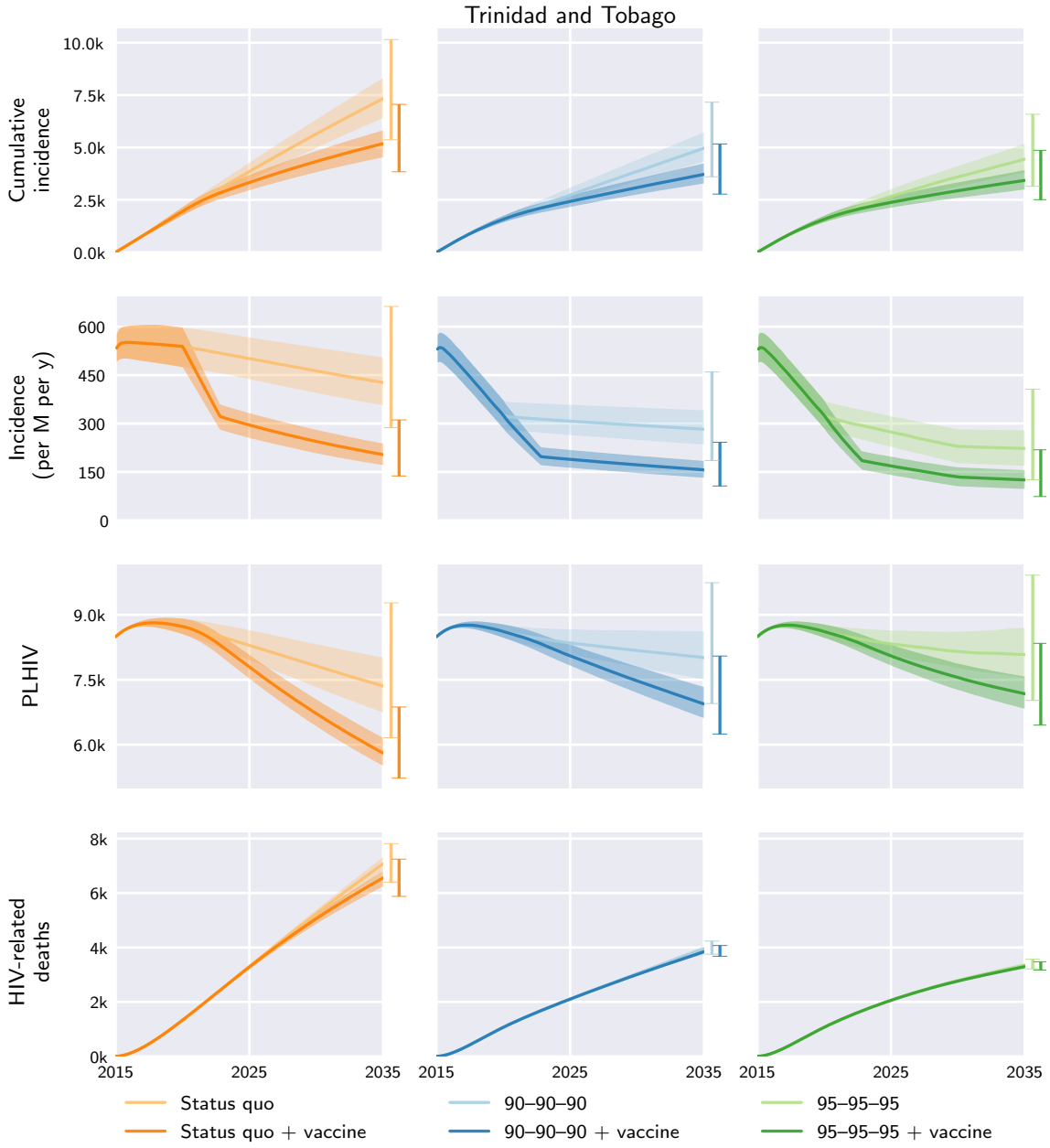

Fig. S127. Trinidad and Tobago model outcomes under the different diagnosis, treatment, and vaccination scenarios. Central curves show the medians over model runs with 1000 samples from parameter distributions, shaded regions show the 1st and 3rd quartiles (i.e. 25th and 75th percentiles), and vertical bars to the right of each axis show the 5th and 95th percentiles at the end time, 2035. Regional and global outcomes were aggregated from the country-level model outcomes.

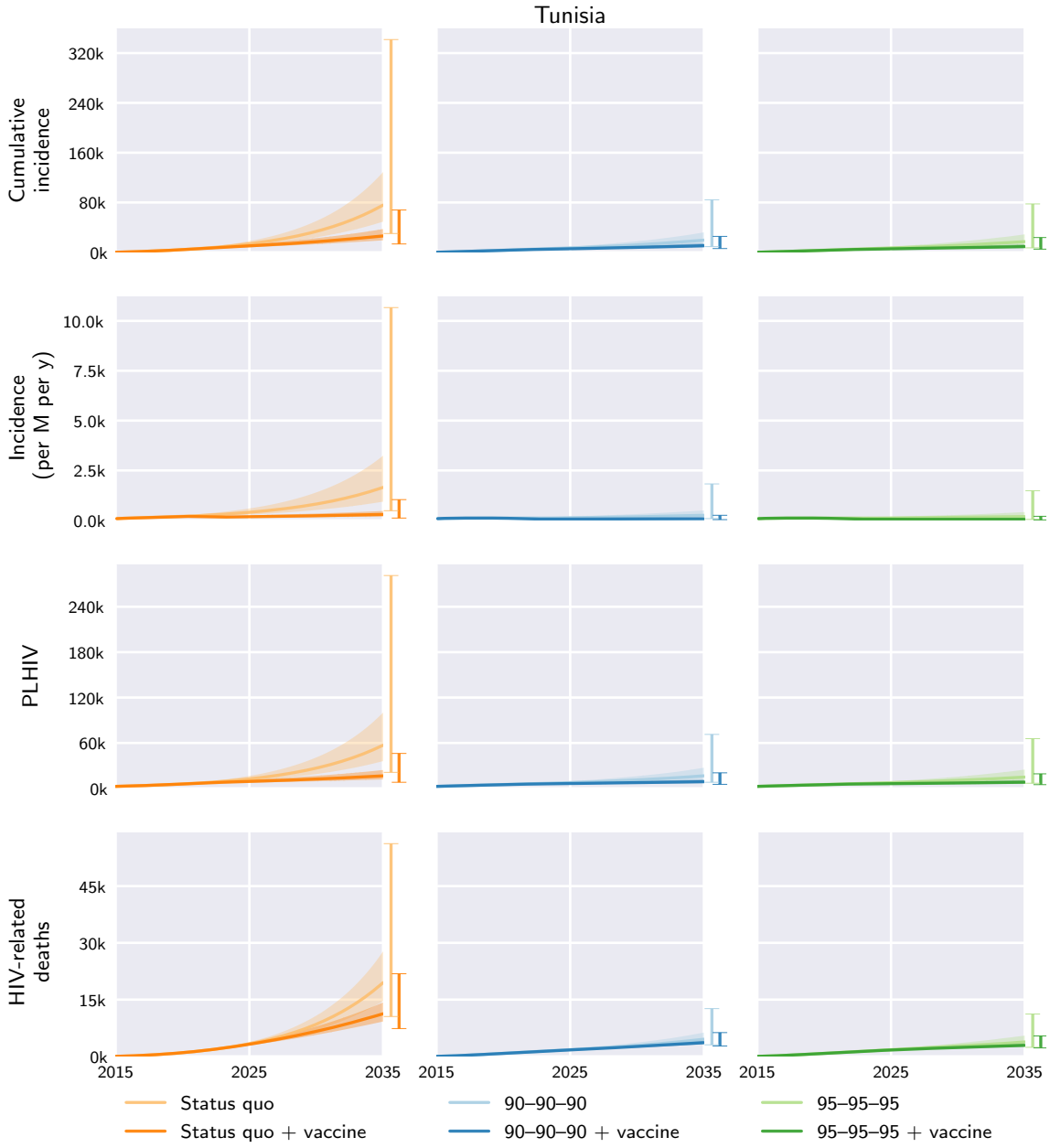

Fig. S128. Tunisia model outcomes under the different diagnosis, treatment, and vaccination scenarios. Central curves show the medians over model runs with 1000 samples from parameter distributions, shaded regions show the 1st and 3rd quartiles (i.e. 25th and 75th percentiles), and vertical bars to the right of each axis show the 5th and 95th percentiles at the end time, 2035. Regional and global outcomes were aggregated from the country-level model outcomes.

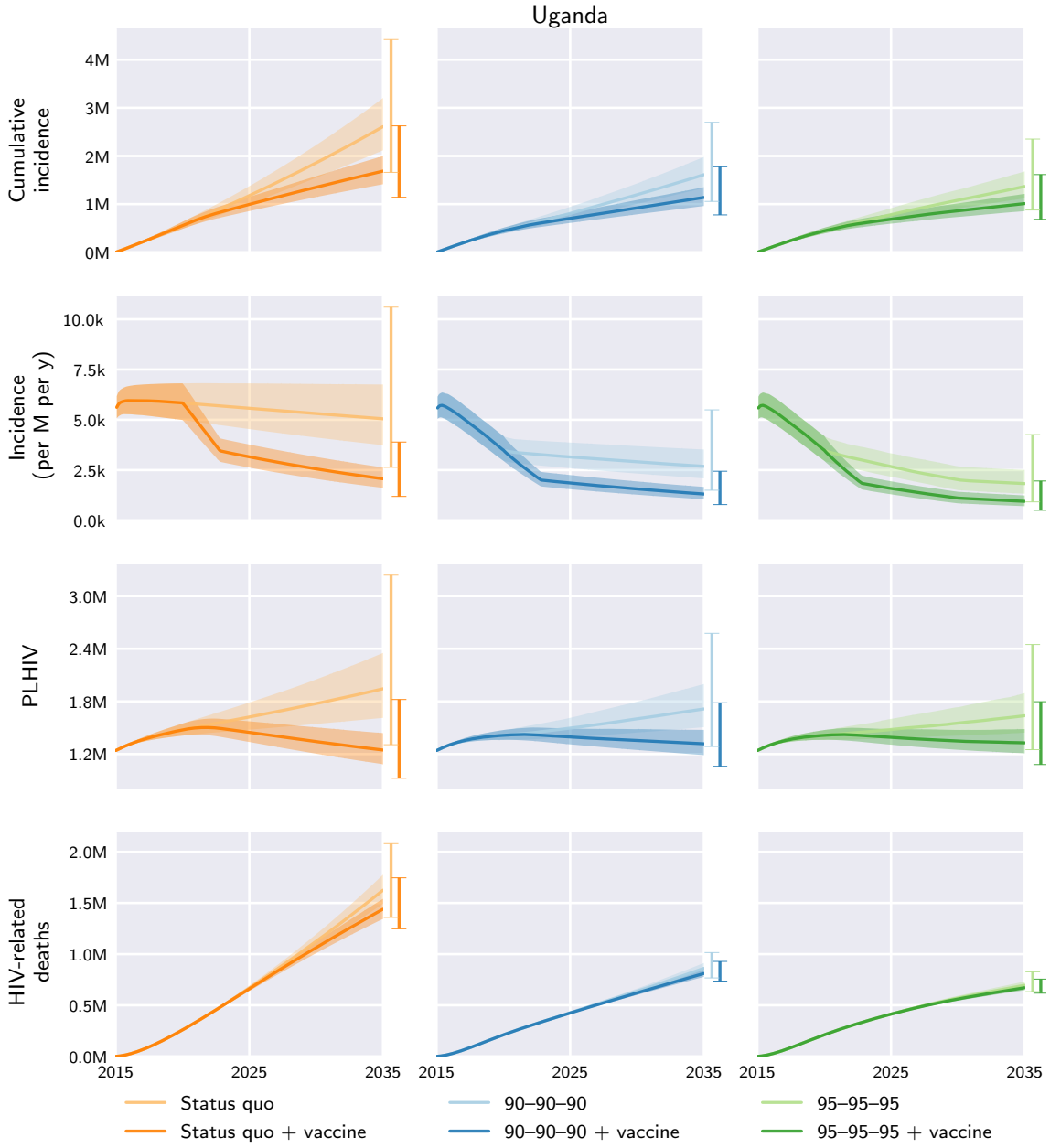

Fig. S129. Uganda model outcomes under the different diagnosis, treatment, and vaccination scenarios. Central curves show the medians over model runs with 1000 samples from parameter distributions, shaded regions show the 1st and 3rd quartiles (i.e. 25th and 75th percentiles), and vertical bars to the right of each axis show the 5th and 95th percentiles at the end time, 2035. Regional and global outcomes were aggregated from the country-level model outcomes.

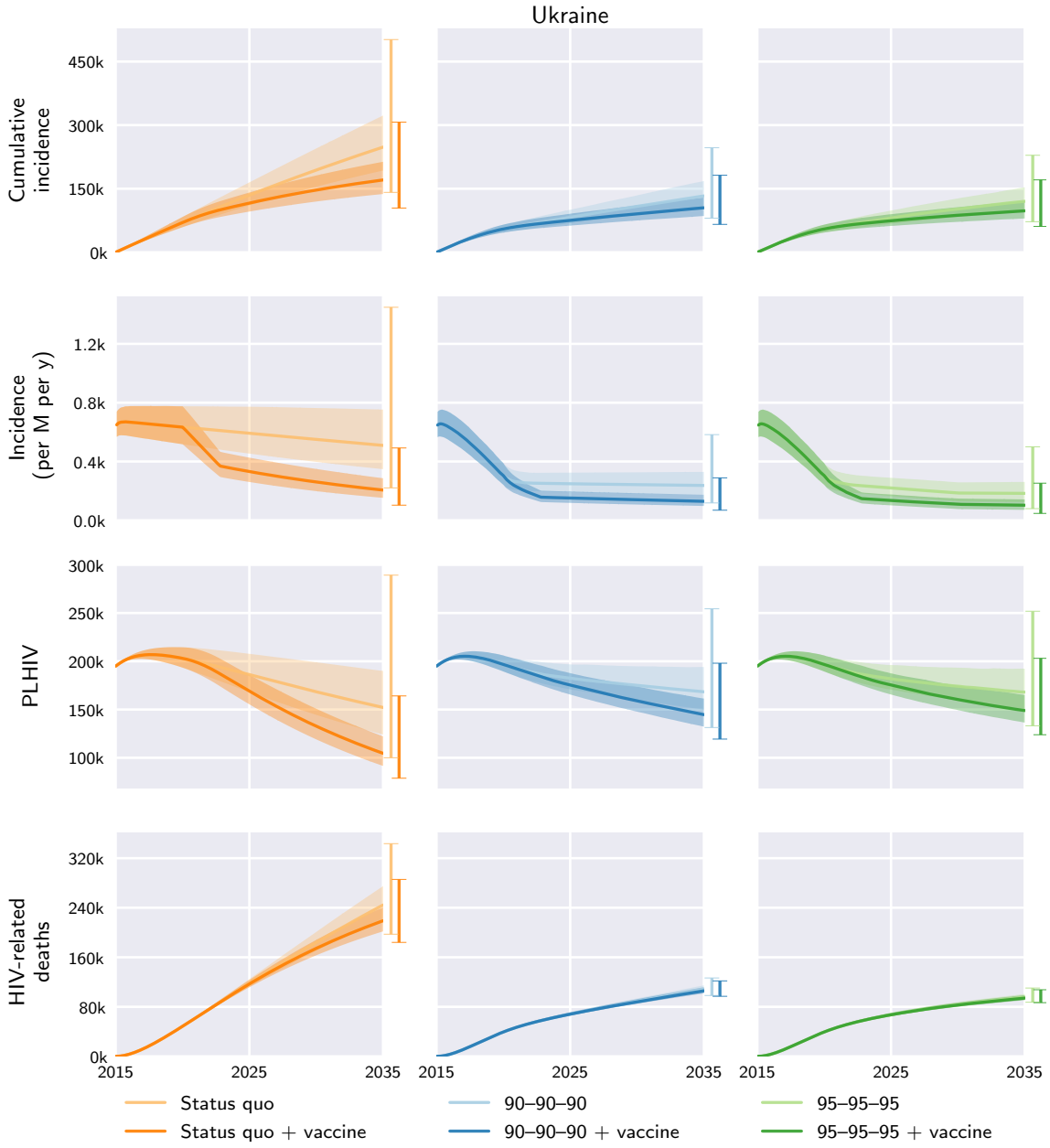

Fig. S130. Ukraine model outcomes under the different diagnosis, treatment, and vaccination scenarios. Central curves show the medians over model runs with 1000 samples from parameter distributions, shaded regions show the 1st and 3rd quartiles (i.e. 25th and 75th percentiles), and vertical bars to the right of each axis show the 5th and 95th percentiles at the end time, 2035. Regional and global outcomes were aggregated from the country-level model outcomes.

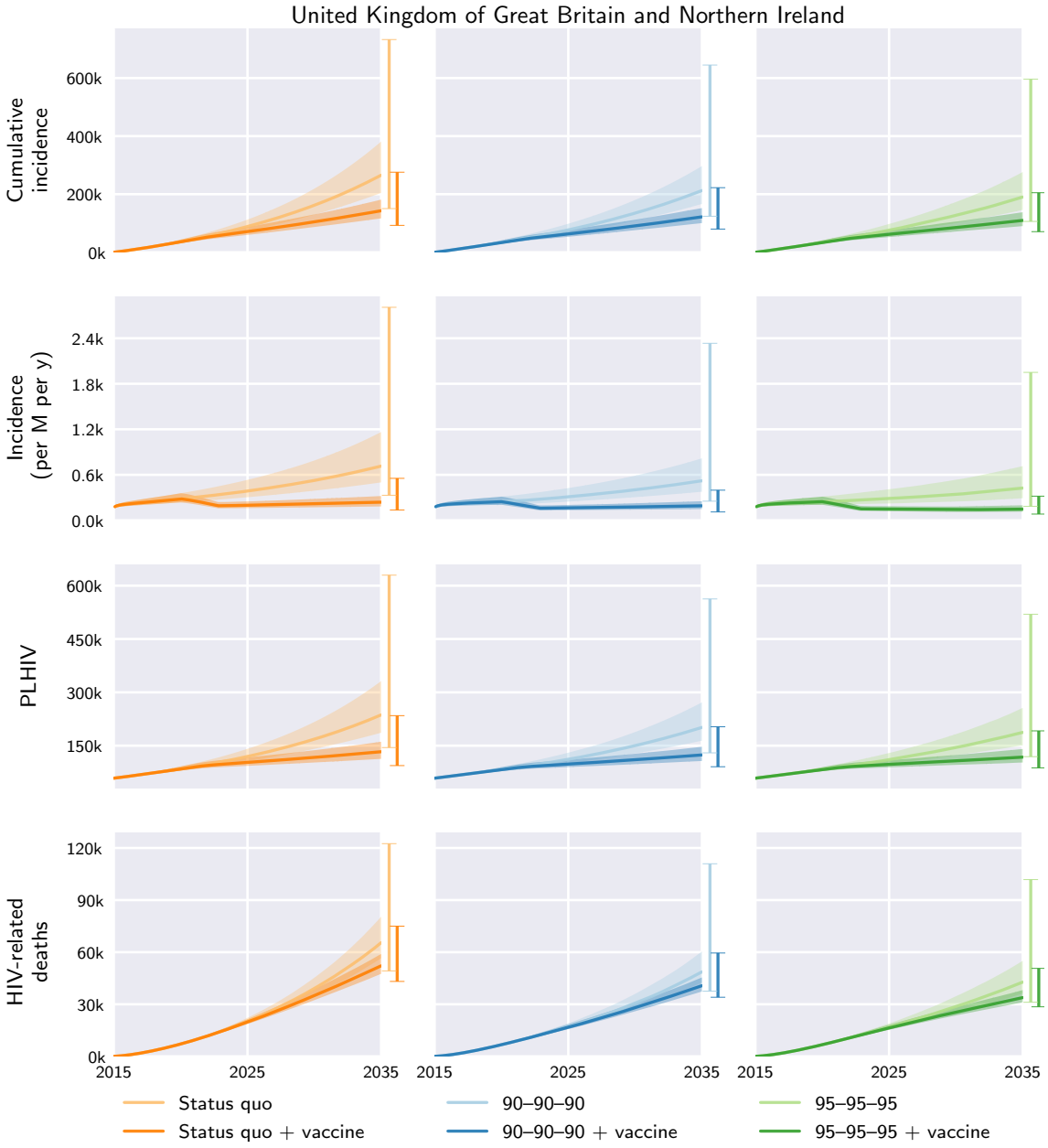

Fig. S131. United Kingdom of Great Britain and Northern Ireland model outcomes under the different diagnosis, treatment, and vaccination scenarios. Central curves show the medians over model runs with 1000 samples from parameter distributions, shaded regions show the 1st and 3rd quartiles (i.e. 25th and 75th percentiles), and vertical bars to the right of each axis show the 5th and 95th percentiles at the end time, 2035. Regional and global outcomes were aggregated from the country-level model outcomes.

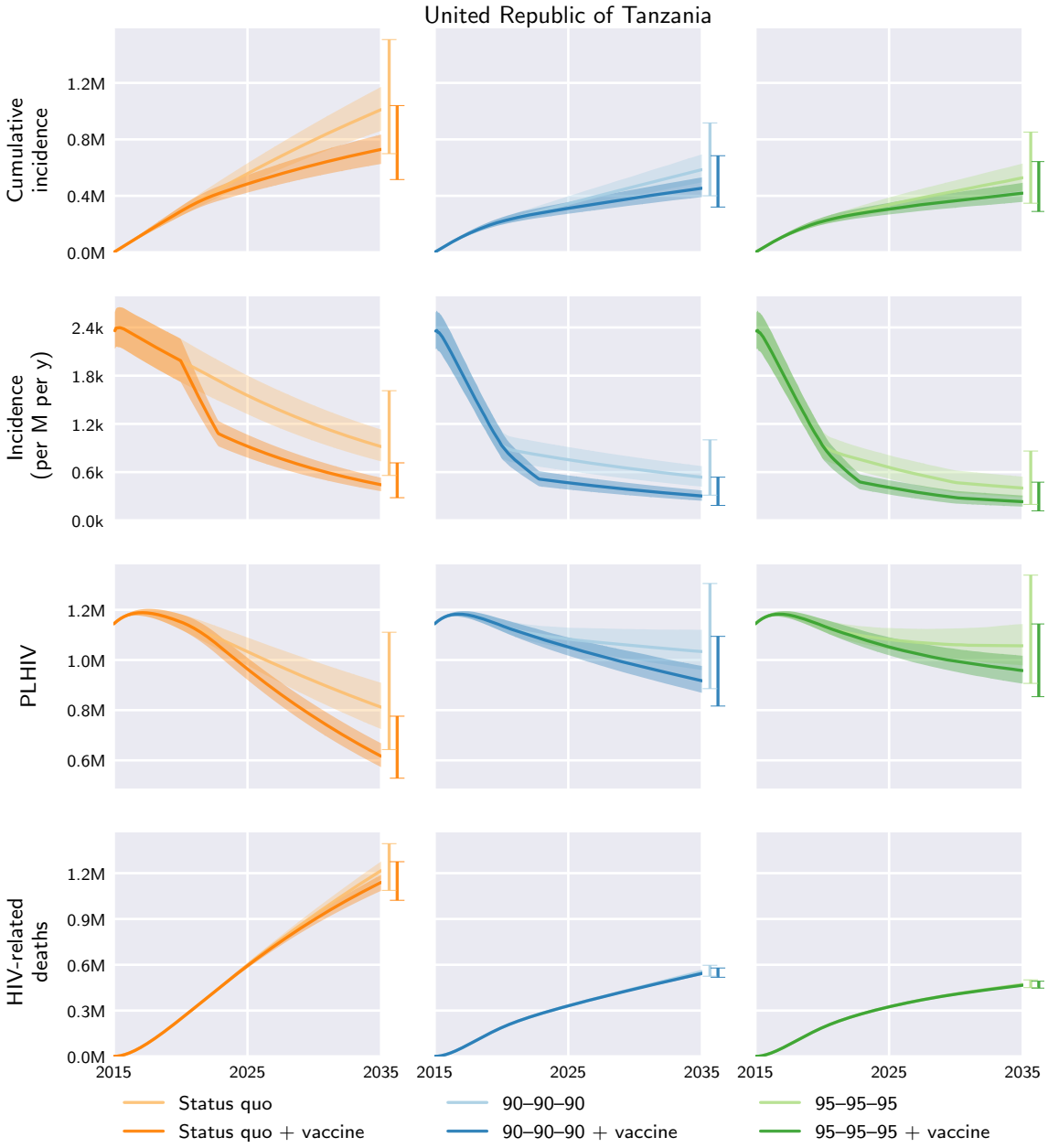

Fig. S132. United Republic of Tanzania model outcomes under the different diagnosis, treatment, and vaccination scenarios. Central curves show the medians over model runs with 1000 samples from parameter distributions, shaded regions show the 1st and 3rd quartiles (i.e. 25th and 75th percentiles), and vertical bars to the right of each axis show the 5th and 95th percentiles at the end time, 2035. Regional and global outcomes were aggregated from the country-level model outcomes.

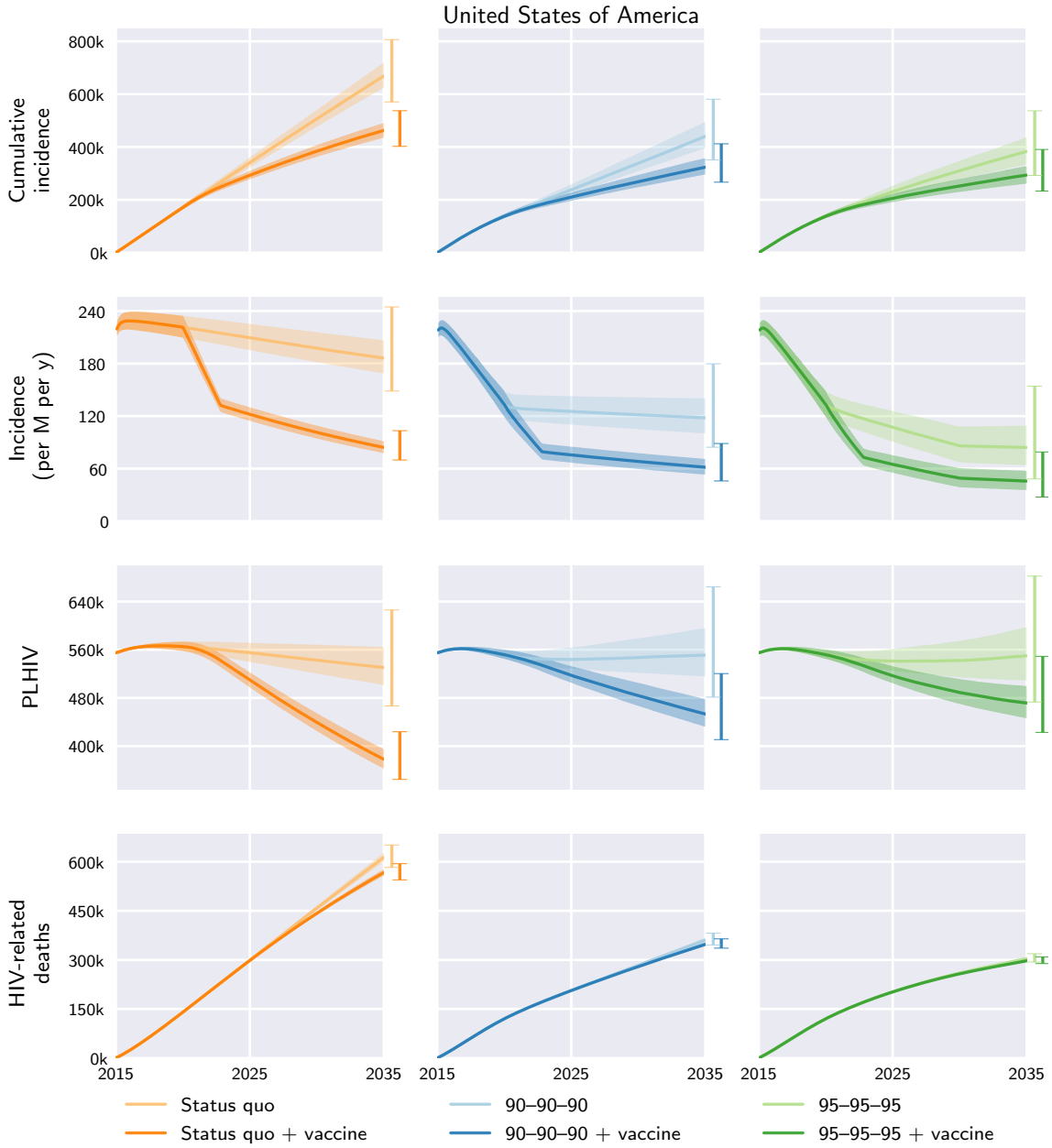

Fig. S133. United States of America model outcomes under the different diagnosis, treatment, and vaccination scenarios. Central curves show the medians over model runs with 1000 samples from parameter distributions, shaded regions show the 1st and 3rd quartiles (i.e. 25th and 75th percentiles), and vertical bars to the right of each axis show the 5th and 95th percentiles at the end time, 2035. Regional and global outcomes were aggregated from the country-level model outcomes.

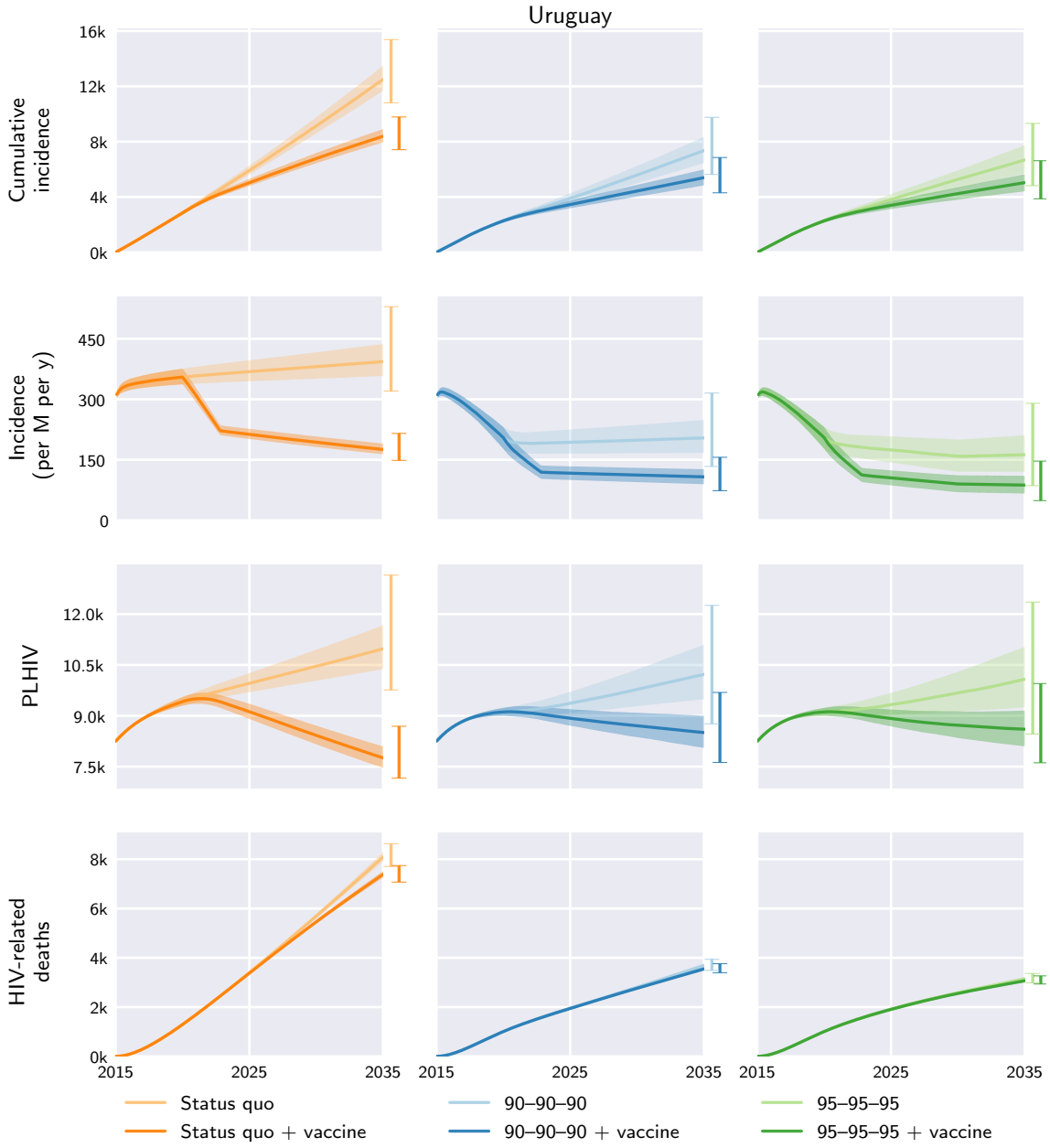

Fig. S134. Uruguay model outcomes under the different diagnosis, treatment, and vaccination scenarios. Central curves show the medians over model runs with 1000 samples from parameter distributions, shaded regions show the 1st and 3rd quartiles (i.e. 25th and 75th percentiles), and vertical bars to the right of each axis show the 5th and 95th percentiles at the end time, 2035. Regional and global outcomes were aggregated from the country-level model outcomes.

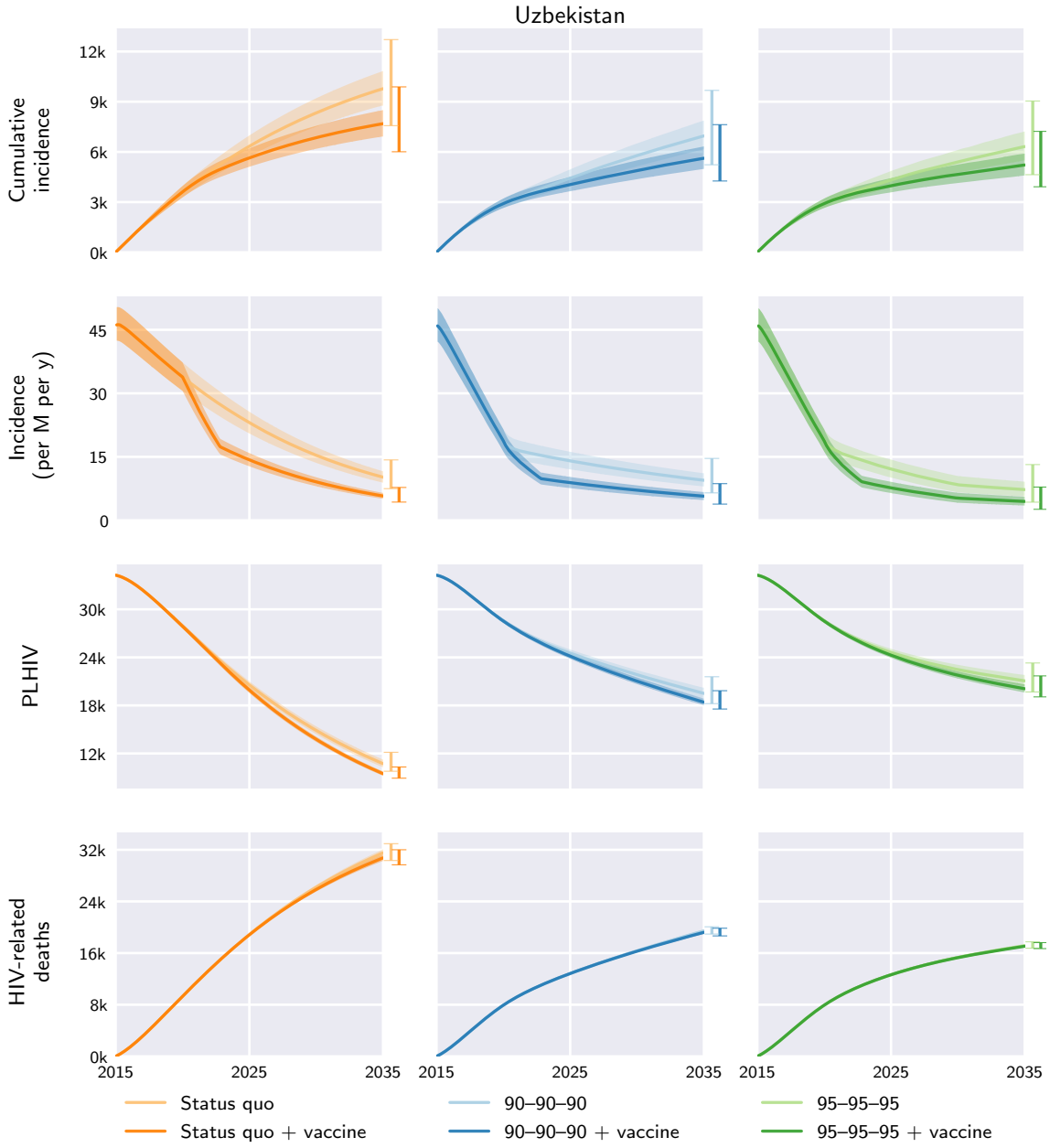

Fig. S135. Uzbekistan model outcomes under the different diagnosis, treatment, and vaccination scenarios. Central curves show the medians over model runs with 1000 samples from parameter distributions, shaded regions show the 1st and 3rd quartiles (i.e. 25th and 75th percentiles), and vertical bars to the right of each axis show the 5th and 95th percentiles at the end time, 2035. Regional and global outcomes were aggregated from the country-level model outcomes.

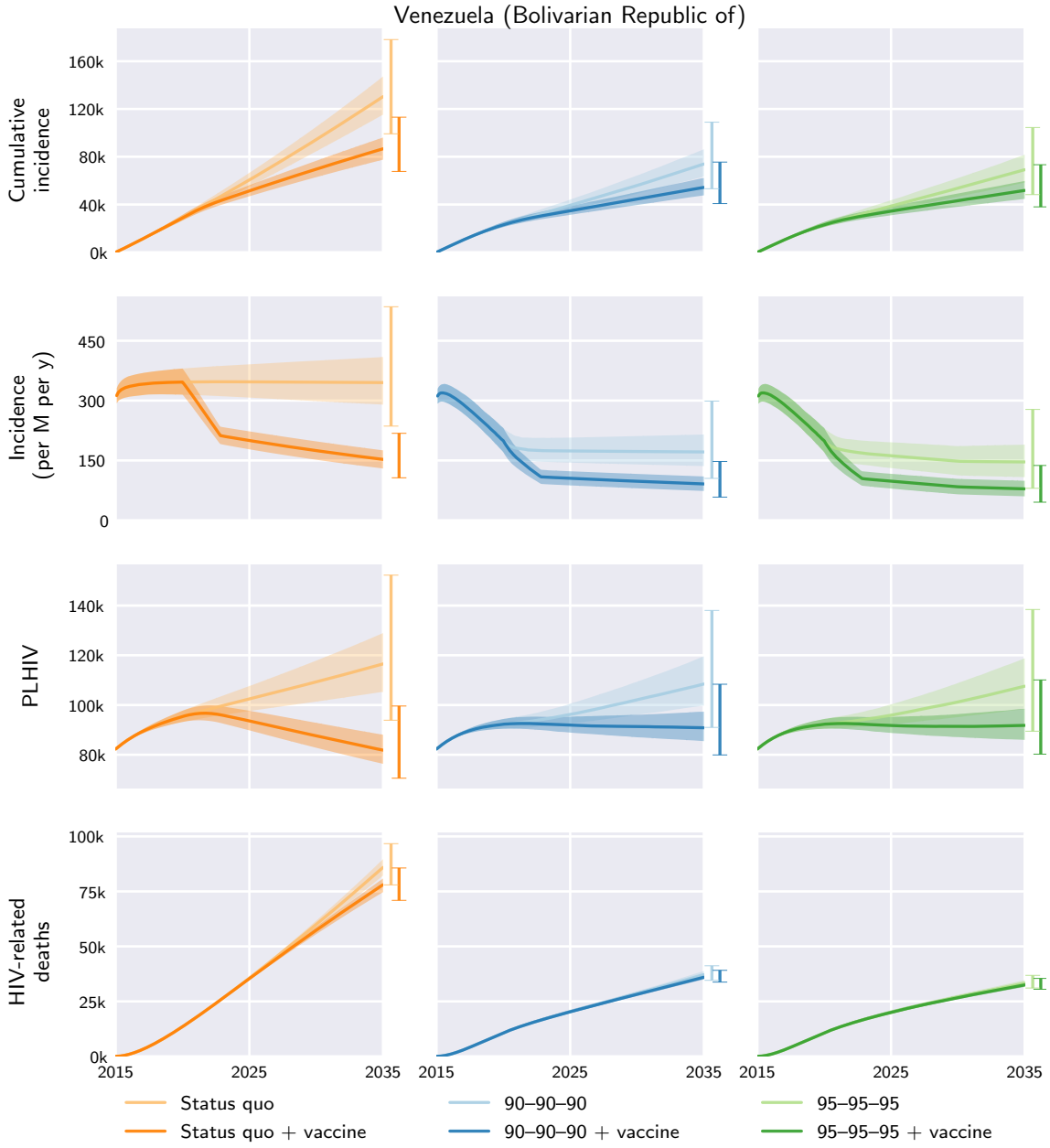

Fig. S136. Venezuela (Bolivarian Republic of) model outcomes under the different diagnosis, treatment, and vaccination scenarios. Central curves show the medians over model runs with 1000 samples from parameter distributions, shaded regions show the 1st and 3rd quartiles (i.e. 25th and 75th percentiles), and vertical bars to the right of each axis show the 5th and 95th percentiles at the end time, 2035. Regional and global outcomes were aggregated from the country-level model outcomes.

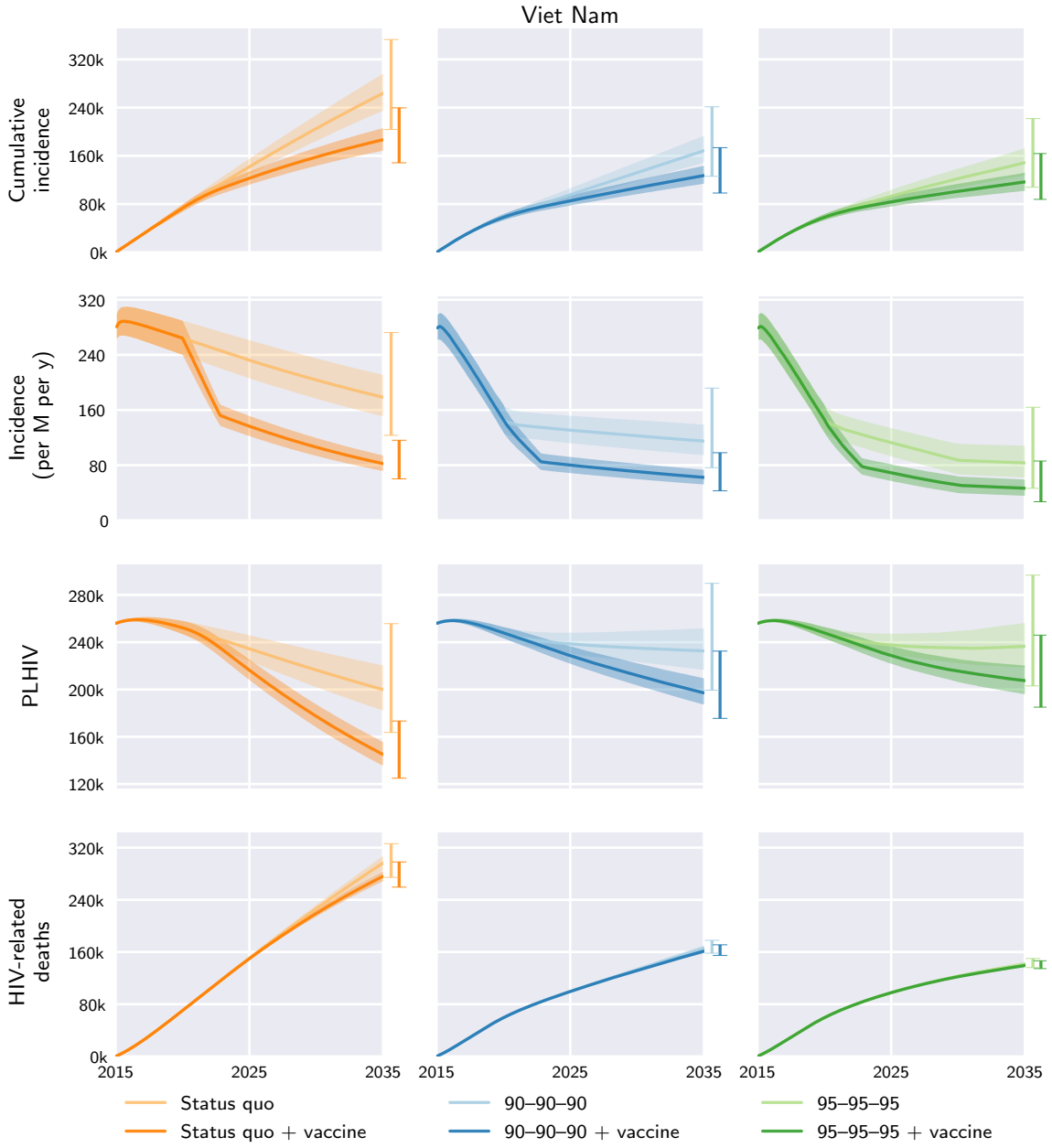

Fig. S137. Viet Nam model outcomes under the different diagnosis, treatment, and vaccination scenarios. Central curves show the medians over model runs with 1000 samples from parameter distributions, shaded regions show the 1st and 3rd quartiles (i.e. 25th and 75th percentiles), and vertical bars to the right of each axis show the 5th and 95th percentiles at the end time, 2035. Regional and global outcomes were aggregated from the country-level model outcomes.

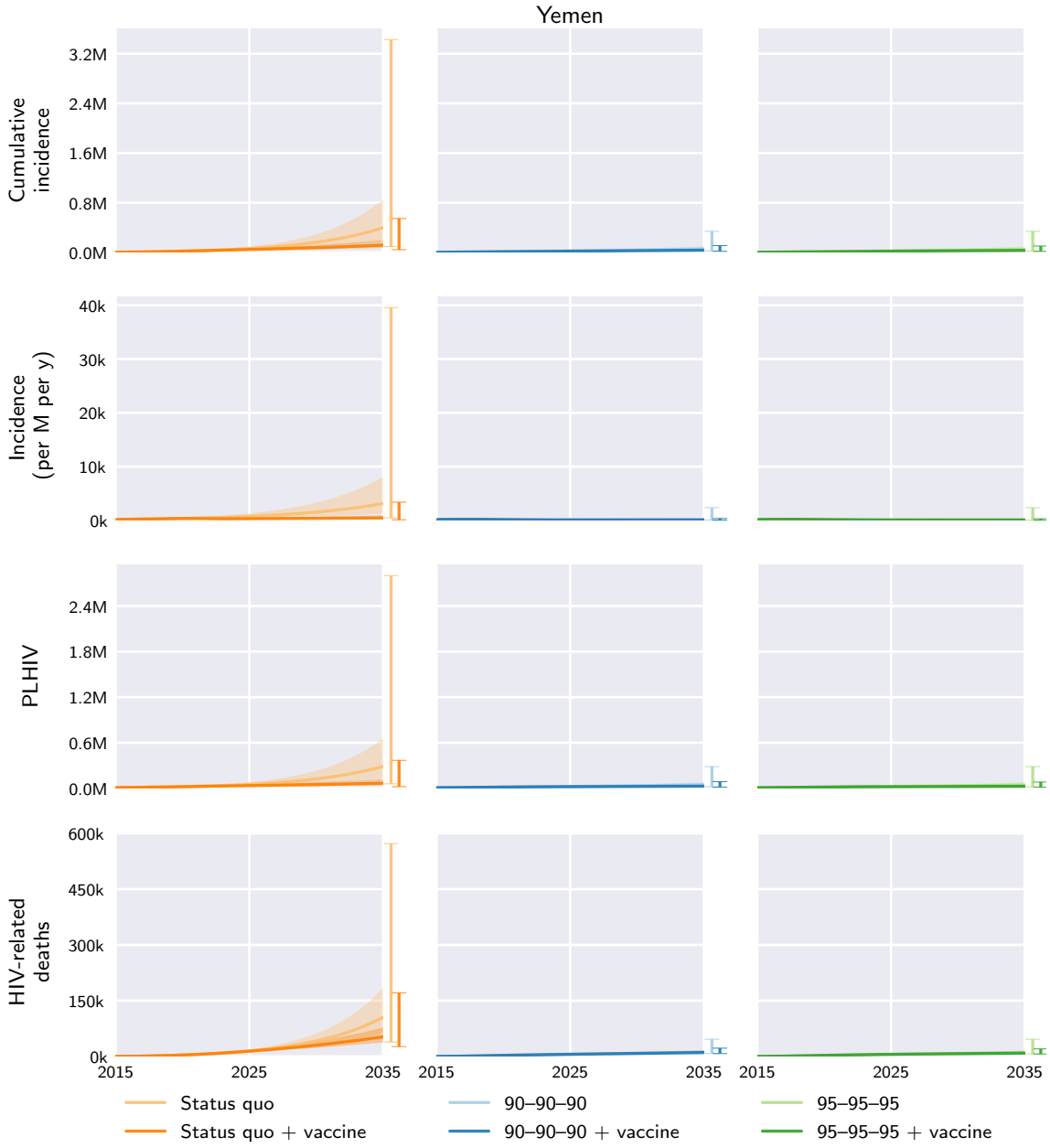

Fig. S138. Yemen model outcomes under the different diagnosis, treatment, and vaccination scenarios. Central curves show the medians over model runs with 1000 samples from parameter distributions, shaded regions show the 1st and 3rd quartiles (i.e. 25th and 75th percentiles), and vertical bars to the right of each axis show the 5th and 95th percentiles at the end time, 2035. Regional and global outcomes were aggregated from the country-level model outcomes.

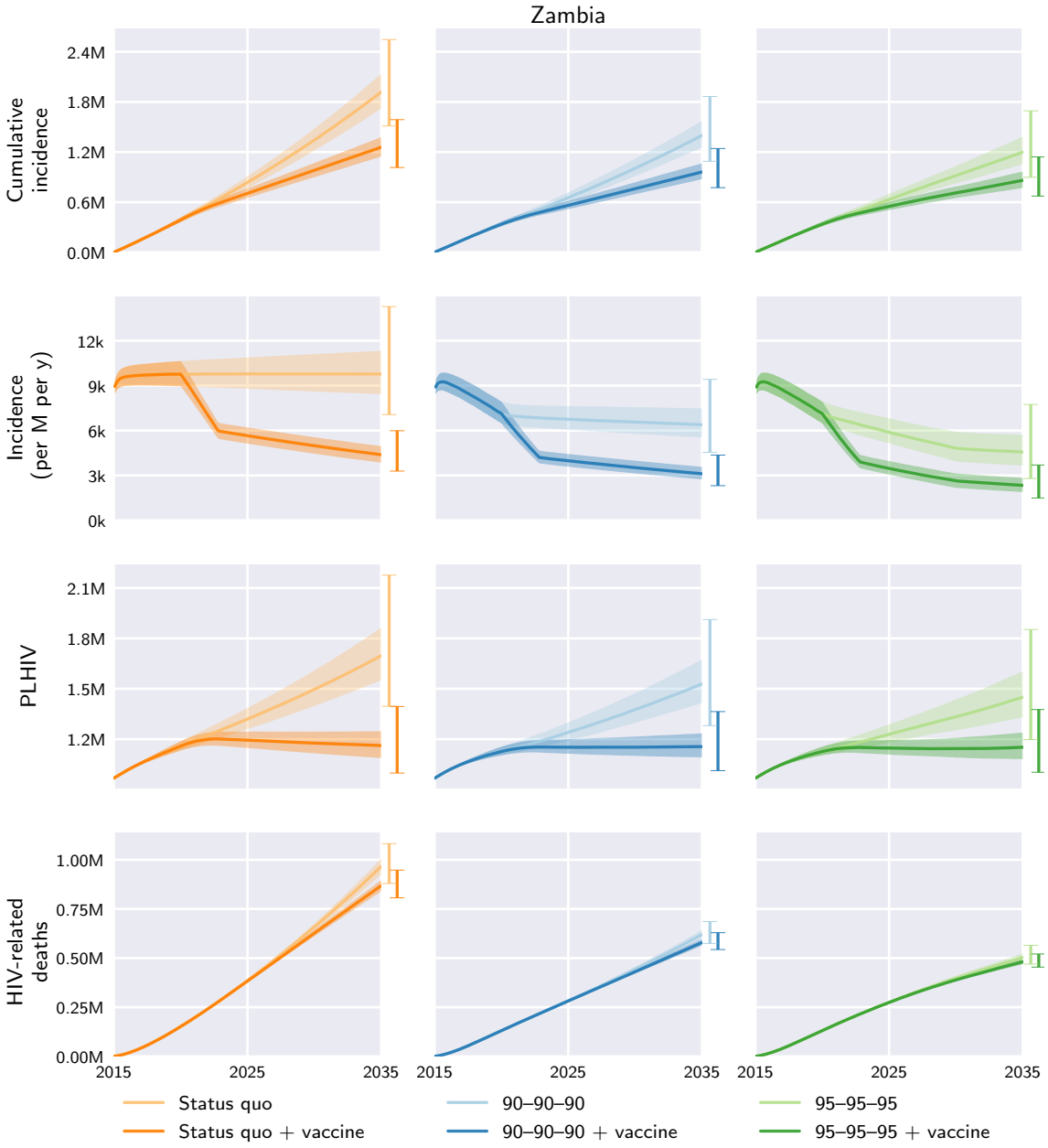

Fig. S139. Zambia model outcomes under the different diagnosis, treatment, and vaccination scenarios. Central curves show the medians over model runs with 1000 samples from parameter distributions, shaded regions show the 1st and 3rd quartiles (i.e. 25th and 75th percentiles), and vertical bars to the right of each axis show the 5th and 95th percentiles at the end time, 2035. Regional and global outcomes were aggregated from the country-level model outcomes.

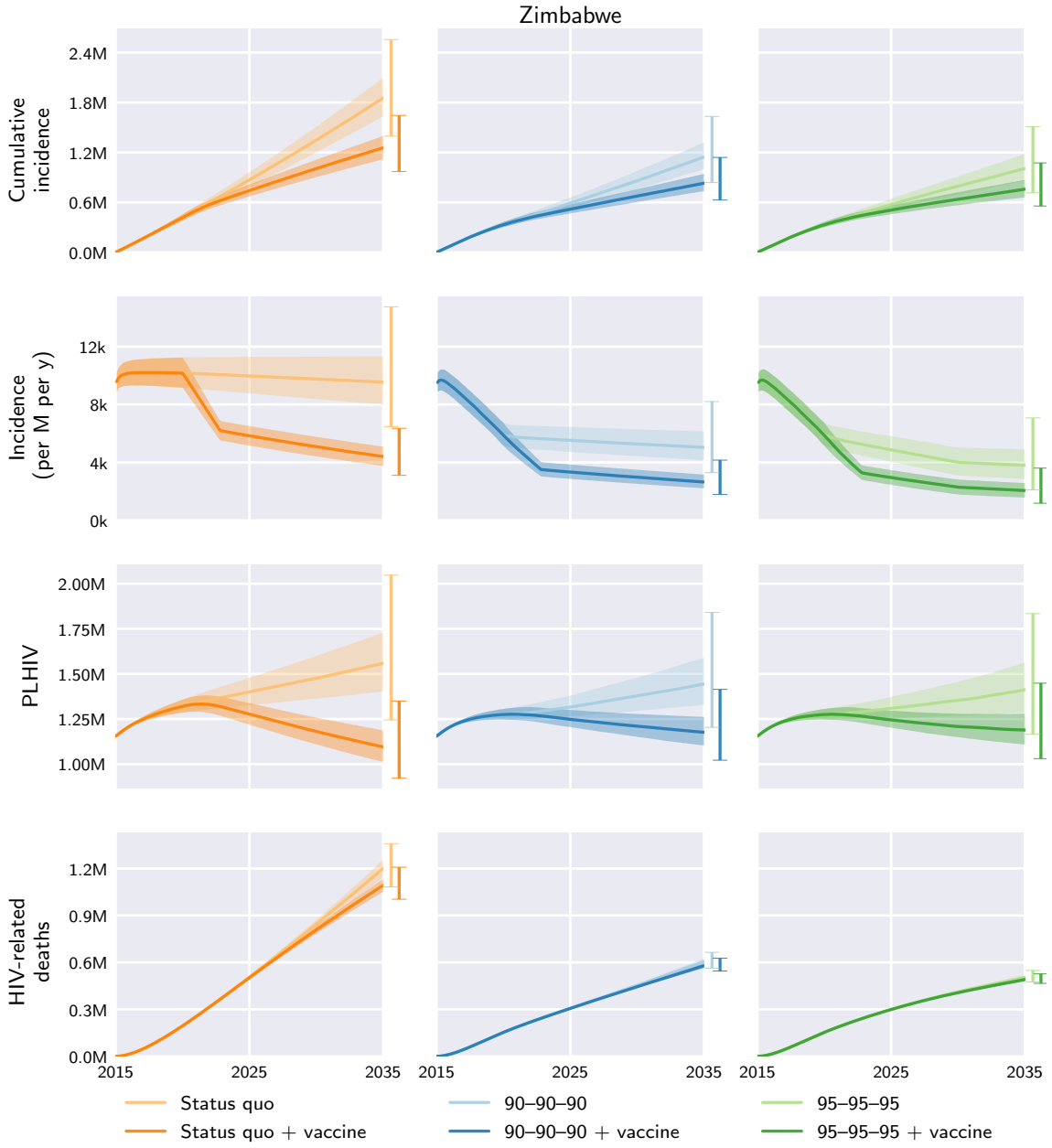

Fig. S140. Zimbabwe model outcomes under the different diagnosis, treatment, and vaccination scenarios. Central curves show the medians over model runs with 1000 samples from parameter distributions, shaded regions show the 1st and 3rd quartiles (i.e. 25th and 75th percentiles), and vertical bars to the right of each axis show the 5th and 95th percentiles at the end time, 2035. Regional and global outcomes were aggregated from the country-level model outcomes.